Analysis of CK2-dependent regulation of Myo5-induced actin polymerization during the endocytic uptake in *S. cerevisiae*

Análisis de la regulación mediada por CK2 de la polimerización de actina inducida por Myo5 durante la internalización endocítica en "S. Cerevisiae"

Isabel M. Fernández Golbano

Analysis of CK2-dependent regulation of Myo5-induced actin polymerization during the endocytic uptake in *S. cerevisiae*

Isabel M. Fernández Golbano

Barcelona 2012

Análisis de la regulación mediada por CK2 de la polimerización de actina inducida por Myo5 durante la internalización endocítica en *S. cerevisiae*

Memòria presentada per Isabel M. Fernández Golbano per optar al grau de doctora per la Universitat de Barcelona

Programa de Doctorat de Biologia Cel·lular

Departament de Biologia Cel·lular

Institut de Biologia Molecular de Barcelona (IBMB-CSIC)

Doctoranda:	Directora:	Tutor:
Isabel M. Fernández Golbano	Maribel Geli Fernández-Peñaflor	Albert Martínez

aa	amino acid
ADP	adenosine 5’-diphosphate
AMP^R	ampicillin resistance gene
ATP	adenosine 5’-triphosphate
Ci	Curie
DNA	deoxyribonucleic acid
g	gravity
GFP	green fluorescent protein
GST	glutathion-S-transferase
GTP	guanosine 5’-triphosphate
HEPES	N-[2-Hydroxyethyl]piperazine-N’-[2-ethanesulfonic acid]
His	histidine
IgG	immunoglobulin G
kDa	kilodalton
Leu	leucin
min	minute(s)
mRFP	monomeric red fluorescent protein
OD_{600}	optical density at 600nm
ORF	open reading frame
PCR	polymerase chain reaction
P_i	inorganic phosphate
PIP_2	phosphatidylinositol 4,5-bisphosphate
PMSF	phenylmethanesulfonyl fluoride
ProtA	protein A of Staphylococcus aureus
RT	room temperature
SDC	synthetic dextrose complete medium
ts	temperature-sensitive
Trp	tryptophan
Ura	uracil
WT	wild type
YPD	yeast peptone dextrose medium

1. INTRODUCTION

Actin filaments, intermediate filaments, and microtubules constitute the cytoskeleton in eukaryotic cells, which serves to organize the cytoplasm, to generate force, to determine the cell shape, and to provide structural integrity. The actin cytoskeleton is composed of linear polymers of actin subunits that assemble forming a double-stranded helix. An important property of actin is its ability to polymerize and depolymerize rapidly, producing movement in the presence and in the absence of motor proteins. For this reason, the actin cytoskeleton plays an essential role in dynamic processes such as muscle contraction, cell migration, intracellular transport, cellular division, and a number of morphogenetic processes. Actin is conserved in all eukaryotic organisms and several studies have identified homologs in prokaryotes as well (reviewed in (Wickstead and Gull, 2011)), indicating the importance of actin during evolution.

Powerful molecular and genetic methods, well-established biochemical techniques, and development of live cell imaging make the budding yeast *Saccharomyces cerevisiae* particularly powerful to study the relation between molecular mechanisms of actin regulation and its biological function. Compared with higher eukaryotes, *S. cerevisiae* has a simple actin cytoskeleton, but at least one member for each class of actin regulators have been identified in yeast (most of them showing a high degree of homology to their counterparts in mammals), suggesting that the molecular mechanisms that control the remodeling of the actin cytoskeleton are conserved from yeast to mammals. The fact that a number of findings in *S. cerevisiae* were applicable to higher eukaryotes validates *S. cerevisiae* as a powerful model system for studying actin-based cellular processes (Ayscough and Drubin, 1996; Engqvist-Goldstein and Drubin, 2003).

This introduction has been divided into two main sections: the first part briefly describes the biochemical activities of the highly conserved actin-binding proteins known to regulate actin dynamics and organization, while the second introduces the actin structures found in *S. cerevisiae* and the major biological functions of actin in this organism -with special attention to the internalization step of endocytosis, which is the focus of this thesis-.

1.1. Molecular mechanism for actin remodeling in *Saccharomyces cerevisiae*

1.1.1. The monomer & the filament: biochemistry of treadmilling and the polarity of the actin filament

Actin is a highly conserved ATPase of 42 kDa found in all eukaryotic cells, being one of the most abundant protein in nearly all organisms. Unicellular organisms have 1 or 2 copies of the actin gene, whereas higher eukaryotes have several genes encoding for different isoforms. α-actin is found in muscle and is associated with muscle contraction, whereas β- and γ-actin are expressed in non-muscle cells. β-Actin mainly polymerizes at the cell leading edge and γ-actin is mainly associated with stress fibers. Actin can be found in two states: a globular monomeric form (namely G-actin) or forming filaments (F-actin), which are assembled in a double helical pattern in a head-to-tail manner, which confers polarity to the filament. Based on the arrowhead pattern observed upon decoration with myosin fragments (Huxley, 1963), one end of the

filament is called the barbed- and the other the pointed-end. Actin filaments are strongly oriented with respect to the cell surface, barbed end outwards (Woodrum et al., 1975).

Formation of a new actin filament starts with the assembly of two or three ATP-charged actin subunits to form the nucleus in a process called nucleation. This step is thermodynamically unfavorable and it is the rate limited step in actin filament formation (Pollard and Cooper, 1986; Sept and McCammon, 2001). However, once the nucleus is assembled, the affinity of an actin monomer for the end of the filament increases. Thus, in the most simple situation, without the contribution of regulatory proteins, actin subunits are added in a rate directly proportional to the concentration of G-actin ($K = C \cdot k_+ - k_-$, where k_+ is the association rate constant, k_- is the dissociation rate constant, and C is the actin monomer concentration) (Oosawa, 1975). As filament grows, C decreases until it reaches the critical concentration ($C_c = k_- / k_+$). At steady state, undergoing addition and loss of actin subunits at both barbed- and pointed-ends, the critical concentration for ATP-actin is much lower at the barbed than at the pointed end, thus filament growth is favorable at this end (Pollard, 1986; Wegner, 1976; Woodrum et al., 1975). Once an ATP-actin monomer is added to the growing end, it promotes irreversible and fast hydrolysis of ATP, leaving actin bound to ADP + P_i. Phosphate is then released more slowly to produce ADP-actin, which shows less affinity to the neighbor subunit and consequently is dissociated from the pointed end (Carlier and Pantaloni, 1988). Then, the free ADP-actin undergoes nucleotide exchange to be recycled for a new round of polymerization at the barbed end (Goldschmidt-Clermont et al., 1992). This turnover cycle is called treadmilling, or head to tail polymerization (Wegner, 1976) (Figure 1).

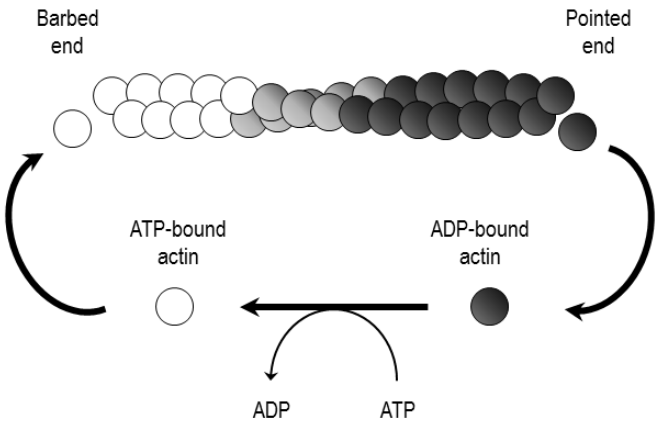

Figure 1. Actin treadmilling.
ATP-bound actin monomers (white) preferentially associate with the fast-growing barbed end of the filament. Once the monomer interacts with the filament, ATP-hydrolysis is triggered, leaving actin bound to ADP+P_i (light gray); the release of P_i generates ADP-bound actin (dark gray) that dissociates from the slow-growing pointed end of the filament. Nucleotide exchange allows the restitution of the assembly-competent pool of ATP-bound actin monomers.

S. cerevisiae has a single actin isoform, Act1, which shows 87 % and 91 % sequence identity with mammalian α- and β-actin, respectively. The crystal structure of the yeast actin has revealed minor differences with the mammalian isoforms (Kabsch et al., 1990; Vorobiev et al., 2003). However, careful examination indicates functional differences between yeast actin and actin from other species. Complementation studies have shown that yeast cells cannot survive with muscle actin as the sole actin isoform, and although the yeast actin can be replaced with a vertebrate non-muscle β-actin, cells exhibited an altered morphology, slower growth and temperature-sensitive lethality (Karlsson et al., 1991). Budding yeast actin can also substitute for actin from metazoan in a wide range of biochemical assays such as activation of an ATPase activity, or actin-myosin motility assays, although it does it less efficiently (Greer and Schekman, 1982; Kron et al., 1992). Yeast actin also displays some differences in the polymerization behavior with respect to mammalian actin. Interestingly, polymerization of budding yeast actin is faster than that of muscle actin (Buzan and Frieden, 1996; Kim et al., 1996). Moreover, the turnover cycle of an actin filament slightly differs in *S. cerevisiae*. Addition of new ATP-bound subunits to the barbed end of the filament is followed by ATP hydrolysis, but instead of retaining the P_i, yeast actin releases it concomitantly with hydrolysis of the bound ATP (Melki et al., 1996; Yao and Rubenstein, 2001). This difference is significant since ADP-actin is less stable than ADP-P_i-bound actin (Orlova and Egelman, 1992).

1.1.2. Actin-binding proteins that regulate actin polymerization/depolymerization

The mechanism of treadmilling predicts a subunit flux from the barbed towards the pointed end at steady state, a flow that was visualized directly at individual actin filaments by fluorescence microscopy (Fujiwara et al., 2002). Remarkably, growth observed in pure actin filaments (of about 1.1 nm/s (Fujiwara et al., 2002)) is two orders of magnitude slower than actin movement observed *in vivo* (Theriot and Mitchison, 1991); thus, regulatory proteins are indispensable to explain the physiological behavior of actin filaments. As seen by the reconstitution of actin-based motility using purified proteins (Loisel et al., 1999), efficient actin-driven, motor-independent motility requires the presence of proteins that accomplish each of the following molecular functions: 1) stabilization of the actin nucleus to enable explosive actin polymerization, 2) monomer binding to either concentrate G-actin close to the growing filament ends or to prevent its polymerization, 3) capping of the actin filament to prevent growth toward unproductive directions and, 4) actin severing to produce new barbed ends or to recycle actin monomers. A high number of proteins can perform each of these functions, most of them conserved among all eukaryotes (Pollard et al., 2000). In *S. cerevisiae* the number of proteins that regulate actin treadmilling is reduced to only 16 highly conserved actin-associated proteins (Table 1). Some of these proteins are essential for viability whereas others display functional redundancy. In addition to the regulation of actin treadmilling, actin filament stabilization and actin-dependent molecular motors play a fundamental role on actin dynamics (see below). In the following sections, the biochemical activities of these relevant actin regulators are briefly described (see also an illustrated overview in Figure 2).

	Yeast protein	Homologue	Molecular activities	Main mutant phenotypes
Actin treadmilling regulation	Cap1/2	Capping protein	Cap barbed ends Stabilizes actin filaments	Abnormal actin distribution Endocytic defects
	Aip1	Aip1	Caps barbed ends Promotes filament disassembly	Abnormal actin distribution Endocytic defects
	Cof1	Cofilin	Disassembles/Severs actin filaments	Lethality or strong growth defects Abnormal actin distribution Endocytic defects
	Aim7	GMF	Actin debranching	Synthetic sickness in combination with mutant *cof1*
	Pfy1	Profilin	Prevents spontaneous actin nucleation Restrict elongation to the barbed end Might promote nucleotide exchange	Lethality or strong growth defects Abnormal actin distribution
	Srv2	Cyclase-associated protein	Promotes nucleotide exchange from Cof1-bound ADP-actin to Pfy1-bound ATP-actin	Lethality or strong growth defects Abnormal actin distribution
	Twf1	Twinfilin	Might sequester actin monomers Severs actin filaments at low pH	Synthetic lethality in combination with mutant *cof1* Endocytic defects
	Vrp1	WIP	Activates de nucleating promoting activity of Myo5	Abnormal actin distribution Endocytic defects Abnormal vacuolar morphology Delayed cytokinesis
	Bni1	Formin	Nucleates actin	Synthetic lethality in combination with mutant *bnr1* Abnormal actin distribution Abnormal budding
	Bnr1	Formin	Nucleates actin	Synthetic lethality in combination with mutant *bni1* Abnormal actin distribution Abnormal budding
	Arp2/3 complex	Arp2/3 complex	Nucleates actin Promotes filament branching	Lethality
	Las17	WASP	Activates the Arp2/3 complex	Growth defect Abnormal actin distribution Endocytic defects
	Myo3/Myo5	Type I myosin	(see molecular motors)	(see molecular motors)
	Pan1	Eps15	Activates the Arp2/3 complex	Lethality or strong growth defects Abnormal actin distribution Endocytic defects
	Abp1	mAbp1	Activates the Arp2/3 complex	Abnormal actin distribution
	Crn1	Coronin	Restricts actin nucleation sites Bundles actin filaments	Endocytic defects
Actin filament stabilization	Tpm1/2	Tropomyosins	Stabilize filaments	Synthetic lethality
	Sac6	Fimbrin	Bundles actin filaments	Abnormal actin distribution Endocytic defects
	Scp1	Calponin	Bundles actin filaments	-
	Iqg1	IQGAP	Bundles actin filaments	Lethality or strong growth defects Cytokinesis defects
	Abp140	-	Bundles actin filaments	-
	Sla2	Hip1R	Links actin to membranes	Strong growth defects Abnormal actin distribution Endocytic defects
Actin-dependent molecular motors	Myo1	Type II myosins	Moves along actin filaments	Lethality or strong growth defects Cytokinesis defects
	Myo2	Type V myosins	Moves along actin filaments	Lethality Transport defects
	Myo4	Type V myosins	Moves along actin filaments	Transport defects
	Myo3	Type I myosins	Activates the Arp2/3 complex Moves along actin filaments	Synthetic lethality in combination with mutant *myo5*
	Myo5	Type I myosins	Activates the Arp2/3 complex Moves along actin filaments	Synthetic lethality in combination with mutant *myo3* Endocytic defects

Table 1. *S. cerevisiae* actin regulators.
List of the most relevant actin regulators identified in budding yeast, including the name of mammalian homologs and an overview of their biochemical activities and mutant phenotypes. See text for further details.

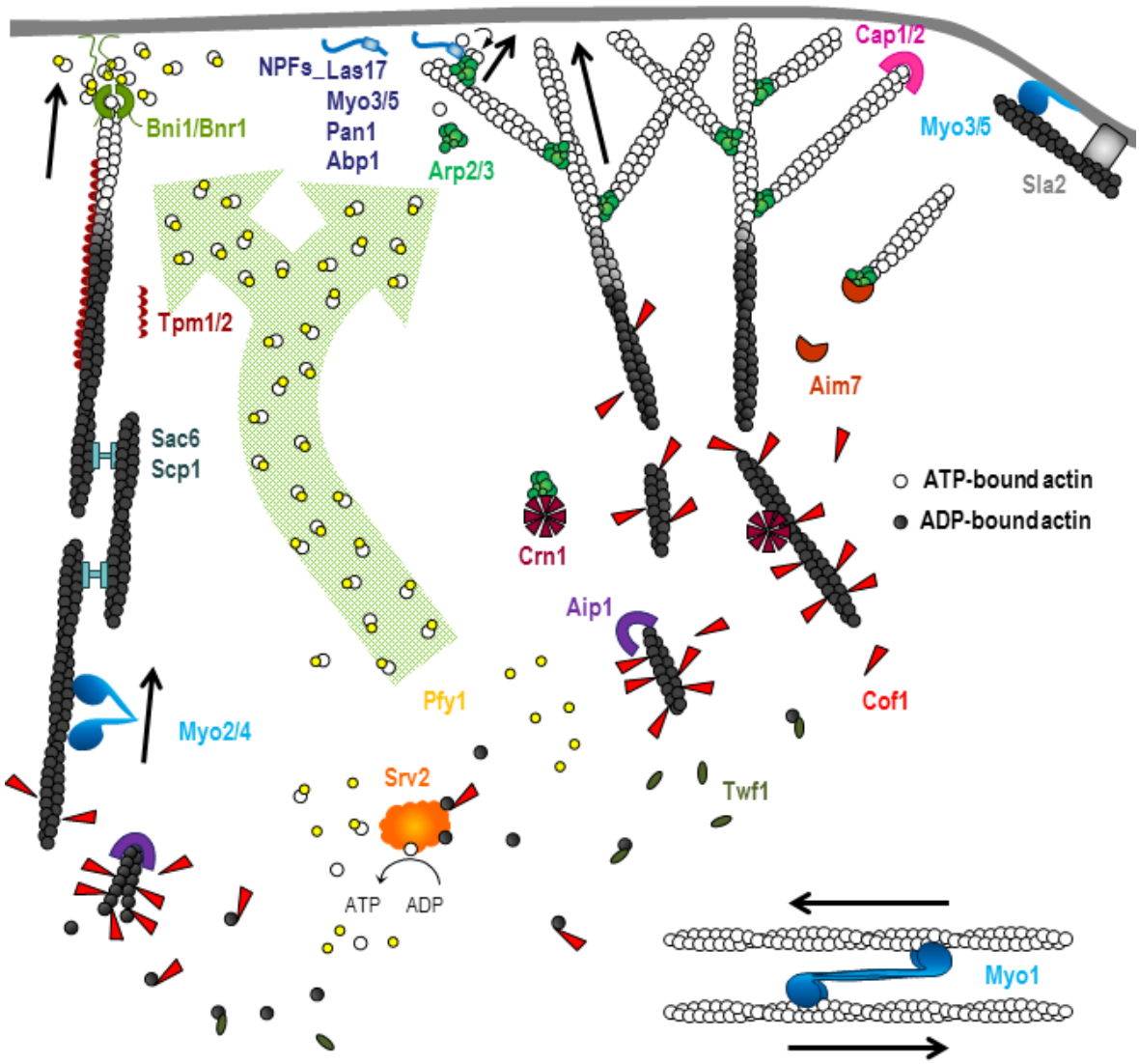

Figure 2. Overview of the molecular activities of *S. cerevisiae* actin regulators.
This figure illustrates the main functions of the most relevant actin regulators in budding yeast. Briefly, the formins Bni1 and Bnr1, and the Arp2/3 complex -with the assistance of nucleation promoting factors- initiate the assembly of ATP-bound actin filaments adjacent to the plasma membrane, with the fast growing barbed end oriented towards the cell surface. Formins assemble unbranched actin filaments while the Arp2/3 complex forms Y-shaped actin branches. Crn1 restricts actin nucleation to sites of dynamic actin assembly. The capping proteins Cap1/2 prevents further polymerization. Aim7 promotes filament debranching. Old actin filaments (formed by ADP-bound actin) are severed and/or dissociated by Cof1, while Aip1 caps the severed oligomer to prevent rapid re-polymerization and stimulate actin disassembly. The ADP-bound actin monomers might be sequestered by Twf1, or be delivered to Srv2 that, together with Pfy1, promotes nucleotide exchange to finally refill the pool of ATP-actin monomers bound to Pfy1. The actin filaments are stabilized by Tpm1/2, and bundled by Sac6, Scp1, or Iqg1 (not depicted). Sla2 and type-I myosins can link the actin polymers to membranes, and myosins move/slide along actin filaments. Arrows represent growth/force directions. See text for details. This illustration has been adapted from (Pollard, 2007) and (Gandhi et al., 2009).

1.1.2.1. Actin nucleators

The spontaneous initiation of a new filament assembly requires the assembly of a trimeric nucleus. Since the actin dimer intermediate is very unstable, proteins that bypass or promote this step are very important for efficient actin dynamics (Pollard and Borisy, 2003). So far, five types of actin nucleators have been identified: proteins of the formin family, Spir proteins, Cordon-bleu, Leiomodin, and the Arp2/3 complex (Ahuja et al., 2007; Chereau et al., 2008; Mullins et al., 1998; Pruyne et al., 2002; Quinlan et al., 2005; Sagot et al., 2002b); of those, only formins and the Arp2/3 complex are conserved in all species. Each type of actin nucleators work by distinct mechanisms and trigger building of specialized actin-based structures (Campellone and Welch, 2010). The molecular mechanisms that control the activity of the conserved actin nucleators, the formins and the Arp2/3 complex, are discussed in the next two sections and depicted in Figure 4.

1.1.2.1.1. The formins: Bni1, Bnr1

Proteins of the formin family are conserved in yeast, plants and animals. Formins assemble structures composed of unbranched actin filaments including stress fibers, filopodia, the cytokinetic contractile ring or polarized actin cables. Yeast cells typically have 2 or 3 genes encoding formin proteins, while mammals have around 15 classified in 7 subfamilies (for a review see (Chesarone et al., 2010)). The conserved active region of formins is located at the C-terminus, and consists of the formin homology domains FH1 and FH2 (Figure 3). The N-terminus confers regulatory roles and varies considerably between different organisms (Chesarone et al., 2010). *S. cerevisiae* contains only 2 genes codifying for formins, *BNI1* and *BNR1*. Deletion of each gene has no effect on viability, but deletion of both genes is lethal, indicating functional redundancy (Imamura et al., 1997). Analysis of mutants point out to an essential role of Bni1 and Bnr1 in cell polarity, cytokinesis and the formation of long filamentous actin cables required for polarized secretion and organelle inheritance, and indicate that both the FH1 and FH2 domains are required for the biological function of formins (Evangelista et al., 1997; Evangelista et al., 2002; Pruyne et al., 2002; Sagot et al., 2002a; Sagot et al., 2002b; Zahner et al., 1996). Formins do not seem to bind actin monomers and how exactly they activate actin nucleation is still unclear. It has been proposed that the FH2 domain, which *in vitro* is sufficient to catalyze nucleation, might bind and stabilize spontaneous formed actin seeds that otherwise would disassembly (Pring et al., 2003; Sagot et al., 2002b). In addition, nucleation-cofactors and monomer-binding sequences outside the FH2 domain might also be required for some formin to efficiently promote actin polymerization. For example, in *S. cerevisiae* the formin-binding protein Bud6 recruits actin monomers to nucleate actin dimers that might be captured by the FH2 domain (Graziano et al., 2011; Moseley et al., 2004). Once an actin seed is formed, the FH2-dimer switches between an open state, which allows addition of new monomers at the filament barbed end (about 100 monomers per second), and a closed state, which prevents elongation of the filaments but also binding of Capping Protein to the fast growing end. The FH1 domain contributes to FH2-dependent elongation by concentrating actin

subunits through its multiple profilin-actin binding domains (Figure 4)(Kovar et al., 2006; Kovar and Pollard, 2004; Pruyne et al., 2002; Sagot et al., 2002b; Vavylonis et al., 2006). Nucleation and processive capping are the two conserved activities found for most formins, but some members of the family have been reported to bundle, severe, and depolymerize actin filaments. Whether these effects on the actin dynamics are functionally relevant is still unknown (Chesarone et al., 2010).

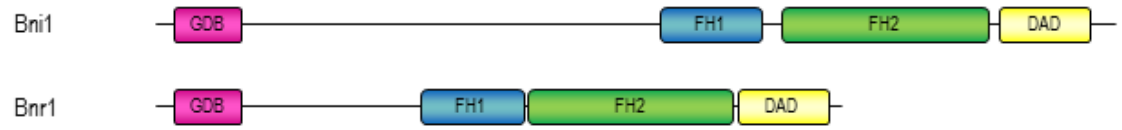

Figure 3. Domain organization of yeast formins.
Domain organization of the yeast formins Bni1 and Bnr1. Both proteins show a similar organization. GDB: GTPase binding domain; FH1: formin homology domain 1; FH2: formin homology domain 2; DAD: diaphanous autoregulatory domain.

Formins are spatially and temporally regulated by different mechanisms. Five of the seven subfamilies of mammalian formins are autoinhibited by interactions between two domains, the diaphanous inhibitory domain DID and the diaphanous autoregulatory domain DAD, located at the N- and C-terminus, respectively. Binding of Rho GTPases and/or other factors and post-translational modifications can disrupt the DID-DAD interaction (Chesarone et al., 2010). In *S. cerevisiae,* the formin Bni1 seems to be autoinhibited by an interaction between the N-terminal region and the DAD domain (Wang et al., 2009). Phosphorylation by the kinases Prk1 and Fus3 release the formin from autoinhibition and regulate its activity and its proper localization (Matheos et al., 2004; Wang et al., 2009). In addition to Fus3, other proteins that regulate the localization of yeast formins are Spa2, Bud6, and distinct members of the Rho family (Dong et al., 2003). Bud14, on the other hand, inhibits the activity of the Bnr1-FH2 domain and displaces the formin from the newly formed actin filament (Chesarone et al., 2009).

1.1.2.1.2. The Arp2/3 complex

The Arp2/3 complex was first isolated from *Acanthamoeba castellanii* (Machesky et al., 1994), and since then it has been purified from several organisms including budding yeast and humans (Welch et al., 1997; Winter et al., 1997). Arp2/3 is a highly conserved complex of seven subunits: Arp2, Arp3, Arpc1 (Arc40 in budding yeast), Arpc2 (Arc35), Arpc3 (Arc18), Arpc4 (Arc19), and Arpc5 (Arc15). Two of the subunits, Arp2 and Arp3, are actin-related proteins - actually Arp2 was first identified based of its sequence similarity to actin (Lees-Miller et al., 1992; Schwob and Martin, 1992)- and it has been recently demonstrated that because of their similarity to actin, they provide the two first 'actin' subunits of the new filament (Egile et al.,

2005; Rouiller et al., 2008). The Arp2/3 complex not only nucleates new actin filaments by mimicking an actin dimer, but it also anchors them to preexisting filaments with an angle of approximately 70º. As a result, the pointed end is capped with the old filament and the new filament grows towards the barbed end direction, forming a characteristic Y-shaped branch with the Arp2/3 complex at the junction (Figure 4) (Mullins et al., 1998)(Svitkina and Borisy, 1999). This tight coupling of nucleation and cross-linking of actin filaments is biased towards the barbed end due to the affinity of Arp2/3 for ATP-actin or ADP-P_i-actin (Amann and Pollard, 2001; Ichetovkin et al., 2002).

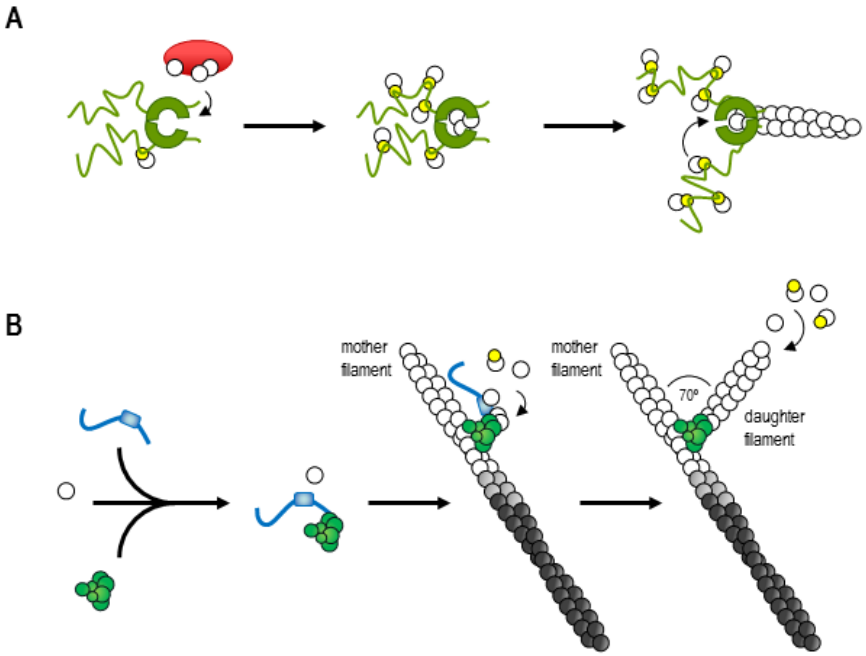

Figure 4. Actin nucleation and elongation by formins and the Arp2/3 complex.
(A) Formins (green) might initiate or stabilize actin nucleation from free actin monomers (white) provided by Bud6 (red), and remain associated with the growing barbed end while allowing the addition of new actin subunits. Profilin-bound actin monomers (yellow and white, respectively) associate with the formins to facilitate the delivery of actin to the barbed end of the filament (arrow). (B) Nucleating promoting factors (blue) bind actin monomers (white) and the Arp2/3 complex (green) through its WH2 and acidic domains. Binding to the side of a preformed filament (mother filament) completes activation and allows growth of the daughter filament with an angle of 70 º with respect to the mother filament. See text for further details.

Purified Arp2/3 is able to nucleate actin *in vitro*, although highly inefficiently (Mullins et al., 1998; Welch et al., 1998); however, the addition of regulatory factors (see next section) enhance Arp2/3 mediated actin polymerization several orders of magnitude (Machesky et al., 1999; Rohatgi et al., 1999; Welch et al., 1998). The crystal structure of the bovine purified complex shows that Arp2 and Arp3 are too far apart to form an actin dimer, suggesting that they are in an inactive state and that regulatory proteins might promote a conformational change to close up the complex in order to trigger nucleation (Robinson et al., 2001). Recent studies have shown that the binding of regulatory proteins collectively known as nucleating

promoting factors (NPFs) induce such a large conformational change (Goley et al., 2004; Rodal et al., 2005). Actin filaments also stimulate actin nucleation by increasing the affinity of regulatory proteins to the Arp2/3 complex (Marchand et al., 2001). In addition, the Arp2/3 complex must also be activated by ATP binding to the actin homologous proteins Arp2 and Arp3 (Dayel et al., 2001; Goley et al., 2004; Le Clainche et al., 2001; Martin et al., 2005). However, the role of ATP hydrolysis in the Arp2/3 complex is far from being understood. It has been proposed that ATP hydrolysis either occurs rapidly and is required for nucleation or that it occurs after nucleation and is necessary for debranching the dendritic network (Dayel and Mullins, 2004) (Le Clainche et al., 2003). Recent work performed in *S. cerevisiae* with an *arp2* mutant that cannot hydrolyze ATP revealed that ATP hydrolysis occurs simultaneously with actin nucleation but is actually required for filament debranching (Martin et al., 2006). Another level of regulation has been reported recently. LeClaire et al. observed that phosphorylation on either threonine or tyrosine conserved residues in the Arp2 subunit is necessary for the nucleating activity of the complex (LeClaire et al., 2008).

Genetic analysis of the Arp2/3 complex in *S. cerevisiae* indicates that depletion of any subunit except Arc18 causes severe growth defects or lethality, depending on the yeast background (Huang et al., 1996; Schwob and Martin, 1992; Winter et al., 1997; Winter et al., 1999b). Generation of mutants early pointed out a role for the Arp2/3 complex in the organization of the actin cytoskeleton and in the uptake step of endocytosis (Moreau et al., 1997; Moreau et al., 1996; Munn and Riezman, 1994; Pan et al., 2004; Winter et al., 1997; Winter et al., 1999b). The mutational analysis of the yeast Arp2/3 complex has provided some important insights into the Arp2/3 nucleation mechanism (Balcer et al., 2010; D'Agostino and Goode, 2005; Daugherty and Goode, 2008). *In vitro*, yeast Arp2/3 complex has more basal nucleation activity than the mammalian Arp2/3 in the absence of NPFs, but addition of NPFs further enhances actin polymerization (Rodal et al., 2005; Wen and Rubenstein, 2005).

Besides the classical NPFs, coronin (Crn1) also regulates the Arp2/3 complex by a completely different mechanism. Crn1 is a multifunctional protein (Figure 5) that interacts with the Arc35 subunit of the complex and inhibits spontaneous nucleation *in vitro* (Humphries et al., 2002). However, Crn1 exhibits high affinity for the newly assembled actin filaments, loaded with ATP-actin, and in contact with those, the inhibition of the Arp2/3 complex by Crn1 is released. Thereby, coronin restricts the Arp2/3 activity to sites where new forming filaments are abundant (Gandhi et al., 2009; Humphries et al., 2002). In addition to this role, Crn1 bundles actin filaments, and synergizes with cofilin and Aip1 to sever ADP-bound actin filaments (Brieher et al., 2006; Gandhi et al., 2009; Goode et al., 1999). Deletion of the single gene encoding coronin in budding yeast, *CRN1*, causes a defect in endocytosis (Burston et al., 2009). Phosphorylation of a serine located in the N-terminus of human coronin 1B by PKC weakens coronin-Arp2/3 interaction (Cai et al., 2005). Yeast Crn1 is phosphorylated at multiple sites *in vivo* but no biological function has been assigned to any of these post-translational modifications (Albuquerque et al., 2008; Chi et al., 2007; Ficarro et al., 2002; Li et al., 2007; Smolka et al., 2007).

Figure 5. Domain organization of yeast coronin.
WD: WD40 repeats –a region rich in tryptophan and aspartic acid; CC: potential coiled-coil domain.

1.1.2.1.2.1. Nucleation promoting factors: Las17, Myo3 and Myo5, Pan1, Abp1

Arp2/3 is activated by a collection of regulatory proteins that are known as nucleation promoting factors (NPFs). The first NPF to be identified was ActA, a protein found in the surface of the intracellular pathogenic bacteria *Listeria monocytogenes* that activates the Arp2/3 complex to produce actin comet tails required for bacterial motility in the host cytoplasm (Welch et al., 1998). Since then, several proteins that activate the Arp2/3 complex have been identified including the well-studied NPF WASP (from Wiskott-Aldrich syndrome protein), whose mutation produces a human immunodeficiency and bleeding disorder (for further information see (Lappalainen, 2007)).

Although the domain organization of different NPFs is remarkably diverse, they all share some common characteristics. The organization of representative NPFs is shown in Figure 6. The main feature for all type of nucleator promoting factors is the presence of an Arp2/3-binding sequence called the CA domain, which consists in a central o connecting region (C) plus an acidic sequence that includes a conserved tryptophan (A). The CA region is necessary and sufficient to bind the Arp2/3 complex but is not sufficient to activate it (Rohatgi et al., 1999). In order to activate the Arp2/3 complex, an NPF must bind either monomeric or filamentous actin (classifying the NPFs in group I or group II, respectively). Class I and II NPFs activate the Arp2/3 complex by slightly different mechanisms:

Class I NPFs contains one or two monomer-binding WH2 domains, also called W or V domains -from WASP homology 2, or Verprolin homology- that is found usually just before the CA domain. Although most class I NPFs contains the triple domain WCA, some members might lack one of the typical sequences or they can even be located in a separate molecule (Lechler et al., 2001). Typical members of this type of NPFs are the Wiskott-Aldrich syndrome protein (WASP) family, including budding yeast WASP homolog Las17 or Scar/WAVE proteins (Machesky et al., 1999; Rohatgi et al., 1999; Winter et al., 1999a; Yarar et al., 1999); proteins from intracellular pathogens such as ActA from *Listeria*, RickA from *Rickettsia*, or p78/83 from a baculovirus (Goley et al., 2006; Gouin et al., 2004; Jeng et al., 2004; Welch et al., 1998); the capping protein Arp2/3 complex and myosin-I linker CARMIL (Jung et al., 2001); WHAMM -from WASP Homolog associated with actin, membranes, and microtubules- (Campellone et al., 2008); the WASP and Scar homologue (WASH) (Derivery et al., 2009; Gomez and Billadeau, 2009); the p53 cofactor JMY (Zuchero et al., 2009); and yeast type I myosins (Geli et al., 2000; Lechler et al., 2001; Lee et al., 2000; Sun et al., 2006).

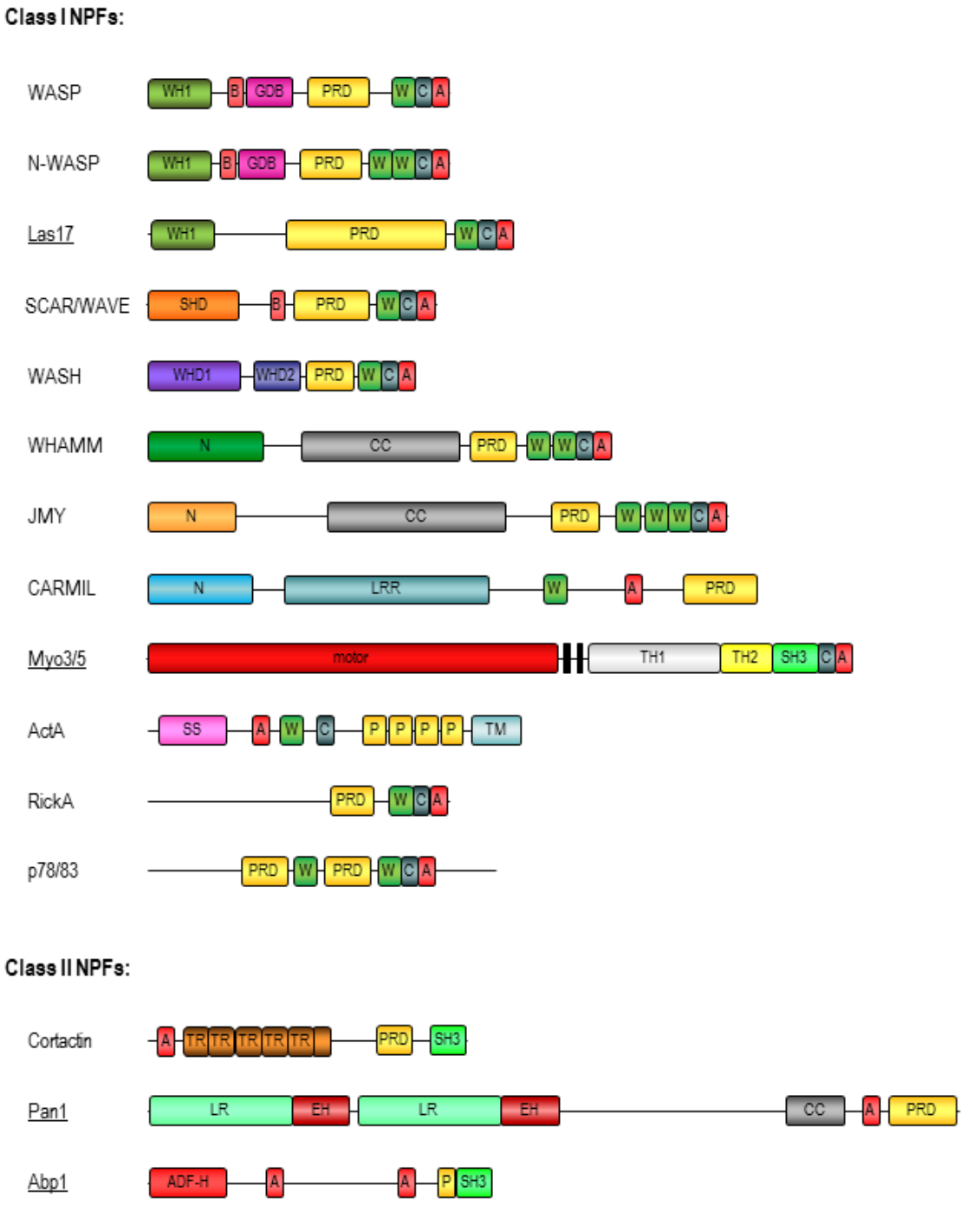

Figure 6. Domain organization of nucleation promoting factors.
S. cerevisiae NPFs are underlined. Class I NPFs contain the monomer-binding WH2 domain (W) and the Arp2/3 binding regions Connecting (C) and Acidic (A). Note that CARMIL does not contain the C region and Myo3/Myo5 does not include the W domain, which are provided by co-activators. Class II NPFs interact with the Arp2/3 complex via the acidic domain and to F-actin through the tandem repeat (TR) of cortactin, the coiled-coil (CC) of Pan1, and the actin-depolymerizing factor homology (ADFH) of Abp1. Other domains are required to bind signaling molecules and/or actin regulators. WH1: WASP-homology 1, verprolin-binding domain; B: basic region, PIP2-binding region; GDB: GTPase binding domain; PRD: proline-rich domain, SH3-binding region; SHD: Scar homology domain; WHD1: WASH homology domain 1; WHD2: WASH homology domain 2; N: N-terminal region; LRR: Leucine-rich repeat; TH1: Tail homology 1, lipid-binding region; TH2: Tail homology 2; SH3: Src homology 3, PRD-binding domain; SS: signal sequence; TM: transmembrane; LR: long repeat; EH: Eps15 homology; black bars: IQ motifs, calmodulin-binding regions.

Arp2/3 activation by class I NPFs requires both the CA and the WH2 domain. Constructs consisting on the WCA domain from WASP-related proteins can activate the Arp2/3 complex, independently of other factors (Machesky et al., 1999; Rohatgi et al., 1999; Winter et al., 1999a). The CA region is thought to bind the Arp2/3 complex and tether the WH2 domain so that the first actin subunit can be positioned to start a new filament. Moreover, it promotes an activating conformational change in the Arp2/3 complex that depends on conserved residues in the C region (Goley et al., 2004; Rodal et al., 2005). Class I NPFs have low affinity for the Arp2/3 complex, thus after transiently interact and stimulate the complex they might dissociate to start a new round of activation.

Class II NPFs do not bind G-actin. Instead, they bind filamentous actin through F-actin binding domains. This is an important difference as class II NPFs are far less powerful activators *in vitro* that class I NPFs (Higgs and Pollard, 2001; Sun et al., 2006). Members of this group of NPFs are cortactin (Uruno et al., 2001; Weaver et al., 2001), yeast Abp1 (Goode et al., 2001), and yeast Pan1 (Duncan et al., 2001). It is not clear how class II activate the Arp2/3 complex, but they lack the connecting region and cannot trigger the Arp2/3 activating conformational change (Goley et al., 2004). Their mechanism of activation might involve the enhancement of the Arp2/3 complex association with the mother filament, which is itself an activator of the complex (Higgs et al., 1999; Machesky et al., 1999). Cortactin remains associated at the branch point, apparently to inhibit branch dissociation (Egile et al., 2005).

Five NPFs are present in *S. cerevisiae*: Las17 and the type I myosins Myo3 and Myo5 (see also section 1.1.4.3), which are class I NPFs, and Abp1 and Pan1, which are class II NPFs and therefore have a lower nucleation promoting activity (NPA).

The *S.cerevisiae* protein Las17 was first found based on its high sequence homology with the Wiskott-Aldrich syndrome protein WASP (Symons et al., 1996). It has a similar organization to WASP (Figure 6), except that Las17 does not contain the GTPase binding domain (GBD), a domain that has been shown to promote WASP auto-inhibition (see below) (Miki et al., 1998; Rohatgi et al., 1999). The WH1 domain of Las17 interacts with Vrp1 while the proline-rich regions of Las17 interact with SH3-domain containing proteins that regulate its activity (see below). Downstream from the poly-proline region, the WH2 domain binds to monomeric actin. At the C-terminus is located the central and the acidic domains (CA), which interact with the Arp2/3 complex (Winter et al., 1999). Purified WCA is able to activate the Arp2/3 complex *in vitro* (Winter et al., 1999) albeit with less efficiency than the full length protein, suggesting that other regions in Las17 might contribute to efficient Arp2/3 activation (Rodal et al., 2003). Deletion of *LAS17* causes severe actin cytoskeleton defects (Li, 1997) and prevents endocytic internalization (Madania et al., 1999; Naqvi et al., 1998). Interestingly, deletion of Las17-WCA domain alone does not cause any detectable phenotype (Winter et al., 1999), indicating that different domains are important for Las17 function in actin organization and that other factors can fulfill its function in actin assembly. Indeed, mutation of the acidic domains of the Arp2/3 activators Pan1 and the myosins-I Myo3 and Myo5 show synthetic defects with deletion of the

acidic domain of Las17, suggesting functional redundancy (Duncan et al., 2001; Evangelista et al., 2000; Lechler et al., 2000; Sun et al., 2006).

Mammalian WASP and N-WASP proteins are autoinhibited by an intramolecular interaction between the GBD and WCA domain, which prevents binding to the Arp2/3 complex. Some WASP ligands, including the Rho-family GTPases Cdc42 and Rac cooperate with PIP2 to release this auto-inhibition by binding to the GBD and displacing the WCA domain, which can then bind and activate the Arp2/3 complex (Takenawa and Suetsugu, 2007). The activity of WASP, N-WASP, and WAVE proteins are also modulated by intermolecular interactions. The N-terminal region of WASP/N-WASP contains a WH1 domain that mediates their interactions with verprolins (WIP, WICH/WIRE, or CR16, see section 1.1.2.2). The binding of verprolins to the NPF seems to have different functions, from maintaining it in the inactive conformation to recruiting the NPF to localized regions where massive actin polymerization is needed; there, a myriad of regulatory mechanisms that are still being characterized release the WIP-WASP inhibitory complex (Takenawa and Suetsugu, 2007). Although Las17 shares high sequence homology with WASP, it does not contain an obvious GBD domain and does not seem to interact with Cdc42 directly (Lechler et al., 2001). This is an important functional difference, because full length Las17 is extremely active *in vitro* while purified WASP is inactive in the absence of Cdc42 or PIP_2 (Rodal et al., 2003)(Higgs and Pollard, 2000). Both, inhibition of actin assembly mediated by Las17 and the release of such inhibition is achieved by interactions with SH3-domain containing proteins (Figure 7). Four proteins have been shown to date to inhibit Las17-induced actin assembly: Sla1, Bbc1, Syp1, and Abp1 (D'Agostino and Goode, 2005; Rodal et al., 2003)(Boettner et al., 2009). Sla1 and Bbc1 both bind Las17 *in vivo*, and they inhibit Las17 *in vitro* by binding to different regions of Las17 (Li, 1997; Rodal et al., 2003; Tong et al., 2002). In contrast, Abp1 attenuates Las17 actin assembly by competing for the Arp2/3 complex (D'Agostino and Goode, 2005). Bzz1 also binds Las17 (Soulard et al., 2002; Tong et al., 2002), but this interaction serves to relieve Las17 inhibition mediated by Sla1 (Sun et al., 2006).

Myosins are a family of actin-activated molecular motors that have a crucial role in actin-dependent processes in eukaryotic cells (see also section 1.1.4). In *S. cerevisiae*, type-I myosins are recruited to the plasma membrane where both motor and nucleating promoting activities plays an important function in endocytic internalization (see section 1.2.3.1.1, and references therein). The domain organization of budding yeast myosins-I is shown in Figure 6. Briefly, Myo3 and Myo5 contain an N-terminal motor domain that carries an actin-based ATPase (Sun et al., 2006), a neck that contains 2 IQ motifs that bind calmodulin (Geli et al., 1998), a basic tail homology 1 (TH1) domain that probably interacts to acidic phospholipids (Pollard et al., 1991), and a C-terminal extension (C_{ext}) that includes the domains required for their nucleation promoting activity: a TH2 domain that contains poly-proline motifs, an SH3 domain, and a central and acidic domains (CA) at the very C-terminus that directly binds to the Arp2/3 complex (Evangelista et al., 2000; Lechler et al., 2000)(Geli et al., 2000). Whether budding yeast were directly capable of activating actin polymerization was initially a matter of debate since Myo3 and Myo5 do not contain the WH2 domain required for G-actin binding. Yet, it was

subsequently demonstrated that the yeast myosins-I interact with the WIP homologue Vrp1 -which contain two WH2 domains- through the SH3 domain located at the myosin C-terminal extension (Evangelista et al., 2000; Geli et al., 2000; Vaduva et al., 1997). Robust evidence now accumulates demonstrating that binding of Vrp1 to the myosins is necessary and sufficient to the develop their potent NPA: 1) our lab has demonstrated that a Myo5 construct consisting on the TH2, SH3 and acidic domains immobilized in Glutathione-Sepharose beads is able to induce the formation of actin patch-like structures in the presence of the Arp2/3 complex and Vrp1 (Geli et al., 2000; Idrissi et al., 2002)(see also section 5.1); 2) a chimeric protein containing the WH2 domain of Vrp1 and the A domain of Myo3 was able to directly promote actin polymerization *in vitro* (Lechler et al., 2001); and 3) more recently, Myo5/Vrp1-induced actin polymerization was observed using purified components (Sun et al., 2006). In fission yeast, although type I myosin alone is able to weakly induce actin polymerization (Lee et al., 2000), this activity is also enhanced by Vrp1 (Sirotkin et al., 2005). Importantly, the NPF activity of the Myo5/Vrp1 complex is very powerful, being comparable to Las17 activity (Sun et al., 2006). As mentioned above, deletion of the acidic domains of Myo3 and Myo5 is synthetically defective with deletions of the acidic domain of Las17 (Evangelista et al., 2000; Lechler et al., 2000; Sun et al., 2006). Thus, although the NPA of Myo5 and Las17 have different functions (see section 1.2.3.1.1.2, and references therein), in the absence of the myosin-I NPA, Las17 can take over and viceversa (Evangelista et al., 2000; Lechler et al., 2000). In addition to its activity as NPFs, type-I myosins have other essential functions that cannot be fulfilled by any other proteins since deletion of both Myo3 and Myo5 results in lethality or strong defects in growth, depending on the yeast strain used (Geli and Riezman, 1996; Goodson et al., 1996).

The nucleating promoting activity of the yeast myosins-I is regulated by intra- and intermolecular interactions (Figure 7). An autoinhibitory interaction between the TH1 domain and the C-terminal extension of the protein, containing the SH3 and CA domains, prevents binding of the co-activator Vrp1 to the myosin SH3 domain. This inhibitory interaction is stabilized by binding of calmodulin to Myo5. Calmodulin is thought to work as a clamp linking the myosin neck adjacent to the TH1 domain and the C-terminal extension. Calmodulin dissociation from the myosin neck at the plasma membrane induced by a still unknown factor, releases the autoinhibitory interaction (Grotsch et al., 2010). In addition, the Myo5 NPA can be regulated by other interacting proteins. Both Vrp1 and Bbc1 interact with the SH3 domain of Myo5, but while Vrp1 is required to activate the NPF activity of Myo5, Bbc1 negatively regulates this function (Anderson et al., 1998; Mochida et al., 2002; Sun et al., 2006). Another SH3-binding protein, Pan1 (see below) has been recently proposed to enhance Myo5-mediated actin polymerization (Barker et al., 2007). Bzz1 also interacts with Myo5 but the functional significance of this interaction is not clear (Soulard et al., 2005; Soulard et al., 2002) (see discussion). Abp1 inhibits Arp2/3 complex activation by Myo5/Vrp1, and although the molecular mechanism that triggers this inhibition has not been demonstrated, it might involve the competition for the Arp2/3 complex (D'Agostino and Goode, 2005)(Sun et al., 2006). The

regulation of Myo5 NPA by phosphorylation (see below) was the subject of this study and is discussed along the dissertation.

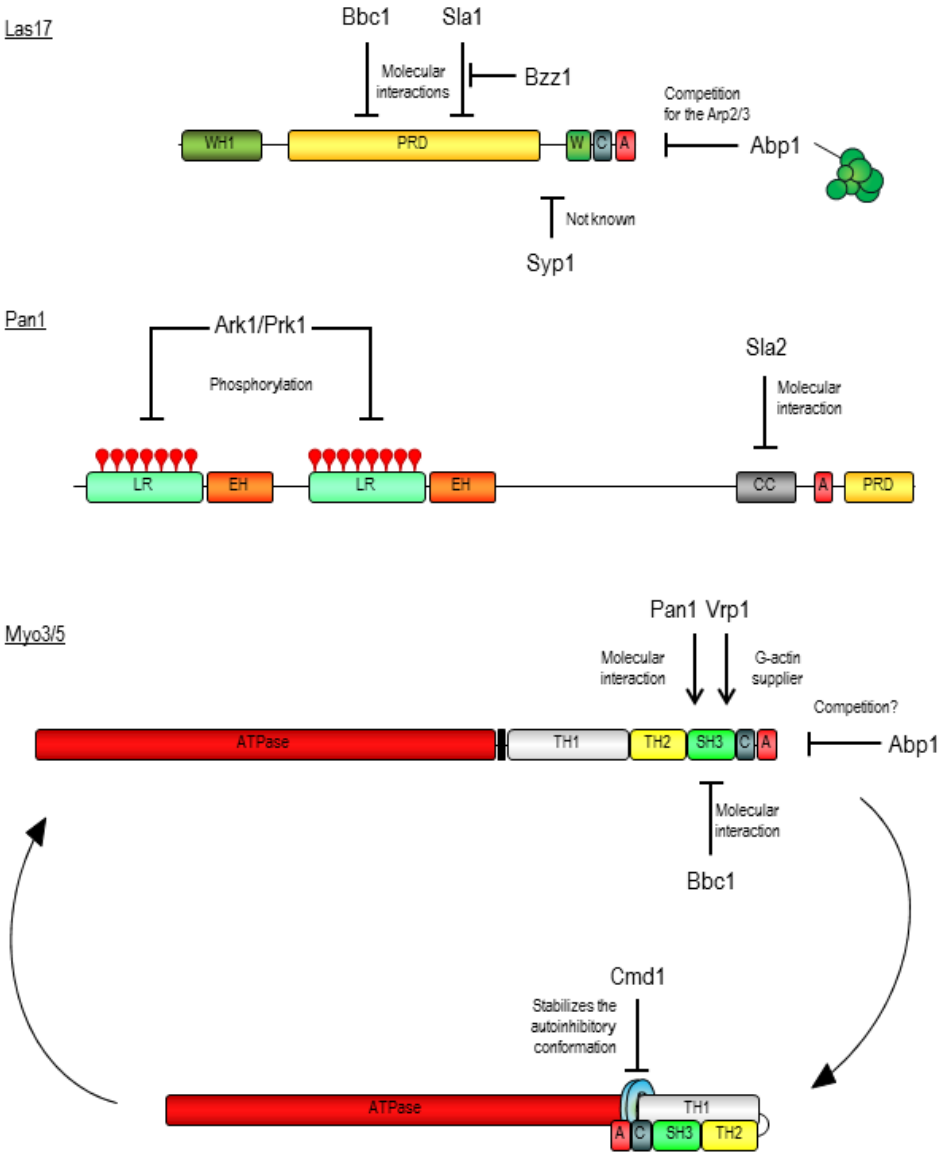

Figure 7. Mechanisms of regulation of *S. cerevisiae* NPFs.
The molecular mechanisms that regulate the nucleating promoting activities of Las17, Pan1, and the myosins Myo3 and Myo5 are depicted. See text for further details.

Pan1 was found in various screens to be required for endocytosis and for normal actin cytoskeleton organization (Tang and Cai, 1996; Wendland et al., 1996). Pan1 contains two long repeat domains at the N-terminus, each embodying an Eps15-Homology domain (EH) (see the domain organization of Pan1 in Figure 6). Through these domains, Pan1 interacts with cargo adaptors and other endocytic proteins (Tang et al., 1997; Tang et al., 2000; Wendland and

Emr, 1998; Wendland et al., 1999). At the central region a coiled-coil domain contains a WH2-like region, which differs from others WH2 domains since it is unable to interact with G-actin. Nevertheless, the coiled-coil domain binds F-actin with high affinity (Toshima et al., 2005). At the C-terminus of the protein an acidic domain interacts with the Arp2/3 complex (Duncan et al., 2001) and a poly-proline region binds to type-I myosins (Barker et al., 2007). Purified Pan1 activates the Arp2/3 complex (Duncan et al., 2001), although much less efficiently than Myo5/Vrp1 or Las17 (Sun et al., 2006). Deletion of Pan1-WA domain does not cause any detectable phenotype, but it shows synthetic defects with deletions of the acidic domains or Las17 and the type-I myosins (Sun et al., 2006; Toshima et al., 2005).

The NPA of Pan1 is regulated by two mechanisms: phosphorylation by the Ark1/Prk1 kinases and inter-molecular interactions (Figure 7). Pan1 contains 15 consensus sites for the kinase Prk1, a kinase required for endocytosis (Sekiya-Kawasaki et al., 2003; Zeng and Cai, 1999). Mutation of all 15 potential phosphorylation residues into non-phosphorylatable amino acids increases the nucleation promoting activity of Pan1, while addition of the kinase inhibits Pan1-mediated actin polymerization (Toshima et al., 2005). In addition, the actin-binding protein Sla2 (see section 1.1.3.3) binds to the WH2-like (CC) domain of Pan1 and also inhibits its NPA *in vitro* (Toshima et al., 2007).

Abp1 was the first actin-associated protein described in yeast (Drubin et al., 1988). Its domain organization is shown in Figure 6. Abp1 contains an ADF-H domain required for F-actin binding (Goode et al., 2001), a proline-rich region of unknown interaction partners, and a SH3 domain that interacts with the kinase Prk1 (Fazi et al., 2002). Moreover, it contains two acidic domains, both required for the activation of the Arp2/3 complex (Goode et al., 2001). Abp1 has been shown to co-fractionate with the Arp2/3 complex and to activate the complex *in vitro* (Goode et al., 2001). However, increasing evidence indicate that Abp1 might negatively regulate actin polymerization *in vivo*, as it inhibits the NPF activity of Las17 and Myo5/Vrp1, which are much powerful Arp2/3 activators than Abp1 (D'Agostino and Goode, 2005; Sun et al., 2006).

1.1.2.2. G-actin binding proteins: Pfy1, Srv2, Twf1, Vrp1

A high number of actin-monomer-binding proteins (>25 in mammals) control actin polymerization and depolymerization, but only six classes are conserved from yeast to mammals: ADF/cofilin (Cof1 in budding yeast), profilin (Pfy1), Srv2/CAP, twinfilin (Twf1), verprolins (Vrp1), and WASP/WAVE (Las17). Paradoxically β–thymosins, which are the major actin-sequestering proteins in vertebrate cells, have not been found in invertebrates or yeast (Safer et al., 1991; Safer et al., 1990). The biochemical functions of Pfy1, Srv2, Twf1, and Vrp1 are explained in this section and their domain organization shown in Figure 8; the general features of Las17 were described above and that of Cof1 are explained in section 1.1.2.4.

Profilin is an evolutionarily conserved small protein that binds G-actin, forming a 1:1 complex with the monomer. It is essential to maintain the normal actin distribution in yeast cells, when not critical for viability (depending on the yeast background), and it seems to function in a post-

internalization step of endocytosis (Haarer et al., 1990; Idrissi et al., 2002; Magdolen et al., 1988; Wolven et al., 2000). *In vitro*, Pfy1 promotes rapid actin turnover in the presence of cofilin (Wolven et al., 2000). Actin monomers bound to profilin are considered the main source of actin for rapid assembly at the barbed ends because it has higher affinity for ATP- than for ADP-bound G-actin; in addition, profilin can bind to actin and to actin nucleators (or NPFs) simultaneously, and with higher affinity than to each one separately (Moseley and Goode, 2006). Moreover, because the profilin-binding site is located in the actin-barbed end (Schutt et al., 1993), profilin inhibits both spontaneous actin nucleation and elongation at the pointed end (Pantaloni and Carlier, 1993; Pollard and Cooper, 1984; Pring et al., 1992). Pfy1 binds to short series of proline residues located in the FH1 domain of yeast Bni1 and Bnr1 formins (Evangelista et al., 1997; Imamura et al., 1997), and while profilin is not required for the processivity of formins, it increases formin-dependent actin filament assembly and elongation *in vitro* (Kovar et al., 2006; Sagot et al., 2002b). Another assigned role of profilin was to promote nucleotide exchange of monomeric actin. However, yeast profilin is almost 2 orders of magnitude less efficient than human profilin in promoting this exchange (Eads et al., 1998); moreover, it requires Srv2 to catalyze this exchange in the physiological substrate cofilin-bound ADP-actin, and indeed Srv2 alone can promote this turnover (Balcer et al., 2003; Quintero-Monzon et al., 2009). Profilin, like other actin-binding proteins, interacts with PIP_2 (Lassing and Lindberg, 1985). The physiological significance of this interaction is not well understood, but PIP_2 can partially dissociate profilin-actin and profilin can inhibit PIP_2 hydrolysis (see (Lappalainen, 2007), chapter 3, and references therein). ROCK-mediated phosphorylation of profilin might also modulate its interaction with actin, at least *in vitro* (Shao et al., 2008). It is not known whether yeast profilin is regulated by the same mechanisms.

Another evolutionary conserved G-actin binding protein is a multifunctional molecule called CAP (Cyclase-associated protein), also named Srv2 in budding yeast. The essential protein Srv2 was first identified in budding yeast for its role in the stimulation of adenylate cyclase, a function independent of its role in actin filament organization and only observed for the budding and fission yeast CAP proteins (Fedor-Chaiken et al., 1990; Field et al., 1990; Hubberstey and Mottillo, 2002). Shortly after, a role for Srv2 in actin regulation was demonstrated (Gerst et al., 1991; Hubberstey and Mottillo, 2002; Vojtek et al., 1991). Profilin only weakly catalyzes nucleotide exchange of cofilin-bound ADP-actin. This activity has recently been attributed to Srv2 based on several observations: 1) it binds to ADF/cofilin-ADP-actin complexes; 2) it promotes ADF/cofilin dissociation; 3) it strongly catalyzes nucleotide exchange on cofilin-bound ADP-G-actin; and 4) it has low affinity for the ATP-actin, and therefore, it might release the monomer to profilin for a new round of polymerization (Balcer et al., 2003; Bertling et al., 2007; Gandhi et al., 2010; Mattila et al., 2004; Moriyama and Yahara, 2002; Quintero-Monzon et al., 2009). Srv2 is linked to actin filaments through the actin-binding protein Abp1 (Balcer et al., 2003; Lila and Drubin, 1997). The association of actin and Srv2/CAP might also be regulated by PIP_2, since PIP_2 partially dissociate actin from CAP, at least in some organisms (Gottwald et al., 1996). Srv2 is phosphorylated *in vivo* but whether this phosphorylation regulates the activity of the protein is unknown (Albuquerque et al., 2008).

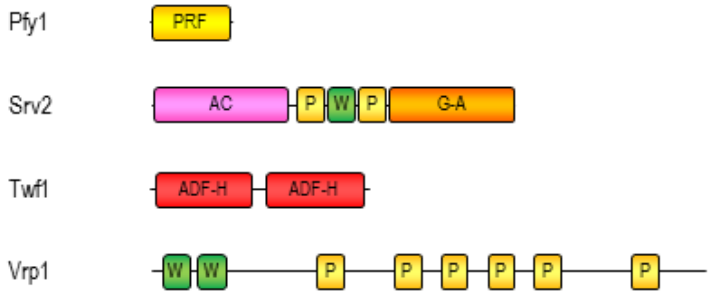

Figure 8. Domain organization of yeast actin-monomer binding proteins.
Domain organization of yeast profilin (Pfy1), the yeast adenylyl cyclase-associated protein (Srv2), twinfilin (Twf1) and verprolin (Vrp1). Different G-actin binding domains are depicted. PRF: profilin domain; G-A: G-actin binding site; W: WH2 domain; ADF-H: actin-depolymerizing factor homology domain. Other domains are required to bind signaling molecules and/or regulators. P: proline-rich domain, SH3-binding region; AC: adenylyl cyclase binding region.

Twf1 has two ADF-H domains, and like cofilin, it is required for endocytic uptake and rapid actin turnover. However its mechanism of function is still not well understood (Burston et al., 2009; Goode et al., 1998; Moseley et al., 2006). Twinfilin binds ADP-G-actin with higher affinity than to ATP-G-actin and inhibits nucleotide exchange, suggesting an actin-sequestering role (Goode et al., 1998; Palmgren et al., 2001). Still, Twf1 stimulates rapid actin disassembly, possibly due to its role in severing at low pH (Moseley et al., 2006). Twf1 also interacts with capping protein, which might localize twinfilin-bound actin monomers to sites of active actin assembly (Falck et al., 2004). This interaction seems to prevent twinfilin's severing activity (Moseley et al., 2006). A capping activity found for mammalian twinfilin is not conserved for yeast Twf1 (Helfer et al., 2006). Twinfilin, like other actin-interacting proteins, binds directly PIP_2 and this binding prevents its interaction with actin (Palmgren et al., 2001). Phosphorylation of Twf1 *in vivo* has also been reported, but still no regulatory role has been assigned to this post-translational modification (Albuquerque et al., 2008).

Verprolins are proline-rich proteins that have been identified in most eukaryotic organisms. The members of this family include WIP, WIRE/WICH, and CR16 in vertebrate cells (Lappalainen, 2007). Besides its high content in prolines, verprolins contain two WH2 domains, one of the most abundant and functional diverse actin binding fold (Vaduva et al., 1997). Yeast Vrp1 shares some homology with the WASP-interacting protein WIP. Deletion of the *VRP1* causes cytoskeletal disorganization, a delayed cytokinesis, and endocytic defects (Donnelly et al., 1993; Munn et al., 1995; Naqvi et al., 2001). Human WIP is able to rescue these phenotypes, indicating functional similarities (Vaduva et al., 1999). Verprolins are important effectors of the regulation of actin dynamics, although its precise role is still not well understood. In mammals, verprolins maintain the nucleating promoting factor N-WASP in an inactive conformation, but

also recruit N-WASP and Arp2/3 to activate localized bursts of actin polymerization and regulate actin dynamics in a N-WASP independent manner (Kato and Takenawa, 2005; Kinley et al., 2003; Martinez-Quiles et al., 2001; Moreau et al., 2000). In *S. cerevisiae*, Las17 binding serves to recruit Vrp1 to sites with active actin dynamics, but the effect of this interaction in the Las17 actin nucleating activity is not well understood (Naqvi et al., 1998; Sun et al., 2006). Vrp1 also associates with another Arp2/3 activator, Myo5 (and probably also Myo3), and activates its nucleating activity, probably by providing the actin monomers binding activity (see above, section 1.1.2.1.2.1) (Evangelista et al., 2000; Geli et al., 2000; Sun et al., 2006). Vrp1 is phosphorylated *in vivo*, but the biological role of this post-translational modifications are still not known (Albuquerque et al., 2008; Smolka et al., 2007)

1.1.2.3. Capping proteins: Cap1/Cap2 and Aip1

Since actin polymerization and depolymerization occur at the end of the filament, regulation of the dynamics and organization of filaments can be achieved by blocking the availability of filament ends and therefore, by preventing further assembly of actin monomers. Paradoxically, although capping proteins prevents both the addition and removal of subunits and therefore, they limit the length of F-actin, they enhance actin-based motility *in vivo* and *in vitro* (Hug et al., 1995; Loisel et al., 1999). The widely accepted actin funneling hypothesis postulate that the number of free actin monomers increases when most actin filaments are capped, resulting in the fast elongation of the few uncapped barbed ends (Carlier and Pantaloni, 1997). However, a recent study indicates that the capping protein CP (also known as β–actinin or capZ in higher eukaryotes) does not influence the kinetics of filament elongation but the rate of Arp2/3-dependent actin polymerization (Akin and Mullins, 2008). The authors propose an alternative hypothesis that postulates that capping protein modifies the architecture of the actin network rather than its kinetics. Two barbed end capping proteins are conserved from yeast to humans, indicating a general mechanism for actin regulation: capping protein (CP) and AIP1. The domain organization of the yeast CP subunits and Aip1 are shown in Figure 9. In addition to CP and Aip1, Eps8 and tropomodulins are capping-proteins only present in metazoan (Di Fiore and Scita, 2002; Weber et al., 1994).

Yeast capping protein (CP) is a heterodimer composed of Cap1 and Cap2 subunits, each encoded by one gene. Disruption of CP results in abnormal actin distribution and endocytic defects (Amatruda and Cooper, 1992; Amatruda et al., 1992; Burston et al., 2009; Kaksonen et al., 2005), and analysis of a set of CP mutants indicate that the actin distribution phenotype correlates with the capping activity of the dimer (Kim et al., 2004). Interestingly, nematode CP can substitute the deletion of yeast CP *in vivo*, indicating that CP function is conserved across evolution (Waddle et al., 1993). By binding to the filament barbed end CP regulates the filament length and modifies the architecture of the actin network (Kaksonen et al., 2005; Kim et al., 2006; Moseley and Goode, 2006). Several proteins are able to bind and inhibit CP in metazoan (either by preventing its binding to actin or by a direct uncapping activity) including CARMIL, V-1/myotrophin, CKIP-1, and CD2AP (Cooper and Sept, 2008), but no protein has been found to

inhibit yeast CP to date. Moreover, the activity of CP from several organisms, including yeast, is inhibited by PIP_2 (Amatruda and Cooper, 1992). Since PIP_2 is enriched at the plasma membrane (Di Paolo and De Camilli, 2006), capping of barbed ends might be prevented near the plasma membrane to locally regulate actin turnover. Moreover, *in vivo* phosphorylation of both CP subunits from a number of organisms including *S. cerevisiae* has been reported, but how phosphorylation regulates the activity of capping protein is not yet known (Albuquerque et al., 2008; Li et al., 2007; Malik et al., 2009; Olsen et al., 2010; Raijmakers et al., 2010).

The actin-interacting protein Aip1 was first identified as an actin-interacting protein by yeast two hybrid (Amberg et al., 1995). Shortly later, it was reported to stimulate cofilin-mediated actin disassembly *in vitro*. Deletion of the *AIP1* gene leads to formation of atypical actin filaments and endocytic defects {Rodal, 1999 #485}(Burston et al., 2009; Okada et al., 2006). Aip1 caps the barbed ends of ADF/cofilin-severed filaments *in vitro*, preventing its further elongation and/or filament re-annealing (Okada et al., 2002) (Balcer et al., 2003), and helping to convert the short actin oligomers into monomeric actin (Okreglak and Drubin, 2010). Proteomic analysis indicates that yeast Aip1 is phosphorylated *in vivo*, but whether this phosphorylation regulates its activity is still unknown (Albuquerque et al., 2008).

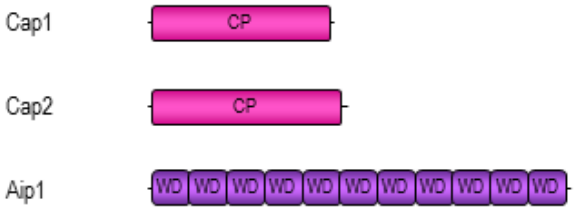

Figure 9. Domain organization of yeast capping proteins.
Domain organization of the yeast subunits of heterodimeric capping protein Cap1 and Cap2, and of yeast Aip1. Aip1 contains eleven WD40 repeats, a region rich in tryptophan and aspartic acid (WD).

Two other conserved proteins, formins and the Arp2/3 complex, also cap actin filaments at their barbed and pointed end, respectively, but their major role is the nucleation of actin filaments and its function was discussed in section 1.1.2.1.

1.1.2.4. Actin depolymerizing/Severing proteins: Cof1, Aim7

Actin depolymerization and severing of filaments are crucial to dynamize filamentous actin, because it increases the availability of actin monomers and provides new barbed ends for the new rounds of actin polymerization. The members of the gelsolin/villin family (gelsolin, villin, adseverin, advillin, supervillin, and flightless I) are actin-severing and barbed-end actin-capping factors widely expressed in metazoan and in plants, but only cofilin (a member of the ADF/cofilin family, see domain organization in Figure 10) is conserved from yeast to mammals.

ADF and cofilin are the best characterized members of a family of essential and conserved proteins collectively known as the ADF/cofilin family. Members of this protein family have in common the presence of a single actin-depolymerizing factor homology domain (ADF-H). The gene *COF1* encodes the only member of the ADF/cofilin family present budding yeast, and its deletion is lethal (Iida et al., 1993; Moon et al., 1993). Analysis of temperature-sensitive cofilin alleles indicate that Cof1 is required for endocytic uptake and stimulates the actin turnover *in vivo* and *in vitro* by the disassembly of actin in a molecular mechanism not yet fully understood (Idrissi et al., 2002; Lappalainen and Drubin, 1997). Growing evidence indicates that Cof1 binding weakens the longitudinal interaction between the actin subunits and shifts the helical twist of the filament (Bobkov et al., 2004; McGough et al., 1997). Cofilin inhibits nucleotide exchange as long as it remains bound to the monomer (Nishida, 1985). Therefore, other interaction partners -Aip1, Srv2, and Pfy1- are required for the recycling of Cof1-bound actin-monomers (Balcer et al., 2003; Quintero-Monzon et al., 2009). Alternative proposed functions for members of the ADF/cofilin are the dissociation of actin branches produced by Arp2/3 (Blanchoin et al., 2000), and actin nucleation when cofilin is present at high concentrations (Andrianantoandro and Pollard, 2006). Due to the essential roles of cofilin, its activity must be tightly regulated. In fact, multiple mechanisms that regulate ADF/cofilins have been described. Phosphorylation of a serine located in the N-terminus prevents its binding to both monomeric and filamentous actin. In mammals, the members of the LIM and TES family of kinases and the members of the SSH family of phosphatases and CIN are responsible for the phosphorylation and dephosphorylation of ADF/cofilin, respectively, via a complex control of several signaling pathways (see (Van Troys et al., 2008). Budding yeast cofilin is also phosphorylated *in vivo* (Albuquerque et al., 2008), but replacement of the corresponding residue does not cause any detectable phenotype, suggesting that phosphorylation of Cof1 does not play a major regulatory role in yeast (Lappalainen et al., 1997). Protonation/deprotonation of the only histidine in human cofilin regulates its binding to actin and to phosphatidylinositol PIP_2, which competes with F-actin to bind cofilin (Bamburg, 1999; Frantz et al., 2008). Yeast cofilin does not seem to be regulated by changes in pH, but it is also regulated by PIP_2 (Ojala et al., 2001). The activity of ADF/cofilin is also modulated by interacting proteins. Aip1 (section 1.1.2.3) and Srv2 (see section 1.1.2.2) cooperate with ADF/cofilin to promote actin disassembly; coronin (section 1.1.2.1.2) collaborate with cofilin to mediate disassembly at old actin regions -rich in ADP-actin- while it prevents Cof1-mediated disassembly at newly assembled actin regions -rich in ATP-actin- (Gandhi et al., 2009). Tropomyosins (see section 1.1.3.1.) are coiled-coil dimers that bind along the length of actin filaments; in general they stabilize actin filaments and prevent the depolymerizing/severing activity of ADF/cofilin, though at least one isoform of tropomyosin seems to recruit ADF/cofilin to dynamic actin structures (Bryce et al., 2003). In contrast, tropomyosin cannot protect yeast F-actin from depolymerization/severing caused by yeast Cof1 (Fan et al., 2008).

Recently, based on structural homology, the glia maturation factor (GMF) was identified as a member of the ADF/cofilin superfamily, although the actin-binding residues of GMT and ADF/cofilins are not conserved (Goroncy et al., 2009). GMF has an homolog in yeast, the altered

inheritance rate of mitochondria Aim7 protein (see Figure 10). Deletion of *AIM7* does not produce any detectable phenotype, but shows synthetic sickness when combined with a mutant allele of cofilin (Gandhi et al., 2010; Hess et al., 2009). In contrast to Cof1, Aim7 does not affect the kinetics of actin assembly or disassembly, but stimulates de-branching of actin filaments produced by Arp2/3 and inhibits the formation of new daughter filaments (Gandhi et al., 2010). Proteomic studies indicate that Aim7 is phosphorylated *in vivo*, but whether this phosphorylation regulates the activity of Aim7 is not yet known (Albuquerque et al., 2008).

Figure 10. Domain organization of yeast actin depolymerizing/severing proteins.
Domain organization of yeast cofilin Cof1 and the yeast homolog of the Glia Maturation Factor (GMF) Aim7, depicting its single actin-depolymerizing factor homology domain (ADF-H).

1.1.3. Organization and stabilization of actin filaments

In *S. cerevisiae*, the total concentration of actin is estimated to be around two orders of magnitude lower than in other species, and is predominantly in the filamentous form, organized in specialized suprastructures (Karpova et al., 1995; Moseley and Goode, 2006; Pollard et al., 2000). Proteins that stabilize, bundle and crosslink actin filaments are in charge of building the functional actin assemblies.

1.1.3.1. The tropomyosins: Tpm1/Tpm2

Tropomyosins are conserved proteins that form parallel coiled-coil dimers and interact head-to-tail to cooperatively associate along the length of actin filaments. Tropomyosins associate mainly with actin filaments nucleated by formins since they stimulate formin activity (Wawro et al., 2007). Besides, the branching induced by Arp2/3 disrupts tropomyosin head-to-tail interactions (Blanchoin et al., 2001). There are two functionally redundant tropomyosins in budding yeast, Tpm1 and Tpm2, which are shorter than metazoan tropomyosins, but structurally related (its domain organization is depicted in Figure 11). Deletion of *TPM1*, but not of *TPM2*, causes morphology defects and loss of actin cables (see section 1.2) (Huckaba et al., 2006; Liu and Bretscher, 1989). Mammalian tropomyosins protect actin filaments from severing and block the myosin-binding site on actin, but these functions might not be conserved in budding yeast (Bernstein and Bamburg, 1982; Fan et al., 2008; Moore et al., 1970). The activity of yeast and metazoan tropomyosins is regulated by acetylation at the N-terminus. Unacetylation of tropomyosins disrupts the coiled-coil conformation, impeding its polymerization and association with actin filaments (Hitchcock-DeGregori and Heald, 1987; Maytum et al., 2000).

Figure 11. Domain organization of yeast tropomyosins.
Domain organization of yeast tropomyosins Tpm1 and Tpm2. Tpm1 contains 5 actin-binding (A_b) regions, while Tpm2 contains four.

1.1.3.2. The actin crosslinking proteins: Sac6, Scp1, Iqg1, Abp140

Actin filament bundling and crosslinking proteins are required to organize filaments into actin-based suprastructures. All actin bundling and crosslinking proteins connect filaments either via the presence of numerous actin-binding sites or via oligomerization. Although pluricellular organisms have an elevate number of actin bundling/crosslinking proteins (for more information see (Kreis and Vale, 1999), only the calponin-homology domain containing proteins fimbrin (also named plastin), smooth muscle transgelin SM22, and IQGAP, are conserved from yeast to mammals (see the domain organization on budding yeast actin crosslinking proteins in Figure 12).

Fimbrins contain two actin-binding domains (ABD), each including two calponin homology domains (CH) also found in other actin bundling proteins. Among its established role in actin bundling, there is also evidence that fimbrin might stabilize the filament and/or have anti-depolymerization activities, at least in fission yeast (Nakano et al., 2001). The *S. cerevisiae* fimbrin Sac6 is required for proper actin organization and endocytic uptake (Adams et al., 1989, 1991; Drubin et al., 1988; Kubler and Riezman, 1993). Sac6 binds to the lateral surface of the actin filament and bundles filaments probably through its two separate ABDs, although the actin binding surfaces on Sac6 have not been identified yet (Brower et al., 1995). In addition to Sac6, Scp1 -the budding yeast homolog of the smooth muscle transgelin SM22- has been suggested to bundle actin filaments via two actin binding sites located outside its single CH domain (Gheorghe et al., 2008). Sac6 and Scp1 might function together to bundle actin filaments, since they show synthetic functional defects (Gheorghe et al., 2008; Goodman et al., 2003; Winder et al., 2003). Both Scp1 and Sac6 are phosphorylated *in vivo* but whether this post-translational modification regulates their bundling activity is not yet known (Albuquerque et al., 2008; Chi et al., 2007; Li et al., 2007; Smolka et al., 2007).

Iqg1 (also called Cyk1) is the third CH-containing protein in budding yeast. Deletion of the IQG1 gene causes lethality or temperature sensitivity -depending on the strain background- due to defects in cytokinesis (Epp and Chant, 1997; Lippincott and Li, 1998). Iqg1 binds F-actin through the region containing the CH domain, and its mammalian homolog IQGAP directly bundles actin filaments, but there is still not direct evidence for this activity in Iqg1 (Epp and Chant, 1997). Moreover, mammalian IQGAP and CaIqg1 from the yeast *Candida albicans* are able to interact with formins, and it has been proposed that they might also control actin

polymerization (Brandt et al., 2007; Li et al., 2008). Direct phosphorylation of CaIqg1 regulates its association with formins (Li et al., 2008).

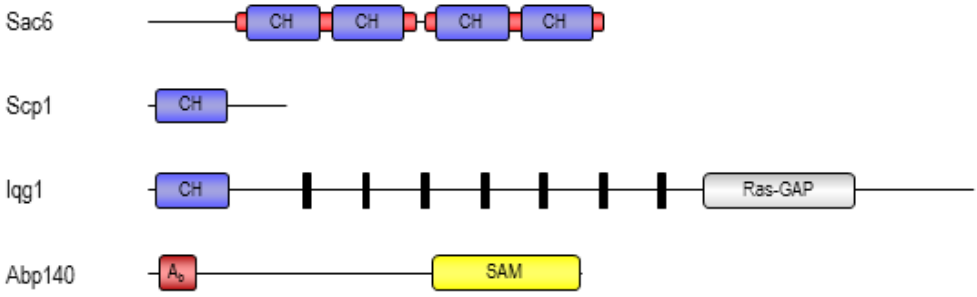

Figure 12. Domain organization of actin crosslinking proteins.
Domain organization of the yeast actin cross linking proteins Sac6, Scp1, Iqg1, and Abp140. The actin-binding calponin homology domain (CH) is shown; note that the CH domains of Sac6 are included within the two actin binding domains (pictured in red). Abp140 does not contain CH domains but a different actin-binding region (A_b). Other important domains are shown. Black bars: IQ motifs, calmodulin-binding regions; Ras-GAP: Ras-GTPase activating region. SAM: S-adenosylmethionine domain.

In addition, to Sac6, Scp1 and Iqg1, *S. cerevisiae* contains another actin-bundling protein that seems to exist only in this organism. Abp140. Abp140 was purified as a protein that binds and bundles F-actin, the ABD of Abp140 is located in the N-terminal region and the protein appears to multimerize (Asakura et al., 1998). Recent studies indicate that while the N-terminus binds F-actin, the C-terminal region of Abp140 binds RNA and has tRNA methyltransferase activity. The N-terminal ABD might function to cotranslationally transport the nascent ABP140 mRNA along actin cables (D'Silva et al., 2011; Kilchert and Spang, 2011; Noma et al., 2011).

1.1.3.3. Linkers of actin to membranes: Sla2

Apart from the group of proteins that bundle and crosslink actin filaments, a number of proteins link the actin cytoskeleton to cellular structures. Several actin-binding proteins have regions that interact with specific lipids or are even linked covalently to lipids (for example the already mentioned capping protein, cofilin, or profilin, which are regulated by PIP_2); certain actin-binding proteins are in fact integral membrane proteins; and numerous actin-binding proteins interact with membranes through intermediate adaptor proteins or adaptor complexes (see (Doherty and McMahon, 2008)). In addition, from yeast to mammals, bidirectional cross-talk between membranes and cytoskeletal proteins is regulated by small GTP-binding proteins -such as the members of the Rho/Rac/Cdc42 family- and their effectors, which include lipid kinases and regulators of actin dynamics such as NPFs or formins (Pruyne et al., 2004b; Ridley, 2006).

In budding yeast two types of actin-binding proteins are known to bind directly to membranes, the unconventional myosins (see next section), and the Hip1R homolog Sla2, which is required for normal cytoskeletal morphology and for endocytosis (Holtzman et al., 1993; Raths et al., 1993). Sla2 binds PIP_2 through its N-terminal ANTH (AP180 N-terminal homology) domain and to F-actin through its C-terminal talin-like domain (McCann and Craig, 1997; Sun et al., 2005) (see its domain organization in Figure 13). In addition, Sla2 contains a coiled-coil domain that mediates Sla2 dimerization and interacts with endocytic proteins including the NPF Pan1 (Henry et al., 2002; Toshima et al., 2007; Yang et al., 1999). Recent biochemical and live cell imaging analyses indicate that Sla2 negatively regulates the nucleation promoting activity of Pan1 *in vitro* by interfering with the WH2-like domain of Pan1, and serves *in vivo* as a linker between endocytic sites at the plasma membrane and the actin cytoskeleton (Kaksonen et al., 2003; Toshima et al., 2007). The biochemical function of Sla2 is controlled by interacting proteins such as the clathrin light chain (Clc1), which seems to spatially regulate the actin-binding activity of Sla2 (Boettner et al., 2011). In addition, Sla2 is phosphorylated *in vivo*, but still no regulatory role has been assigned to this post-translational modification (Albuquerque et al., 2008; Ficarro et al., 2002; Gruhler et al., 2005; Li et al., 2007; Smolka et al., 2007).

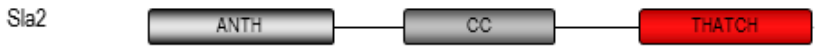

Figure 13. Domain organization of Sla2.
Sla2 interacts with PIP2 via its AP180 N-terminal homology domain (ANTH), and to F-actin through the talin-HIP1R/Sla2 actin-tethering C-terminal homology domain (THATCH). Between the ANTH and THATCH domains Sla2 contains a coiled-coil region (CC).

1.1.4. Actin-dependent molecular motors

Myosins are molecular motors that bind to and move along actin filaments. They typically consist of monomeric or dimeric heavy chains bound to a variable number of light chains. Phylogenetic analysis classifies the myosin superfamily into ~24 different types (Foth et al., 2006). Some myosin types are widely expressed and others have members only present in specific organisms (Sellers, 2000). Type II myosins, which were the first discovered, are called 'conventional' myosins. Other myosins are collectively referred as 'unconventional' myosins.

Most myosin heavy chains share a common structural organization, with an N-terminal motor domain, a neck region that binds myosin light chains, and a type-conserved C-terminal tail region that is responsible for cargo binding and/or dimerization. The motor uses the chemical energy of ATP to produce mechanical force in a process known as the actomyosin ATPase cycle

(depicted in Figure 14). Briefly, in the absence of ATP, myosin is tightly bound to actin; when ATP binds the myosin, it induces a conformational change and the myosin is released from the actin filament; ATP-hydrolysis causes a second conformational change that allows myosin to bind weakly to the filament; and finally, dissociation of the P_i, which is the rate-limiting step of the cycle, restores the original conformation producing a force-generating power-stroke that causes the movement of the filament relative to the myosin. The mechanical and motile properties of myosin classes and isoforms are influenced by the lifetime of the entire cycle and by the fraction of time a myosin spends in the strong actin-bound state (the duty ratio). A high duty ratio is required for continuous movement of myosins; otherwise the assembly of several motors is necessary for processivity (De La Cruz and Ostap, 2004). The neck serves as a lever arm, transducing small conformations of the motor domain into bigger movement at the C-terminal tail domain. The neck consists of one or more IQ consensus motifs, which serve as binding sites for one or more types of myosin light chains (calmodulin molecules or other members of the EF-hand domain containing protein family). The nature of the light chain bound to the neck domain affects the mechanochemical properties of myosins (Coluccio, 2008).

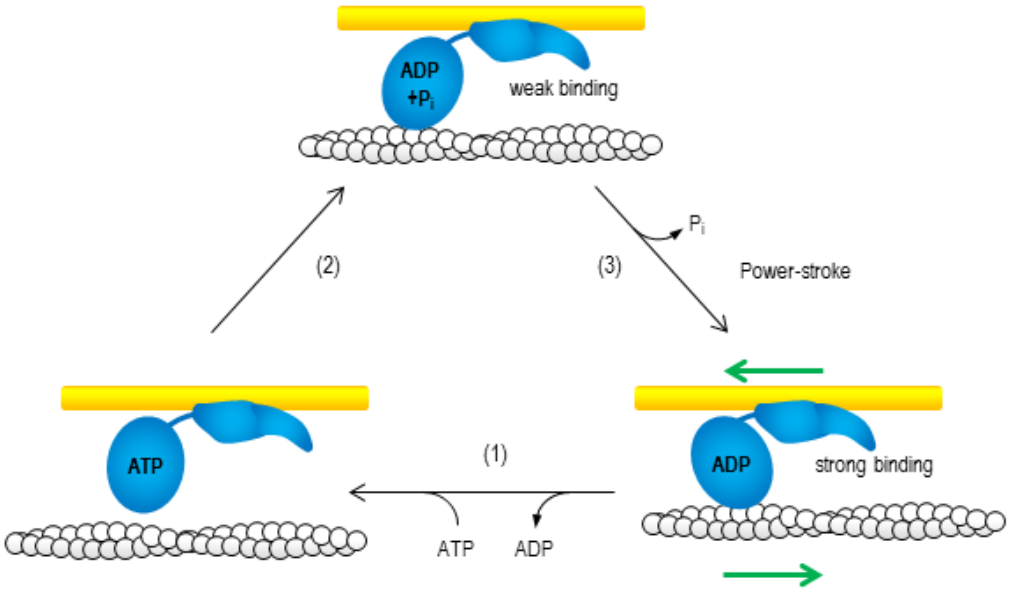

Figure 14. A simplified model for the actomyosin ATPase cycle.
In the absence of ATP, myosin (blue) binds tightly to actin (white), while the tail of the myosin mediates its interaction to other proteins and/or membranes (yellow). ATP binding (1) induces a conformational change in the myosin that weakens its actin affinity and causes myosin to detach from actin. ATP hydrolysis causes a second conformational change and the myosin rebinds to the actin filament with low affinity (2). When Pi is finally released, the myosin can bind with high affinity to actin and the force-generating power-stroke causes the filament and/or the myosin to slide (green arrows)(3). ADP is released and ATP can rebind to repeat the cycle. See text for further details.

The tail of myosins remarkably varies, both in sequence and structural organization. Consequently, the tails as considered as the region that mainly defines the localization and function of specific myosin subtypes. However, variations in the motor and neck regions are also important to define their function. Numerous myosins contain protein-protein interaction domains, such as the coiled-coil domain that mediates dimerization of myosin heavy chains, the SH3 domain that mediate the interaction with poly-proline-rich domain containing proteins, the MyTH4/FERM domain that links the heavy chain to specific membrane proteins, or the Dilute domain that mediates the interaction of type V myosins with their cargoes, among others. Some myosins contain also domains to link the myosin to membranes, such as the pleckstrin homology domains present in some type I and type X myosins (Coluccio, 2008).

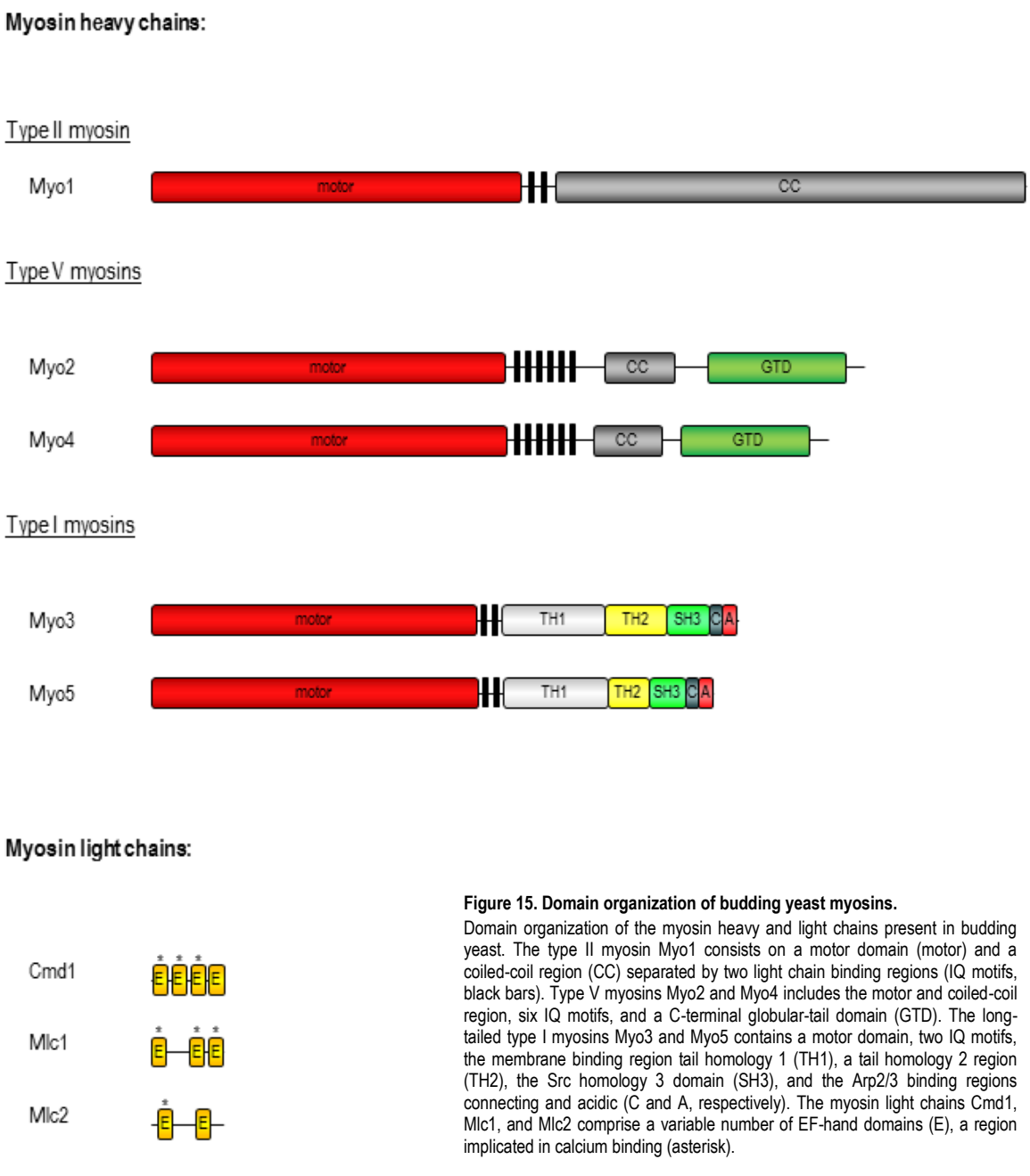

Figure 15. Domain organization of budding yeast myosins.
Domain organization of the myosin heavy and light chains present in budding yeast. The type II myosin Myo1 consists on a motor domain (motor) and a coiled-coil region (CC) separated by two light chain binding regions (IQ motifs, black bars). Type V myosins Myo2 and Myo4 includes the motor and coiled-coil region, six IQ motifs, and a C-terminal globular-tail domain (GTD). The long-tailed type I myosins Myo3 and Myo5 contains a motor domain, two IQ motifs, the membrane binding region tail homology 1 (TH1), a tail homology 2 region (TH2), the Src homology 3 domain (SH3), and the Arp2/3 binding regions connecting and acidic (C and A, respectively). The myosin light chains Cmd1, Mlc1, and Mlc2 comprise a variable number of EF-hand domains (E), a region implicated in calcium binding (asterisk).

Five myosins are present in *S. cerevisiae*, and are comprised into three classes: the type II myosin Myo1, that localizes at the bud-neck interphase and plays a role in cytokinesis and in retrograde actin cable flow (Bi et al., 1998; Huckaba et al., 2006; Lippincott and Li, 1998); two type-V myosins, Myo2 and Myo4, that transport diverse cargoes such as organelles, vesicles, and specific proteins and mRNA along actin cables towards the growing bud (Pruyne et al., 2004b); and two type-I myosins, Myo3 and Myo5, that promote actin polymerization and are required for endocytosis. In addition, budding yeast possesses three light chains: calmodulin (Cmd1), and the myosin light chains Mlc1 and Mlc2. The domain organization of budding yeast myosin heavy and light chains is depicted in Figure 15.

1.1.4.1. Type II myosins: Myo1

Until the isolation and characterization of type I myosins from *Acanthamoeba* in the early 70's (Pollard and Korn, 1973), the only known myosins were the double-headed type II myosins. Myosins were first described in the mid-19th century as a component of the skeletal muscle extract, while their contractile capacities were revealed almost a century later. Actin and myosin-II form thin and thick filaments of the muscle cells, respectively, which slide into each other during muscle contraction (Huxley and Niedergerke, 1954; Huxley and Hanson, 1954). The contractile ability of non-muscle type II myosin functions in a variety of cellular processes including cytokinesis, cell adhesion, cell migration, and cell shape change. The type II myosins are constituted by two heavy chains and four light chains. The heavy chain is composed of a relatively low duty ratio motor domain; a neck, which binds to two different myosin light chains (one essential light chain and one regulatory light chain); and a C-terminal coiled-coil domain, which mediate the dimerization with another heavy chain (Coluccio, 2008).

The sole conventional myosin Myo1 was the first myosin identified in *S. cerevisiae*, it interacts with the essential light chain Mlc1 and the regulatory light chain Mlc2 through its IQ1 and IQ2 motifs, respectively. Myo1 forms the typical double-headed structure of other type II myosins (Fang et al., 2010; Luo et al., 2004; Watts et al., 1985). Deletion of *MYO1* does not cause cell lethality but severely affects cytokinesis and cell separation due to a motor-independent role of Myo1 in actomyosin ring formation and targeted membrane deposition (Bi et al., 1998; Lord et al., 2005). In addition, Myo1 is required for retrograde actin flow (Huckaba et al., 2006).

The regulation of type II myosins in metazoan involves the phosphorylation in the regulatory light chain. Phosphorylation of the light chain prevents the myosin to adopt an autoinhibited folded conformation, at least *in vitro*. This mechanism is not conserved in yeast though (Coluccio, 2008). In addition, regulation of type II myosins also involves phosphorylation(s) in the heavy chain (reviewed in (Redowicz, 2001)).

1.1.4.2. Type V myosins: Myo2 and Myo4

Unconventional type V myosins are double-headed molecular motors that transport cargo within the cell by 'walking' hand-over-hand upon actin filaments (Sellers and Veigel, 2006). With some

exceptions such as such as budding yeast myosins-V, the heavy chain of type V myosins bears a high-duty-ratio motor domain (with some exceptions (Reck-Peterson et al., 2001)), which allow processive transport of cargo along actin cables. Downstream of the myosin ATPase, follow a long neck with six IQ motifs that bind light chains and determines the step length; a coiled-coil domain, which mediate its dimerization; and a C-terminal globular-tail domain (GTD or Dilute domain) implicated in cargo transport (Coluccio, 2008).

The essential Myo2 and the non-essential Myo4 constitute the two myosin-V heavy chains present in budding yeast (Haarer et al., 1994; Johnston et al., 1991). Although they are closely related, they transport distinct cargoes by different mechanisms. Myo2 transports membrane-bound cargoes such as vesicles and organelles (such as secretory vesicles, the vacuole, late Golgi, peroxisomes, or mitochondria) and microtubules (Pruyne et al., 2004b). Myo2 functions as a dimer to transport its cargo and binds to the light chains calmodulin (Cmd1) and Mlc1 (Brockerhoff et al., 1994; Stevens and Davis, 1998). However, since it is a weakly processive motor, efficient transport of cargoes likely requires the presence of several Myo2 dimers (Dunn et al., 2007; Reck-Peterson et al., 2001). Myo4, on the other hand, transports cortical ER and mRNA protein complexes and its light chains have not been determined (Pruyne et al., 2004b). Myo4 is a non-processive monomeric motor, but recently data suggests that efficient transport is achieved by the recruitment of multiple Myo4 monomers by its cargo (Chung and Takizawa, 2010; Dunn et al., 2007).

Generally type V myosins adopt a folded conformation when not bound to cargo. Autoinhibition can be released by calcium (Trybus, 2008). The interaction of type V myosins and their cargo can be regulated by phosphorylation of the globular cargo-binding domain, at least in some organisms (Karcher et al., 2001). The cargo-binding domain of yeast myosin-V Myo2 is also found phosphorylated *in vivo*, but the physiological significance of this phosphorylation has not been determined (Legesse-Miller et al., 2006).

1.1.4.3. Type I myosins: Myo3 and Myo5

Unconventional type I myosins are single-headed molecular motors that perform specialized functions that differ between distinct types of cells (Kim and Flavell, 2008). The heavy chain is composed of a low duty ratio motor domain (De La Cruz and Ostap, 2004); a long neck with a variable number of IQs, whih bind to light chains and also to specific proteins and lipids (Coluccio, 2008; Cyr et al., 2002; Hirono et al., 2004); and either a short or a long C-terminal tail that classifies type I myosins into two subgroups. Most amoeboid and fungal type I myosins are long-tailed, whereas higher organisms usually expresses both short- and long-tailed myosins- (Berg et al., 2001). Both short- and long-tailed type I myosins contain a characteristic positively charged tail homology 1 (TH1) domain, which binds to negatively charged lipids and protein stripped membranes and might help to localize the myosin to membranes (Adams and Pollard, 1989; Hayden et al., 1990; Miyata et al., 1989). The TH1 domain of some type I myosins includes a pleckstrin homology (PH) domain that mediates the interaction with PIP_2, although not all PH-containing type I myosins binds lipids through this domain (Brzeska et al.,

2008; Feeser et al., 2010; Hokanson et al., 2006). In addition, long-tailed myosins-I bear a C-terminal extension (C_{ext}) adjacent to the TH1 domain. The C_{ext} includes a region rich in glutamine, alanine and proline (called TH2 or QPA-domain), which binds F-actin in an ATP-insensitive manner (Doberstein and Pollard, 1992; Jung and Hammer, 1994; Rosenfeld and Rener, 1994), and a SH3 domain that mediates interaction with proline-rich motifs (Kuriyan and Cowburn, 1997). In addition, several long-tailed myosins forms a linkage with the Arp2/3 complex by two alternative mechanisms: fungal heavy chains bear an acidic region directly involved in the activation of the Arp2/3-dependent actin polymerization (the CA, see section 1.1.2.1.2) while some protozoal myosins-I recruit the Arp2/3 complex indirectly, via a WH2- and acidic domain-containing protein called CARMIL (Jung et al., 2001).

Myo3 was the first type I heavy chain discovered in *S. cerevisiae*, and shortly later the second myosin-I, Myo5, was identified (Geli and Riezman, 1996; Goodson et al., 1996; Goodson and Spudich, 1995). Both proteins follow the typical structure of long-tailed type I myosins: an N-terminal ATPase motor domain; a neck that contains 2 IQ motifs and bind Cmd1 in the absence of calcium (Geli et al., 1998); a TH1 domain that binds to acidic phospholipids and is involved in Myo5 autoinhibition (see below) (Grotsch et al., 2010); and a C-terminal extension (C_{ext}) required for the actin nucleation promoting activity of Myo5 (Geli et al., 2000) (see also section 1.1.2.1.2.1 and Figure 15). Deletion of either *MYO3* or *MYO5* has not effect in cell growth, but deletion of both genes caused synthetic lethality or sickness depending on the strain background; analysis of mutant alleles revealed the essential function of budding yeast myosins in endocytic uptake. Both the motor and the actin nucleation promoting activity of type I myosins are required for this cellular function (Geli and Riezman, 1996; Goodson et al., 1996; Goodson and Spudich, 1995; Sun et al., 2006).

The biochemical and physiological function(s) of type I myosins are tightly regulated. The motor activity of amoeba, fungi and yeast type I myosins (and also myosins-VI from vertebrates and flies) is controlled by phosphorylation of a conserved serine or threonine located in a surface loop that contacts the actin filament, the so called TEDS site (reviewed in (Redowicz, 2001)). In the TEDS site, the serine or threonine residues susceptible of phosphorylation are replaced by negatively charged aspartic- or glutamic-acid residues in others type I myosins, which indicates that a negative charge at this position is important for their function (Bement and Mooseker, 1995). Actually, phosphorylation of the TEDS site increases 20 to 50 fold the actin-activated ATPase activity of protozoal type I myosins *in vitro* and is required for some type I myosin functions *in vivo* (Albanesi et al., 1983; Baines et al., 1995; Brzeska et al., 1997; Cote et al., 1985; Lynch et al., 1989; Maruta and Korn, 1977; Novak and Titus, 1998). Phosphorylation of the TEDS site has been shown to be mediated by members of the PAK (p21-activated kinase) family in protozoa (Brzeska et al., 1997; Lee et al., 1996). In vertebrate type I myosins, the motor activity is inhibited by calcium, which might trigger the dissociation of at least a fraction of the calmodulin bound to the heavy chain since addition of exogenous calmodulin restores the biochemical function. It has been proposed that calmodulin acts as a mechanical lever and/or protects the function of the neck as a lever arm (Block, 1996; Williams and Coluccio, 1994). In

addition, a large conformational reorganization of the tail can also be observed upon calmodulin dissociation of the brush border myosin-I (Whittaker and Milligan, 1997). Whether type I myosins are regulated by binding to specific signaling lipids is less clear. Most myosins-I interact with PIP_2 via the TH1 domain, either with high affinity via a PH domain embedded within the TH1 domain or by electrostatic interactions with the positively charged residues of this domain (Feeser et al., 2010; Hokanson et al., 2006). Whether this interaction serves only to localize the myosin or also modulates its activity has not been addressed.

In *S. cerevisiae*, the motor and nucleation promoting activities of Myo3 and Myo5 function independently and might be controlled by different mechanisms. Phosphorylation/dephosphorylation of Myo5 TEDS site controls the motor activity *in vitro* and the endocytic uptake rate *in vivo*, but has no effect on the NPA activity of budding yeast myosins-I (Grosshans et al., 2006; Sun et al., 2006). Interestingly, although the Myo5 TEDS site is phosphorylated by members of the PAK (p21-activated kinase)/Ste20 family *in vitro* (Wu et al., 1997), a second signaling cascade involving the yeast PDK1 (3-phosphoinositide-dependent protein kinase-1) and SGK (serum and glucocorticoid-induced kinase) homologues -Pkh1/2 and Ypk1/2, respectively- seems to activate Myo5 for its endocytic function *in vivo* (Grosshans et al., 2006). As described in sections 1.1.2.1.2.1, the C-terminal NPA is regulated by an autoinhibitory interaction between the TH1 domain and the C_{ext}, which is stabilized by calmodulin. The IQ motifs of Myo5 bind calmodulin in the absence of calcium; addition of calcium triggers calmodulin dissociation and as a consequence, activation of the Myo5 NPA (Geli et al., 1998)(Grotsch et al., 2010). However, it is not known whether calcium influences calmodulin-binding to the neck under physiological conditions.

1.2. Physiological functions of actin in *Saccharomyces cerevisiae*

Actin filaments in *S. cerevisiae* are organized in three main suprastructures, which can be visualized by fluorescence microscopy upon staining with phalloidin coupled to fluorescent dies (Figure 16): the cortical actin patches, actin cables and the actomyosin contractile ring. Actin cables and the actomyosin ring are both believed to be formed by parallel bundles of short actin filaments. Actin cables are polarized along the mother-bud axis, whereas the actomyosin ring is located perpendicular to this axis and it is only present in large-budded cells (at G2-M transition). Cortical actin patches, in contrast, are formed by a dendritic array of branched filaments and are located at the cell cortex (Adams and Pringle, 1984; Bi et al., 1998; Kilmartin and Adams, 1984; Lippincott and Li, 1998)(Young et al., 2004). Cortical patches, actin cables and the cytokinetic ring are dynamic structures that undergo rapid turnover, as they disappear soon after the addition of the monomer sequestering drug Latrunculin-A (Ayscough et al., 1997)(Karpova et al., 1998). All three actin structures undergo dramatic rearrangements during the cell cycle. When a cell is about to bud, the actin cables and patches converge at the nascent bud site. During bud growth, actin patches accumulate at the daughter cells, whereas actin cables align along the mother-bud axis. When the daughter cell reaches a certain size, the asymmetric distribution of actin patches and cables is lost. Finally, when cytokinesis starts, both

patches and cables reorient towards the mother-bud neck junction and the cytokinetic ring is assembled (Adams and Pringle, 1984; Amberg, 1998; Kilmartin and Adams, 1984); see Figure 16. When the actin cytoskeleton is depolarized, the asymmetric distribution of actin patches and cables is lost, and the actin structures distribute uniformly in the cell. The different location and composition of these structures suggests that they might perform different physiological functions. In the following sections, the protein composition and the physiological role of the three actin structures is briefly described.

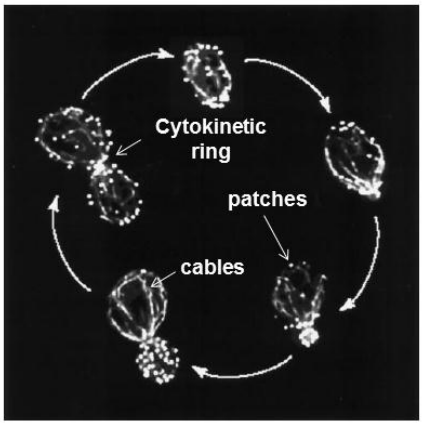

Figure 16. The yeast actin cytoskeleton through the cell cycle.
Fluorescence images showing *S. cerevisiae* cells from an asynchronous culture that were chemically fixed and stained with rhodamine-phalloidin to visualize the filamentous actin structures. In non-dividing yeast cells both actin patches and cables are randomly distributed. During bud emergence and bud growth, actin patches are polarized to the growing bud and cables align parallel to the polarity axis. During isotropic growth, the asymmetric distribution of actin patches and cables is lost. During cytokinesis, the cytokinetic ring appears and cables are polarized towards the cytokinetic ring. Image obtained from Amberg, 1998.

1.2.1. Cell division: assembly and contraction of the cytokinetic ring

An actomyosin contractile ring is essential to divide two cells during cytokinesis in almost all eukaryotic cells (Balasubramanian et al., 2004). However, in *S. cerevisiae* the actomyosin ring is required for efficient cell division but is not essential. For this reason, the presence of an actomyosin contractile ring was questioned until its direct observation (Bi et al., 1998; Lippincott and Li, 1998). Actin assembly at the bud neck occurs at G2-M transition, and requires the formins Bni1 and Bnr1, profilin, Iqg1, and tropomyosin (Epp and Chant, 1997; Lippincott and Li, 1998; Tolliday et al., 2002). In contrast to actin, the type II myosin Myo1 is recruited to the bud neck earlier during the cell cycle (at G1). Disassembly after constriction requires the regulatory light chain Mlc2, while the essential light chain Mlc1 is dispensable for Myo1 function in the contractile ring but is still required for cytokinesis and cell viability (Bi, 2001; Luo et al., 2004; Shannon and Li, 2000; Watts et al., 1985). The role of Myo1 in the assembly and the contraction of the cytokinetic ring is still not understood, since its function does not require the motor domain (Lord et al., 2005). In fact, deletion of *MYO1* only delays cytokinesis and cell separation but does not prevent it (Bi et al., 1998). This is probably due to the existence of other complementary mechanism that drives cytokinesis, which is the septum deposition. The actomyosin ring and septum deposition are interdependent pathways: the actomyosin ring regulates the proper alignment of the septum whereas septum deposition is required for ring constriction, and together cooperate to efficiently separate the two cells during cytokinesis (reviewed in (Bi, 2001)).

1.2.2. Polarized secretion and organelle inheritance: the actin cables

After bud emergence and the establishment of an axis of polarity, cell growth is restricted to the bud (or to the bud neck at mitosis). Transport of secretory vesicles and organelle inheritance is directed by the actin cables (Pruyne et al., 2004a). Actin cables are formed by bundles of actin filaments anchored at the bud tip (or nascent bud site) and the bud neck. Actin cables are oriented with the barbed ends towards the nascent bud during cell division and towards the bud tip or the bud neck during bud growth; this is due to the restricted location of the formins Bni1 (at the tip) and Bnr1 (at the neck) (Pruyne et al., 2004a). The assembly of actin cables relies in the nucleating activity of the formins Bni1 and Bnr1, but profilin and Bud6 are also important for this activity (Evangelista et al., 2002)(Sagot et al., 2002a)(Pruyne et al., 2002)(Amberg et al., 1997; Sagot et al., 2002b). In addition, Sac6, tropomyosins, and Abp140 localize to actin cables (Adams et al., 1991; Asakura et al., 1998; Drees et al., 1995; Liu and Bretscher, 1989). Actin cables serve as tracks for the type V myosins Myo2 and Myo4 to transport secretory vesicles, daughter-specific mRNA and organelles towards the daughter cell. In addition, actin cables help during mitotic spindle elongation and are implicated in the retrograde movement of endosomes and other mother-specific molecules (Bretscher, 2003; Pruyne et al., 2004)(Huckaba et al., 2004)(Kilchert and Spang, 2011; Toshima et al., 2006). While anterograde transport is driven by the molecular motor myosin-V, retrograde movement relies on the retrograde flow of actin caused by addition of actin subunits by formins at the bud tip or at the bud neck (Yang and Pon, 2002). In addition, Myo1 located at the bud neck (see above) increases the rate of retrograde actin cable flow. In contrast to the contraction of the cytokinetic ring retrograde actin flow requires the motor domain of Myo1, suggesting that myosin-II actively pulls away the actin filaments that are being assembled at the bud neck (Huckaba et al., 2006).

1.2.3. The role of actin in endocytosis

Endocytosis is an evolutionary conserved cellular process whereby the flat plasma membrane bends to form an endocytic vesicle that detaches from the cell surface and travels through the cytosol to fuse with early endosomes. From the endosomes internalized cargo is either recycled back to the plasma membrane or sorted into the endolysosomal system for degradation. Endocytosis, together with exocytosis, controls the lipid and protein composition of the cell surface, and consequently, it regulates multiple aspects of biology such as nutrient uptake, cell signaling, cell migration, or pathogen entry, among others.

Several mechanisms of endocytosis have been described in mammals (reviewed in (Doherty and McMahon, 2009; Mayor and Pagano, 2007)). In budding yeast, only the clathrin-mediated endocytic was described until now. However, evidence for an alternative clathrin-independent endocytic mechanism have recently been reported (Prosser et al., 2011). Interestingly, a dynamic actin cytoskeleton is mandatory for endocytosis in *S. cerevisiae*. Mutations on actin and several actin-regulating proteins cause strong internalization defects and endocytosis is blocked in the presence of G-actin sequestering or F-actin stabilizing drugs (Ayscough, 2000; Ayscough et al., 1997). In higher eukaryotes, the role of actin in clathrin-mediated endocytosis is more

controversial. An increasing number of results indicate that actin polymerization is also required in at least a subset of clathrin dependent budding events (reviewed in (Doherty and McMahon, 2009; Engqvist-Goldstein and Drubin, 2003; Girao et al., 2008)). Interestingly, recent data indicates that membrane tension might determine the actin requirement for clathrin-coat assembly in mammalian cells (Boulant et al., 2011).

In the next section, the current general model for the formation of clathrin- and actin-dependent endocytic vesicles in budding yeast is discussed; the section is followed by a brief description of the role of actin in post-internalization endocytic traffic.

1.2.3.1. Endocytic vesicle budding from the plasma membrane

1.2.3.1.1. The classical clathrin and actin-dependent endocytic pathway in yeast: the cortical actin patches

The first evidence indicating that actin was associated to endocytosis in yeast was obtained almost two decades ago, when a genetic screen to isolate mutants with defects in the formation of endocytic vesicles at the plasma membrane identified genes encoding actin and several actin patch-associated proteins (Kubler and Riezman, 1993; Munn et al., 1995; Raths et al., 1993). During the next years, more actin patch-components whose mutation leads to endocytic defects were identified and, in addition, most endocytic proteins -such as endocytic adaptors and scaffolds- were found by immunofluorescence or live cell imaging to localize to punctate cortical structures that total or partially colocalize with actin patches (table 2)(Engqvist-Goldstein and Drubin, 2003). However, a direct functional link between cortical actin patches and endocytosis was missing until new advances in live-cell imaging (dual-color time-lapse fluorescence microscopy, particle tracking, or total internal reflection microscopy (TIRF)) were applied to the study of endocytic budding in yeast. These studies demonstrated that endocytic cargo transiently joint the components of cortical patches before being internalized (Kaksonen et al., 2003; Toshima et al., 2006). Dual color live cell fluorescence microscopy has been particularly valuable to order the sequence of molecular events during actin patch maturation and vesicle budding from the plasma membrane. Proteins involved in endocytic uptake are transiently recruited in a invariable, sequential, and partially-overlapping manner at the cortical sites where an endocytic vesicle is being produced (Figure 17) ((Weinberg and Drubin, 2012) and references therein). Based on their dynamics at the endocytic sites, the endocytic proteins have been assigned into different functional modules (Table 2, Figure 17).

More recently, quantitative immunoelectron microscopy applied to the study of endocytic budding in yeast has increased the spatial resolution to define the nature of the primary endocytic profiles at the plasma membrane and to unveil how the molecular complexes that deform the plasma membrane reorganize as the endocytic profile matures (Idrissi et al., 2012; Idrissi et al., 2008). These experiments demonstrate that the endocytic profiles in yeast are tubular invaginations of 50 nm in diameter and up to 180 nm in length, capped by a

hemispherical clathrin coat of about 40 nm, which moves into the cytosol as the tubular profile elongates and matures (Idrissi et al., 2008)(Figure 18).

The current model for clathrin- and actin-dependent endocytic budding in *S. cerevisiae* is explained in the next sections, separated in four main steps: assembly of the endocytic coat, actin-driven membrane deformation, vesicle scission, and uncoating (Figure 19).

Module	Protein or complex	Homolog	Function
Early	Ede1	Eps15	Scaffold protein
	Syp1	FCho1/2	Endocytic adaptor Membrane curvature sensing/bending
Early coat	Chc1/Clc1	Clathrin	Formation of clathrin cage Possible regulatory function
	yAP1801/2	AP180	Endocytic adaptor Scaffold protein that links the endocytic coat to the plasma membrane
	Pal1	-	Not known
	AP2	AP2	Endocytic adaptor
Intermediate coat	Sla2	Hip1R	Scaffold protein that links the endocytic coat to the actin cap and the plasma membrane Regulation of actin dynamics (inhibits Pan1 NPA)
	Ent1/2	Epsin	Scaffold protein that links the endocytic coat to the plasma membrane
Late coat	End3	-	Scaffold protein
	Pan1	Intersectin	Nucleation promoting factor Scaffold protein
	Sla1	Intersectin/CIN85	Endocytic adaptor Regulation of actin dynamics (inhibits Las17 NPA)
WASP/Myosin	Las17	WASP	Nucleation promoting factor Recruits Vrp1 to the endocytic patch
	Vrp1	WIP	Regulation of actin dynamics (co-activator of Myo5 NPA)
	Bzz1	Syndapin	Regulation of actin dynamics (relieves Sla1 inhibition on Las17)
	Myo5	Myosin-I	Motor protein Nucleation promoting factor (requires Vrp1)
	Bbc1	-	Regulation of actin dynamics (inhibits Myo5 and Las17 NPA)
Actin	Arp2/3	Arp2/3	Actin nucleator Promotes actin filament branching
	Abp1	ABP1	Nucleation promoting factor Regulation of actin dynamics (inhibits Las17 NPA, recruits Ark1/Prk1 kinases, and Sjl2)
	Sac6	Fimbrin	Actin filament bundling
	Scp1	Transgelin	Actin filament bundling
	Cap1/2	Capping protein	Actin filament capping at barbed ends
Amphiphysin	Rvs161/167	Amphiphysin	Membrane curvature sensing/bending Promotes vesicle scission
	Vps1	Dynamin	Might help to promote vesicle scission
Uncoating/Disassembly	Ark1/Prk1	AAK1	Pan1 and Sla1 phosphorylation Regulation of actin dynamics (inhibits Pan1 NPA) Vesicle uncoating
	Sjl2	Synaptojanin-1	PIP2 dephosphorylation
	Cof1	Cofilin	Regulation of actin dynamics (filament severing/disassembly)
	Aip1	Aip1	Regulation of actin dynamics (filament severing/disassembly)
	Crn1	Coronin	Regulation of actin dynamics (filament severing/disassembly)

Table 2. Budding yeast endocytic patch components.
List of the most representative endocytic proteins localizing to cortical patches, grouped by modules and including the name of mammalian homologs and a general overview of their main molecular functions in endocytosis. See text for further details.

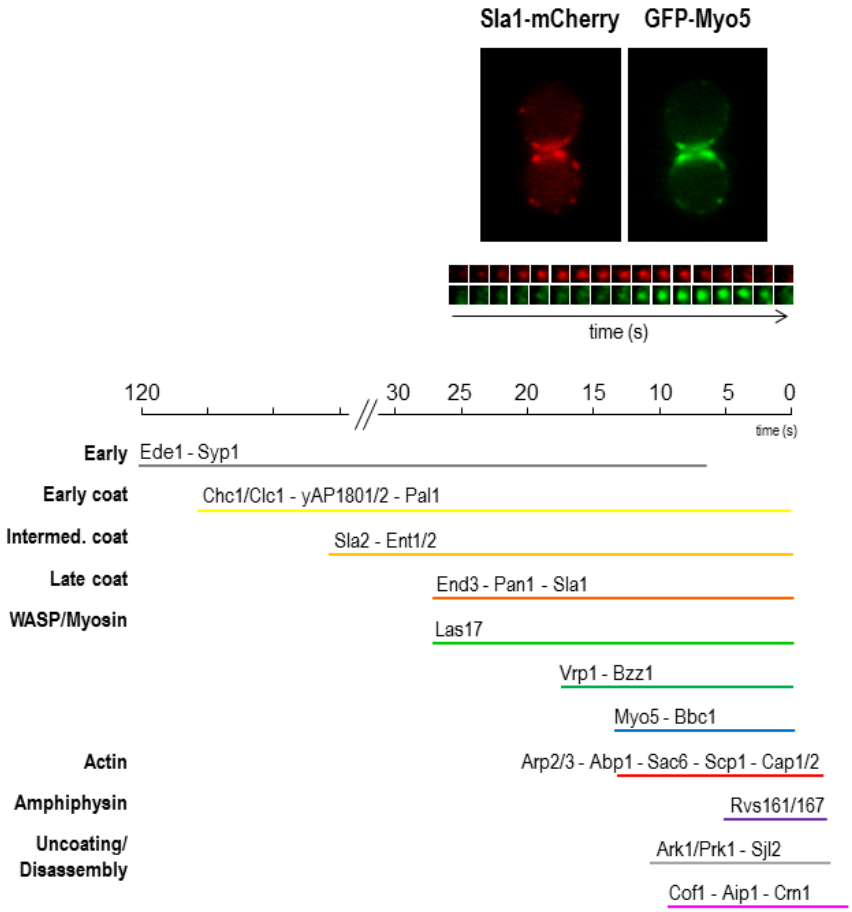

Figure 17. Pathway for the recruitment and disassembly of endocytic proteins at cortical patches.
(A) Single frames from a double-color time-lapse movie showing the localization of mCherry- and GFP-fused endocytic markers (Sla1 and Myo5) in *S. cerevisiae* cells. The consecutive frames from the double-color time-lapse movie displaying a selected cortical patch are shown below. (B) Cortical dynamics of endocytic proteins. The proteins have been grouped in functional modules (see text for details). Time 0 correspond to scission.

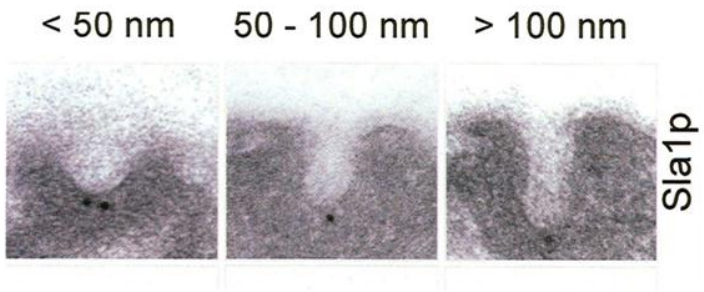

Figure 18. Primary endocytic profiles of budding yeast.
Electron micrographs of ultrathin sections from S. cerevisiae showing plasma membrane associated invaginations shorter than 50 nm, between 50 nm and 100 nm, and longer that 100 nm decorated with gold particles against the HA-tagged endocytic coat protein Sla1. Taken from (Idrissi et al., 2008).

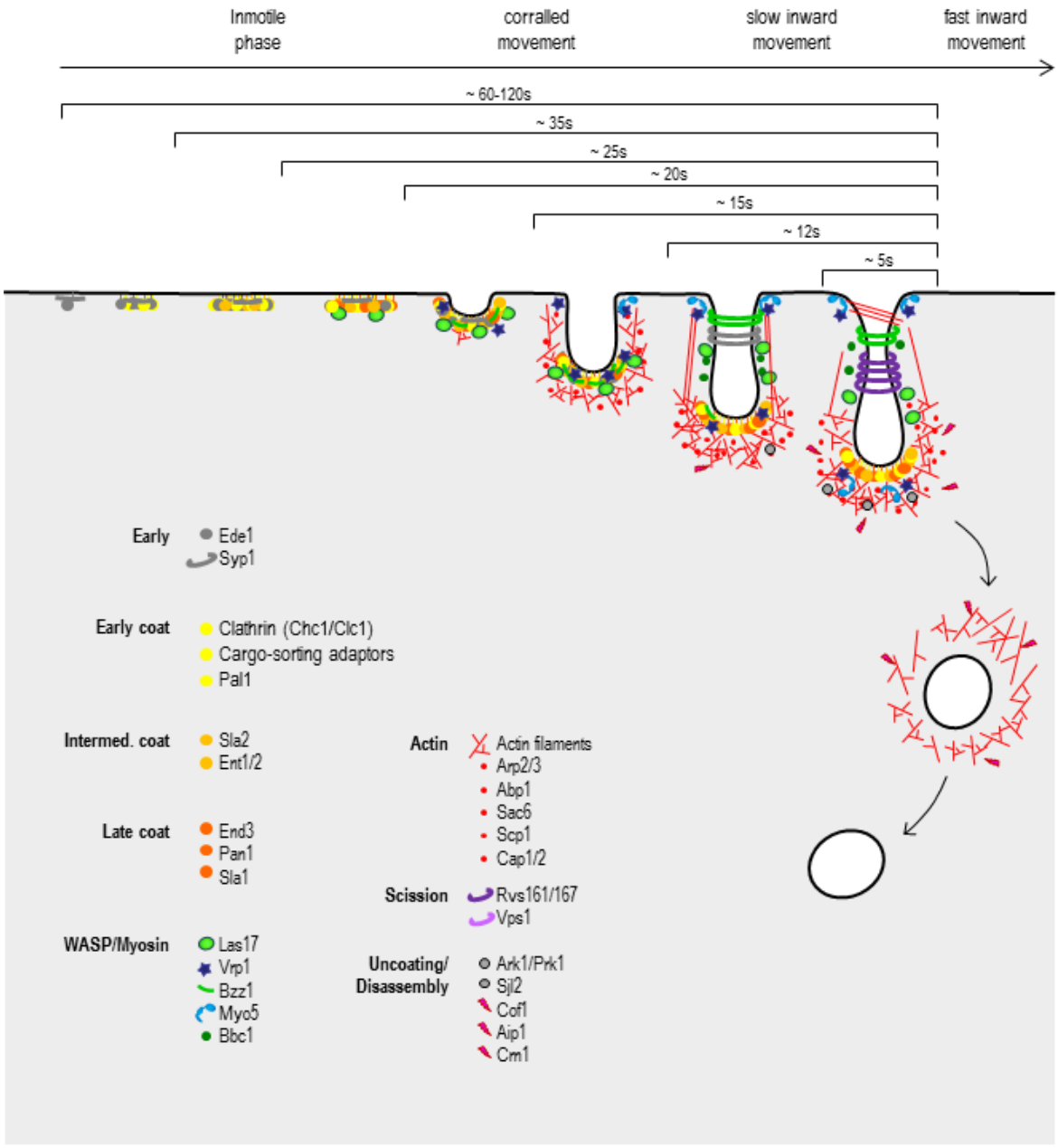

Figure 19. Model for the spatiotemporal organization of endocytic proteins on primary endocytic profiles at the plasma membrane.
The figure shows the spatiotemporal organization of yeast endocytic proteins along growing endocytic profiles based on the different studies cited in the text. The process can be dissected into different stages: sequential recruitment of the early, early coat, intermediate coat, and late coat modules on the flat plasma membrane; emergence of initial curvature after recruitment of the WASP/Myosin members Las17, Vrp1, and Bzz1; formation of an actin cap coupled with a corralled movement of the endocytic patch; elongation of the tubular invagination combined with the accumulation of myosin-I at the base of primary endocytic profiles and with a slow inward movement of the endocytic patch; narrowing of the tubular invagination that coincides with translocation of BAR proteins at the neck and requires the mechanochemical activity of myosin-I; scission of the endocytic profiles coupled with a fast inward movement; and disassembly of the endocytic coat followed by disassembly of the actin cap. See text for further details. This illustration has been adapted from Idrissi et al., 2012, Boettner et al., 2012; Weinberg and Drubin, 2012.

1.2.3.1.1.1. Assembly of the endocytic coat

Although our understanding of the sequence of events that trigger endocytic budding in *S. cerevisiae* has improved in the last few years, it is still unknown how the process is initiated in a particular region of the plasma membrane. But once an endocytic site is marked by the arrival of the early module, composed by Ede1 (the yeast homolog of the scaffolding protein Eps15) and Syp1 (FCHo1/2) (Boettner et al., 2009; Stimpson et al., 2009; Toshima et al., 2006), the rest of the components follow in a sequential manner. Immediately after the arrival of Syp1 and Ede1, the early coat module components -including clathrin, cargo-sorting adaptors (yeast AP-2 complex and Yap1801/2 (AP180/CALM)), and Pal1- appear at the cortical endocytic sites (Boettner et al., 2009; Carroll et al., 2012; Kaksonen et al., 2005; Newpher et al., 2005; Reider et al., 2009; Stimpson et al., 2009; Toshima et al., 2006). The early and the early coat components are classified into two different modules because, despite they arrive to the endocytic site at the same time, Ede1/Syp1 disassembles from the patch earlier than the coat (Boettner et al., 2009; Stimpson et al., 2009). Fluorescence-tagged cargo can be observed joining the cortical patch shortly after, and since the lifetime of the early proteins is highly variable, it has been proposed that a transition point might delay endocytic budding progression until the endocytic site is fully loaded with cargo (Carroll et al., 2012). The role of the proteins that participate in this early phase of endocytic budding is still being dissected. Cargo-sorting adaptors are multimeric or multidomain proteins that might simultaneously interact with lipids, membrane proteins destined for internalization, and clathrin (Maldonado-Baez and Wendland, 2006). The function of the early component Pal1 is still unknown (Carroll et al., 2012). Clathrin has classically been considered as a scaffold for cargo adaptors and a driving force for endocytic budding. However, in *S. cerevisiae* clathrin might rather have a regulatory role. Mutations in *CHC1* and *CLC1* (the genes that codify for clathrin heavy and light chain, respectively) only causes a 50 % decay in the endocytic uptake rate and does not affect the morphology of the primary endocytic profiles or the hemispherical position of the endocytic adaptors at the ultrastructural level (Idrissi et al., 2012; Payne et al., 1988). Depletion of clathrin reduces the number of endocytic sites and shortens the lifespan of some late endocytic proteins, suggesting that invagination of the plasma membrane might occur before the buds are loaded (Kaksonen et al., 2005; Newpher and Lemmon, 2006). Interestingly, the *ede1Δ* mutant seems to have a similar phenotype, indicating that both proteins regulate the same function (Kaksonen et al., 2005; Stimpson et al., 2009). In contrast Syp1 -which is a member of the membrane curvature sensing/bending F-BAR family- seems to have multiple functions: to recruit certain endocytic cargo, to constrict the invagination neck, to down regulate the NPA of Las17, and to localize endocytic budding close to the bud neck (Boettner et al., 2009; Idrissi et al., 2012; Kaksonen et al., 2005; Reider et al., 2009; Stimpson et al., 2009).

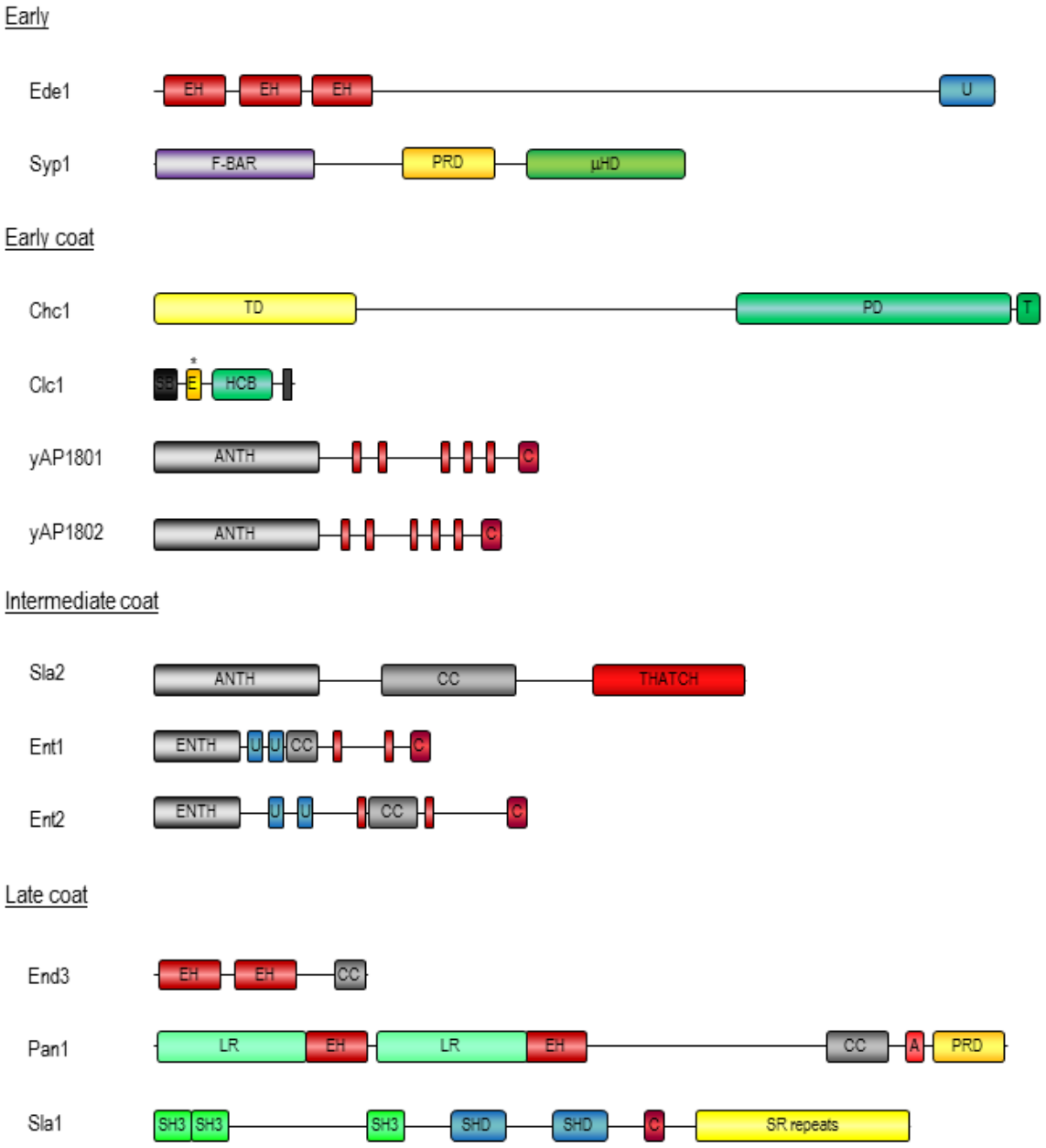

Figure 20. Domain organization of early and coat components.
Domain organization of the most representative endocytic proteins present in the early and coat modules. Several domains involved in protein-membrane interactions are shown. ANTH: AP180 N-terminal homology; ENTH: Epsin N-terminal homology; F-BAR: Fes/CIP4 homology-Bin/Amphiphysin/Rvs domain. A number of protein-protein interaction domains are also represented. EH: Eps15-homology domains, they bind to NPF motifs; red bars: asparagine-proline-phenylalanine-rich regions (NPF motifs); PRD: proline-rich domain, they bind to SH3 domains; SH3: Src homology 3 domain; CC: coiled-coil domain; U: ubiquitin associated domain, or UBA domain; CHB: heavy chain binding region; C: clathrin box domain, also involved in clathrin binding; TD: Chc1 terminal domain, required for the interaction with endocytic adaptors; PD: Chc1 proximal domain, it mediates binding to the clathrin light chain Clc1; T: trimerization domain; SB: Sla2-binding region; black bar: calmodulin-interacting motif; THATCH: talin-HIP1R/Sla2 actin-tethering C-terminal homology domain, it mediates interaction with actin filaments; µHD: µ-adaptin homology domain, it is involved in cargo sorting and/or Ede1 binding. Other domains depicted are: E: EF-hand or calcium-binding region; SHD: Sla1 homology domain; LR: long repeats; SR repeats: serine-arginine-rich regions.

Shortly after clathrin, the intermediate coat module arrives. This functional module comprises the proteins Sla2 (Hip1R) and the yeast epsins Ent1 and Ent2 (Kaksonen et al., 2003; Toret et al., 2008). Both Sla2 and Ent1/2 are multidomain proteins that are believed to function as linkers between endocytic proteins and the plasma membrane, because they bind to PIP_2 through their ANTH (AP180 N-terminal homology) and ENTH (Epsin N-terminal homology) domains, respectively. Deletion of both *ENT1* and *ENT2* genes cause synthetic lethality and analysis of ts alleles indicated the essential role of epsins in endocytosis (Wendland et al., 1999). Epsins interact with Ede1 and clathrin, and contain ubiquitin-interacting motifs that might mediate protein-protein interactions to stabilize the endocytic network. This function seems to be shared with Yap1801/2 (Aguilar et al., 2003; Dores et al., 2010; Maldonado-Baez et al., 2008; Wendland et al., 1999). Sla2 (see also section 1.1.3.3) also binds to actin filaments via its talin-like domain and to endocytic partners through a central coiled-coil domain, and thereby, it has been proposed to crosslinking the endocytic coat to the actin cytoskeleton (Kaksonen et al., 2003).

The recruitment of the intermediate coat module is closely followed by the arrival of the late coat module, formed by End3, Pan1, and Sla1, three proteins that might act as a complex to have adapting, scaffolding and actin regulatory functions, similar to intersectin in mammals. End3 is essential for endocytosis, and via its two EH (Eps15-homology) domains might interact with cargo adaptors and other endocytic proteins. Actually, mutation of the End3 EH domains causes a defect in coat maturation and endocytic internalization (Suzuki et al., 2012). Deletion of the two EH domains of Pan1 lead to controversial results, from a strong to a minor defect in coat maturation, depending on the study (Maldonado-Baez et al., 2008; Suzuki et al., 2012). Pan1 seems to perform a dual role in endocytosis, acting as a scaffolding protein and as nucleating promoting factor (see section 1.1.2.1.2.1). Similarly, Sla1 is a multifunctional cargo-sorting adaptor/scaffold that also functions as a regulator of actin dynamics at the endocytic patch (see below).

1.2.3.1.1.2. Actin-driven membrane deformation

The WASP homolog Las17 is recruited to the plasma membrane together with the late coat components (Kaksonen et al., 2003). Although Las17 possesses a strong nucleating promoting activity *in vitro* (see also section 1.1.2.1.2.1), actin polymerization only starts about 10 seconds after its recruitment, suggesting that its NPA activity is tightly controlled (Kaksonen et al., 2003; Rodal et al., 2003). The earlier arriving proteins Syp1 and Sla1, which are known Las17 inhibitors *in vitro* and colocalize with Las17 at the ultrastructural level at this initial phase, might maintain Las17 inactive (Boettner et al., 2009; Idrissi et al., 2012; Idrissi et al., 2008; Rodal et al., 2003). Likewise, the weak NPA of Pan1 might at this time be inhibited by Sla2 (Toshima et al., 2007).

About 10 seconds after the recruitment of Las17, Vrp1 (WIP) (see section 1.1.2.2) and Bzz1 (syndapin) joint the endocytic patch (Sun et al., 2006). Its arrival coincides with the initiation of an actin-dependent corralled movement of the endocytic coat. Interestingly, ultrastructural

analysis has recently demonstrated that the recruitment of these two factors coincides with the initial bending of the plasma membrane, indicating that the early and the coat modules remain flat until this stage (Idrissi et al., 2012). Bzz1 bears an F-BAR domain, which is predicted to recognize membrane curvature, and it has been shown to release the Sla1 inhibition on Las17. Therefore, it has been proposed that initial membrane curvature might prompt Vrp1 and Bzz1 recruitment, which in turn will initiate actin polymerization at sites of endocytic budding (Soulard et al., 2002; Sun et al., 2006). What generates initial curvature is still unknown, but recent result from our laboratory indicate that actin polymerization ignited by Las17 is unlikely to generate this initial bending since pharmacological treatment with the G-actin sequester Latrunculin A does not prevent assembly of the endocytic coat and the formation of shallow pits (Idrissi et al., 2012).

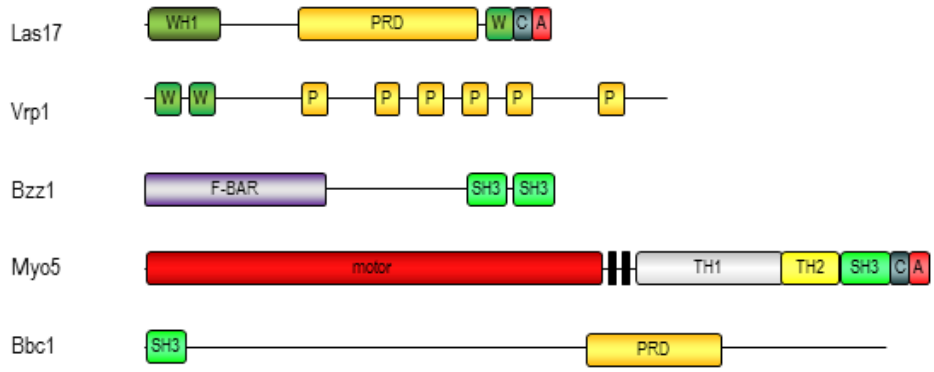

Figure 21. Domain organization of the WASP/Myosin module components.
Domain organization of the members of the WASP/Myosin module. F-BAR: Fes/CIP4 homology-Bin/Amphiphysin/Rvs domain, involved in membrane curvature sensing/bending; WH1: WASP-homology domain 1, involved in Vrp1 binding; W: WASP-homology domain 2, a G-actin binding region; PRD or P: proline-rich domain, they bind to SH3 domains; SH3: Src homology 3 domain; CA: Arp2/3 binding regions connecting and acidic; motor: myosin motor domain; black bars: IQ motifs, calmodulin-binding regions; TH1: tail homology 1, involved in lipid binding; TH2: tail homology 2.

At this initial stages of membrane invagination, Las17 and Pan1 localize on the endocytic coat, which covers the tip of the endocytic invaginations (Figure 19)(Idrissi et al., 2008), and trigger the formation of an actin cap (Galletta et al., 2008; Idrissi et al., 2012; Kaksonen et al., 2003). Actin polymerization occurs concomitant with the recruitment of a number of actin-binding proteins, which organize the endocytic actin structures. Those include the Arp2/3 complex (section 1.1.2.1.2), Abp1 (section 1.1.2.1.2.1), the yeast fimbrin Sac6, the transgelin homolog Scp1 (section 1.1.3.2), and the capping proteins Cap1/Cap2 (section 1.1.2.3). They all compose the endocytic actin module (Kaksonen et al., 2003; Kaksonen et al., 2005)(Gheorghe et al., 2008). Mutations of the essential components of the Arp2/3 complex or depletion of the actin bundling (Sac6 and Scp1) and capping proteins (Cap1 and Cap2) do not prevent actin assembly but impair productive internalization of the coat, indicating that the formation of an actin network with a defined architecture is essential to generate productive forces capable of driving membrane bending and vesicle scission (Kaksonen et al., 2005)(Gheorghe et al., 2008). Abp1

does not have a clear role in this task; instead, it seems to be important for the recruitment of coat disassembly factors that will function in a later step (see below).

About 10 seconds after the recruitment of Vrp1 and Bzz1, the second potent endocytic NPF, the type-I myosin Myo5 (probably also Myo3) and its interacting protein Bbc1 are recruited to the endocytic site. Arrival of the type I myosins coincides with a burst of massive actin polymerization and with the switch between the corralled and undirected movement of the coat to the onset of a slow directed inward movement, which corresponds to the growth of the endocytic tubular profiles from 70 to about 200 nm before fission (Jonsdottir and Li, 2004) (Sun et al., 2006) (Idrissi et al., 2008)(Idrissi et al., 2012) As explained in section 1.1.2.1.2.1, yeast type-I myosins are actin-dependent molecular motors with a strong NPA comparable to that of Las17, while Bbc1 negatively regulates actin polymerization mediated by both Myo5 and Las17 (Rodal et al., 2003; Sun et al., 2006). Live cell imaging analysis of Myo5 mutants have demonstrated that both the motor and nucleating promoting activities of Myo5 are strongly required for the slow inward movement of the coat whereas Pan1 and Las17 seem play a major role earlier in the process (Galletta et al., 2008; Sun et al., 2006). Ultrastructural studies have shown that on invaginations of intermediate length (about 70 nm in length), Las17 colocalize with its inhibitors Bbc1 and Syp1 at the neck of the profiles while Myo5 and Vrp1 accumulate at the base of the endocytic invaginations (Idrissi et al., 2012; Idrissi et al., 2008). The molecular interactions described at the ultrastructural levels suggest that at this point the NPA of Las17 on the endocytic coat is replaced by that of the Myo5/Vrp1 pair situated at the base of the invaginations. Indeed, fluorescence recovery after photobleaching (FRAP) analysis indicated that *de novo* addition of actin monomers actually occurs close to the plasma membrane as the coat moves into the cytosol (Kaksonen et al., 2003).The location of the active NPF Myo5/Vrp1 at this stage favors the accumulation of actin filaments with barbed ends facing the plasma membrane, which can then be pushed into the cytosol by the mechanochemical activity of the myosin head (Figure 23). If these actin filaments are firmly connected to the apical actin cap and the endocytic coat, the motor activity of the myosin is then well-positioned to power the directed movement of the coat into the cytosol.

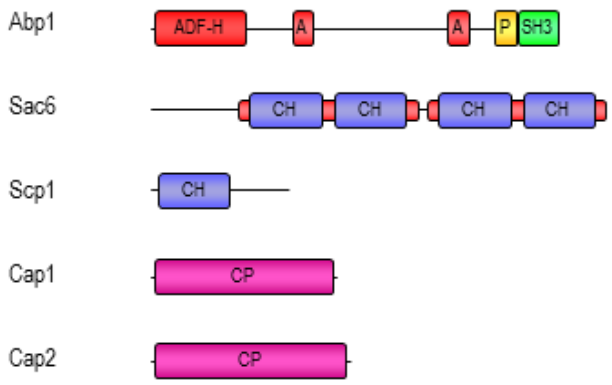

Figure 22. Domain organization of the actin module.
Domain organization of the representative members of the actin module, the multi-protein organization of the Arp2/3 complex is shown in Figure 4. ADF-H: actin-depolymerizing factor homology domain; CH: calponin-homology domain; A: Acidic domain, involved in the activation of the Arp2/3 domain; P: proline-rich domain, it binds to SH3 domain-containing proteins; SH3: Src homology 3 domain; CP: capping protein domain.

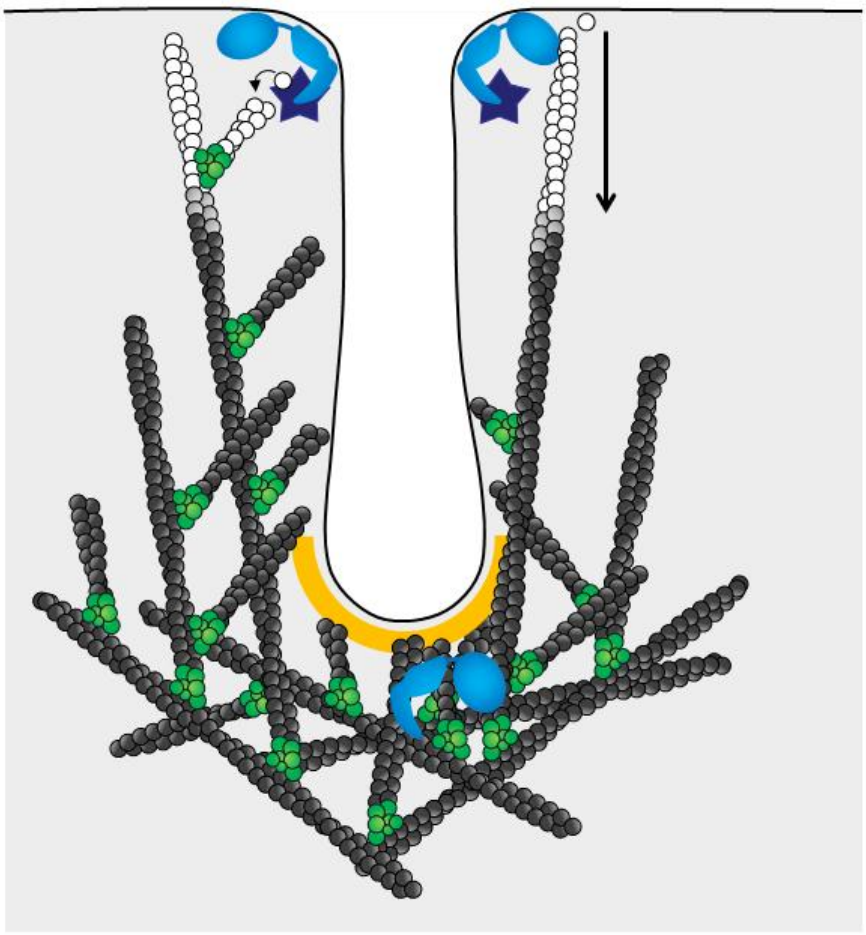

Figure 23. Model for the role of the mechanochemical and nucleating promoting activities of Myo5 in membrane deformation.
Myo5 (light blue) is located at the base of the invagination together with its co-activator Vrp1 (dark blue). The nucleating promoting activity of Myo5/Vrp1 might promote the accumulation of growing barbed ends near the plasma membrane (left), while the myosin motor activity could push the growing actin filaments away from the membrane (right). The arrow indicates movement's direction. A pool of Myo5 near the tip might serve to generate tension along the endocytic profile, which might be required for scission. The actin cap surrounding the endocytic tip is linked to the endocytic coat (yellow). The Arp2/3 complex is represented in green. See text for further details.

1.2.3.1.1.3. Vesicle scission

Arrival of the yeast amphiphysins Rvs161 and Rvs167 marks the time point when vesicle fission occurs, approximately when endocytic invaginations have elongated to reach 200 nm in length (Kukulski et al., 2011). Rvs167 and Rvs161 bear N-BAR domains that are predicted to recognize and stabilize membrane curvature (reviewed in (Rao and Haucke, 2011)). Yeast amphiphysins localize to the neck region of the endocytic invaginations, and have recently been shown to significantly contribute to narrow the neck of the endocytic invaginations (Idrissi et al., 2008; Kishimoto et al., 2011). However, the fluorescence microscopy experiments suggest that the

yeast amphiphysins are probably not the only molecules involved in fission. Null mutations of *RVS161* or *RVS167* do not prevent the slow inward movement but causes the retraction of the endocytic patch, a phenotype that has been attributed as a defect in vesicle scission (Kaksonen et al., 2005; Kishimoto et al., 2011). Interestingly though, retraction only occurs in 25 % of endocytic sites, whereas other endocytic profiles undergoes proper scission from the plasma membrane. In higher eukaryotes, the GTPase dynamin is required for the scission of clathrin-coated pits (Damke et al., 1994; Herskovits et al., 1993; van der Bliek et al., 1993). Several models have been proposed for the mechanism of membrane fission induced by dynamin polymerization around the neck of an endocytic pit. Upon dynamin polymerization, GTP hydrolysis coupled to a structural reorganization of the dynamin helix might promote scission by either constricting or stretching the membrane tubule; alternatively, dynamin helix disassembly after GTP hydrolysis might promote membrane destabilization and produce fission (reviewed in (Ferguson and De Camilli, 2012)). Although purified dynamin is sufficient to trigger membrane scission in cell-free studies (Bashkirov et al., 2008; Pucadyil and Schmid, 2008; Roux et al., 2006), other factors might also cooperate to support fission *in vivo*. In fact, dynamin interacts with a number of BAR-domain containing and actin regulatory proteins, and regulate its recruitment at endocytic sites in a mechanism that depends on the GTPase cycle (Ferguson and De Camilli, 2012; Taylor et al., 2012). In yeast, the role of dynamin in the scission of clathrin coated vesicles at the plasma membrane is still controversial. The dynamin-like protein Vps1 has recently been shown to join at least some endocytic patches, and two different studies report that depletion of this protein exacerbates the fission defects of amphiphysin mutants (Nannapaneni et al., 2010; Smaczynska-de et al., 2010). However, other studies seem to indicate that this is not the case (Kishimoto et al., 2011).

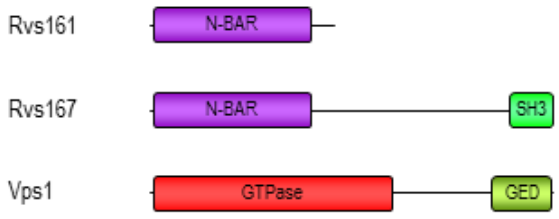

Figure 24. Domain organization of the scission module.
Domain organization of the yeast amphiphysins Rvs161 and Rvs167, and of the yeast dynamin-like protein Vps1. N-BAR: N-terminal amphipathic helix-Bin/Amphiphysin/Rvs domain; SH3: Src homology 3 domain, it binds to proline-rich regions; GTPase: dynamin-like GTPase; GED: GTPase effector domain.

Recent results indicate that a combination of different biochemical activities such as membrane shaping by BAR domains, lipid reorganization, and actin polymerization might cooperate to achieve membrane fission. In mammalian cells, it has been recently shown that depletion of dynamin cause an elongation of the neck at clathrin-coated pits that very much reminds the primary endocytic profiles found in yeast: a tubular structure stabilized by actin polymerization and accumulation of BAR-containing proteins (Ferguson et al., 2009; Idrissi et al., 2008). In *S. cerevisiae*, mutations in the N-BAR protein Rvs167 shows a synergistic defect in tubule

constriction and membrane scission when combined with the F-BAR containing protein Bzz1 (Kishimoto et al., 2011). Similarly, depletion of the actin nucleating promoting activity of Myo5 and Las17 also exacerbate the fission defects of the yeast amphiphysin mutants (Kishimoto et al., 2011). The possibility that type I myosins have a second endocytic function in vesicle scission is consistent with the observation that, actin and Myo5 reorganize to form two distinct apical and basal structures in very long invaginations (>110 nm in length), previous to fission (Idrissi et al., 2008). The actin network located in the base of the invagination might form a ring-like structure to promote constriction of the invagination neck (Idrissi et al., 2008; Mulholland et al., 1994(Idrissi et al., 2012). The distal actomyosin network might function to promote the tension required for scission (Idrissi et al., 2008)(Roux et al., 2006). In the very long invaginations -preceding scission- Las17 locates at the invagination neck (Idrissi et al., 2008). Reactivation of the NPF activity of Las17 at this point might assist membrane fission and/or push the endocytic invagination into the cytoplasm, as proposed for mammalian cells (Collins et al., 2011; Yarar et al., 2005). Disassembly of the Las17 inhibitor Syp1 from the endocytic neck before scission (see above) and the arrival of the amphiphysins, which have been recently found to activate N-WASP in metazoan cells (Yamada et al., 2009), supports a possible reactivation of Las17 at this point.

Besides BAR-containing protein accumulation and actin polymerization, lipid reorganization along the tubular endocytic profiles might also be crucial to achieve scission. The phospholipid PIP_2 is concentrated at endocytic sites and disappears concomitantly with scission, shortly after the recruitment of the PIP_2 phosphatase Sjl2 (yeast synaptojanin) (Sun et al., 2007). Genetic analysis of synaptojanin mutants and mathematical modeling has led to the proposal that PIP_2 might be hydrolyzed at the tip of the endocytic site but not at the tubular neck -which is protected by BAR proteins-, creating a lipid phase segregation that might squeeze the endocytic profile (Liu et al., 2006; Liu et al., 2009; Sun et al., 2007).

1.2.3.1.1.4. Uncoating

After pinching off from the plasma membrane, the internalized vesicle travels into the cytosol while undergoing coat and actin disassembly. The actin module component Abp1 recruits several coat disassembly factors, such as the PIP_2 phosphatase Slj2 (see above), and the Ser/Thr protein kinases Ark1/Prk1 (Cope et al., 1999; Stefan et al., 2005; Toret et al., 2008). PIP_2 accumulates at the endocytic sites, and it is probably important for the recruitment of the ENTH domain containing proteins Ent1 and Ent2, and ANTH domain containing proteins Sla2 and yAP1801/1802 to the endocytic sites (Sun et al., 2007). Recruitment of Sjl2 might favor detachment of these coat proteins from the lipid bilayer, since deletion of the synaptojanin leads to a defect in the uncoating of Sla2, Ent1, and Ent2, but does not affect the uncoating of Sla1 (Toret et al., 2008). Similarly, Ark1/Prk1-mediated phosphorylation of the coat proteins Sla1 and Pan1 disrupt their interaction, which may lead to their disassembly from the vesicle (Zeng and Cai, 1999; Zeng et al., 2001). In fact, inhibition of Ark1/Prk1 activity results in an accumulation of Sla1- and actin-labeled endocytic vesicles (Sekiya-Kawasaki et al., 2003).

Other factors involved in actin disassembly, such as cofilin (see section 1.1.2.4), Aip1 (see section 1.1.2.3), and coronin (see section 1.1.2.1.2), are also recruited about this time (Lin et al., 2010; Okreglak and Drubin, 2007). Comparison of mutant alleles indicates that cofilin plays a more important role than Aip1 and coronin in actin patch disassembly after endocytic internalization. In addition these experiments show that internalization is delayed in cofilin mutants alleles, a phenotype that has been attributed to a possible decrease in the G-actin pool due to defects in actin filament turnover (Lin et al., 2010; Okreglak and Drubin, 2007) or a decrease in actin polymerization due to a reduced number of available barbed ends (Idrissi 2002).

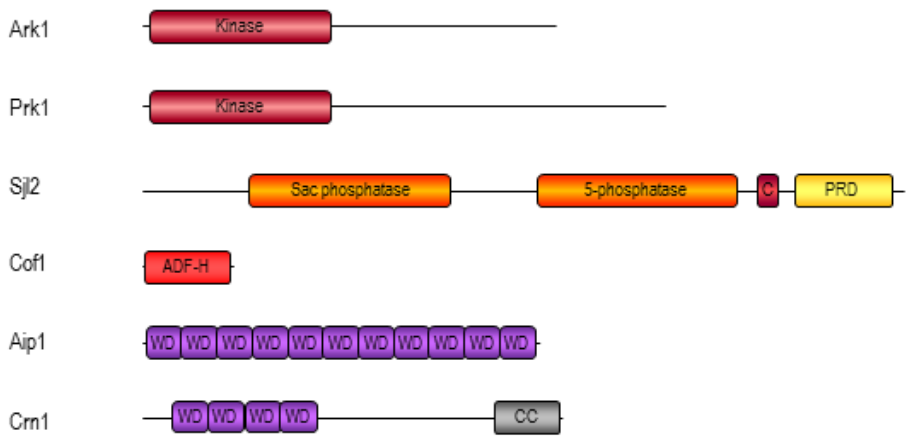

Figure 25. Domain organization of the uncoating/disassembly module.
Domain organization of representative members of the uncoating/disassembly module. Kinase: protein kinase domain. 5-phosphatase: PI(4,5)P2-5-phosphatase domain; Sac phosphatase: PI(4)P-phosphatase region; C: clathrin box motifs; PRD: proline-rich domain, it binds to SH3 domain-containing proteins; ADF-H: actin-depolymerizing factor homology domain; WD: WD40 repeats, region rich in tryptophan and aspartic acid; CC: coiled-coil domain.

1.2.3.1.2. Evidence for an actin-dependent but clathrin-independent endocytic pathway in yeast.

In higher eukaryotic cells, several clathrin-independent endocytic pathways have been described, including phagocytosis, macropinocytosis, caveolae-mediated endocytic uptake, or clathrin- and dynamin-independent carrier/glycosylphosphatidylinositol-anchored protein-enriched early endosomal compartment (CLIC–GEEC) pathway, among others (reviewed in (Mayor and Pagano, 2007)). In yeast though, the classical clathrin- and actin-mediated endocytic pathway was the only pathway identified until the recent finding of a novel clathrin-independent endocytic pathway (Prosser et al., 2011). This novel pathway does not require functional clathrin, protein adaptors, Arp2/3 complex, or actin bundling proteins, but involves the GTPase Rho1 and the formin Bni1 (Prosser et al., 2011). It is still not known the

contribution of this endocytic pathway in cells with an intact classical clathrin- and actin-mediated endocytic pathway, nor are the cargoes that might enter through this endocytic pathway (Prosser et al., 2011).

1.2.3.1.2. Post internalization roles of actin in the endocytic traffic: retrograde traffic of endocytic vesicles, endosome motility, and homotypic vacuole fusion.

The actin cytoskeleton also participates in post-internalization traffic of released vesicles, although the molecular mechanisms that drive these movements are far from being understood (Figure 26). After scission from the plasma membrane, the endocytic vesicles travel into the cytosol following an apparently random trajectory (Kaksonen et al., 2003). Whether Arp2/3 mediated actin assembly is required for this undirected movement is unknown. Upon membrane fission, Myo5 and Las17 remain attached at the plasma membrane, the NPF activity of Pan1 is inhibited via phosphorylation by Ark1/Prk1 kinases, and depletion of Abp1 does not prevent vesicle movement. However, a fraction of Las17 and/or Myo5 below current detection limits, or a still uncharacterized NPF, might travel with the vesicle. Alternatively, actin disassembly by the coordinated activities of cofilin, Aip1, coronin and Srv2 might also propel the vesicle into the cytosol in a random movement (Jonsdottir and Li, 2004; Kaksonen et al., 2003; Kaksonen et al., 2005; Sun et al., 2006)(Toshima et al., 2005). In mammalian cells though, newly formed endocytic vesicles moving at the tip of actin tails have been observed (Kaksonen et al., 2000; Merrifield et al., 1999).

After the first undirected trajectory, a subpopulation of the newly formed endocytic vesicles undergoes a directed linear retrograde movement attached to the actin cables (Huckaba et al., 2004; Toshima et al., 2006). In mammalian cells, the type VI myosin Myo6 facilitates the transport on endocytic vesicles towards the cell interior (Aschenbrenner et al., 2003). However, *S. cerevisiae* does not possess any member of type-VI myosins, the only known class of myosins found to move towards the pointed end of the actin filament. Further, the vesicles do not make net movement along the actin cables but rather follow the retrograde actin cable flow (Huckaba et al., 2004). It is still unknown how the endocytic vesicle associates with the actin cables. Fusion of endocytic vesicles to early endosomes occurs within a few seconds after scission. The efficient docking and fusion of endocytic vesicles with early endosomal compartments is prompted by the retrograde movement of the vesicles along the actin cables combined with the anterograde movement of early endosomes towards the cortical endocytic sites (Toshima et al., 2006). This forward movement of the endosomes along actin cables could be driven by a myosin, but the molecular motor responsible has not been identified yet. Strikingly, the type V myosins Myo2 and Myo4, which drive the anterograde transport of most cellular structures along actin cables, do not seem to participate in the translocation of the early endosomes (Toshima et al., 2006).

Actin might also be involved for movement and/or fusion of endocytic compartments in *S. cerevisiae*. Live cell imaging of the plasma membrane receptor Ste2 fused to GFP used to label intracellular compartments -that were later shown to correspond to late endosomes- has shown

that the NPF activity of Las17 is required to sustain late endosome motility, and neither actin cables nor type V myosins are needed (Chang et al., 2005; Chang et al., 2003)(Toshima et al., 2006). A caveat on this observation is that neither Las17 nor the Arp2/3 complex have ever been observed in late endocytic compartments, thought they might be present below the detection limits (Chang et al., 2005). In mammalian cells, short-range movement of endosomes at actin-rich regions also seems to rely on Arp2/3- and/or formin-dependent actin polymerization (Durrbach et al., 1996; Gasman et al., 2003; Llado et al., 2008; Southwick et al., 2003; Taunton et al., 2000), while long-range endosome transport occurs via microtubules (reviewed in (Soldati and Schliwa, 2006)).

Wild type budding yeast cells contain 1 to 3-4 vacuoles at steady state, which undergo constant homotypic fusion and fission (Wickner, 2002). Several proteins involved in actin regulation, such as Vrp1 and a subunit of the Arp2/3 complex were identified in a genetic screen conceived to uncover non-essential genes involved in vacuole fusion, while point or null mutations introduced into actin and other actin-associated proteins –members of the Arp2/3 complex, Las17, Vrp1, Myo5, and Sac6- also resulted in a defective homotypic vacuole fusion (Eitzen et al., 2002; Seeley et al., 2002). Actin disassembly seems to be important in the early steps of the vacuole fusion pathway, while actin polymerization at the vertex of docked vacuoles, where fusion occurs, is required to drive the final stage of homotypic fusion (Eitzen et al., 2002; Wang et al., 2002). Similarly, actin might also be involved in the transport to and fusion with lysosomes in mammalian cells (Durrbach et al., 1996; Kjeken et al., 2004; van Deurs et al., 1995).

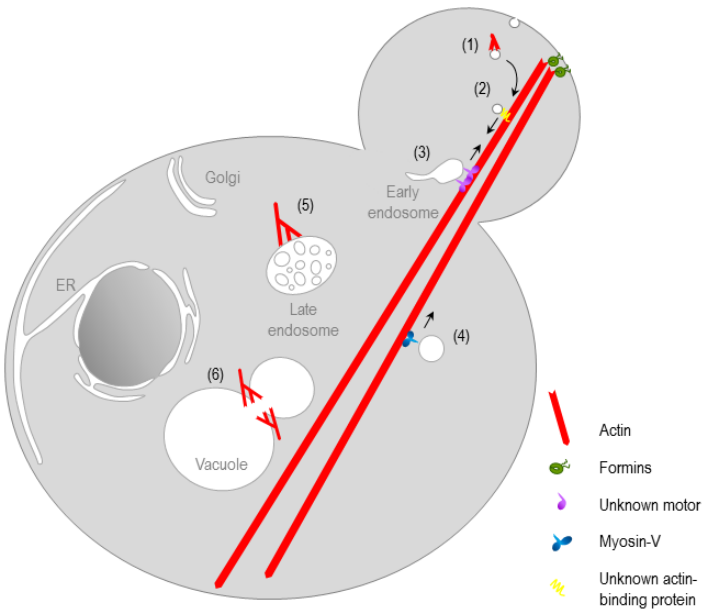

Figure 26. Model for the post-internalization roles of actin in the endocytic pathway.
Upon vesicle release from the plasma membrane vesicles travel following a random trajectory, attached to uncharacterized actin structures (1). A subpopulation of the endocytic vesicles then travel to towards the cell center connected by an unknown factor to the actin cables assembled by formins (2). Early endosomes move towards the endocytic vesicle -to which they fuse- by an unknown molecular motor (3). Type-V myosins could also carry recycled cargo towards the plasma membrane (4). Actin polymerization associated to late endosomes might also contribute to organelle motility (5). Arp2/3-dependent dynamic actin structures are also important for homotypic vacuoles fusion in budding yeast (6). Arrows indicate movement direction. See text for further details. This illustration has been adapted from Girao et al., 2008.

2. ANTECEDENTS AND OBJECTIVES

2.1. Antecedents

2.1.1. The assembly of Myo5-induced actin *foci in vitro* recapitulates the assembly of actin structures required for endocytic budding *in vivo*

2.1.1.1. Assembly of Myo5-induced actin *foci* is temperature and cytosol-dependent

The nucleating promoting activity of the type I myosin Myo5 plays an important role in endocytic internalization (Sun et al., 2006). This activity must be tightly regulated to generate the productive forces required for actin-driven membrane deformation (see introduction, sections 1.1.2.1.2.1, 1.1.4.3, and 1.2.3.1.1.2). In order to study this matter, our laboratory established an *in vitro* actin polymerization assay that allows monitoring the assembly of actin structures induced by the C-terminal extension of Myo5 (C_{ext}, amino acids 984 to 1219) in the presence of cell extracts (Geli et al., 2000; Idrissi et al., 2002). Briefly, a Myo5-C_{ext} recombinant fusion protein is purified from *E. coli*, bound to glutathione-Sepharose beads, and incubated at 26ºC in the presence of yeast extract, an ATP regeneration system, and rhodamine-labeled actin (see materials and methods, section 6.6). Building of actin structures on the coated beads was directly examined by fluorescence microscopy (Figure 27). Strikingly, although the beads were homogeneously covered by Myo5-C_{ext}, the rhodamine-actin signal appeared as discrete actin *foci* that grew centrifugally (Idrissi et al., 2002).

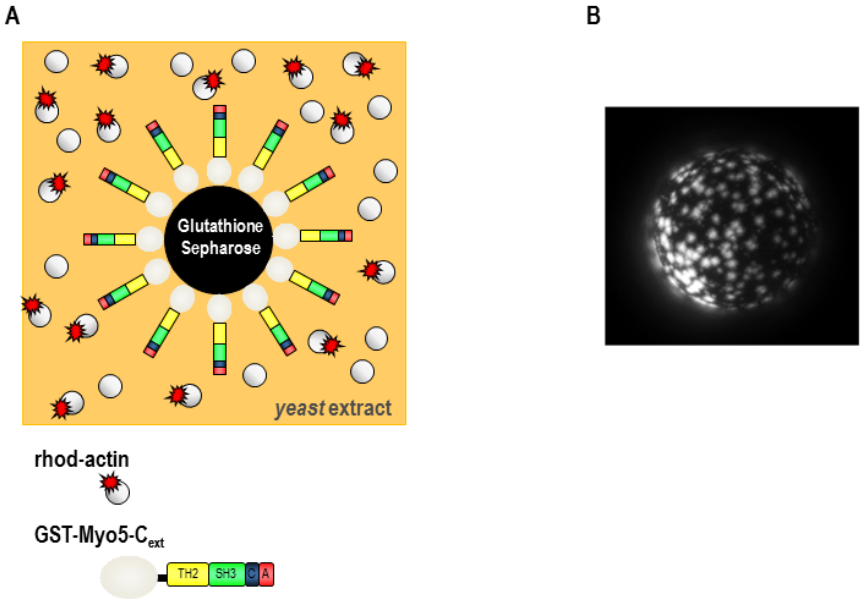

Figure 27. Myo5-C_{ext} induces the formation of actin *foci* on the surface of glutathione-Sepharose beads.
(A) Illustration describing the Myo5-C_{ext}-induced *in vitro* actin polymerization assay. See materials and methods for details. (B) Fluorescence micrograph of a GST-Myo5-C_{ext} –coated glutathione-Sepharose bead incubated with yeast extracts from wild type cells and 1μM rhodamine-labeled actin for 10 min at 26°C.

Initial characterization of the process indicated that the actin *foci* contained filamentous actin, since they could be decorated with fluorescently labeled phalloidin. Building of the actin structures required *de novo* actin polymerization given that depletion of filamentous actin from the yeast extracts by ultracentrifugation did not prevent their assembly, and addition of the actin depolymerizing drug Latrunculin A completely impeded its appearance (Geli et al., 2000; Idrissi et al., 2002). The actin structures were not assembled simply by the recruitment of actin filaments preformed in the yeast extract, because no actin *foci* were observed when actin was allowed to polymerize in the absence of GST-Myo5-C_{ext}-coated glutathione-Sepharose, and beads were subsequently added to allow binding at 0°C (Idrissi et al., 2002). Finally, the formation of the actin structures appeared to be a complex process that required the presence of one or more cytosolic components, since they were not assembled when buffer instead of yeast extract was used in the reaction (Geli et al., 2000).

2.1.1.2. Assembly of Myo5-induced actin *foci* requires the Myo5 TH2, SH3 and acidic domains and the presence of the Arp2/3 complex and Vrp1, but does not require Las17 or Pan1

The morphology of the Myo5-induced actin *foci* was reminiscent of the yeast endocytic actin patches (see introduction, section 1.2). Consistent with the hypothesis that the assay reconstituted the formation of an endocytic actin structures and with the role of the Arp2/3 complex in endocytosis, yeast extracts prepared from *arp2-2* and *arp3-63* mutants were unable to induce Myo5-dependent actin polymerization *in vitro* (Geli et al., 2000; Idrissi et al., 2002). Addition of purified Arp2/3 reconstituted the ability of the mutant yeast extracts to sustain Myo5-induced actin polymerization (Idrissi et al., 2002)(Figure 28). Activation of the Arp2/3 complex was likely triggered by Myo5 and not by other NPFs that might be recruited by direct or indirect interaction with the myosin, because the structures were still formed when yeast extracts from *las17Δ* or *pan1-4* mutant cells were used ((Idrissi et al., 2002), F. Idrissi personal communication), but deletion of the Myo5 CA domain completely abolished the nucleation of actin structures on the surface of the beads (F. Idrissi and V. Paradisi, personal communication).

Even though the presence of functional Arp2/3 complex in the extracts was clearly required for the formation of actin patch like structures *in vitro*, mutational analysis of the Myo5 C_{ext} suggested that other cytosolic factor might be required. Besides the CA domain, directly involved in the activation of the Arp2/3 complex, the Myo5 SH3 and TH2 domains were also required to build the actin structures on the myosin coated beads (Geli et al., 2000). Binding of Vrp1 to the SH3 domain of Myo5 also turn out to be essential to build up the actin *foci in vitro*. Thus, a point mutation in the Myo5 SH3 domain that completely abolished the Myo5-Vrp1 interaction (Myo5-C_{ext}-W1123S) or depletion of Vrp1 prevented building of the actin structures (Geli et al., 2000). The molecular function of the TH2 domain has not been elucidated yet. The TH2 domain of protozoal type-I myosins is thought to provide an ATP-insensitive actin filament-binding site (Brzeska et al., 1988; Doberstein and Pollard, 1992). However, actin pelleting

assays using different Myo5 fragments indicated that deletion of the TH2 domain does not affect the interaction of Myo5 with F-actin (Geli et al., 2000). Subsequent analysis of the myosin-I-induced actin polymerization using a pyrene-actin assay and purified components indicated that, besides the WH2 domain of Vrp1, actin and the Arp2/3 complex, only the CA domain of the myosins-I was strictly required to trigger actin polymerization ((Lechler et al., 2001; Sun et al., 2006), see section 1.1.2.1.2.1). However, this assay only monitors incorporation of monomeric actin into filaments. Thus, it is likely that the TH2 domain participates in the assembly or stabilization of more complex endocytic actin structures (see below).

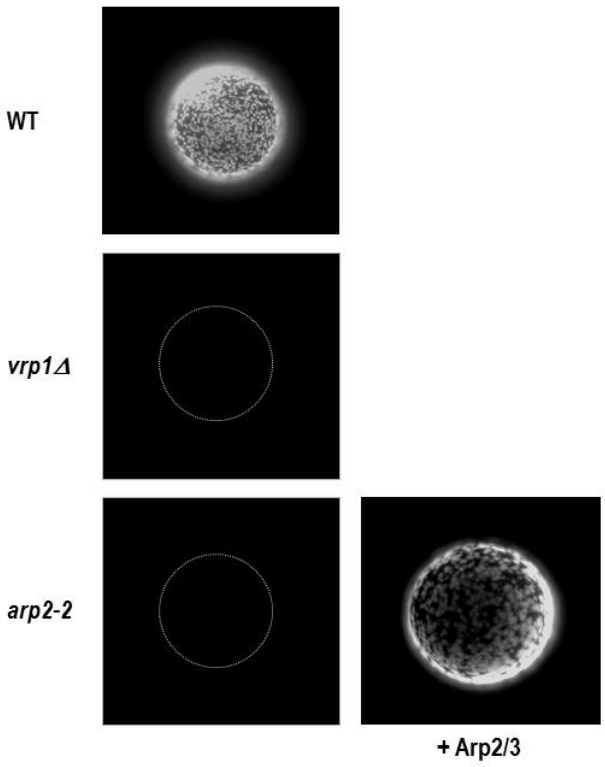

Figure 28. The Myo5 co-activator Vrp1 and the Arp2/3 complex are required for the formation of Myo5-Cext-mediated actin *foci*.
Fluorescence micrographs of glutathione-Sepharose beads coated with GST-Myo5-C_{ext} incubated with either *WT* (RH2881), *vrp1Δ* (SCMIG48), or *arp2-2* (RH4165) yeast extracts (left) or GST-Myo5-C_{ext} pre-bound to purified Arp2/3 and *arp2-2* (RH4165) yeast extracts (right), plus 1μM rhodamine-labeled actin for 10 min at 26°C. These data were taken from (Idrissi et al., 2002) and (Geli et al., 2000).

The results strongly support the hypothesis that Myo5 immobilized on the surface of Sepharose beads can trigger Arp2/3-mediated actin polymerization and that development of the myosin full NPA requires binding to Vrp1.

2.1.1.3. The composition of the Myo5-induced actin *foci* recapitulates that of the endocytic actin patches *in vivo*

Preliminary analysis of the composition of Myo5-C_{ext}-induced actin *foci* also suggested that these structures specifically recapitulated the yeast endocytic actin patches (see introduction, section 1.2.3.1.1.2.). Antibodies against the endocytic actin patch component Abp1 were able to decorate the Myo5-C_{ext} induced actin *foci*, while antibodies against the actin cables component Tpm1 could not (Idrissi et al., 2002), see Figure 29.

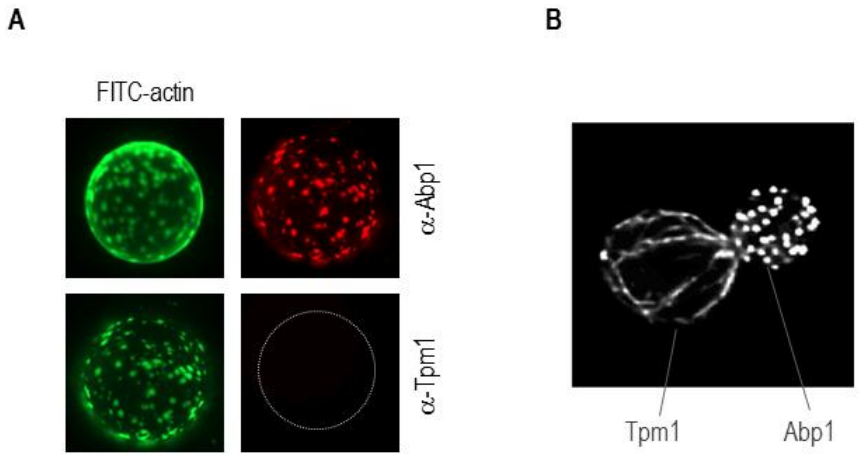

Figure 29. The Myo5-C_{ext}-induced actin *foci* contain the actin patch component Abp1 but not the actin cable component Tpm1.
(A) Fluorescence micrographs of glutathione-Sepharose beads coated with GST-Myo5-C_{ext} incubated with a wild type (RH2881) yeast extract and 1μM FITC-labeled actin for 10 min at 26ºC, fixed, and decorated with α-Abp1 or α-Tpm1 antibodies. This data was taken from (Idrissi et al., 2002). (B) Fluorescence image of a *S. cerevisiae* cell chemically fixed and stained with rhodamine-phalloidin to visualize the filamentous actin structures showing the localization of the actin cables component Tpm1 and the actin patch component Abp1. Image obtained from Amberg, 1998.

To further characterize the actin *foci* generated *in vitro*, the reaction was scaled up and the proteins bound to the beads under conditions that allowed actin polymerization were identified by mass spectrometry. Several endocytic proteins including Sla1, Bbc1, Abp1, Sac6, and Crn1 accumulated in these structures (M. Geli, personal communication). Analysis of their localization using yeast extracts from cells in which these proteins with GFP indicated that the members of the endocytic actin or actin disassembly modules –Abp1, Sac6, and Crn1- co-localized with Myo5-C_{ext}-induced actin *foci*, whereas the endocytic coat component Sla1 and the WASP/Myosin module factor Bbc1 localize on the surface of Myo5-C_{ext}-covered beads. Actually Bbc1 act as a negative modulator of the actin *foci* growth and it was excluded from the actin structures (see section 1.1.2.1.2.1) (F. Idrissi, personal communication). A summary of this data is shown in Figure 30.

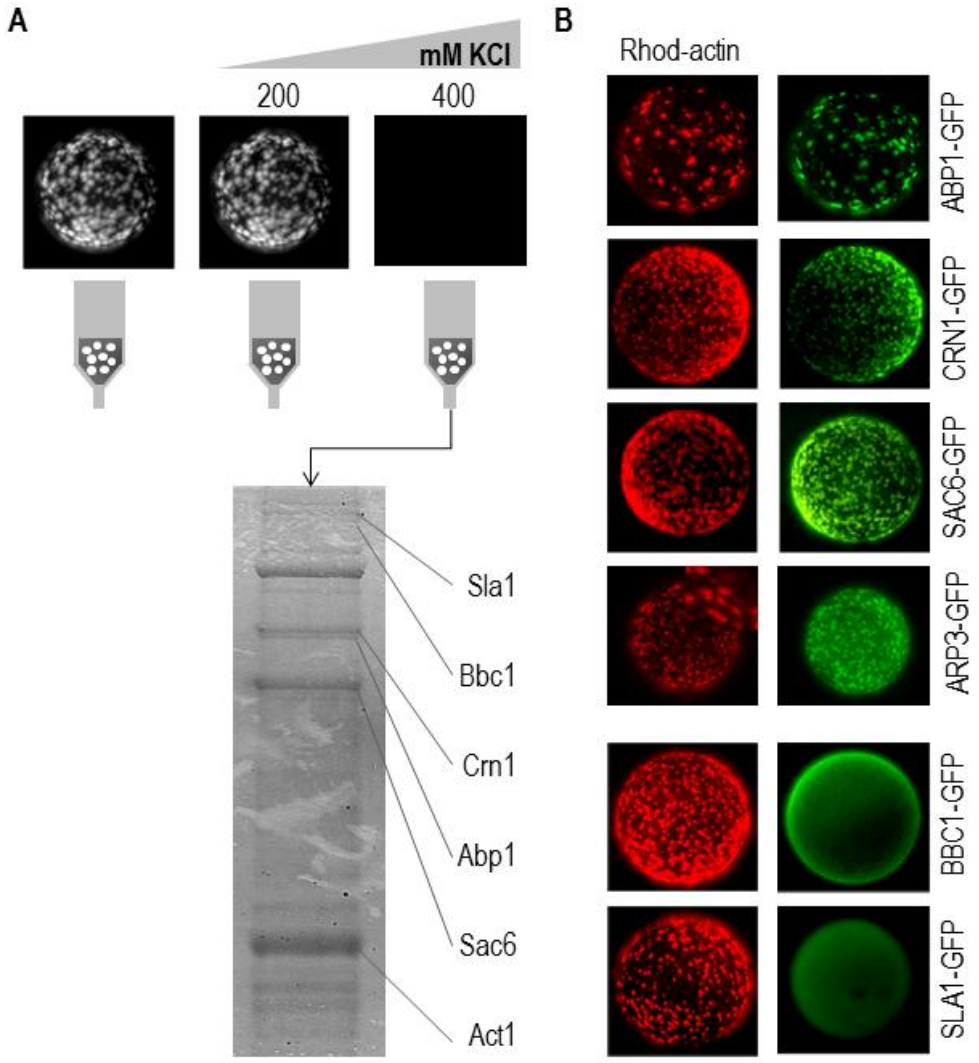

Figure 30. The composition of Myo5-C_{ext}-induced actin *foci* recapitulates that of the endocytic actin patch.
(A) Fluorescence micrographs of glutathione-Sepharose beads coated with GST-Myo5-C_{ext} incubated with a wild type (RH2881) yeast extract and 1µM rhodamine-labeled actin for 10 min at 26ºC, subsequently washed to remove the yeast extract, and finally treated with the indicated concentrations of KCl to collect the components of the actin patches (upper panel). The lower panel displays a Coomassie stained SDS-PAGE gel showing multiple bands that correspond to actin patch components and the proteins identified by mass spectrometry. (B) Fluorescence micrographs of glutathione-Sepharose beads coated with GST-Myo5-C_{ext} incubated with yeast extract from wild type cells transformed with centromeric plasmids expressing GFP-tagged version of the genes indicated under their own promoters and 1µM rhodamine-labeled actin for 10 min at 26ºC. The experiments shown here were done by M. Geli and F. Idrissi.

2.1.2. The assembly of Myo5-induced actin *foci is* down-regulated by phosphorylation

The observation that the actin *foci* appeared as discrete structures while Myo5-C_{ext} homogeneously covered the beads and neither actin nor the Arp/3 complex were limiting in the assay, strongly suggested that the process might be regulated by cytosolic components (Idrissi et al., 2002). In order to study whether the formation of Myo5-induced actin *foci* was regulated by phosphorylation, the former lab member Dr. Bianka Grosshans performed a pharmacological analysis of the assay. As shown in Figure 31, the presence of a cocktail of kinase inhibitors in

the Myo5-C_{ext}-induced actin polymerization assay strongly enhanced the assembly of actin structures on the surface of the beads, whereas addition of phosphatase inhibitors significantly inhibited the process (Dr. Bianka Grosshans, unpublished results). These results suggested that one or more phosphatases might be required to initiate the formation of the Myo5-C_{ext}-induced actin-patch-like structures while one or more protein kinases might down-regulated their assembly.

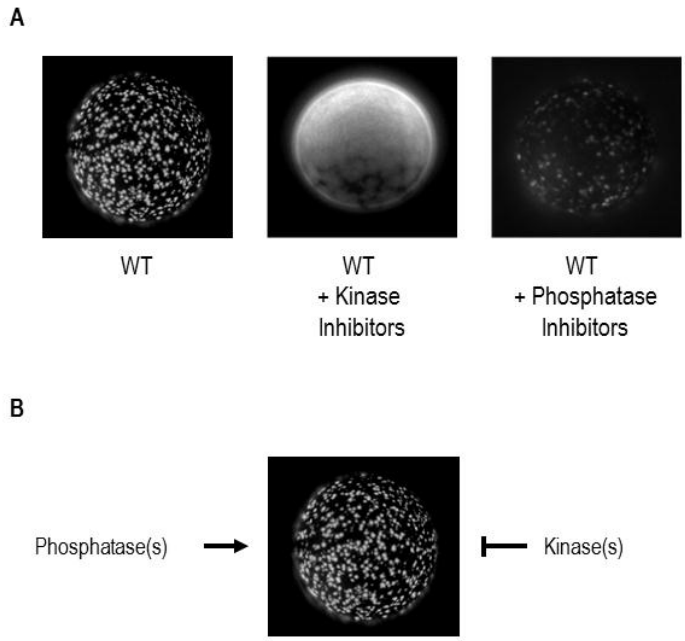

Figure 31. Myo5-C_{ext}-mediated actin *foci* formation seems to be negatively regulated by phosphorylation.
(A) Fluorescence micrographs of glutathione-Sepharose beads coated with GST-Myo5-C_{ext} incubated with a wild type (RH2881) yeast extract and 1µM rhodamine-labeled actin for 10 min at 26ºC either in the absence (WT) or in the presence of kinase inhibitors (WT+KI) or phosphatase inhibitors (WT+ PPI). (B) Schematic drawing of the working hypothesis that Myo5-C_{ext}-mediated actin *foci* formation is up-regulated by protein phosphatase(s) and down-regulated by protein kinase(s). This data was obtained B. Grosshans.

2.1.3. Myo5 S1205 is phosphorylated by CK2 *in vitro*

In order to study whether Myo5-C_{ext} was itself phosphorylated in the assay, GST-Myo5-C_{ext} recombinant fusion protein was bound to glutathione-Sepharose beads and incubated at 26ºC in the presence of yeast extract, γ-^{32}P-ATP, and unlabeled actin. The GST-Myo5-C_{ext}–coated glutathione-Sepharose beads were then recovered and incorporation of radioactivity measured by autoradiography. As shown in Figure 32, Myo5-C_{ext} was heavily phosphorylated by cytosolic factor(s) under the same conditions used for the *in vitro* actin polymerization assay. N-terminal truncation of the Myo5-C_{ext} fragment mapped the phosphorylated amino acid(s) within the most C-terminal portion of the protein, in an area comprising amino acids 1142 to 1219 (Dr. Bianka Grosshans, unpublished results).

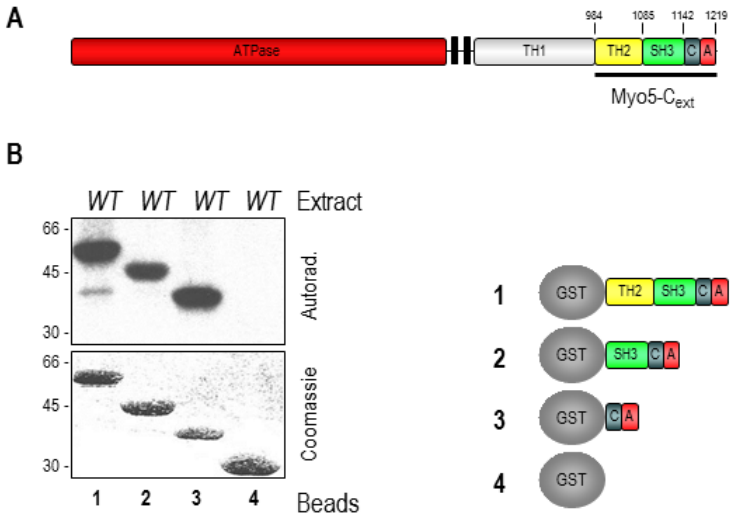

Figure 32. The Myo5-C_{ext} region comprising the central and acidic domains is phosphorylated *in vitro*.
(A). Domain organization of Myo5 (B) Autoradiography (left-upper panel) of a Coomassie stained SDS-PAGE gel (left-lower panel) showing GST fused to the indicated N-terminal truncations of Myo5-C_{ext} (1 to 3) or GST alone (4), depicted in the right panel. Glutathione-Sepharose beads coated with the indicated proteins were incubated with a wild-type yeast (RH2881) extract and γ-^{32}P-ATP for 30 min at 26°C. Beads were pelleted, rinsed several times and boiled in the presence of SDS-PAGE sample buffer. GST and GST fusion proteins were separated in a 12.5 % SDS-PAGE gel and analyzed by Coomassie staining to demonstrate equivalent protein loading and autoradiography to demonstrate protein phosphorylation. This experiment was done by Dr. B. Grosshans.

Sequence analysis of this polypeptide identified of a phosphorylatable serine (S1205) (Figure 33A). Exchanging S1205 into alanine abolished Myo5-C_{ext} phosphorylation *in vitro*, indicating that Myo5 S1205 was the residue predominantly phosphorylated in the assay (Dr. Bianka Grosshans unpublished results; Figure 33B). Analysis of the S1205 context evidenced that the residue lied within a consensus motif for protein kinase CK2 (former casein kinase II). The CK2 consensus consists of a serine or threonine surrounded by acidic amino acids that may extend from positions -2 to 5 (Meggio et al, 1994). An acidic residue at +3 was shown to be most important but not crucial in an otherwise acidic environment (Pinna, 2002). Myo5 1025 is located in an acidic context that extends from amino acid -1 to +4 (Figure 33A), giving an excellent putative CK2 consensus site. To test whether CK2 was the cytosolic factor that phosphorylates Myo5-C_{ext}, GST-Myo5-C_{ext} recombinant fusion protein was bound to glutathione-Sepharose beads and incubated at 26ºC in the presence of γ-^{32}P-ATP, unlabeled actin, and either a wild type cytosolic extract or yeast extract from a temperature sensitive CK2 mutant (*ck2-ts*). As shown in Figure 33C, the *ck2-ts* yeast extract was unable to phosphorylate Myo5-C_{ext} while the yeast extract from wild type cells strongly phosphorylated the construct (Dr. Bianka Grosshans unpublished results). Altogether, this data indicates that the protein kinase CK2 is able to phosphorylate Myo5-C_{ext} at serine 1205.

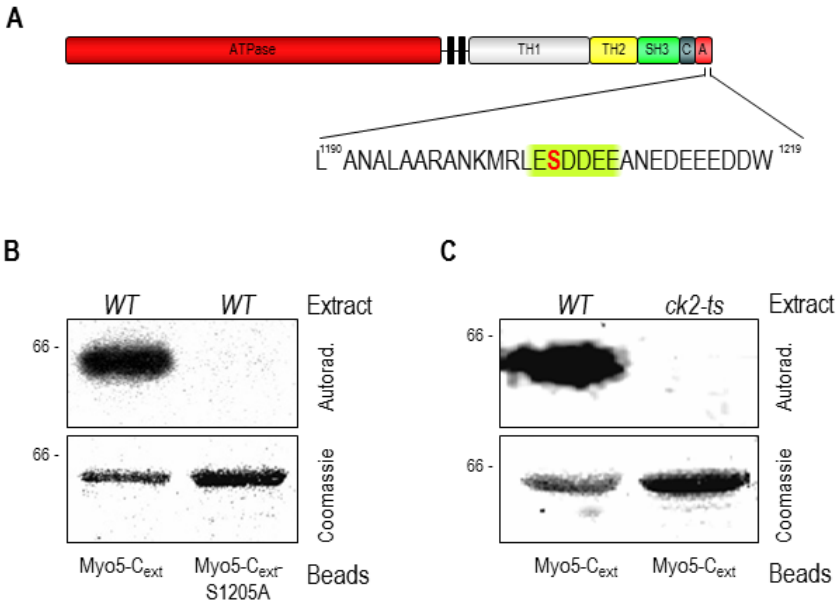

Figure 33. Myo5 serine 1205 is phosphorylated *in vitro* by the protein kinase CK2.
(A) Amino acid sequence of the C-terminal region of Myo5 (amino acids 1190 to 1219), which is still phosphorylated *in vitro*. Serine 1205 is labeled in red and the protein kinase CK2 consensus sequence highlighted in green. (B) Autoradiography (upper panel) of a Coomassie stained SDS-PAGE gel (lower panel) showing glutathione-Sepharose beads coated with GST-Myo5-C_{ext} or GST-Myo5-C_{ext}–S1205A incubated with WT (RH2881) yeast extracts and γ–^{32}P-ATP for 30 min at 26°C. Beads were pelleted, rinsed several times and boiled in the presence of SDS-PAGE sample buffer. GST fusion proteins were separated in a NuPAGE Bis-Tris 4-12 % gradient gel and analyzed by Coomassie staining to demonstrate equivalent protein loading and autoradiography to demonstrate protein phosphorylation. (C) Autoradiography of a Coomassie stained SDS-PAGE gel showing glutathione-Sepharose beads coated with GST-Myo5-C_{ext} incubated with either wild type (*WT*, RH2881) or *cka1Δ cka2-ts* (*ck2-ts*, YDH13) yeast extracts and γ–^{32}P-ATP for 30 min at 26°C. Beads were pelleted, rinsed several times and boiled in the presence of SDS-PAGE sample buffer. GST fusion proteins were separated in a NuPAGE Bis-Tris 4-12 % gradient gel and analyzed by Coomassie staining to demonstrate equivalent protein loading and autoradiography to demonstrate protein phosphorylation. These experiments were done by Dr. B. Grosshans.

2.2. Objectives

Our previous published and unpublished results indicated that the Myo5 C-terminal extension (Myo5-C_{ext}) that comprises the TH2, SH3 and CA domains induced the formation of actin *foci in vitro* that recapitulate the cortical actin structures required for endocytic budding *in vivo*; that a phosphorylation/dephosphorylation event regulates the formation of Myo5 *foci*; and that Myo5-C_{ext} is phosphorylated by CK2 at a residue located in the CA domain, a region involved in the binding of Myo5 to the Arp2/3 complex. In this context, the objectives of this study were:

- To further characterize the kinase activity present in yeast extracts that phosphorylates Myo5 S1205.
- To investigate whether the phosphorylation of Myo5 S1205 by CK2 regulates the assembly of endocytic actin structures both *in vitro* and *in vivo*.
    - If so, dissect the molecular mechanisms responsible for the CK2-dependent regulation of Myo5-induced actin polymerization at the endocytic sites.
    - If so, understand the functional significance of the CK2-dependent regulation of Myo5-induced actin polymerization at the endocytic sites.

3. RESULTS

3.1. Analysis of Myo5 S1205 phosphorylation by CK2

3.1.1. Phosphorylation of Myo5 at S1205 *in vitro* is Cka2-dependent but Cka1- and Ckb1/Ckb2-independent

3.1.1.1. Depletion of Cka2, but not Cka1 or Ckb1 and Ckb2, prevents phosphorylation of the Myo5 S1205 by yeast extracts

Our previous unpublished results indicated that a cytosolic activity present in yeast extracts, the casein kinase 2 (CK2), phosphorylates Myo5 at S1205 (see antecedents, section 2.1.3). CK2 is a pleiotropic and highly conserved serine/threonine protein kinase ubiquitously expressed in eukaryotic cells. Protein kinase CK2 exists primarily as a tetrameric protein composed of two catalytic (α) and two regulatory (β) subunits that form the holoenzyme (Figure 34). Although the stoichiometry of the enzyme is conserved from yeast to mammals, the number of genes encoding the catalytic and regulatory subunits is not preserved. In many organisms, two genes encode two different catalytic isoforms, α and α' (Litchfield, 2003). The regulatory β subunit is generally codified by a single gene, but distinct isoforms have also been reported in some organisms including *S. cerevisiae* (see below). The holoenzyme can contain identical – the homotetramers $\alpha_2\beta_2$ and $\alpha'_2\beta_2$- or different –the heterotetramer $\alpha\alpha'\beta_2$- catalytic subunits (Gietz et al., 1995). In *S. cerevisiae*, the catalytic subunits are encoded by the genes *CKA1* and *CKA2*, while another two genes, *CKB1* and *CKB2*, encode the regulatory subunits. The regulatory subunits are dispensable for viability under standard growth conditions (Bidwai et al., 1995). However, while deletion of either *CKA1* or *CKA2* does not cause any obvious phenotype, disruption of both genes is synthetically lethal (Chen-Wu et al., 1988; Padmanabha et al., 1990). Lethality can be rescued by expression of *Drosophila* α subunit, indicating functional conservation (Chen-Wu et al., 1988; Padmanabha et al., 1990). Interestingly, although the two catalytic subunits are able to compensate for each other in the context of viability, increasing evidence suggest that they might have independent functions (Berkey and Carlson, 2006; Glover, 1998; Hanna et al., 1995; Kobayashi and Nagiec, 2003; Rethinaswamy et al., 1998; Schmidt et al., 2011).

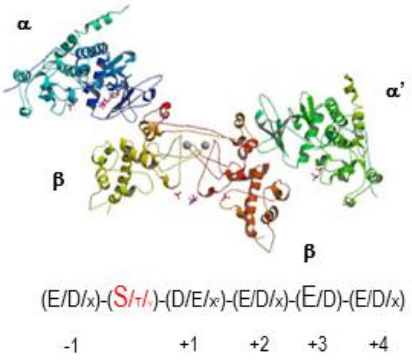

Figure 34. Ribbon diagram illustrating the high-resolution structure of tetrameric CK2.
(A) Illustration of human CK2 tetramer obtained from the protein data bank (identification number IJWH). Both catalytic (α and α') and regulatory (β) subunits are shown in different colors although the regulatory subunits are often codified by the same gene. The consensus motif for CK2 is shown below: X is any residue except basic residues and X' is any residue except basic or proline residues. The size of the letters is proportional to the frequency of a given residue at that position.

To examine the contribution of each CK2 subunit to the Myo5 S1205 phosphorylation, isogenic wild type, *cka1Δ, cka2Δ, cka1Δ cka2-13, cka2Δ cka1-13* and *ckb1Δckb2Δ* strains were generated, where the *cka2-13* and *cka1-13* are temperature sensitive alleles of the catalytic subunits (Hanna et al., 1995; Rethinaswamy et al., 1998) (see materials and methods, section 6.2.3.4). As previously shown (Bidwai et al., 1995; Chen-Wu et al., 1988; Padmanabha et al., 1990; Rethinaswamy et al., 1998), loss of one catalytic activity or loss of both regulatory subunits did not cause any obvious growth phenotype, while the *cka2Δ cka1-13* and *cka1Δ cka2-13* strains displayed a temperature-sensitive lethal phenotype (Figure 35A).

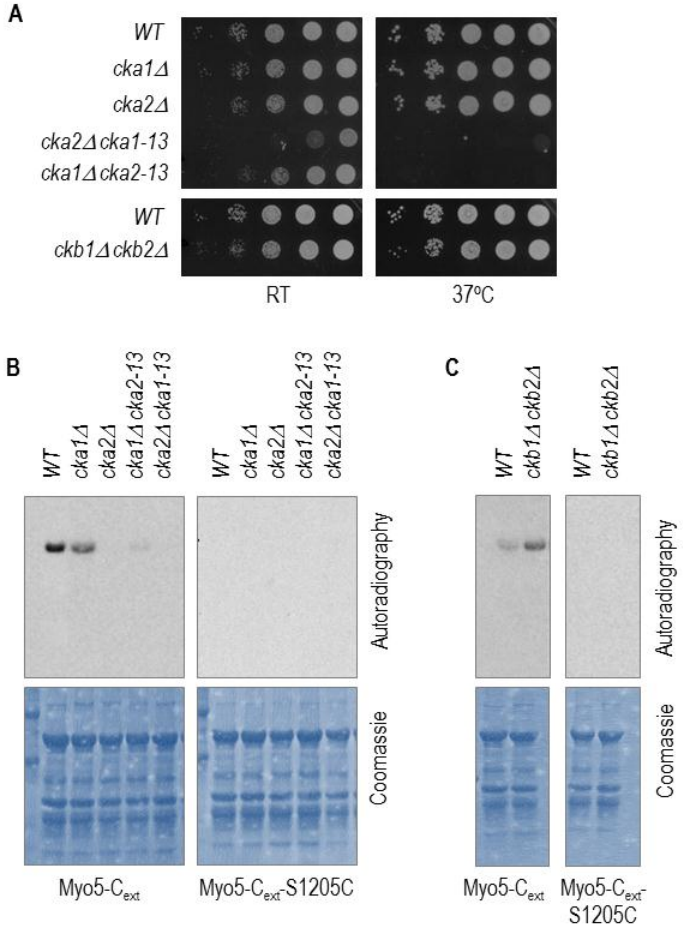

Figure 35. Depletion of the CK2 catalytic subunit Cka2, but not depletion of Cka1 or the regulatory subunits Ckb1 and Ckb2, prevents phosphorylation of Myo5 S1205 *in vitro*.

(A) Serial dilutions of *WT* (BY4741), *cka1Δ* (SCMIG1178), *cka2Δ* (SCMIG1182), *cka2Δ cka1-13* (SCMIG1180), *cka1Δ cka2-13* (SCMIG1176), and *ckb1Δ ckb2Δ* (SCMIG1173) cells from a mid-log phase culture spotted onto SDC plates and let grown for 24 hours at room temperature or 37°C. (B) Autoradiography (upper panel) of a Coomassie stained SDS-PAGE gel (lower panel) showing glutathione-Sepharose beads coated with GST-Myo5-C_{ext} or GST-Myo5-C_{ext}–S1205C incubated with either *WT* (SCMIG1182 +p*CKA2.leu2Δ::URA3*), *cka1Δ* (SCMIG1178), *cka2Δ* (SCMIG1182), *cka2Δ cka1-13* (SCMIG1180), or *cka1Δ cka2-13* (SCMIG1176) yeast extracts and γ-^{33}P-ATP for 30 min at 26°C. Beads were pelleted, rinsed several times and boiled in the presence of SDS-PAGE sample buffer. GST fusion proteins were separated in a NuPAGE Bis-Tris 4-12 % gradient gel and analyzed by Coomassie staining to demonstrate equivalent protein loading and autoradiography to demonstrate protein phosphorylation. (C) Autoradiography (upper panel) of a Coomassie stained SDS-PAGE gel (lower panel) showing glutathione-Sepharose beads coated with GST-Myo5-C_{ext} or GST-Myo5-C_{ext}–S1205C incubated with either *WT* (BY4741) or *ckb1Δ ckb2Δ* (SCMIG1173) yeast extracts and γ-^{33}P-ATP for 30 min at 26°C. Beads were pelleted, rinsed several times and boiled in the presence of SDS-PAGE sample buffer. GST fusion proteins were separated in a NuPAGE Bis-Tris 4-12 % gradient gel and analyzed by Coomassie staining to demonstrate equivalent protein loading and autoradiography to demonstrate protein phosphorylation.

The ability of yeast extracts from the CK2 mutants to phosphorylate the Myo5 S1205 *in vitro* was examined using a Myo5 C-terminal fragment comprising amino acids 982 to 1219 (Myo5-C_{ext}) fused to GST, expressed and purified from *E. coli* (Geli et al., 2000). GST-Myo5-C_{ext}-coated glutathione-Sepharose beads were incubated with extracts from the above described strains, in the presence of radiolabeled ^{33}P-γ-ATP. The GST-Myo5-C_{ext}-coated beads were then separated from the extracts and the incorporation of radioactivity in Myo5 was determined by autoradiography. As previously shown, an extract from a wild type yeast was capable of phosphorylating GST-Myo5-C_{ext} but not an analogous construct bearing a serine to cysteine substitution at the Myo5 S1205 (Myo5-C_{ext}-S1205C) (Figure 35B). This result confirmed that the S1205 is the residue predominantly phosphorylated by yeast extracts in the Myo5-C_{ext} terminus. Consistent also with the previous observations that CK2 phosphorylates the Myo5-S1205, extracts from cells lacking the catalytic subunit *CKA2* (*cka2Δ and cka2Δ cka1-13*) were unable to phosphorylate GST-Myo5-C_{ext}. Interestingly though, disruption of the *CKA1* gene (*cka1Δ*) showed a very mild phenotype, as compared with the isogenic *cka2Δ* strains. Interestingly also, the regulatory subunits seemed to be dispensable for the Myo5 S1205 phosphorylation (*ckb1Δ ckb2Δ*) (Figure 35C). Actually, deletion of the regulatory subunits enhanced phosphorylation of GST-Myo5-C_{ext} but not that of GST-Myo5-C_{ext}-S1205C, indicating that the classical tetrameric CK2 was not responsible for Myo5 S1205 phosphorylation *in vitro*.

3.1.1.2. Overexpression of *CKA2,* but not *CKA1,* strongly increases phosphorylation of the Myo5 S1205 *in vitro*.

To further investigate if the catalytic subunits might play a differential role in the Myo5 S1205 phosphorylation, GST-Myo5-C_{ext}-coated beads were incubated with radiolabeled ^{33}P-γ-ATP and extracts from cells overexpressing either *CKA1* or *CKA2* from multicopy plasmids (+*CKA1* and +*CKA2*, respectively). As shown in Figure 36A, yeast extracts overexpressing *CKA2*, but not those overexpressing *CKA1* strongly increased the radioactive signal associated to GST-Myo5-C_{ext}, but not that associated to GST-Myo5-C_{ext}-S1205C. The increased phosphorylation was a direct consequence of the kinase activity of Cka2 since a point mutation in a conserved residue of its active site (*cka2-K79A*) (Hanks and Hunter, 1995; Vilk et al., 1999) significantly disrupted its ability to phosphorylate the Myo5-S1205. Further, tetramerization did not seem to be required for the observed effect since overexpression of *CKA2* in a *ckb1Δ ckb2Δ* background increased the Myo5 S1205 phosphorylation to the same extend as its overexpression in an isogenic wild type (Figure 36B). Immunoblot analysis demonstrated that differences in the expression level of the wild type and mutant catalytic subunits of CK2 could not explain the phenotypes observed (Figure 36C).

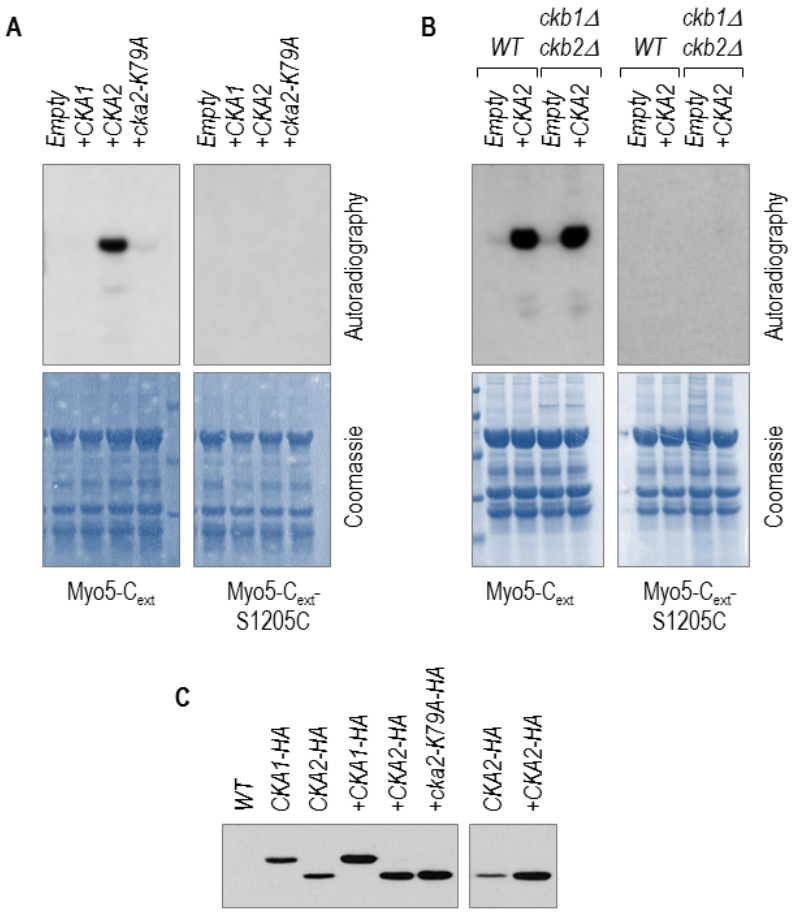

Figure 36. Overexpression of the catalytic subunit Cka2 but not of Cka1 increases phosphorylation of Myo5 S1205 *in vitro* independently of the tetramerization of CK2.

(A) Autoradiography (upper panel) of a Coomassie stained SDS-PAGE gel (lower panel) showing glutathione-Sepharose beads coated with GST-Myo5-C_{ext} or GST-Myo5-C_{ext}–S1205C incubated with yeast extracts from WT cells (BY4741) transformed with either a multicopy empty plasmid (Empty, pYEplac181), a multicopy plasmid encoding the catalytic subunit Cka1 (+CKA1, p181*CKA1*), a multicopy plasmid encoding the catalytic subunit Cka2 (+CKA2, p181*CKA2*), or a multicopy plasmid encoding a kinase-dead version of the catalytic subunit Cka2 (+*cka2-K79A*, p181*cka2-K79A*), and γ-^{33}P-ATP for 30 min at 26°C. Beads were pelleted, rinsed several times and boiled in the presence of SDS-PAGE sample buffer. GST fusion proteins were separated in a NuPAGE Bis-Tris 4-12 % gradient gel and analyzed by Coomassie staining to demonstrate equivalent protein loading and autoradiography to demonstrate protein phosphorylation. (B) Autoradiography (upper panel) of a Coomassie stained SDS-PAGE gel (lower panel) showing glutathione-Sepharose beads coated with GST-Myo5-C_{ext} or GST-Myo5-C_{ext}–S1205C incubated with yeast extracts from either WT (BY4741) or *ckb1Δ ckb2Δ* (SCMIG1173) cells transformed with either a multicopy empty plasmid (Empty, pYEplac181) or a multicopy plasmid encoding the catalytic subunit Cka2 (+*CKA2*, p181*CKA2*) and γ-^{33}P-ATP for 30 min at 26°C. Beads were pelleted, rinsed several times and boiled in the presence of SDS-PAGE sample buffer. GST fusion proteins were separated in a NuPAGE Bis-Tris 4-12 % gradient gel and analyzed by Coomassie staining to demonstrate equivalent protein loading and autoradiography to demonstrate protein phosphorylation. (C) Immunoblot of total protein extracts from *WT* (BY4741), *CKA1-HA* (SCMIG1202), *CKA2-HA* (SCMIG1155) cells; from wild type cells (BY4741) transformed with either a multicopy plasmid encoding the catalytic subunit Cka1 tagged with HA (+*CKA1-HA*, p181*CKA1-HA*), a multicopy plasmid encoding the catalytic subunit Cka2 tagged with HA (+*CKA2-HA*, p181*CKA2-HA*), or a multicopy plasmid encoding a kinase-dead version of the catalytic subunit Cka2 tagged with HA (+*cka2-K79A-HA*, p181*cka2-K79A-HA*); from *ckb1Δ ckb2Δ CKA2-HA* (SCMIG1200) cells; and from *ckb1Δ ckb2Δ* (SCMIG1173) cells transformed with a multicopy plasmid encoding the catalytic subunit Cka2 tagged with HA *(+CKA2-HA*, p181*CKA2-HA*). An antibody against HA (α-HA) was used to detect the HA-tagged constructs. 15 μg of total protein was loaded per lane. The autoradiograms shown in A and B were less exposed that those shown in Figure 35. Longer exposure also evidenced phosphorylation in samples of GST-Myo5-C_{ext} incubated with extracts from cells not overexpressing *CKA2*.

3.1.2. A non-cytosolic CK2 activity predominantly phosphorylates Myo5 S1205.

To further characterize the CK2 activity phosphorylating Myo5-S1205, we investigated its subcellular localization. For this purpose, the yeast extracts used in the *in vitro* phosphorylation assays (obtained from the supernatant after centrifugation at 13,000 g, see materials and methods) were sub-fractionated by centrifugation at 100,000 g for 1 hour and the supernatant (S100) and the pellet (P100) were recovered to perform separated phosphorylation assays. As shown by the relative enrichments of the cytosolic marker Hxk2, the membrane-associated protein Gas1 and actin, the S100 corresponds to the cytosolic fraction whereas the P100 contained cellular membranes and possibly cytoskeletal elements (Figure 37A). Interestingly, under the same experimental conditions that allowed phosphorylation of the Myo5 S1205 by the yeast extracts used in previous assays (S13), we found that the cytosolic fraction (S100) was less able to phosphorylate the GST-Myo5-C_{ext} construct than the equivalent amount of P100, even though the protein concentration in this fraction was lower than that of the cytosolic extract (Figure 37B and 37C).

The P100 fraction was unable to phosphorylate the GST-Myo5-C_{ext}-S1205C construct and the kinase activity phosphorylating this residue was reduced when the P100 was prepared from a *cka2Δ* strain, but not when it was prepared from *cka1Δ* mutants, supporting a major role of Cka2 for Myo5 S1205 phosphorylation (Figure 37C). Consistent with a specific membrane or cytoskeletal-associated Cka2 activity responsible for the Myo5 S1205 phosphorylation, Cka2 was found enriched in the P100 fraction (Figure 37A). Analysis of subcellular fractions containing heavier membranes such as the plasma membrane or the nuclear envelope (P13, see materials and methods) indicated that the kinase activity phosphorylating the Myo5 S1205 was also associated with some of these compartments. Consistently, Cka2 also appeared enriched in the P13 fraction, as compared to Cka1 (Figure 37A and 37B).

The P100 fraction was unable to phosphorylate the GST-Myo5-C_{ext}-S1205C construct and the kinase activity phosphorylating this residue was reduced when the P100 was prepared from a *cka2Δ* strain, but not when it was prepared from *cka1Δ* mutants, supporting a major role of Cka2 for Myo5 S1205 phosphorylation (Figure 37C). Consistent with a specific membrane or cytoskeletal-associated Cka2 activity responsible for the Myo5 S1205 phosphorylation, Cka2 was found enriched in the P100 fraction, as compared to Cka1 (Figure 37A). Analysis of subcellular fractions containing heavier membranes such as the plasma membrane or the nuclear envelope (P13, see materials and methods) indicated that the kinase activity phosphorylating the Myo5 S1205 was also associated with some of these compartments. Consistently, Cka2 also appeared enriched in the P13 fraction, as compared to Cka1 (Figure 37A and 37B).

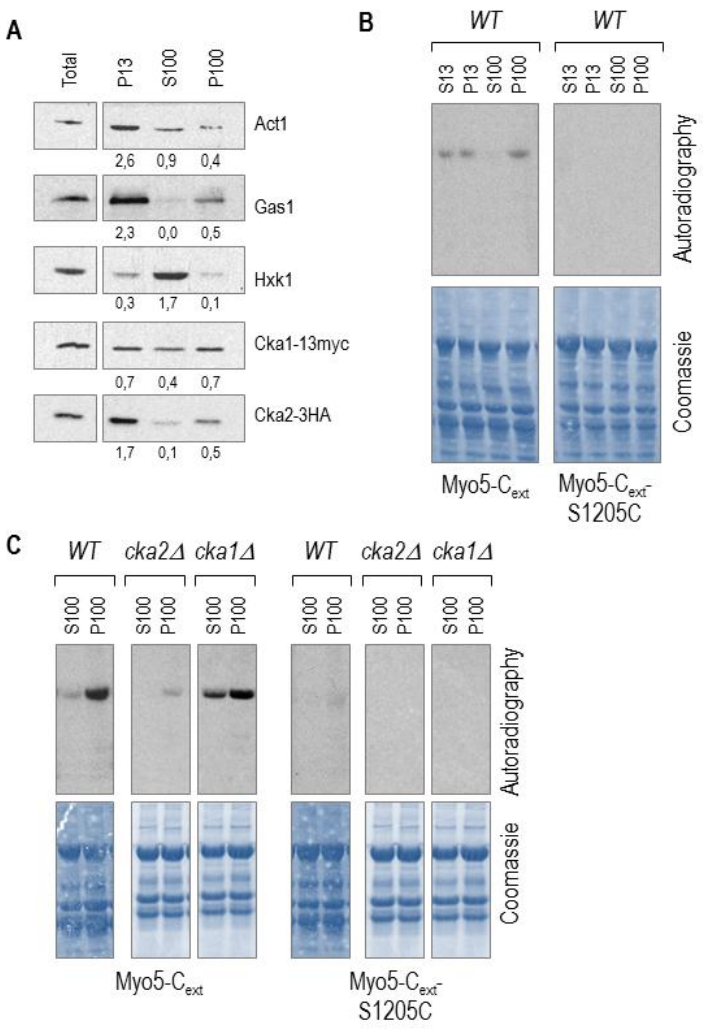

Figure 37. The catalytic activity that phosphorylates Myo5-C_{ext}, Cka2, is associated with a particulate fraction. (A) Immunoblot of a total protein extract (Total), the 13,000 g pellet of a total protein extract (P13), and the 100,000 g supernatant (S100) and pellet (P100) of a 13,000 g supernatant (S13) from a total protein extract, from *CKA1-MYC CKA2-HA* cells (SCMIG1152). . Samples were boiled in the presence of SDS-PAGE and analyzed by immunoblot .An antibody against actin (α-Act1) was used to identify cytoskeletal elements; the plasma membrane marker Gas1 and the cytosolic marker hexokinase were identified with α-Gas1 and α-Hxk1 antibodies, respectively; and α-myc and α-HA antibodies were used to detect Cka1 and Cka2, respectively. 10 μg of total protein was loaded per lane. Numbers indicate enrichment with respect to the total protein extract (B) Autoradiography (upper panel) of a Coomassie stained SDS-PAGE gel (lower panel) showing glutathione-Sepharose beads coated with GST-Myo5-C_{ext} or GST-Myo5-C_{ext}–S1205C incubated with γ-^{33}P-ATP and the supernatant and the pellet from a protein extract fractionated at 13,000 g (S13 and P13, respectively), and the supernatant and the pellet from the S13 protein extract sub-fractionated at 100,000 g (S100 and P100, respectively) of wild type cells (BY4741) for 30 min at 26°C. Beads were pelleted, rinsed several times and boiled in the presence of SDS-PAGE sample buffer. GST fusion proteins were separated in a NuPAGE Bis-Tris 4-12 % gradient gel and analysed by Coomassie staining to demonstrate equivalent protein loading and autoradiography to demonstrate protein phosphorylation. (C) Autoradiography (upper panel) of a Coomassie-stained SDS-PAGE gel (lower panel) showing glutathione-Sepharose beads coated with GST-Myo5-C_{ext} or GST-Myo5-C_{ext}–S1205C incubated with γ-^{33}P-ATP and the 100,000 *g* supernatant (S100) and pellet (P100) from the LSP protein extract, of *WT* (BY4741), *cka2Δ* (SCMIG1182), or *cka1Δ* (SCMIG1178) cells for 30 min at 26°C. Beads were pelleted, rinsed several times and boiled in the presence of SDS-PAGE sample buffer. GST fusion proteins were separated in a NuPAGE Bis-Tris 4-12 % gradient gel and analyzed by Coomassie staining to demonstrate equivalent protein loading and autoradiography to demonstrate protein phosphorylation.

3.2. Analysis of the regulatory role of Myo5 S1205 phosphorylation by Cka2 in Myo5-induced actin polymerization

3.2.1. The formation of Myo5-induced actin *foci* is down or up-regulated by mutations that mimic the constitutively phosphorylated or unphosphorylated Myo5 S1205 states, respectively

As explained above (see section 2.1), previous work from our laboratory has demonstrated that a chimeric protein containing GST and the C-terminus of Myo5, comprising the TH2, SH3 and Acidic domains (Myo5-C_{ext}, amino acids 984 to 1219), is capable of inducing the formation of actin structures on the surface of glutathione-Sepharose beads in a cytosol and temperature-dependent manner. The structures can be visualized as fluorescent *foci* under the microscope when they are formed in the presence of rhodamine-labeled actin. Further, the recruitment of specific proteins to the actin *foci* can be investigated by using extracts from yeast expressing the adequate GFP-tagged polypeptides. This kind of analysis have established that the morphology and the composition of the Myo5-induced actin *foci* built *in vitro* recapitulate those of the yeast cortical endocytic actin patches *in vivo* (Geli et al., 2000; Idrissi et al., 2002). On the other hand, the observation that the Myo5-induced actin structures appear as discrete *foci* despite Myo5 covers the bead homogenously and neither actin nor the Arp2/3 complex are limiting in the reaction, led to the proposal that their assembly is regulated by components present in the extract (Idrissi et al., 2002).

Our previous results also showed that Myo5 is phosphorylated at S1205. This residue is located adjacent to the acidic domain, which is required for the activation of the Arp2/3 complex. This observation prompted us to analyze whether the Myo5 tail phosphorylation might regulate the formation of actin structures *in vitro*. For that purpose, the S1205 was mutated to cysteine (C) or to aspartic acid (D) to mimic the un-phosphorylated or the phosphorylated states, respectively. GST fusion proteins of the C-terminus of wild type (Myo5-C_{ext}) and mutant Myo5 (Myo5-C_{ext}-S1205C and Myo5-C_{ext}-S1205D) were bound to glutathione-Sepharose beads and incubated with wild type yeast extracts and rhodamine-labeled actin. The formation of actin *foci* was then visualized under the fluorescence microscope. As shown in Figure 38A and 38B, the construct bearing the mutation mimicking the constitutively unphosphorylated Myo5 (Myo5-C_{ext}-S1205C) showed a significant increase in the number of fluorescently labeled actin patches generated per surface area, as compared to the wild type Myo5-C_{ext}. On the contrary, the construct bearing the mutation mimicking the constitutively phosphorylated Myo5 (Myo5-C_{ext}-S1205D) showed a significant decrease. The fact that the GST-Myo5-C_{ext}-S1205C and the GST-Myo5-C_{ext}-S1205D constructs bind the same amount of Arp3 (see Figure 41) indicated that down-regulation of actin polymerization was not the result of miss-folding of the Myo5-C_{ext}-S1205D construct. These findings suggested that Myo5 phosphorylation at S1205 negatively regulates the formation of actin patch-like structures *in vitro*.

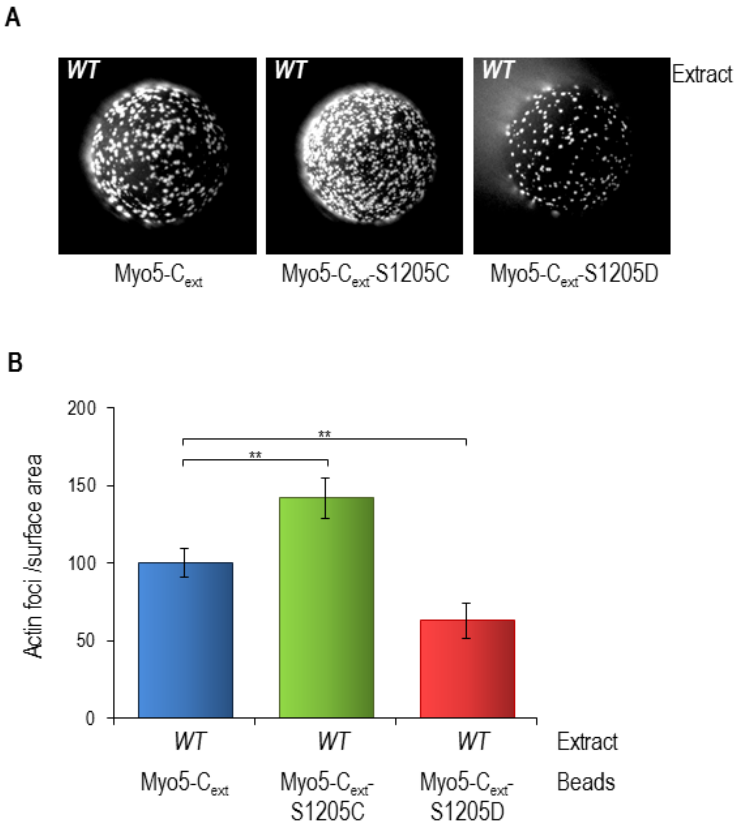

Figure 38. Phosphorylation of Myo5 S1205 negatively regulates Myo5-C_{ext} mediated actin polymerization.
(A) Fluorescence micrographs of glutathione-Sepharose beads coated with GST-Myo5-C_{ext} (Myo5-C_{ext}), GST-Myo5-C_{ext}–S1205C (Myo5-C_{ext}-S1205C) and GST-Myo5-C_{ext}–S1205D (Myo5-C_{ext}-S1205D), incubated with yeast extracts from wild type cells (SCMIG100) and 1 μM rhodamine-labeled actin for 10 min at 26°C. (B) Average patch density of the experiments described in (A). Actin *foci* were counted on a 25 x 25 μm^2 surface area of at least 10 different beads per experiment. At least three independent experiments were performed per each sample. The average actin *foci* density was normalized with respect to the average density of actin *foci* generated on beads coated with GST-Myo5-C_{ext} (Myo5-C_{ext}). Statistical analysis was performed using the two-tailed Student's t-test. ** represents a p-value ≤ 0.001.

3.2.2. Cka2 down-regulates the formation of Myo5-induced actin *foci*

3.2.2.1. Depletion of Cka2, but not Cka1 up-regulates the formation of Myo5-induced actin *foci*.

As shown above, the Cka2 subunit of CK2 plays a predominant role in the phosphorylation of Myo5 at position S1205, and this activity seems to be independent of the regulatory subunits. Besides, a mutation mimicking phosphorylation at this position inhibits Myo5-induced actin polymerization. Thus, we questioned whether Cka2 specifically down-regulates the formation of actin structures. To address this point, extracts from *WT*, *cka1Δ,* and *cka2Δ* mutants were prepared and tested for their ability to generate actin *foci* over the surface of GST-Myo5-C_{ext} coated beads in the presence of rhodamine-labeled actin. As shown in Figure 39A and 39B, Myo5-C_{ext} induced the assembly of comparable amounts of actin *foci* when incubated with either

wild type or *cka1Δ* extracts. However, the number actin *foci* per surface area were significantly higher when the Myo5-C_{ext}-covered beads were incubated with yeast extract from *cka2Δ* cells. These results suggested that Cka2 specifically down-regulates Myo5-induced actin-patch assembly. Moreover, we could demonstrate that up-regulation of Myo5-induced actin polymerization by depletion of Cka2 was at least partially caused by unphosphorylation of the Myo5 S1205, since the Myo5 S1205D mutation (mimicking the constitutive phosphorylated state) down-regulated the formation of actin *foci* in a *cka2Δ* mutant extract to the wild type density (Figure 39A and 39B). However, depletion of Cka2 could still up-regulate (even though to a lesser extent) actin polymerization on the beads coated with the GST-Myo5-C_{ext}-S1205D construct (compare actin *foci* density on the GST-Myo5-C_{ext}-S1205D-coated beads incubated with wild type (Figure 38) or *cka2Δ* extracts (Figure 39)). This result suggested that Cka2 might also target other proteins involved in the assembly of the Myo5-induced actin patches.

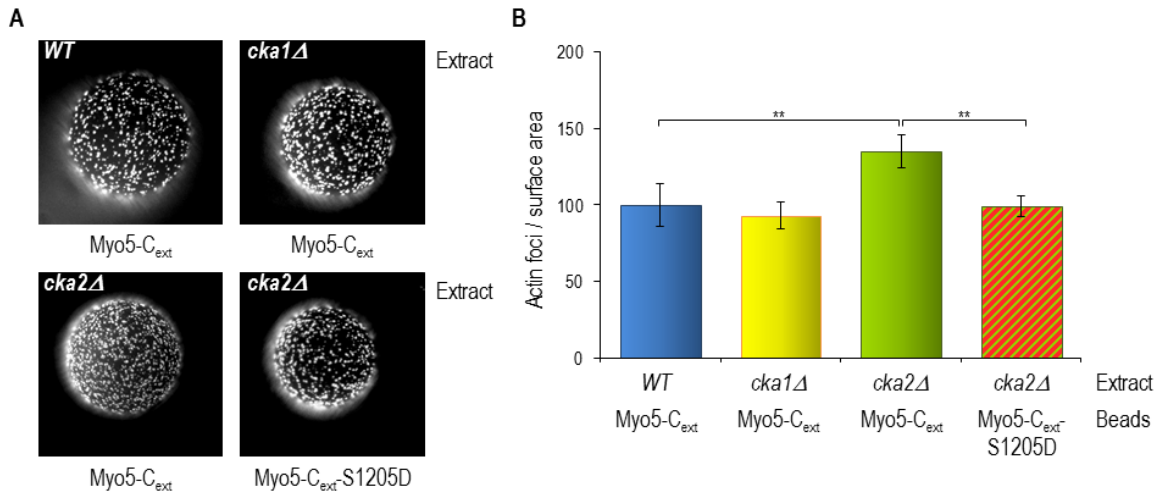

Figure 39. Depletion of the CK2 catalytic subunit Cka2, but not Cka1, up-regulates Myo5-C_{ext}-induced actin polymerization.
(A) Fluorescence micrographs of glutathione-Sepharose beads coated with GST-Myo5-C_{ext} (Myo5-C_{ext}) or GST-Myo5-C_{ext}–S1205D (Myo5-C_{ext}-S1205D) incubated with either *WT* (SCMIG100), *cka1Δ* (SCMIG716), or *cka2Δ* (SCMIG717) yeast extracts and 1 μM rhodamine-labeled actin for 10 min at 26°C. (B) Average patch density of the experiments described in (A). Actin *foci* were counted on a 25 x 25 μm^2 surface area of at least 10 different beads per experiment. At least two independent experiments were performed per each sample. The average actin *foci* density was normalized with respect to the average density of actin *foci* generated on beads incubated with the *WT* yeast extract. Statistical analysis was performed using the two-tailed Student's t-test. ** represents a p-value ≤ 0.001.

3.2.2.2. Overexpression of *CKA2,* but not *CKA1*, down-regulates the formation of Myo5-induced actin *foci*.

To further demonstrate the specificity of Cka2 in the down-regulation of Myo5-induced actin polymerization, GST-Myo5-C_{ext} was bound to glutathione-Sepharose beads and incubated with yeast extracts from cells over-expressing either *CKA1* or *CKA2* from multicopy plasmids (+*CKA1* and +*CKA2*, respectively). Consistent with the specific up-regulation of Myo5 S1205 phosphorylation observed upon over-expression of Cka2 (Figure 36A), increased levels of this

catalytic subunit specifically down-regulated the formation of Myo5-induced actin *foci* (Figure 40). Again, the observed effect was a direct consequence of the kinase activity of Cka2 since a point mutation in the conserved residue of its active site (K79A) (+*cka2-K79A*) not only disrupted the ability of Cka2 to down-regulate the assembly of actin *foci* but significantly increased it. This result suggested that the mutant protein probably interferes with phosphorylation by the endogenous wild type Cka2. Again though, the results indicated that Cka2 substrates other than Myo5 might also contribute to the observed effects, because the Myo5 S1205C mutation alone (Myo5-C_{ext}-S1205C) did not prevent the inhibition of actin polymerization caused by overexpression of *CKA2* nor did it prevent up-regulation of actin polymerization by overexpression of the *cka2-K79A* mutant (Figure 40).

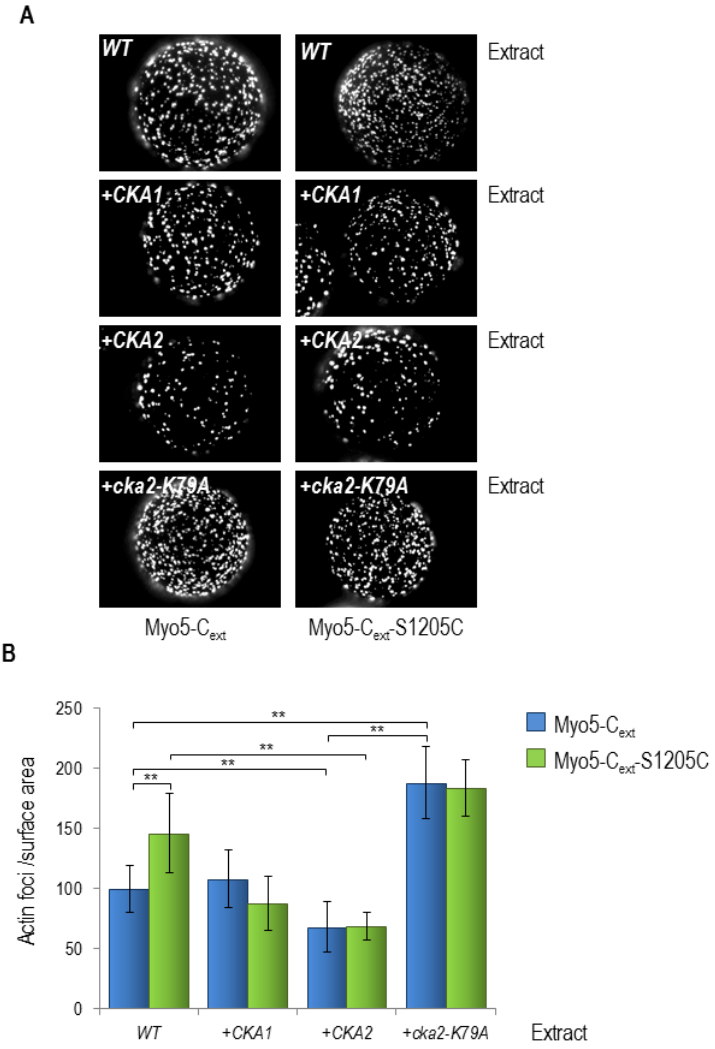

Figure 40. Overexpression of the catalytic subunit Cka2, but not Cka1 or a kinase-dead version of Cka2, down-regulates Myo5-C_{ext} mediated actin polymerization.
(A) Fluorescence micrographs of glutathione-Sepharose beads coated with GST-Myo5-C_{ext} (Myo5-C_{ext}) or GST-Myo5-C_{ext}–S1205C (Myo5-C_{ext}-S1205C) incubated with yeast extracts from WT cells (BY4741) transformed with a multicopy plasmid either empty (WT, pYEplac181), or encoding the catalytic subunit Cka1 (+CKA1, p181*CKA1*), the catalytic subunit Cka2 (+CKA2, p181*CKA2*), or a kinase-dead version of the catalytic subunit Cka2 (+cka2-K79A, p181*cka2-K79A*) and 1μM rhodamine-labeled actin for 10 min at 26°C. (B) Average patch density of the experiments described in (A). Actin *foci* were counted on a 25 x 25 μm^2 surface area of at least 10 different beads per experiment. At least two independent experiments were performed per each sample. The average actin *foci* density was normalized with respect to the average density of actin *foci* generated on beads coated with GST-Myo5-C_{ext} (Myo5-C_{ext}). Statistical analysis was performed using the two-tailed Student's t-test. ** represents a p-value ≤ 0.001.

3.3. Analysis of the influence of the Myo5 S1205 phosphorylation on the Myo5 interactome

3.3.1. Mutants mimicking the constitutive phosphorylated and unphosphorylated Myo5 S1205 states show reciprocal differential affinities for the Myo5-coactivator Vrp1 and the clathrin adaptor Sla1

The data presented in previous sections indicated that phosphorylation of Myo5 S1205 negatively regulates myosin-I-induced actin polymerization. However, the molecular mechanisms underlying this regulation were unknown. In order to investigate this matter, we decided to analyze the relative affinities of mutants mimicking the constitutive unphosphorylated or phosphorylated Myo5 S1205 states for known Myo5 interacting proteins: the Arp2/3 complex, Vrp1, Las17, Pan1, Bbc1, Abp1, and Sla1 (See Introduction). From those, the Arp2/3 complex and Vrp1 were already known to be required for assembly of Myo5-induced actin patches in the presence of cell extracts (Geli et al., 2000; Idrissi et al., 2002). In addition, Bbc1 and Abp1 had been demonstrated to inhibit Myo5/Vrp1-induced actin polymerization in pyrene-actin assays with purified components, whereas Pan1 and Las17 well established NPFs (Duncan et al., 2001; Sun et al., 2006; Winter et al., 1999). Extracts from yeast cells expressing myc- or HA-tagged versions of the proteins cited above were subjected to pull-downs by glutathione-Sepharose beads coated with GST-Myo5-C_{ext} bearing the S1205C or S1205D mutations (Myo5-C_{ext}-S1205C and Myo5-C_{ext}-S1205D, respectively) and their presence in the precipitates was analyzed by immunoblot. Surprisingly, we could not detect differential affinities of the Myo5 mutants for the Arp2/3 complex (Figure 41A and 41B). However, we observed clear differential binding for Vrp1 and Sla1 and, to a lesser extent, for Pan1. Interestingly, Vrp1 showed more affinity for Myo5-C_{ext}-S1205C and Pan1 and Sla1 for Myo5-C_{ext}-S1205D. Altogether, our results suggested that phosphorylation at S1205 might at least in part down-regulate Myo5-induced actin polymerization by lowering the affinity of Myo5 for its co-activator Vrp1.

The differential affinities were confirmed *in vivo* by using a two hybrid assay. For that purpose, the LexA DNA binding domain fused to the Myo5 C-terminus of the wild type myosin (LexA-Myo5-C_{ext}) or the mutants mimicking the constitutive unphosphorylated (LexA-Myo5-C_{ext}-S1205C) or phosphorylated (LexA-Myo5$_{ext}$-C-S1205D) states were co-expressed with the B42 transcriptional activator fused to either Vrp1 (B42-Vrp1) or Sla1 (B42-Sla1), in yeast bearing a reporter gene encoding β-galactosidase under the control of the LexA operator (Gyuris et al., 1993). The LexA constructs were also co-expressed with the Arc40 subunit of the Arp2/3 complex fused to B42 as a control (B42-Arc40), since the complex did not exhibited significant differences in its affinity for the mutants mimicking the constitutive phosphorylated or unphosphorylated states in the pull down assays. As shown in Figure 41C, and consistent with the pull down assays, Vrp1 demonstrated higher affinity for the LexA-Myo5-C_{ext}-S1205C construct, as compared to the wild type or the S1205D mutant. In contrast, Sla1 showed more affinity for the LexA-Myo5-C_{ext}-S1205D construct ($p < 0.001$). It should be noticed that

although we could not detect differential binding of GST-Myo5-C_{ext}-S1205C and GST-Myo5-C_{ext}-S1205D for the Arp2/3 component Arp3 in the pull-down, LexA-Myo5-C_{ext}-S1205D showed a small but significantly reduced interaction with Arc40, as compared with wild type Myo5-C_{ext}.

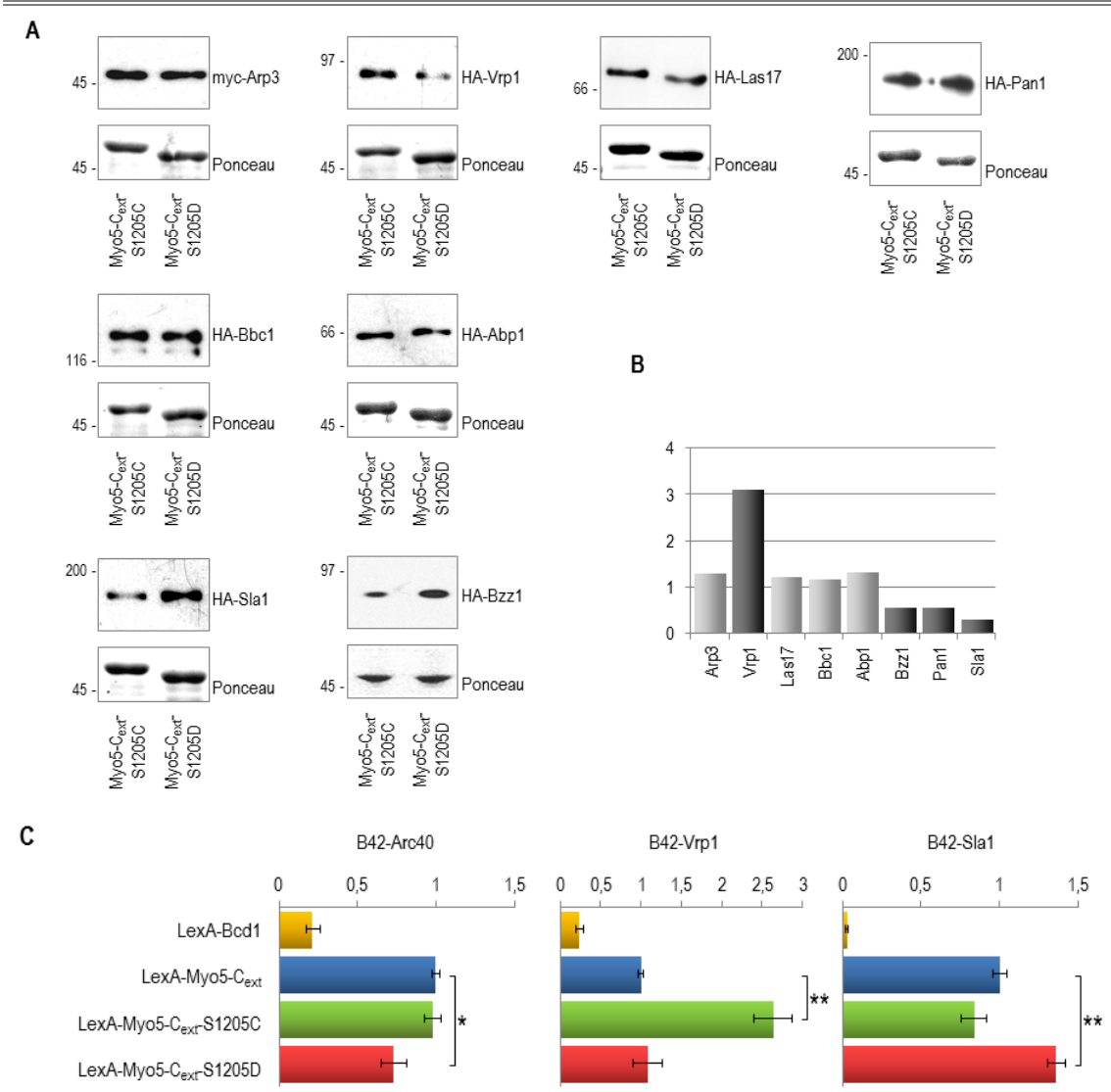

Figure 41. Phosphorylation of Myo5 S1205 regulates the affinity of Myo5-C_{ext} for Vrp1 and Sla1.
(A) Immunoblot (upper panel) of glutathione-Sepharose beads coated with GST-Myo5-C_{ext}–S1205C (Myo5-C_{ext}-S1205C) or GST-Myo5-C_{ext}–S1205D (Myo5-C_{ext}-S1205D) and incubated with yeast extracts from a wild type strain (BY4741) or strains expressing epitope tagged versions of *ARP3-5MYC* (RH4157), *LAS17-3HA* (SCMIG516), *BBC1-3HA* (SCMIG903), *ABP1-3HA* (SCMIG723) and *BZZ1-3HA* (SCMIG1216) tagged cells from the chromosomal genes, or from plasmids (*VRP1-3HA* (p111*VRP1-3HA*), *PAN1-3HA* (p195*PAN1-3HA*), and *SLA1-3HA* (p111*SLA1-HA*)). Constructs were expressed under the control of their own promoters. Incubations were performed in the presence of 1 μM unlabeled actin for 10 min on ice. Beads were pelleted, rinsed several times and boiled in the presence of SDS-PAGE sample buffer. GST fusion proteins and associated polypeptides were separated SDS-PAGE and transferred to a nitrocellulose filter. Ponceau red staining was used to detect the GST-fused proteins (lower panel), and antibodies against myc (α-myc) or against HA (α-HA) were used to detect the myc- and HA-tagged constructs, respectively. Approximately 5 μg of GST-Myo5-C_{ext} constructs was loaded per lane. (B) Quantification of the pull downs shown in (A). The graph represents the relative amount of myc- or HA-tagged protein pulled down by GST-Myo5-C_{ext}-S1205C, respect to the amount of myc- or HA-tagged protein pulled down by GST-Myo5-C_{ext}-S1205D. The most remarkable differences are shown in dark grey. Quantifications were performed with Image J. (C) Yeast two hybrid interactions of the indicated constructs. The EGY48 strain bearing the β-galactosidase reporter on plasmid pSH18-34 and co-transformed with the LexA binding domain fused to the indicated *myo5* versions -or the gene *BCD1* as a control- and the B42 transcriptional activator fused to either full length *ARC40*, *VRP1*, or *SLA1* was grown to early logarithmic phase. Quantification of β-galactosidase activity was recorded by the addition of MUGAL and spectrofluorometry analysis. * represents a p-value ≤ 0.01; ** represents a p-value ≤ 0.001

3.3.2. Sla1 is an inhibitor of Myo5-induced actin patch assembly

The observation that Vrp1 showed higher affinity for the Myo5-C_{ext}-S1205C mutant was consistent with our previous observations that Vrp1 is required for assembly of Myo5-induced actin patches and that phosphorylation of Myo5 S1205 down-regulates the process. More unexpected was the observation that Sla1 interacted more strongly with the Myo5 mutant that mimics the phosphorylated state, since no effect for Sla1 mutants on Myo5-induced actin polymerization was previously reported. Interestingly, a preliminary genetic screen designed to hunt for endocytic proteins that might regulate Myo5-C_{ext} NPA pointed out the potential role of Sla1 in the inhibition of Myo5-C_{ext} mediated actin patch assembly (Dr. Fatima Idrissi, unpublished results). Therefore, to investigate if Sla1 might act as a negative regulator of Myo5-induced actin polymerization, we decided to first characterize the Myo5 and Sla1 domains involved in the interaction to subsequently analyze if mutations that specifically disrupted such interaction might have an influence in the assembly of Myo5-induced actin *foci in vitro*.

3.3.2.1. The Myo5/Sla1 interaction is direct and requires the Myo5 TH2 domain and the two N-terminal SH3 domains of Sla1

A physical interaction between the myosins-I and Sla1 has previously been observed in high-throughput analysis of the yeast SH3 domain interactome, using a yeast two hybrid assay (Tonikian et al., 2009). However, the occurrence of such interaction *in vivo* was not confirmed by other techniques and proper demonstration that the interaction is direct was also missing. In addition, the Myo5 and Sla1 domains involved in the interaction were not defined in detail. In order to first confirm that the Myo5/Sla1 interaction occurred *in vivo*, yeast extracts from cells expressing Protein A-tagged full length Myo5 (ProtA-Myo5) and HA-tagged Sla1 (Sla1-HA) were subjected to IgG pull downs, and the presence of the tagged proteins in the precipitates was analyzed by immunoblot. Consistent with Sla1 and Myo5 interacting *in vivo*, a fourth of the total Sla1-HA co-immunoprecipitated with ProtA-Myo5. No HA signal was detected when the pull downs were performed with strains expressing non-tagged versions of either Sla1 or Myo5. In addition, deletion of the C-terminus of Myo5 (ProtA-Myo5-$C_{ext}\Delta$) completely abolished the interaction (Figure 42), indicating that a domain embedded within this fragment might mediate the interaction with Sla1.

To define the domains involved in the Myo5/Sla1 interaction the yeast two hybrid was used as a first approach. Plasmids encoding the TH2, SH3 an Acidic domains of Myo5 –either alone or in combination, fused to the LexA DNA binding domain and plasmids encoding the B42 transcriptional activator fused to the full length Sla1 or different truncated forms, were co-transformed in yeast bearing the reporter gene β-galactosidase expressed under the LexA operon. As shown in Figure 43, the interaction between Sla1 and Myo5 seemed to occur between the two N-terminal SH3 domains of Sla1 ($Sla1_{SH3(1,2)}$) and the TH2 domain of Myo5 ($Myo5_{TH2n}$), which encompasses a poly-proline region. Interestingly, addition of a poly-proline rich Sla1 fragment to the construct bearing the two N-terminal SH3 domains ($Sla1_{SH3(1,2).P}$)

weakened the Sla1-Myo5 interaction, indicating that a putative intramolecular interaction within Sla1 might control its association with the myosin.

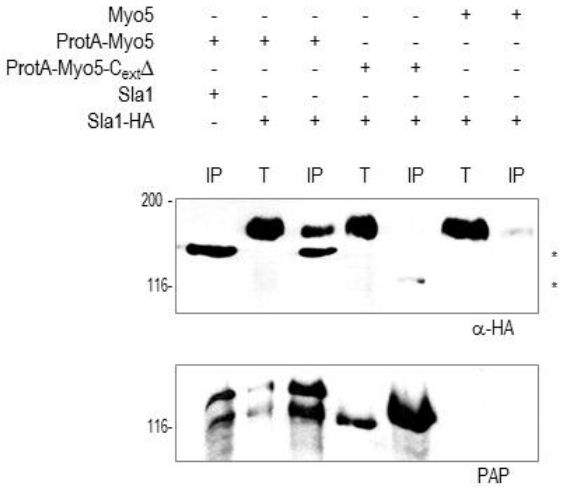

Figure 42. Sla1 interacts with Myo5 through the C-terminal domain.
Immunoblots of IgG-Sepharose pull-downs of *myo5Δ* cells (Y06549) transformed with a plasmid encoding a Protein A-tagged Myo5 construct (p33*ProtA-MYO5*, lane 1), or *myo5Δ sla1Δ* cells transformed with a Sla1-HA tagged construct (SCMIG1164, lanes 2 to 7) and either a Protein A-tagged Myo5 construct (p33*ProtA-MYO5*, lanes 2 and 3), a ProtA-tagged myo5 lacking the Cext domain (p33*ProtA-myo5-Cext Δ*, lanes 4 and 5), or an untagged MYO5 version (p33*MYO5*, lanes 6 and 7). All constructs were expressed in centromeric plasmids under the control of their own promoters. Cells were lysed and proteins were immunoprecipitated with IgG-Sepharose for 1 hour at 4ºC. ProtA-tagged proteins and associated polypeptides were separated by SDS-PAGE and transferred to a nitrocellulose filter. Precipitated proteins were analyzed using PAP (lower panel) and a α-HA antibody (upper panel) to detect ProtA-Myo5 and Sla1-HA fusion proteins, respectively. The asterisks in the upper panel show cross-reactivity of the protA- tagged Myo5 constructs

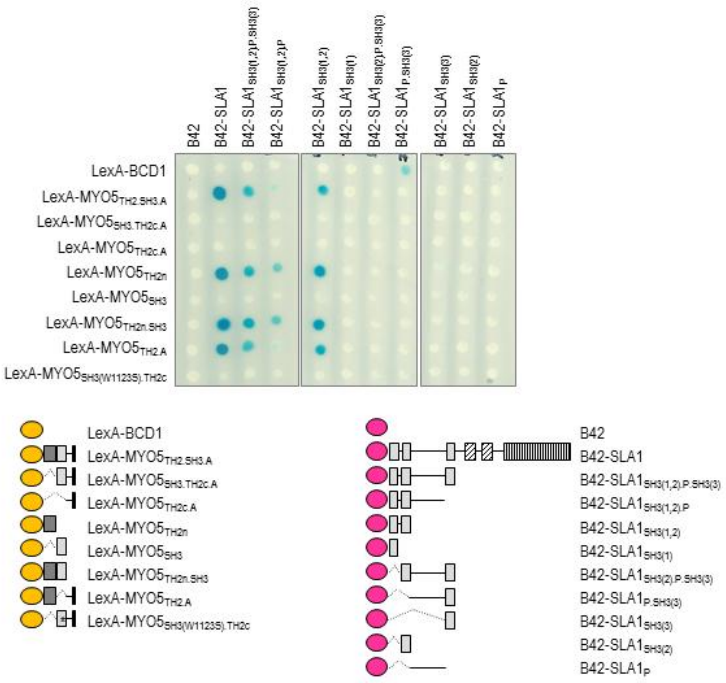

Figure 43. The two first SH3 domains of Sla1 interact with the TH2 domain of Myo5.
Plate assay (upper panel) for the yeast two hybrid interactions of the Myo5 and Sla1 constructs represented in the lower panel. The EGY48 strains bearing the β-galactosidase reporter on plasmid pSH18-34 and co-transformed with plasmids encoding the LexA binding domain fused to the indicated *myo5* constructs -or the gene *BCD1* as a control- and the B42 transcriptional activator alone – as a control- or fused to the indicated *SLA1* fragments, were spotted onto X-Gal containing plates and let them grow for 24 hours at 28ºC. An interaction was scored as positive when cells developed a blue color darker than the control strains.

To investigate if the interaction between the Myo5-C and the SH3 domains of Sla1 was direct, pull-down experiments with purified components were performed. Since the B42-Sla1 constructs used for yeast two hybrid experiments were also tagged with the HA epitope (see Table II, at section 6.3.3), the $Sla1_{SH3(1,2)}$ could be purified from yeast by affinity chromatography using agarose covalently coupled to an anti-HA antibody (see material and methods, section 6.4.3.1). A GST fusion construct bearing the Myo5 C-terminus was expressed and purified from *E. coli* using glutathione-Sepharose beads. As shown in Figure 44, glutathione-Sepharose beads coated with GST-Myo5-C_{ext} but not those coated with GST alone could efficiently pull down purified $Sla1_{SH3(1,2)}$.

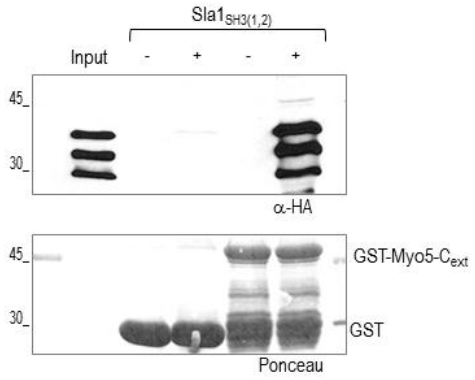

Figure 44. The interaction between the two first SH3 domains of Sla1 and Myo5-C_{ext} is direct.
Immunoblot (upper panel) of glutathione-Sepharose beads coated with GST or GST-Myo5-C_{ext} purified from E. coli, incubated with the HA-tagged SH3(1,2) domains of Sla1 (amino acids 1 to 136) purified from yeast. Beads were pulled down, rinsed several times and resuspended is SDS-PAGE sample buffer. Precipitated polypeptides were separated by SDS-PAGE and transferred to a nitrocellulose filter. Ponceau red staining was used to detect the GST-fused proteins (lower panel), and an antibody against HA (α-HA) was used to detect the HA-tagged Sla1-SH3(1,2) construct. Approximately 5 % of the total input and 20 μg of GST and the GST-Myo5-C_{ext} construct were loaded.

3.3.2.2. Depletion of Sla1 or disruption of the Myo5/Sla1 interaction enhances Myo5-induced actin polymerization.

Our previous results indicated that a Myo5 mutant mimicking the constitutive S1205 phosphorylated state had low capacity to induce the formation of actin *foci* but strongly interacted with Sla1. Sla1 is a known inhibitor of Las17-mediated actin polymerization, and as mentioned, our preliminary data indicate that Sla1 might also down-regulate Myo5-C_{ext} NPA (Dr. Fatima Idrissi, unpublished results). At that moment though, the domains involved in the Myo5/Sla1 interaction were not characterized. Therefore, to investigate whether two N-terminal SH3 domains of Sla1 are involved in the regulation of Myo5-C_{ext} NPA, *sla1Δ* extracts from yeast covered with a plasmid encoding the wild type *SLA1* (*WT*), an empty plasmid (*sla1Δ*), or a mutant *sla1* version lacking the two first SH3 domain (*sla1-SH3(1,2)Δ*) were prepared and incubated with GST-Myo5-C_{ext}-coated glutathione-Sepharose beads and rhodamine-labeled actin. The assembly of Myo5-induced actin *foci* was followed under the microscope. As shown in Figure 45A and 45B, the number of actin *foci* over the surface of Myo5-C_{ext} coated beads was significantly increased when incubated with *sla1Δ* extracts as compared with the isogenic wild type. Further, deletion of the two N-terminal SH3 domains of Sla1, which mediate direct binding

to the Myo5-C_{ext}, increased the number of *foci* assembled per surface area to the same extend as the complete depletion of Sla1. This result suggests that Sla1 directly inhibits Myo5-induced actin polymerization in the presence of yeast extracts and maps to the $Sla1_{SH3(1,2)}$ region the inhibitory activity of Sla1.

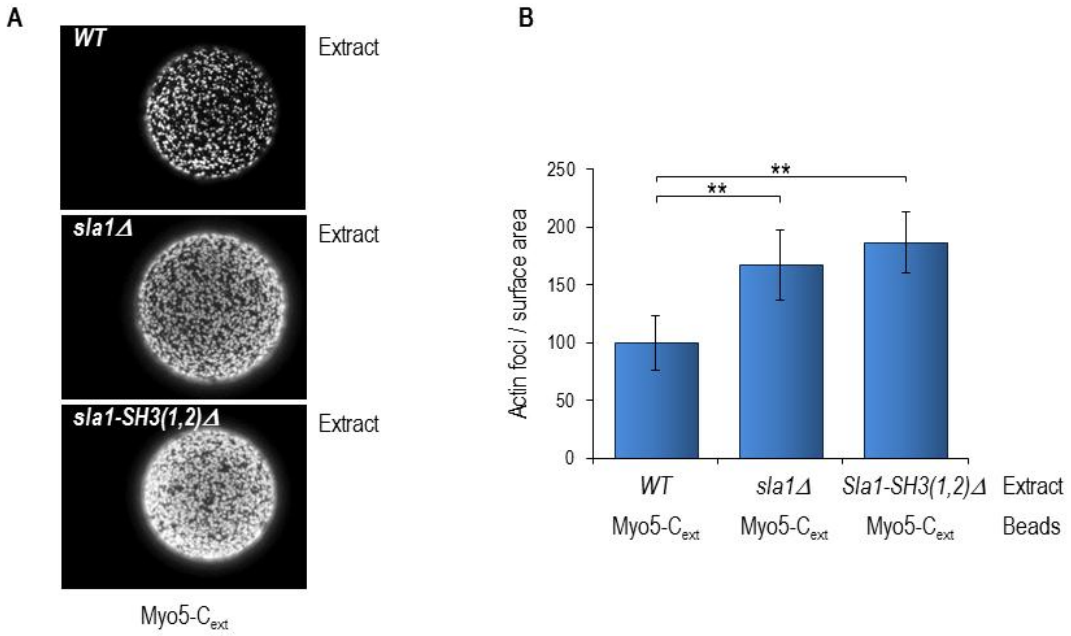

Figure 45. The Sla1 region required for Myo5 interaction down-regulates Myo5-C_{ext} mediated actin polymerization.
(A) Fluorescence micrographs of glutathione-Sepharose beads coated with GST-Myo5-C_{ext} (Myo5-C_{ext}) and incubated with yeast extracts from *sla1Δ* cells (Y03033) transformed either with a centromeric plasmid encoding Sla1 fused to HA (*WT*, p111*SLA1-HA*), a centromeric empty plasmid (*sla1Δ*, pYCplac111), or a centromeric plasmid encoding a Sla1 version lacking the SH3(1,2) domains (amino acids 1 to 136) (*sla1-SH3(1,2)Δ*, p111*sla1-SH3(1,2)Δ-HA*)) and 1μM rhodamine-labeled actin for 10 min at 26°C. (B Average patch density of the experiments described in (A). Actin *foci* were counted on a 25 x 25 μm^2 surface area of at least 10 different beads per experiment. At least two independent experiments were performed per each sample. The average actin *foci* density was normalized with respect to the average density of actin *foci* generated on beads coated with GST-Myo5-C_{ext} (Myo5-C_{ext}). Statistical analysis was performed using the two-tailed Student's t-test. ** represents a p-value ≤ 0.001.

3.4. Analysis of the regulatory role of the Myo5 S1205 phosphorylation by Cka2 in the endocytic uptake

Our previous data suggested that the Cka2 subunit of CK2 phosphorylates Myo5 S1205 *in vitro*, and that this phosphorylation negatively regulates the assembly of Myo5-induced actin *foci* in the presence of yeast extracts. On the other hand, the morphology and composition of the actin *foci* generated *in vitro* suggested that the assay specifically recapitulates the formation of the cortical actin structures that are essential for the formation of the primary endocytic vesicles at the plasma membrane (see above and introduction, section 1.2.3.1.1.2). Therefore, we decided to analyze how Myo5 S1205 phosphorylation by Cka2 might influence the endocytic internalization.

3.4.1. Phosphorylation of Myo5 S1205 delays the internalization of the endocytic coat and the dissociation of Myo5 from the plasma membrane

3.4.1.1. Mutations mimicking the constitutive phosphorylated or unphosphorylated Myo5 S1205 states have a limited influence on the ligand-induced Ste2 internalization rate

To investigate the possible influence of the Myo5 S1205 phosphorylation in the endocytic uptake, we first use a classical assay that quantitatively measures the internalization rate of exogenously added radioactive α-factor. The α-factor is a yeast pheromone, which binds to and activates the G-protein-coupled receptor Ste2 to trigger the matting response. The Ste2 receptor is constitutively internalized at a slow rate in the absence of α-factor, but it is stimulated ~10 fold in the presence of the ligand, as part of a pheromone desensitization program (Jenness and Spatrick, 1986). To investigate the possible influence of the Myo5 S1205 phosphorylation in the ligand-induced and constitutively internalization rates of Ste2, we constructed strains expressing the wild type Myo5 or the Myo5 mutants mimicking the constitutively unphosphorylated and phosphorylated S1205 states as the only source of myosin-I (*myo3Δ MYO5, myo3Δ myo5-S1205C* and *myo3Δ myo5-S1205D*, respectively).

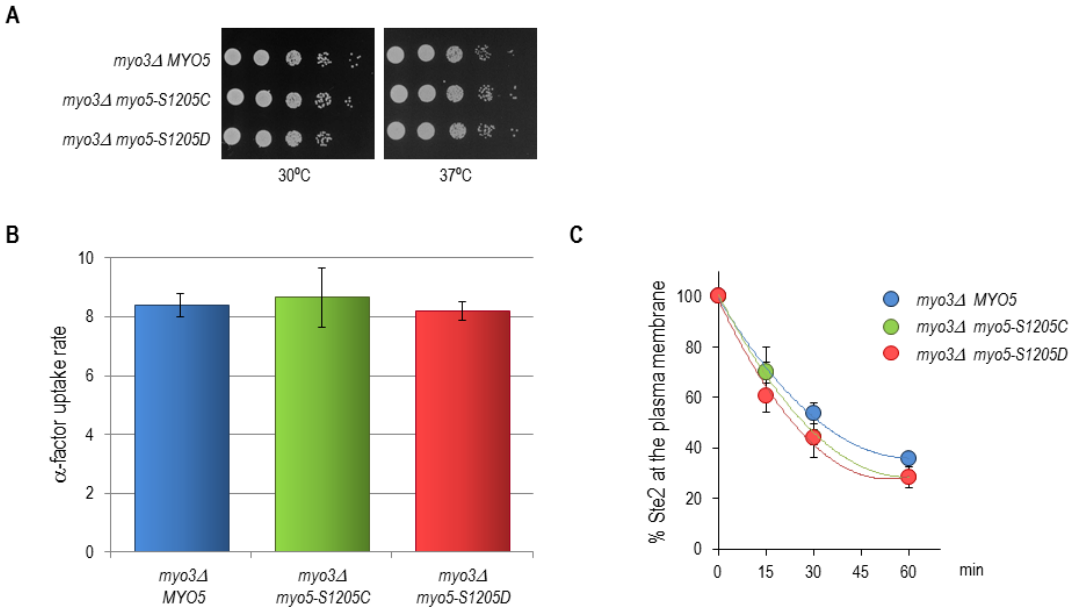

Figure 46. Phosphorylation of Myo5 S1205 does not seem to influence endocytic uptake of the Ste2 receptor.
(A) Serial dilutions of *myo3Δ MYO5* (SCMIG1097), *myo3Δ myo5-S1205C* (SCMIG1099), and *myo3Δ myo5-S1205D* (SCMIG1101) cells from a mid-log phase culture spotted onto YPD plates and let grown for 24 hours at either 30ºC or 37ºC. (B) ^{35}S-labeled α-factor internalization kinetics of *myo3Δ MYO5* (SCMIG1097), *myo3Δ myo5-S1205C* (SCMIG1099), and *myo3Δ myo5-S1205D* (SCMIG1101) strains. Cells grown to early-logarithmic phase were incubated at 37ºC in the presence of ^{35}S-labeled α-factor. Graph show the uptake rates (cell-bound α-factor internalized per min) within the linear range, during the first 9 min. At least three independent assays were performed for each strain. (C) Constitutive Ste2 internalization kinetics of *myo3Δ MYO5* (SCMIG1097), *myo3Δ myo5-S1205C* (SCMIG1099), and *myo3Δ myo5-S1205D* (SCMIG1101) strains. Cells grown to logarithmic phase were incubated at 30ºC in the presence of cycloheximide to prevent protein synthesis. Samples were taken at the indicated time points and endocytosis was stopped by incubating the cells at 0ºC in the presence of NaF and NaN_3. Graphs show the percentage of cell surface exposed Ste2 per time point. At least three independent assays were performed for each strain.

MYO3 was deleted in order to unveil possible phenotypes of the Myo5 S1205 mutants, which might be masked by the functionally redundant Myo3. Since deletion of the Arp2/3 binding domain of Myo5 (amino acids 1186-1219) does not cause synthetic lethality in combination with *myo3Δ* (Lechler et al., 2000; Sun et al., 2006), probably due to the presence of other activators of the Arp2/3 complex, we already expected the double mutants to be viable (Figure 46A). As shown in Figure 46B and 46C, although the Myo5 S1205 phosphorylation regulates the formation of Myo5-C_{ext}-induced actin structures, neither mutation of serine 1205 to cysteine (*myo3Δ myo5-S1205C*) nor to aspartate (*myo3Δ myo5-S1205D*) significantly altered the kinetics of Ste2 internalization. Functional redundancy among endocytic proteins often masks their individual contributions. Thus, we reasoned that the effect of the mutations might be covered by other NPFs *in vivo* (Engqvist-Goldstein and Drubin, 2003). In *S. cerevisiae*, four nucleating promoting factors (NPF) drive endocytic internalization: Las17, Pan1, and the type-I myosins Myo3 and Myo5 (Sun et al., 2006) (see introduction for details).

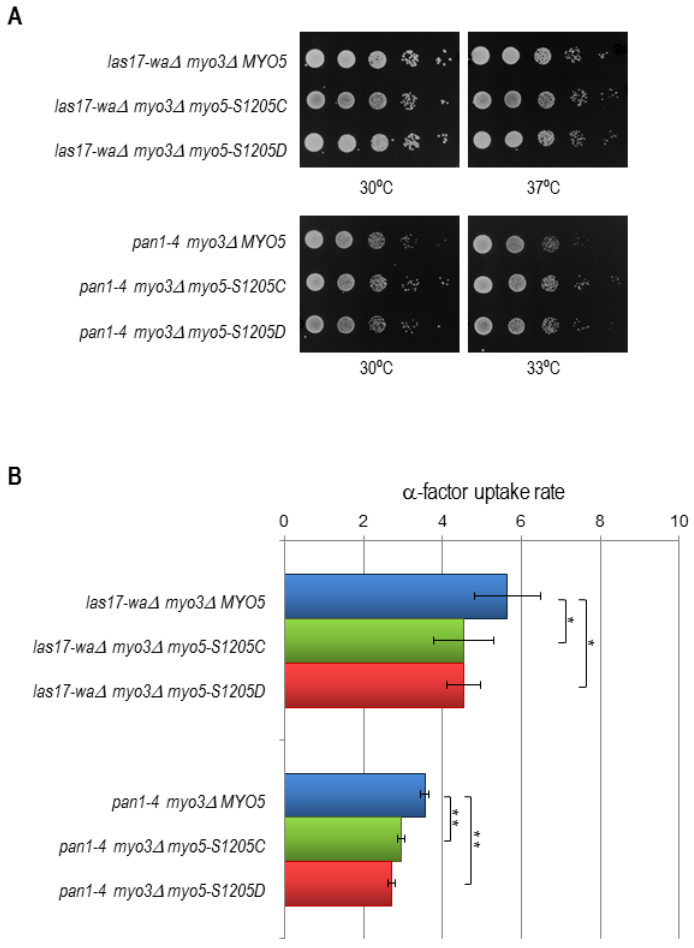

Figure 47. Mutation of Myo5 S1205 to C or D cause mild synthetic endocytic defects in combination with *las17* and *pan1* mutants. (A) Serial dilutions of *las17-waΔ myo3Δ MYO5* (SCMIG1108), *las17-waΔ myo3Δ myo5-S1205C* (SCMIG1110), *las17-waΔ myo3Δ myo5-S1205D* (SCMIG1112), *pan1-4 myo3Δ MYO5* (SCMIG1103), *pan1-4 myo3Δ myo5-S1205C* (SCMIG1105), and *pan1-4 myo3Δ myo5-S1205D* (SCMIG1107) cells from a mid-log phase culture spotted onto YPD plates and let grown for 24 hours at the indicated temperatures. (B) ^{35}S-labeled α-factor internalization kinetics of *las17-waΔ myo3Δ MYO5* (SCMIG1108), *las17-waΔ myo3Δ myo5-S1205C* (SCMIG1110), *las17-waΔ myo3Δ myo5-S1205D* (SCMIG1112), *pan1-4 myo3Δ MYO5* (SCMIG1103), *pan1-4 myo3Δ myo5-S1205C* (SCMIG1105), and *pan1-4 myo3Δ myo5-S1205D* (SCMIG1107) strains. Cells grown to early-logarithmic phase were incubated either at 37° (in the case of *las17-waΔ myo3Δ MYO5*, *las17-waΔ myo3Δ myo5-S1205C*, and *las17-waΔ myo3Δ myo5-S1205D* cells) or at 30°C (in the case of *pan1-4 myo3Δ MYO5*, *pan1-4 myo3Δ myo5-S1205C*, and *pan1-4 myo3Δ myo5-S1205D* cells) in the presence of ^{35}S-labeled α-factor. Graph show the uptake rates (cell-bound α-factor internalized per min) within the linear range, during the first 9 min. At least three independent assays were performed for each strain. Statistical analysis was performed using the two-tailed Student's t-test. * represents a p-value ≤ 0.1; ** represents a p-value ≤ 0.001

Abp1 also induces Arp2/3-dependent actin polymerization *in vitro* but appears to function as a general NPF inhibitor *in vivo,* since its deletion suppresses the *las17Δ* temperature sensitive growth phenotype (D'Agostino and Goode, 2005; Goode et al., 2001; Sun et al., 2006) and the *myo3Δ myo5Δ* synthetic lethality (data not shown). To explore the possibility that functional redundancy might mask the effect of the S1205 mutations, cells expressing the wild type or mutant Myo5 as the only source of myosin-I, were mated with cells lacking the acidic domain in the genes codifying for Las17 (*las17-waΔ*) or Pan1 (*pan1-4) (Tang and Cai, 1996)*. Genetic interactions and the kinetics of ligand-induced endocytosis were analyzed in the triple mutants covered with the *MYO5*, *myo5-S1205C* or *myo5-S1205D* alleles (Figure 47).

As shown in Figure 47B, a limited but significant decrease of the endocytic rate was observed in the *myo3Δ myo5Δ pan1-4* strain covered with the S1205 mutants, as compared to the isogenic strain covered with the wild type myosin ($p < 0.001$). A less significant effect was also observed in the *myo5Δ myo3Δ las17-waΔ* background ($p < 0.1$). The endocytic defect was independent of the charge imposed on this position indicating that both, phosphorylation and dephosphorylation might be required to sustain efficient internalization.

3.4.1.2. The Myo5-S1205D mutation significantly delays the internalization of the endocytic coat and the dissociation of Myo5 from the plasma membrane

Our previous results indicated that Myo5 phosphorylation at S1205 might play a role in endocytic budding. However, the α-factor internalization assay might not be sensitive enough to unequivocally unveil the effects of the S1205C and S1205D mutations in the presence of redundant mechanisms. On the other hand, mild but significant abnormalities in the cortical dynamics of GFP-tagged versions of proteins involved the endocytic uptake are often observed in mutants that do not show changes in the Ste2 internalization rate (Kaksonen et al., 2005). Thus, even though the type I myosins and the Arp2/3 complex are essential for the α-factor internalization, a Myo5 mutant lacking the acidic peptide, which is completely unable to sustain Arp2/3-dependent actin polymerization *in vitro* (F. Idrissi and V. Paradisi, personal communication), does not show a significant Ste2 internalization defect in a *myo3Δ myo5Δ* background (Sun et al., 2006). However, when the mutant is analyzed by time-lapse fluorescence live imaging a significant fraction of ABP1-RFP patches (about 35 %) have extended life spans and fail to internalize in this myosin mutant (versus only 8 % in the wild type).

Therefore, to further dissect the possible role of Myo5 S1205 phosphorylation in the endocytic uptake, we decided to investigate the effect of the Myo5-S1205C and S1205D mutations on the cortical dynamics of the myosin and Abp1. Abp1 is a marker of the endocytic actin module that travels into the cytosol with the endocytic vesicles, while Myo5 mainly remains associated with the plasma membrane. For that purpose, we generated *myo3Δ myo5Δ* strains expressing GFP-tagged versions of the wild type and the mutant myosins expressed from centromeric plasmids and a RFP tagged version of the actin module marker Abp1. The tagged versions of Myo5 and Abp1 had previously been shown to be functional (Grotsch et al., 2010).

As shown in Figure 48 and Table 3, the Myo5-S1205C mutation did not have an obvious influence in the life span of either GFP-Myo5 or Abp1-RFP, when compared with the wild type Myo5. In contrast though, the life span of both Abp1-RFP and GFP-Myo5 was significantly extended in cells expressing the Myo5-S1205D mutant. Thus, in cells expressing the wild type Myo5, the life spans of Abp1-RFP and GFP-Myo5 were 11.9 ± 2.9 s and 13.1 ± 2.9 s, respectively, whereas the Myo5-S1205D mutant remained in the cortex 15.8 ± 3.9 s in average before disappearing. Concomitantly, the life span of Abp1-RFP was extended to 15.6 ± 3.4 s in the *myo3Δ GFP-myo5-S1205D* mutant. In this strain, nearly 33 % of GFP-Myo5-S1205D cortical patches had life spans longer than 16 s versus only 5 % in the wild type.

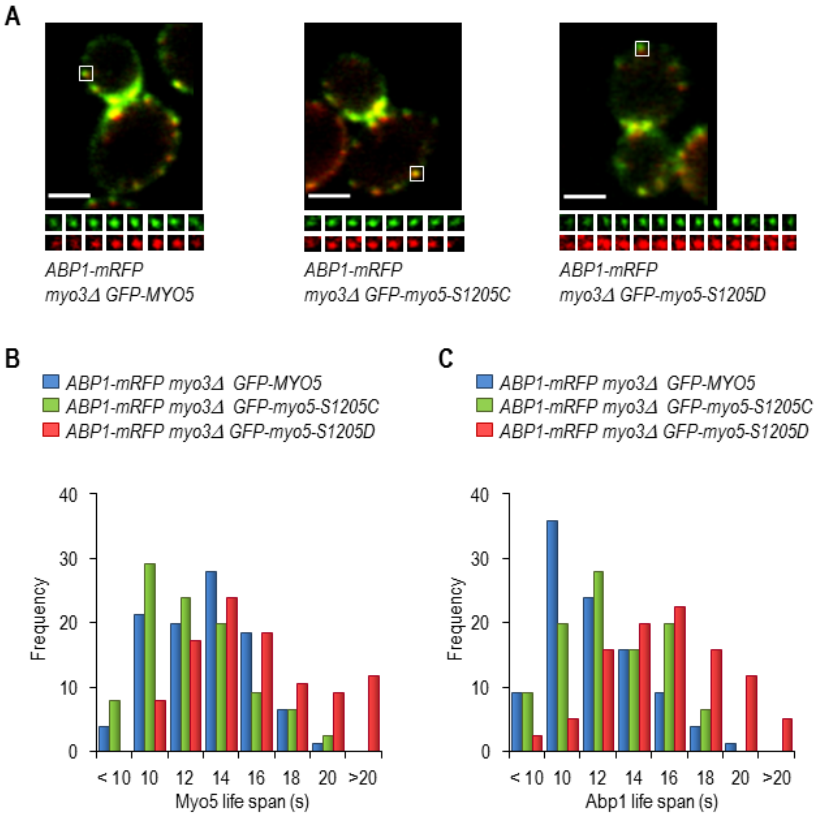

Figure 48. The Myo5 S1205D mutation, mimicking the constitutively phosphorylated state, extents the Myo5 and Abp1 lifespans at cortical patches.

(A) Fluorescence micrographs from a two-color time-lapse video microscopy of *myo3Δ myo5Δ ABP1-mRFP* cells covered with p33*GFP-MYO5* (*ABP1-mRFP myo3Δ GFP-MYO5,* strain SCMIG1126) or the indicated GFP-Myo5 mutant versions: p33*GFP-myo5-S1205C* (*ABP1-mRFP myo3Δ GFP-myo5-S1205C,* strain SCMIG1127) and p33*GFP-myo5-S1205D* (*ABP1-mRFP myo3Δ GFP-myo5-S1205D,* strain SCMIG1128). The different GFP-Myo5 versions were expressed from centromeric plasmids under the *MYO5* promoter. The upper panels show a single frame of representative cells, whereas the lower panels show consecutive frames of the boxed area, which were recorded every 2 seconds. Bar: 2 μm. n= 75 patches (B,C) Frequency distribution of the life span of 75 GFP-Myo5 (B) and Abp1-mRFP (C) cortical patches from the strains described in (A).

Since a fraction of endocytic patches in Myo5 mutant cells lacking the acidic peptide fail to internalize (Sun et al., 2006) and the Myo5-S1205D mutant down-regulated Arp2/3 dependent

actin polymerization (Figure 38), we decided to analyze the effect of Myo5 S1205 phosphorylation in the displacement of Abp1-mRFP patches from the cell cortex towards the cell interior. As shown in Figure 49, neither the Myo5-S120C nor the Myo5-S120D mutations seemed to influence the Abp1-mRFP inward movement.

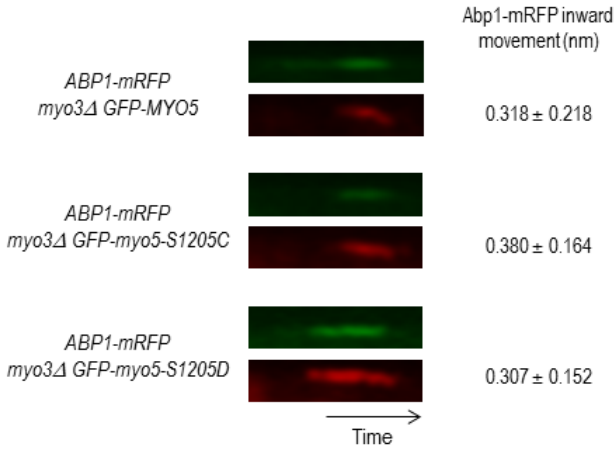

Figure 49. Mutation of the Myo5 S1205 does not prevent internalization of endocytic patches. Kymographs of representative individual endocytic patches from the strains described in Figure 48A. The mean distance covered by Abp1 from the cell cortex is shown. n= 30 patches.

	Abp1-mRFP		GFP-Myo5	
Strains	**avg ± s.d**	**p**	**avg ± s.d**	**p**
ABP1-mRFP myo3Δ GFP-MYO5	11.9 ± 2.9		13.1 ± 2.9	
ABP1-mRFP myo3Δ GFP-myo5-S1205C	12.7 ± 2.8	0.607	12.5 ± 3.0	0.037
ABP1-mRFP myo3Δ GFP-myo5-S1205D	15.6 ± 3.4	1.6×10^{-6}	15.8 ± 3.9	5.5×10^{-6}
ABP1-mRFP myo3Δ GFP-MYO5	11.4 ± 2.6		11.1 ± 2.2	

Table 3. Life spans of Abp1-mRFP and GFP-Myo5 patches of the stains described in Figure 48.
The average (avg) and standard deviation (s.d.) are indicated in seconds. 'p' represents the p-value of the two-tailed Student's t-test compared with the isogenic wild type. p-values under 0.001 indicate statistically significant differences. n= 75 patches.

Our *in vitro* and *in vivo* data was consistent with the view that phosphorylation of Myo5 S1205 down-regulates Myo5-induced actin polymerization and as a consequence, it delays the internalization of Abp1. However, at this point, we could not discard the possibility that the extended life spans of the myosin and Abp1 in the *myo3Δ GFP-myo5-S1205D* mutant reflected a premature association of the myosin to the clathrin coat, accompanied by an early onset of actin polymerization. This view could actually be consistent with the observation that the Myo5-S1205D mutation increased the affinity of the myosin for the clathrin adaptor Sla1, which arrive early to the endocytic sites. To further dissect the molecular mechanism behind the observed phenotypes, *myo3Δ myo5Δ* strains expressing GFP-tagged versions of the wild type and the mutant myosins and a mCherry tagged version of Sla1 were generated and the departure and arrival time of Myo5 relative to the endocytic coat was inspected.

As shown in Table 4, the arrival time of the myosin with respect to Sla1 was unaffected by the S1205D mutation, not even when only the long-lived GFP-Myo5-S1205D patches (ls longer than 16s) were considered in the analysis. If at all, arrival of Myo5 was slightly delayed (Table 4). This result indicated that phosphorylation of the Myo5 S1205 did not cause premature arrival of Myo5 but rather slowed down the internalization of the endocytic coat. Consistent with this view, the life span of Sla1 was significantly extended in the long-lived Myo5-GFP subpopulation of patches (from 23.1 ± 4.9 s in the wild type to 29.9 ± 7.5 s in the mutant, $p<0.001$; n=30), see also Figure 50. On the other hand, we also noticed that the departure time of Myo5 relative to Sla1 was significantly extended in the long-lived Myo5-S1205D mutants (from 6.5 ± 2.9 s in the wild type to 10.6 ± 4.7 s in the mutant, $p<0.001$; n=30), indicating that phosphorylation at this position might also interfere with the dissociation of Myo5 from the plasma membrane, once the vesicle has departed into the cytosol.

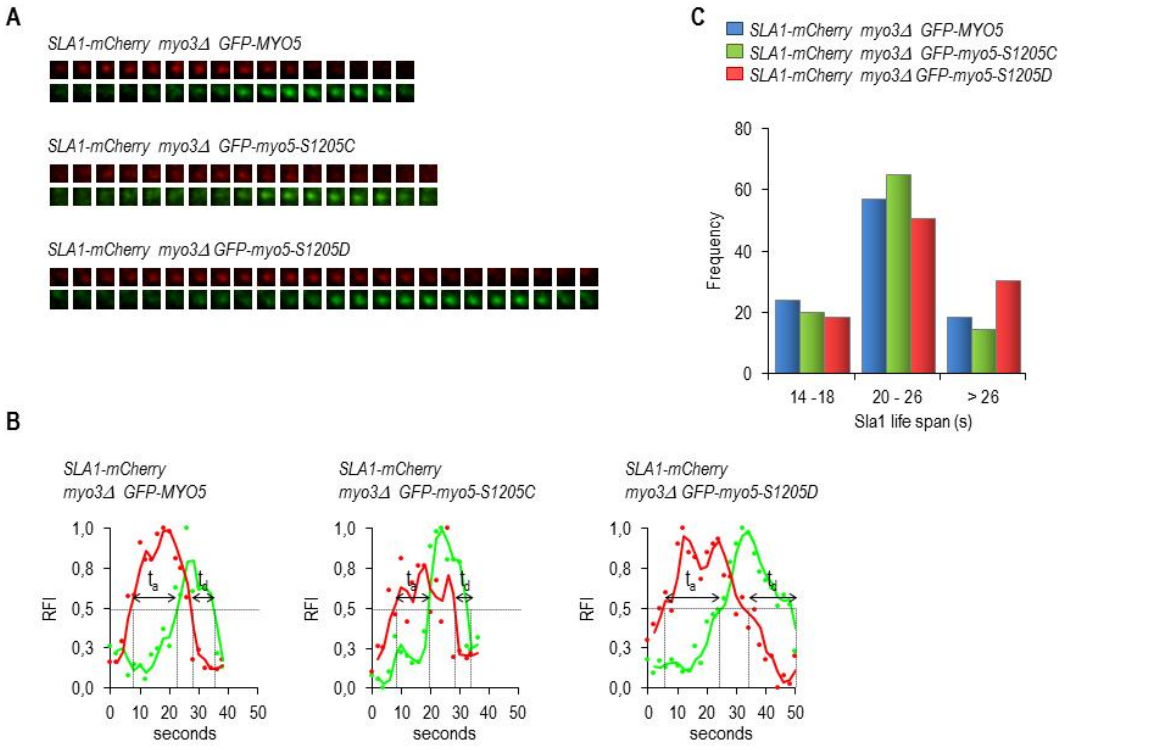

Figure 50. The Myo5 S1205D mutation, mimicking the constitutively phosphorylated state, causes a delay in the internalization of the endocytic coat.

(A) Fluorescence micrographs of consecutive frames from a two-color time-lapse video microscopy of *myo3Δ myo5Δ SLA1-mCherry* cells covered with p33*GFP-MYO5* (*SLA1-mCherry myo3Δ GFP-MYO5,* strain SCMIG1160) or the indicated GFP-Myo5 mutant versions: p33*GFP-myo5-S1205C* (*SLA1-mCherry myo3Δ GFP-myo5-S1205C,* strain SCMIG1162) and p33*GFP-myo5-S1205D* (*SLA1-mCherry myo3Δ GFP-myo5-S1205D,* strain SCMIG1163). The different GFP-Myo5 versions were expressed from a centromeric plasmid under the *MYO5* promoter. For the strain *SLA1-mCherry myo3Δ GFP-myo5-S1205D* only patches with Myo5 life spans longer than 16 s are represented. Frames were recorded every 2 seconds. (B) Graphs showing the relative fluorescence intensity (RFI) plotted against time for the Sla1-mCherry (red) and the different GFP-Myo5 versions (green) two-color time-lapse movies shown in (A). t_a and t_d represents the arrival and departure times of GFP-Myo5 relative to Sla1-mCherry. (C) Frequency distribution of the life span of 75 Sla1-mCherry cortical patches from the strains described in (A).

Strains	*SLA1-mCherry myo3Δ GFP-MYO5*	*SLA1-mCherry myo3Δ GFP-myo5-S1205D*	
	avg ± s.d	avg ± s.d	p
Ls Sla1-mCherry	23.1 ± 4.9	29.9 ± 7.5 (*)	1.2×10^{-4}
Ls GFP-Myo5 or GFP-Myo5-S1205D	13.1 ± 2.5	20.5 ± 3.8 (*)	9.2×10^{-12}
t_a GFP-Myo5 or GFP-Myo5-S1205D	16.0 ± 4.5	20.2 ± 6.6 (*)	0.006
t_d GFP-Myo5 or GFP-Myo5-S1205D	6.5 ± 2.9	10.6 ± 4.7 (*)	2.3×10^{-5}

Table 4. Phosphorylation of Myo5 S1205 does not affect its recruitment but interferes with its dissociation at endocytic sites.
Lifespans (Ls) of correlative Sla1-mCherry and either GFP-Myo5 or *GFP-myo5-S1205D* patches and arrival (t_a) and departure times (t_d) of GFP-Myo5 relative to Sla1-mCherry, analyzed in the indicated strains. The average (avg) and standard deviation (s.d.) are indicated in seconds. p represents the p-value of the two-tailed Student's t-test. p-values under 0.001 indicate statistically significant differences. (*)Subpopulation associated with *GFP-MYO5* or *GFP-myo5-S1205D* cortical patches with lifespans longer than 16 s. n= 30 patches

The phenotype installed by the S1205D mutation were relatively mild but they appear to be highly significant and specific since they clearly differed from those imposed by a mutation in calmodulin (*cmd1-226*), which disrupts the interaction with Myo5, releases autoinhibition and promotes early association of the myosin with the endocytic patch (Figure 51) (Grotsch et al., 2010). In this calmodulin mutant the Myo5 and Abp1 life spans were also extended to 19.5 ± 5.7 and 18.5 ± 5.7 s, respectively. However, in the long-lived GFP-Myo5 patches analyzed in the *cmd1-226* mutant, the life span of Sla1 appeared unaltered as compared with the strain expressing the wild type calmodulin (*CMD1*) and the arrival time of Myo5 and Abp1 relative to Sla1 was shortened about 5 seconds (Figure 51 and Table 5).

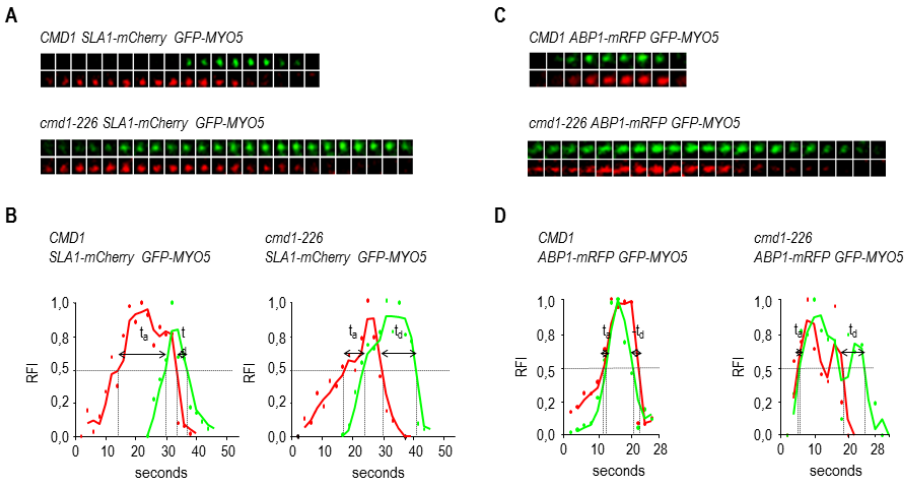

Figure 51. GFP-Myo5 arrives earlier to and departs later from the endocytic sites in the *cmd1-226* mutant.
(A, C) Fluorescence micrographs of consecutive frames from three representative double-color time-lapse movies of cortical patches from *cmd1Δ myo5Δ* strains with mCherry tagged *SLA1* (A), expressing GFP-Myo5 from a centromeric plasmid under the *MYO5* promoter and either the wt *CMD1* (SCMIG1077) or the *cmd1-226* mutant (SCMIG1078), or from *cmd1Δ myo5Δ* strains with mRFP tagged *ABP1* (C), expressing GFP-Myo5 from a centromeric plasmid under the *MYO5* promoter and either the wt *CMD1* (SCMIG1063) or the *cmd1-226* mutant (SCMIG1064). Frames were recorded every 2 s. GFP-Myo5 patches with life spans longer than 16 s were analyzed for the *cmd1-226* strain. (B, D) Graphs demonstrating the relative fluorescence intensity (RFI) plotted against time for the Sla1-mCherry (red) and GFP-Myo5 (green) (B) double-colour time-lapse movies shown in (A), or for the Abp1-mRFP (red) and GFP-Myo5 (green) (D) double-colour time-lapse movies shown in (C). t_a and t_d indicate the arrival and departure times of GFP-Myo5 relative to Sla1-mCherry (B) or to Abp1-mRFP (D), respectively. Data published in (Grotsch et al., 2010).

Strains	*SLA1-mCherry GFP-MYO5 CMD1*	*SLA1-mCherry GFP-MYO5 cmd1-226*	
	avg ± s.d	avg ± s.d	p
Ls Sla1-mCherry	26.0 ± 3.3	24.9 ± 4.6 (*)	0.389
Ls GFP-Myo5	13.1 ± 2.2	23.8 ± 4.6 (*)	1.0×10^{-5}
t_a GFP-Myo5	17.7 ± 4.0	12.3 ± 4.6 (*)	2.5×10^{-4}
t_d GFP-Myo5	4.8 ± 2.9	10.5 ± 3.7 (*)	1.0×10^{-5}

Table 5. GFP-Myo5 arrives earlier to and departs later from the endocytic sites in the cmd1-226 mutant.
Life spans (Ls) of correlative Sla1-mCherry and GFP-Myo5 patches and arrival (t_a) and departure times (t_d) of GFP-Myo5 relative to Sla1-mCherry, analyzed in the indicated strains. The average (avg) and standard deviation (s.d.) are indicated in seconds. 'p' represents the p-value of the Student's t-test. p-values < 0.001 indicate statistically significant differences. (*)Subpopulation associated with *GFP-MYO5* or *GFP-myo5-S1205D* cortical patches with life spans longer than 16 s. n= 20 patches. Data published in (Grotsch et al., 2010).

3.4.2. Overexpression of *CKA2*, but not *CKA1*, delays the internalization of the endocytic coat and the dissociation of Myo5 from the plasma membrane

Our previous results indicated that phosphorylation of the Myo5 S1205 down-regulates Myo5-induced actin polymerization at the endocytic sites. Since the catalytic subunit Cka2 of CK2 seemed to be specifically involved in the phosphorylation of this residue, we next investigated if overexpression of this kinase phenocopied the Myo5 mutant mimicking the constitutively phosphorylated S1205 state. For this purpose, a *myo3Δ* strain expressing a GFP tagged versions of Myo5 and a RFP-tagged version of Abp1 was transformed with a multicopy plasmid encoding *CKA2* and the life span of Myo5 and Abp1 in this strain was compared to that of GFP-Myo5 in the isogenic strain bearing the empty vector. Consistent with the previous data indicating that Cka2 phosphorylated Myo5 S1205 and that phosphorylation of Myo5 at this residue extended its life span, a slight but statistically significant increase of the myosin life span at cortical sites was observed in the strain overexpressing *CKA2* (Table 3, compare the *ABP1-mRFP myo3Δ GFP-MYO5* and *ABP1-mRFP myo3Δ GFP-MYO5 +CKA2* strains; see also Figure 52A and 52B). Similar also to what was observed in the Myo5-S1205D mutant, the Abp1-RFP life span was also extended in the cells overexpressing Cka2, but the inward movement of Abp1-mRFP patches from the cell cortex appeared unaffected (Figure 52A and 52C, and Figure 53). Finally, analysis of the long-lived Myo5 patches in a *myo3Δ GFP-MYO5 SLA1-mCherry* strain overexpressing Cka2 demonstrated that the life span of Sla1-RFP patches was also slightly extended but the arrival of GFP-Myo5 relative to Sla1-mCherry appeared unaltered, as compared with the isogenic strain bearing the empty plasmid (Table 6). The Myo5 life span extension could be specifically attributed to the overexpression of *CKA2* since no significant difference in the dynamics of the type I myosin nor in Abp1 were observed in cells overexpressing *CKA1* (Table 3 and Figure 52; *ABP1-mRFP myo3Δ GFP-MYO5 +CKA1*). Also, the effect observed upon overexpression of *CKA2* required its kinase activity since a point mutation in the enzyme active site (K79A) abolished the observed phenotype (Table 3 and Figure 52; *ABP1-mRFP myo3Δ GFP-MYO5 +cka2-K79A*). Finally, we could demonstrate that the effect installed by overexpression of Cka2 was at least partially dependent of the Myo5 S1205 phosphorylation, since overexpression

of *CKA2* failed to elongate the life span of the Myo5-S1205C mutant (Table 3 and Figure 52; *ABP1-mRFP myo3Δ GFP-myo5-S1205C +CKA2*). In essence, our results indicated that phosphorylation of Myo5 S1205 by Cka2 down-regulates Myo5-induced actin assembly at endocytic sites.

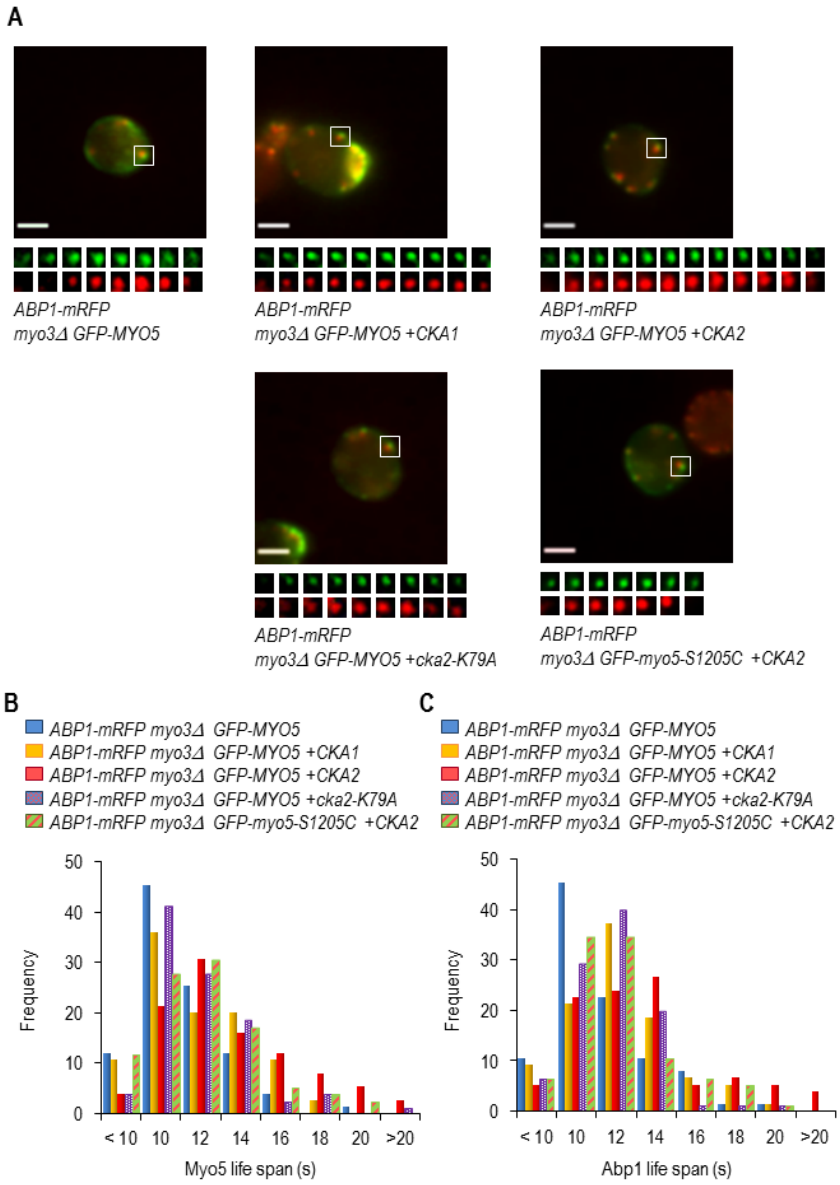

Figure 52. Overexpression of the catalytic subunit Cka2, but not of Cka1 or a kinase-dead version of Cka2, extents the Myo5 and Abp1 life spans in a fraction of endocytic patches.

(A) Fluorescence micrographs from a two-color time-lapse video microscopy of *myo3Δ myo5Δ ABP1-mRFP* cells covered with p33*GFP-MYO5* (*ABP1-mRFP myo3Δ GFP-MYO5,* strain SCMIG1126) transformed with a multicopy plasmid either empty (*ABP1-mRFP myo3Δ GFP-MYO5*, pYEplac181) or encoding the catalytic subunit Cka1 (*ABP1-mRFP myo3Δ GFP-MYO5 +CKA1*, p181*CKA1*), the catalytic subunit Cka2 (*ABP1-mRFP myo3Δ GFP-MYO5 +CKA2*, p181*CKA2*), or a kinase-dead version of the catalytic subunit Cka2 (*ABP1-mRFP myo3Δ GFP-MYO5 +cka2-K79A*, p181*cka2-K79A*), and *myo3Δ myo5Δ ABP1-mRFP* cells covered with the Myo5 mutant versions p33*GFP-myo5-S1205C* (*ABP1-mRFP myo3Δ GFP-myo5-S1205C,* strain SCMIG1127) transformed with a multicopy plasmid encoding the catalytic subunit Cka2 (*ABP1-mRFP myo3Δ GFP-myo5-S1205C +CKA2*, p181*CKA2*). The upper panels show a single frame of representative cells, whereas the lower panels show consecutive frames of the boxed area, which were recorded every 2 seconds. Bar: 2.5 um. (B,C) Frequency distribution of the life span of 75 GFP-Myo5 (B) and Abp1-mRFP (C) cortical patches from the strains described in (A).

Strains	Abp1-mRFP avg ± s.d	p	GFP-Myo5 avg ± s.d	p
ABP1-mRFP myo3Δ GFP-MYO5	11.4 ± 2.6		11.1 ± 2.2	
ABP1-mRFP myo3Δ GFP-MYO5 +CKA1	12.3 ± 2.6	0.034	11.8 ± 2.6	0.070
ABP1-mRFP myo3Δ GFP-MYO5 +CKA2	13.3 ± 3.5	1.4×10^{-4}	13.4 ± 3.4	3.2×10^{-6}
ABP1-mRFP myo3Δ GFP-MYO5 +cka2-K79A	11.8 ± 2.1	0.269	11.9 ± 2.5	0.056
ABP1-mRFP myo3Δ GFP-myo5-S1205C +CKA2	11.9 ± 2.6	0.166	12.0 ± 2.8	0.041

Table 6. Life spans of Abp1-mRFP and GFP-Myo5 patches of the stains described in Figure 52.
The average (avg) and standard deviation (s.d.) are indicated in seconds. 'p' represents the p-value of the two-tailed Student's t-test compared with the isogenic wild type. p-values under 0.001 indicate statistically significant differences. n= 75 patches.

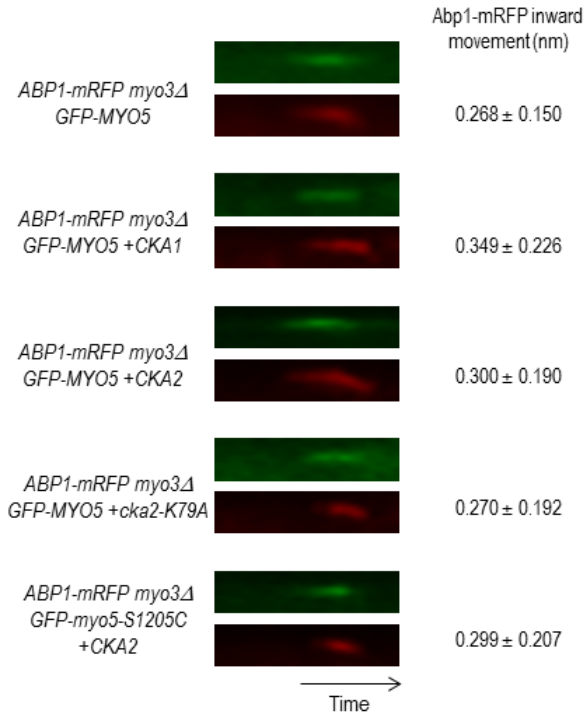

Figure 53. Overexpression of the catalytic subunit Cka2 does not prevent internalization of endocytic patches.
Kymographs of representative individual endocytic patches from the strains described in Figure 53A. The mean distance covered by Abp1 from the cell cortex is also shown. n= 30 patches.

Strains	*SLA1-mCherry myo3Δ GFP-MYO5* avg ± s.d	*SLA1-mCherry myo3Δ GFP-MYO5 +CKA2* avg ± s.d	p
Ls Sla1-mCherry	19.9 ± 3.2	26.0 ± 7.7 (*)	3.4×10^{-4}
Ls GFP-Myo5	12.3 ± 2.2	22.8 ± 4.2 (*)	3.0×10^{-15}
t_a GFP-Myo5	11.5 ± 3.8	14.4 ± 7.0 (*)	0.029
t_d GFP-Myo5	3.9 ± 2.4	11.8 ± 4.9 (*)	1.5×10^{-9}

Table 7. Overexpression of the catalytic subunit Cka2 does not affect the recruitment of Myo5 but interferes with Myo5-dissociation at endocytic sites.
Life spans (Ls) of correlative Sla1-mCherry and GFP-Myo5 patches and arrival (t_a) and departure times (t_d) of GFP-Myo5 relative to Sla1-mCherry, analyzed in the indicated strains. The average (avg) and standard deviation (s.d.) are indicated in seconds. 'p' represents the p-value of the two-tailed Student's t-test. p-values under 0.001 indicate statistically significant differences. (*)Subpopulation associated with *GFP-MYO5* or *GFP-myo5-S1205D* cortical patches with life spans longer than 16 s. n= 30 patches.

3.4.3. Cka2 has endocytic functions others than the phosphorylation of Myo5 S1205

3.4.3.1. Depletion of Cka2, but not of Cka1, significantly accelerates internalization of Ste2

Even though the mutants mimicking the constitutive phosphorylated and unphosphorylated Myo5 S1205 states did not exhibited obvious differences in the internalization rate of Ste2, we reasoned that Cka2 might have endocytic targets other than the myosins and therefore, strains lacking or overexpressing this kinase might have more pronounced uptake defects. Actually, overexpression of Cka2 down-regulated the assembly of Myo5-induced actin patches by a mechanism that was partially independent of the phosphorylation of the Myo5 S1205 (see above). Interestingly, even though overexpression of Cka2 still did not cause any significant α-factor uptake defect (Figure 54), we could observe a small acceleration of ligand-induced Ste2 internalization in a *cka2Δ* strain, as compared to the isogenic wild type (Figure 55A). The observed effect was specific for Cka2 since depletion of the other catalytic subunit Cka1, did not have any effect on the α-factor internalization rate. A more obvious acceleration of the Ste2 internalization in the *cka2Δ* strain could be demonstrated when the constitutive uptake of the receptor was measured. A 1.69 fold acceleration of the constitutive Ste2 uptake rate could be measured in the *cka2Δ* strain, as compared to the wild type or the isogenic *cka1Δ* strain (Figure 55B). Probably as a result of the acceleration in the constitutive internalization of Ste2, the total expression level and the surface exposure of the receptor were diminished (Figure 55C and 55D).

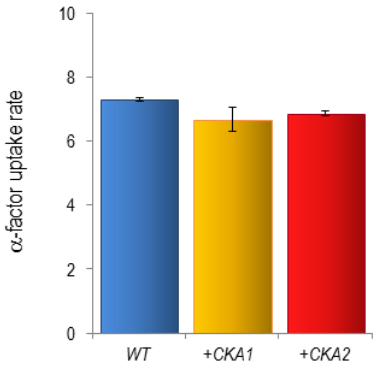

Figure 54. Overexpression of neither Cka1 nor Cka2 significantly influences ligand-induced endocytic uptake of the Ste2 receptor.
^{35}S-labeled α-factor internalization kinetics of WT cells (BY4741) transformed with a multicopy plasmid either empty (Empty, pYEplac181) or encoding the CK2 catalytic subunit Cka1 (+CKA1, p181*CKA1*) or the catalytic subunit Cka2 (+CKA2, p181*CKA2*). Cells grown to early-logarithmic phase were incubated at 28ºC in the presence of ^{35}S-labeled α-factor. Graph shows the uptake rates (cell-bound α-factor internalized per min) within the linear range, during the first 9 min. At least three independent assays were performed for each strain. Statistical analysis was performed using the two-tailed Student's t-test. The p-value was ≥ 0.1.

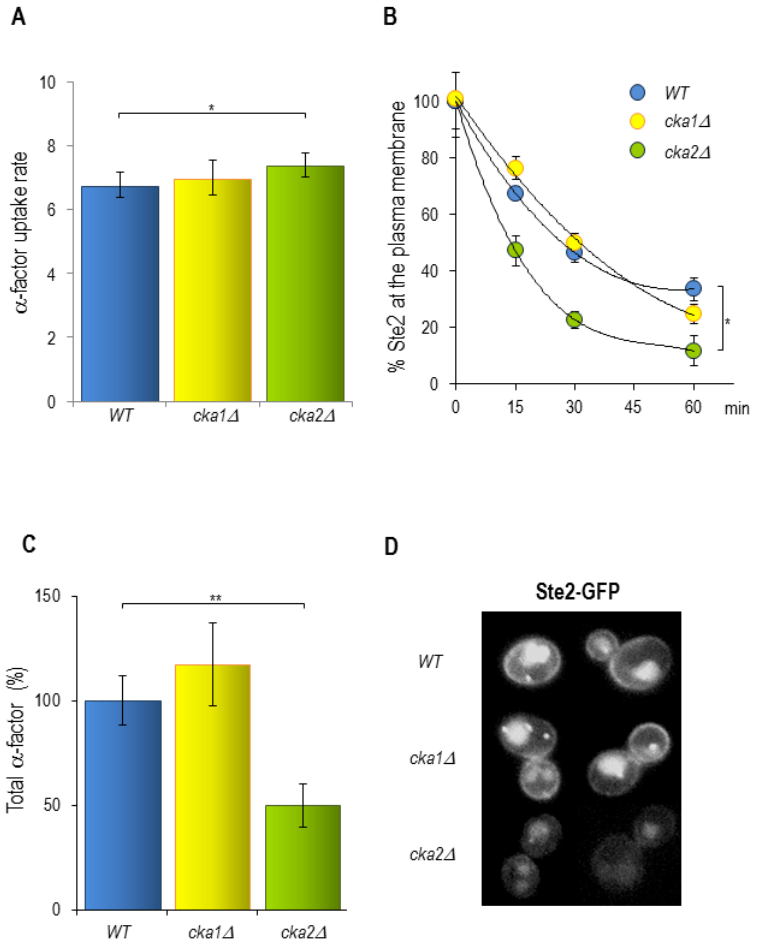

Figure 55. Depletion of the CK2 catalytic subunit Cka2, but not of Cka1, accelerates the endocytic uptake of the Ste2 receptor. (A)^{35}S-labeled α-factor internalization kinetics of wild type (SCMIG100), *cka1Δ* (SCMIG716), and *cka2Δ* (SCMIG717) strains. Cells grown to early-logarithmic phase were incubated at 37ºC in the presence of ^{35}S-labeled α-factor. Graph shows the uptake rates (cell-bound α-factor internalized per min) within the linear range, during the first 9 min. At least three independent assays were performed for each strain. (B) Constitutive Ste2 internalization kinetics of wild type (SCMIG100), *cka1Δ* (SCMIG716), and *cka2Δ* (SCMIG717) strains. Cells grown to logarithmic phase were incubated at 30ºC in the presence of cycloheximide to prevent protein synthesis. Samples were taken at the indicated time points and endocytosis was stopped by incubating the cells at 0ºC in the presence of NaF and NaN_3. Graphs show the percentage of cell surface exposed Ste2 per time point. At least three independent assays were performed for each strain. (C) Graph showing the % of total cell-bound α-factor for the strains described in A and B. The total cell-bound α-factor measures the total radioactive counts (at pH6) at the first time point taken (at 3 min) normalized with respect to the total radioactive counts of the wild type strain. (D) Fluorescence micrographs of wild type (SCMIG100), *cka1Δ* (SCMIG716), and *cka2Δ* (SCMIG717) cells carrying a centromeric plasmid encoding C-terminal GFP tagged Ste2 expressed under the STE2 promoter (Ste2-GFP, p111*STE2-GFP*). Statistical analysis was performed using the two-tailed Student's t-test. * represents a p-value ≤ 0.1. ** represents a p-value ≤ 0.01.

The acceleration in the internalization rate observed in the *cka2Δ* strain was not a consequence of a general acceleration in membrane traffic since the biosynthetic traffic of the carboxypeptidase Y (CPY) from the ER to the vacuole appeared unaltered, as assessed by following its maturation kinetics in a ^{35}S-Met and ^{35}S-Cys pulse-chase experiment (see materials and methods, section 6.9.2) (Figure 56). Upon translocation into de ER (p1) CPY travels to the Golgi where it is glycosylated (p2). Transport to late endosomal compartments and the vacuole coincides with its cleavage to generate the active mature form (m) (Stevens et al., 1982). As shown in Figure 56, maturation and traffic of CPY to the vacuole appeared unaffected in the *cka2Δ* strain, as compared to the wild type.

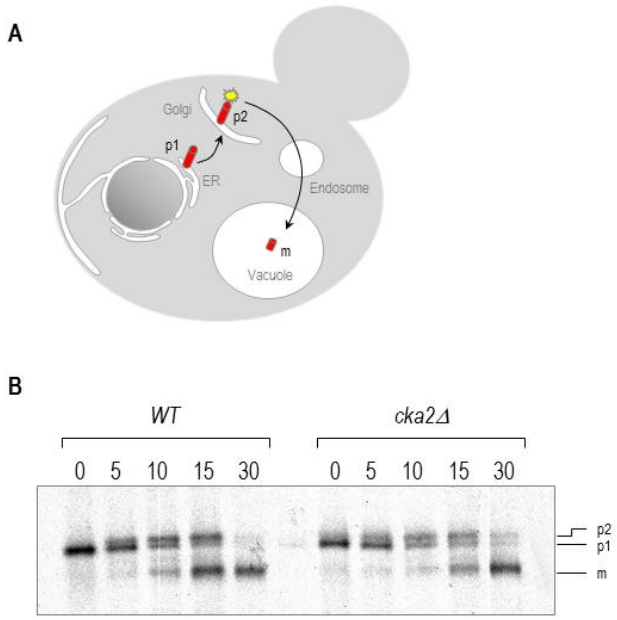

Figure 56. Biosynthetic traffic to the vacuole is not significantly affected in the *cka2Δ* mutant.
(A) Schematic representation of the vacuolar protein sorting of carboxypeptidase Y (CPY). CPY is synthesized in the endoplasmic reticulum (ER) as an inactive precursor. Upon removal of the N-terminal signal sequence it undergoes N-linked glycosylation to generate the ER-modified form (p1). After transport to the Golgi apparatus it suffers further glycosyl modifications that produce the Golgi-modified form (p2). Finally, the CPY precursor is targeted to the vacuole where it is cleaved by luminal proteases to form the active mature CPY form (m). (B) Autoradiography showing carboxypeptidase Y maturation in wild type (SCMIG100) and *cka2Δ* (SCMIG717) cells. Cells were pulsed with a ^{35}S-labeling mix containing ^{35}S-methionine and ^{35}S-cysteine for 5 min and chased by addition of non-labeled methionine and cysteine. CPY was immunoprecipitated from samples taken at the indicated time points, subjected to SDS-PAGE and analyzed by autoradiography. p1, endoplasmic reticulum form; p2, Golgi form; m, mature vacuolar form.

In *Saccharomyces cerevisiae*, depletion of Myo5 causes a partial endocytic defect at 37ºC, which is not observed after depletion of the less abundant Myo3 (Geli and Riezman 1998, Ghaemmaghami 2003). Interestingly, the *myo5Δ* uptake defect can be suppressed by overexpression of Vrp1, indicating that stimulation of the residual Myo3 NPA can overcome the defects installed in the *myo5Δ* mutant (Geli et al., 2000). Since Cka2 negatively modulated Myo5-induced Arp2/3-dependent actin polymerization (see above) and Myo3 also bears a serine at this position (S1257), we investigated if deletion of *CKA2* was able to suppress the endocytic defect of the *myo5Δ* strain. As shown in Figure 57A, deletion of *CKA2* partially restored endocytosis in a *myo5Δ* background. Consistent with the *in vitro* actin polymerization assay, suppression was specific for depletion of Cka2, since the α-factor uptake rate of the double *myo5Δ cka1Δ* strain was indistinguishable from that of the *myo5Δ* single mutant. However, depletion of *CKA2* also partially suppressed the endocytosis defects of other mutants such as *sac6Δ*, indicating that this kinase down-regulates functions required for endocytic budding other than the type I myosin NPA (Figure 57B). Also consistent with the hypothesis that Cka2 might have endocytic targets other than the Myo5 S-1205, we failed to observe acceleration of the ligand-induced or constitutive internalization of Ste2 in the mutant mimicking the constitutive unphosphorylated state in a *myo3Δ* background, as compared with the strain expressing the *myo5-S1205D* mutant or the wild type Myo5 (Figure 46B and 46C).

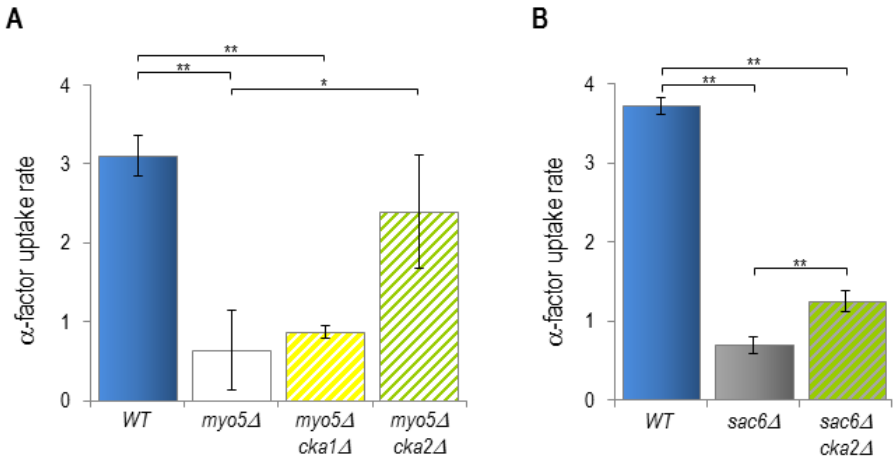

Figure 57. Depletion of the CK2 catalytic subunit Cka2, but not Cka1, suppresses the endocytic defect of *myo5Δ* and *sac6Δ* strains.
(A) ^{35}S-labeled α-factor internalization kinetics of wild type (RH2881), *myo5Δ* (SCMIG275), *myo5Δ cka1Δ* (SCMIG812), and *myo5Δ cka2Δ* (SCMIG811) strains transformed with a multicopy plasmid encoding the Ste2 receptor (p181*STE2*). Cells grown to early-logarithmic phase were incubated at 37ºC in the presence of ^{35}S-labeled α-factor. Graph shows the uptake rates (cell-bound α-factor internalized per min) within the linear range, during the first 9 min. At least three independent assays were performed for each strain. (B) ^{35}S-labeled α-factor internalization kinetics of wild type (RH2881), *sac6Δ* (RH2565), and *sac6Δ cka2Δ* (SCMIG814) strains transformed with a multicopy plasmid encoding the Ste2 receptor (p181*STE2*). Cells grown to early-logarithmic phase were incubated at 37ºC in the presence of ^{35}S-labeled α-factor. Graph show the uptake rates (cell-bound α-factor internalized per min) within the linear range, during the first 9 min. At least three independent assays were performed for each strain. Statistical analysis was performed using the two-tailed Student's t-test. * represents a p-value ≤ 0.01; ** represents a p-value ≤ 0.001.

3.4.3.2. Depletion of Cka2 up-regulates the assembly of endocytic patches and slightly accelerates their maturation, independently of Myo5 phosphorylation at S1205

The results presented above showed an acceleration of ligand-induced and constitutive Ste2 internalization in the *cka2Δ* mutant strain, which might be caused by an increase in the number of endocytic events, a faster maturation of the endocytic vesicles derived from the plasma membrane and/or a more efficient packing of Ste2 in the endocytic vesicles. Since cortical patches are sites of Ste2-mediated α-factor endocytic uptake (Kaksonen et al., 2003; Toshima et al., 2006) see introduction for details), the number and life span of cortical patches of the clathrin coat marker Sla1 were analyzed in *cka2Δ* cells and compared with that of the wild type to gain insight into the mechanisms that trigger this acceleration.

Wild type and *cka2Δ* cells expressing a mCherry-tagged *SLA1* version (*SLA1-mCherry* and *cka2Δ SLA1-mCherry*, respectively) were grown to early logarithmic phase and directly visualized using a wide-field epifluorescence microscope at room temperature. Interestingly, we found that the number of endocytic patches per cell appeared increased and the life span of the endocytic patches was slightly shortened in the *cka2Δ* strain, as compare to the wild type. The number of Sla1-mCherry cortical patches per cell was 8.9 ± 2.4 for a wild type unbudded cell, and it was significantly increased in the *cka2Δ* strain to 9.8 ± 3.0 ($p<0.001$; n=250 cells; see histogram in Figure 58A). In addition, the average life span of Sla1-mCherry cortical patches was slightly reduced, from 21.5 ± 3.8 s in the wild type to 20.0 ± 3.3 s in the *cka2Δ* strain ($p<0.01$; n=75).

As shown in Figure 51B, nearly 40 % of the patches had life spans between 14 and 18 s in Cka2 depleted cells versus only ~ 20 % in the isogenic wild type. This effect was not an artifact due to a decreased intensity of the Sla1-mCherry patches in the *cka2Δ* strain, since we did not observe in this strain a difference in the average intensity of the patches, as compared to the wild type. The shorter Sla1 life span in the *cka2Δ* mutant could not be demonstrated for GFP-Myo5, indicating that either the differences were too small to be unveiled by the methodology used or the acceleration of the endocytic process occurred in the initial stages, before Myo5 arrived (Figure 58C). Consistent also with the view that the effects observed by depletion of Cka2 were at least partially independent of the Myo5 S1205 phosphorylation was the observations that the dynamics of Sla1-mCherry patches were not altered in the *myo3Δ GFP-Myo5-S1205C* mutant (from 23.1 ± 6.4 s in the wild type to 23.6 ± 4.6 s in the mutant, p>0.1; n=75). In summary, our results indicate that Cka2 might control the assembly and the maturation rate of endocytic patches by mechanisms that are at least partially independent from the phosphorylation of Myo5-S1205.

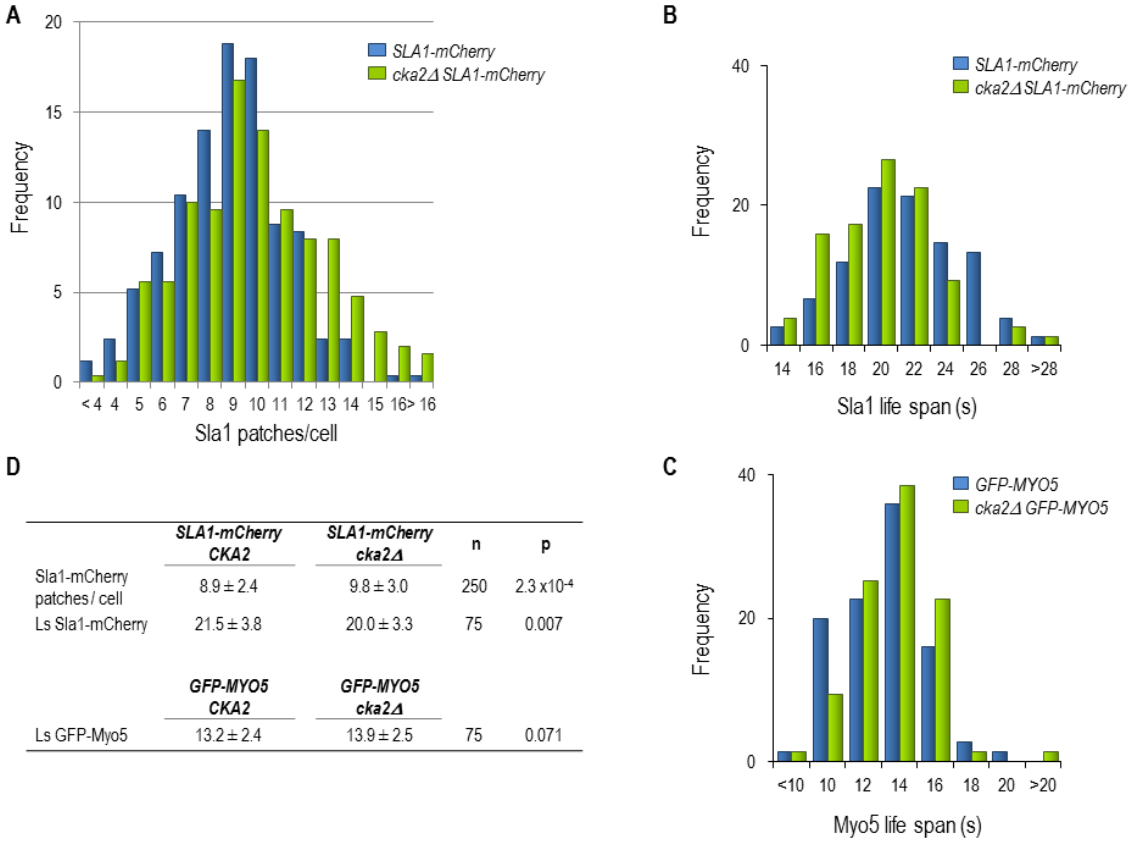

D

	SLA1-mCherry CKA2	SLA1-mCherry cka2Δ	n	p
Sla1-mCherry patches / cell	8.9 ± 2.4	9.8 ± 3.0	250	2.3×10^{-4}
Ls Sla1-mCherry	21.5 ± 3.8	20.0 ± 3.3	75	0.007
	GFP-MYO5 CKA2	**GFP-MYO5 cka2Δ**		
Ls GFP-Myo5	13.2 ± 2.4	13.9 ± 2.5	75	0.071

Figure 58. Depletion of the CK2 catalytic subunit Cka2 slightly up-regulates the assembly of endocytic patches and accelerated their maturation.
(A) Frequency distribution of the number of Sla1-mCherry cortical patches from *cka2Δ SLA1-mCherry* cells (SCMIG 1172) covered either with a centromeric plasmid encoding the CK2 catalytic subunit Cka2 under the *CKA2* promoter (*SLA1-mCherry*, p111*CKA2*), or a centromeric empty plasmid (*cka2Δ SLA1-mCherry*, YCplac111). n=250 cells. (B) Frequency distribution of the life span of 75 Sla1-mCherry cortical patches from the strains described in (A). (C) Frequency distribution of the life span of 75 GFP-Myo5 cortical patches from *myo5Δ* cells covered with p33*GFP-MYO5* (*GFP-MYO5,* strain SCMIG1137) and *myo5Δ cka2Δ* cells covered with p33*GFP-MYO5* (*cka2Δ GFP-MYO5,* strain SCMIG1135). (D) Table showing the number of Sla1 patches/cell and the cortical patch Sla1 and Myo5 life spans from the strains described in (A) and (C).

4. DISCUSSION

Previous results from our group indicated that the Myo5 C-terminal extension comprising amino acids 984 to 1219 (referred as Myo5-C_{ext}) induced the formation of Arp2/3 complex-mediated actin structures *in vitro* when incubated in the presence of a wild type yeast extract (Geli et al., 2000; Idrissi et al., 2002). The analysis of the protein composition of these actin structures indicated that they recapitulate the actin cap that is formed around the endocytic coat *in vivo* (Figure 30). The actin structures generated *in vitro* not only contained the Arp2/3 complex but also the Abp1, Sac6 and Crn1, three actin-associated proteins involved in endocytic uptake *in vivo* (Figure 30B, Dr. Fatima Idrissi and Dr. Maribel Geli unpublished results, (Burston et al., 2009; Idrissi et al., 2012; Kaksonen et al., 2005; Kubler and Riezman, 1993). Further, the structures did not contain Tpm1, an actin binding protein that decorates the actin cables but not the cortical actin patches in yeast (Idrissi et al., 2002; Liu and Bretscher, 1989). Strikingly, the ability of the Myo5-C_{ext} to induce the formation of these structures was negatively regulated by phosphorylation, since incubation of the yeast extract with a cocktail of phosphatase inhibitors led to a significant decrease in actin assembly while incubation with a cocktail of kinase inhibitors increased it (Figure 31, B. Grosshans unpublished results). On the other hand, the results indicated that an enzymatic activity present in a wild type yeast extract phosphorylated the Myo5-C_{ext} when incubated in the presence of ^{32}P-γ-ATP. Mutagenesis analysis of the Myo5-C_{ext} identified the Myo5 S1205 as the residue predominantly phosphorylated in the conditions assayed (Figure 33, B. Grosshans unpublished results), a residue that has been shown phosphorylated *in vivo* in high-throughput proteomic assays (Li et al., 2007). Finally, preliminary experiments indicated that the protein kinase CK2 was the enzymatic activity that phosphorylated the Myo5 S1205 *in vitro* (Figures 35, 36, and 37).

In the present study we further characterize the CK2 activity that phosphorylates the Myo5-C_{ext} and investigate the functional significance of this phosphorylation event, both *in vitro* and *in vivo*. We find that a non-canonical particulate-associated CK2 activity that involves the catalytic subunit Cka2, but no other catalytic or regulatory subunits of the enzyme, phosphorylates the Myo5 S1205. Further, we provide evidence supporting that this phosphorylation event down-regulates the Myo5 NPA required for endocytic uptake. Finally, our data suggest that Cka2 have endocytic targets other than Myo5 and that its activity might also regulate early steps during the assembly of the endocytic coat.

4.1. Phosphorylation at Myo5 S1205 by CK2 regulates the NPA of the type-I myosin

The observations that 1) Myo5-C_{ext} NPA was negatively regulated by phosphorylation and 2) Myo5 was phosphorylated in a residue adjacent to the acidic domain required for the activation of the Arp2/3 complex (Evangelista et al., 2000; Lechler et al., 2000), strongly suggested that this post-translational modification might down-regulate the assembly of Myo5-C_{ext}-induced actin *foci*. Indeed, our results indicated that this was actually the case. A mutation that introduced a negative charge at the Myo5 S1205 (Myo5 S1205D), which mimicked the constitutive phosphorylated state, significantly decreased the density of Myo5-induced actin *foci* generated *in vitro*. Conversely, a conservative substitution of the S1205 to a non-

phosphorylatable residue (Myo5 S1205C) significantly increased the density of actin structures on the surface of the myosin-I-coated beads (Figure 38). The up-regulation of actin polymerization required a conservative mutation since substitution of the S1205 by alanine did not have any effect on the assay (Dr. Bianka Grosshans, personal communication). On the other hand, down-regulation of actin polymerization by the S1205D mutation was not the consequence of protein miss-folding since the Myo5-Cext-S1205D construct interacted with a number of functionally relevant interacting partners with an affinity similar to the wild type protein (Figure 41).

The ability of different mutant cytosols to phosphorylate the Myo5 S1205 inversely correlated with their ability to sustain Myo5-induced actin polymerization. Thus, deletion of the CK2 catalytic subunit Cka2, but not Cka1, prevented Myo5 S1205 phosphorylation and conversely enhanced Myo5-C_{ext}-mediated actin polymerization to the same extent than the Myo5-C_{ext}-S1205C mutant. The Myo5-C_{ext} S1205D mutation was able to partially suppress the up-regulated actin assembly phenotype observed by depletion of Cka2, providing strong evidence that the kinase regulates Myo5-induced actin assembly through phosphorylation of the Myo5 S1205, at least partially (Figure 39). Further, overexpression of Cka2, but not Cka1 or a kinase-dead Cka2, highly increased the level of Myo5-S1205 phosphorylation and conversely decreased the number of actin *foci* to a similar extent than the Myo5-C_{ext} S1205D mutation (Figure 40). It is important noticing that inhibition of actin polymerization by the Myo5-C_{ext}-S1205D mutant was not complete. This result indicated that either the phosphorylation of Myo5 S1205 down-regulates but not abolishes actin polymerization, or that the mutation to aspartic acid does not quite mimic the Myo5 S1205 phosphorylated state. Alternatively, although actin polymerization mediated by Myo5-C_{ext} does not require other NPFs such as Las17 or Pan1 (see section 5.1.1.2), they can still interact with the myosin-C_{ext} and therefore, their activity might potentially sustain the residual actin polymerization on the surface of the mutant myosin coated beads.

Actin-driven membrane deformation is a key step during endocytic internalization. In order to generate productive forces to trigger endocytic budding, the actin architecture at endocytic sites must be perfectly adjusted in time and space. In particular, the force generated by actin polymerization is essential for the inward-movement of the endocytic coat, which corresponds to the elongation of the endocytic tubular invaginations capped by the clathrin coat. Further, it also plays an important role during membrane fission (see introduction, section 3.2.3.1.1) (Galletta et al., 2008; Idrissi et al., 2008; Sun et al., 2006). Since phosphorylation of the Myo5 S1205 Cka2 down-regulates the assembly of endocytic actin structures *in vitro*, we reasoned that Cka2-mediated phosphorylation of Myo5 S1205 might control actin-driven membrane deformation during endocytic budding. In agreement with this hypothesis, we observed that a phospho-mimetic Myo5-S1205 mutant, Myo5-S1205D, significantly delayed the internalization of the endocytic coat in a *myo3Δ myo5Δ* background. The internalization delay was evidenced by a significant extension of the Myo5 and Abp1 life spans at cortical patches (Tables 3 and 4, and Figures 48 and 50). Further, a consistent phenotype was obtained upon overexpression of the Cka2 kinase. Overexpression of Cka2 also elongated the cortical life spans of Myo5 and

Abp1 (even though to a lesser extent than the S1205D mutation). Despite the phenotype was rather subtle, the data clearly indicated that it was a consequence of the Cka2-mediated phosphorylation of the Myo5 S1205, since it could be suppressed by the expression of a non phosphorylatable Myo5 version (Myo5-S1205C) or by a point mutation in the Cka2 active site (*cka2-K79A*) (Tables 6 and 7, and Figure 52).

Even though the endocytic deficiencies observed in these mutants were statistically very significant, their absolute effect was mild (Figures 46 and 54). Several studies demonstrate that although deletion of the Myo5 acidic domain severely impairs its NPA *in vitro*, it only causes limited endocytic defects *in vivo,* even in the absence of Myo3. The data suggested that when the Myo5 NPA is reduced, other NPFs might take over. Further supporting functional redundancy, combined deletion of the type I myosin and Las17 acidic domains causes important synergistic defects in the elongation of the endocytic invaginations, as observed by live-cell fluorescence microscopy (Galletta et al., 2008; Sun et al., 2006). Consistent with these observations, we could demonstrate a significant defect in the endocytic uptake of radioactive α-factor when mutants in the Myo5-S1205 were combined with a truncated Las17 lacking the acidic domain (Figure 47). Strikingly, a similar phenotype was also observed when the mutations were combined with a C-terminally truncated form of Pan1, lacking approximately half of the protein (Tang and Cai, 1996). Deletion of the acidic domains of the myosins-I and Pan1 does not cause additive defects (Sun et al., 2006) and therefore, it is unlikely that the observed effects were in this case a consequence of functional redundancy for the nucleation promoting activity. Alternatively, and consistently with a role for the C-terminal proline-rich region of Pan1 in the regulation of the Myo5 NPA *in vitro* (Barker et al., 2007), Pan1 might co-regulate the same Myo5 activity controlled by Cka2.

It is interesting noticing that both, the phospho-mimicking and the non-phosphorylatable Myo5 S1205C mutations caused endocytosis defects in combination with the *las17-waΔ* or *pan1-4* mutants. This observation strongly indicates that a cycle of Myo5-phosphorylation and dephosphorylation is required to sustain efficient endocytic internalization. We are now generating strains that combine the Myo5 S1205C or Myo5 S1205D mutations with mutations in the acidic domains of either Las17 or Pan1 to analyze the dynamics of the endocytic factors by live-cell imaging and the ultrastructure of the endocytic actin coat by immunoelectron microscopy (Idrissi et al., 2012; Idrissi et al., 2008).

Since our data strongly suggested that Cka2-dependent Myo5 S1205 phosphorylation regulates the myosin NPA, both *in vitro* and *in vivo*, much effort has been focused to directly confirm that phosphorylation at Myo5 S1205 is mediated by the catalytic activity Cka2 *in vivo*. Unfortunately, although different procedures such as radioactive cell labeling experiments using exogenously supplied $^{33}PO_4^{3-}$ or 2-dimensional gel electrophoresis were applied to purified ProtA-tagged Myo5 and Myo5-S1205C, we were unable to identify any Myo5 modification that could be attributed to phosphorylation at S1205. We also collaborated with one of the groups that first identified the Myo5 S1205 phosphorylation by mass spectrometry from whole cell extracts (Dr.

Judit Villén (Dr. Steve Gygi lab, Harvard Medical School, MA, Boston)). Unfortunately again, we were not able to detect any phosphorylated residue in the most C-terminal region of the purified Myo5, including S1205 (Figure 59C and 59D). Interestingly, all proteomic studies that were able to identify Myo5 S1205 phosphorylated *in vivo* were performed using crude cell extracts (Gnad et al., 2009; Holt et al., 2009; Li et al., 2007; Wu et al., 2011). Even though the samples were treated with phosphatase inhibitors, the Myo5 S1205 phosphorylation might have been lost during the purification procedure or the phosphorylated form might be underrepresented after immuno-precipitation. Actually, we have recently observed that the plasma membrane-associated Myo5 is poorly immuno-precipitated as compared with the cytosolic myosin (data not shown). Therefore, future experiments are now being designed to detect Myo5 S1205 phosphorylation *in vivo* from crude extracts and/or Myo5 purified from plasma membrane fractions using the phosphate-binding-tag-based Phos-tag™ Acrylamide system (Wako). Besides, we intended to compare the Myo5 phosphorylation state in a wild type and a *cka2Δ* mutant from crude extracts using a quantitative mass spectrometry method such as SILAC (Nikolov et al., 2012).

Although the phosphorylated Myo5 S1205 could not be detected by proteomic analysis of purified ProtA-Myo5, this analysis led to the identification of one ubiquitinated and 11-phosphorylated residues, six of which had not been described before (Figure 59D). Interestingly, in the conditions used in our *in vitro* phosphorylation assays (see material and methods, section 8.6), Myo5 S1205 was the residue predominantly phosphorylated by cytosolic extracts in the Myo5 region comprising amino acids 984 to 1219 (Figures 33, 35, 36, and 37), even when six other phosphorylation residues were found in this area (Figure 59D). It is possible that these phosphorylation events result from signaling-transducing cascades that are not activated in our assays or that the kinase(s) involved are not significantly present in the extracts. Phosphorylation of some of these residues by still undefined kinases could cooperate with Cka2 to down-regulate the myosin-I NPA *in vivo*. If this is the case, functional redundancy between the phosphorylated residues and the kinases involved could explain the relative mild effects of the Myo5-S1205D and Myo5-S1205C, and *cka2Δ* mutations.

A

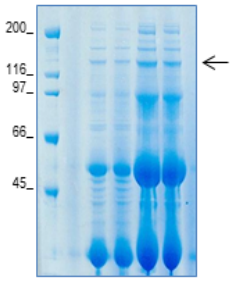

B

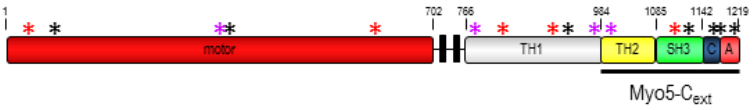

C

Sequence*	Position§	Domain	Reference(s)
KAT*FDSSK	**T27**	Head	This study
EVGVS*DLT*LLSKISDEAINENLK	S39, T42	Head	(Wu et al., 2011)
GS*VYHVPLNIVQADAVR	S357	Head	(Gruhler et al., 2005)
GSVY*HVPLNIVQADAVR	Y359	Head	(Li et al., 2007)
TIKPNETKS*PNDYDDR	***S613***	Head	This study
S*MS*LLGYR	S775, S777	TH1	(Ficarro et al., 2002; Holt et al., 2009)
RQVS*IKEK	**S806**	TH1	This study
LND**K#**IQIKIGSAIEY*QK	***Y923***	TH1	This study
KPGKLHS*VKCQINES*APK	S932, S940	TH1	(Holt et al., 2009)
KKS*SISSGYHASSSQATR	S973	TH1	(Holt et al., 2009)
RPVS*IAAAQHVPTAPASR	S992	TH2	(Li et al., 2007)
KGDVIY*IT*R	**Y1114, T1116**	SH3	This study
PHS*GNNNIPTPPQNRDVPK	S1146	SH3	(Wu et al., 2011)
GNNNIPT*PPQNR	T1153	-	(Gnad et al., 2009)
PVLNSVQHDNTS*ANVIPAAAQASLGDGLANALAARANK	S1174	-	(Wu et al., 2011)
MRLES*DDEEANEDEEEDDW	S1205	Acidic	(Li et al., 2007)

Figure 59. Identification of new Myo5 phosphorylation sites by mass spectrometry.
(A) Coomassie stained SDS-PAGE gel of IgG-Sepharose pull-downs of *myo5Δ* cells (Y06549) transformed with a centromeric plasmid encoding a Protein A-tagged Myo5 construct (p33*ProtA-MYO5*) expressed under the control of its own promoter. Cells were lysed and proteins immuno-precipitated with IgG-Sepharose for 1 hour at 4ºC in the presence of phosphatase inhibitors. The arrow points to the band corresponding to ProtA-Myo5, which was excised from the gel to be analyzed by mass spectrometry. (B) Domain organization of Myo5. Red asterisk: Not previously reported phosphorylation sites found in the study. Lila asterisk: Previously reported phosphorylation sites found in the study. Black asterisk: Previously reported phosphorylation sites not found in the study. (D) Table displaying identified Myo5 phosphorylation sites. * Phosphorylated residues are followed by an asterisk. Residues shown in red represent the Myo5 phosphorylated residues found in this study. Previously non-identified phosphorylated residues are shown in bold letters. The lysine shown in green indicates an ubiquitinated residue. § Phosphorylated residues have been localized with >95% certainty, except when they are shown in italic. The position may change in the literature depending on the sequence database used. Residues annotated in this table came from the Uniprot/KB (Universal Protein Resource Knowledgebase) database.

4.2. The molecular mechanism explaining the down-regulation of myosin-I-induced actin polymerization by CK2

The results discussed above indicate that Cka2-mediated phosphorylation at Myo5 S1205 regulate the formation of complex actin structures *in vitro*, which recapitulate those required for endocytic uptake *in vivo*. Further, analysis of the influence of the Myo5 S1205 phosphorylation on the Myo5 interactome outlined the molecular mechanism explaining the regulation of the Myo5 NPA by CK2. Even though the S1205 residue is embedded within the CA domain required for the interaction with the Arp2/3 complex, we found that phosphorylation of Myo5 S1205 did not seem to grossly affect the interaction with the actin nucleating complex. In contrast, we observed that the phosphorylation state of Myo5 S1205 significantly down-regulated the interaction of Myo5 with its co-activator Vrp1. Vrp1 binds to the SH3 domain of Myo5 and it is thought to provide G-actin binding sites (WH2), which are missing in the Myo5 C_{ext} but required for efficient actin nucleation. Accordingly, the Myo5/Vrp1 interaction is needed for the development of the myosin NPA *in vitro* (Geli et al., 2000) (Lechler et al., 2001) (Sun et al., 2006). In addition, Vrp1 participates in the recruitment of Myo5 to the endocytic sites (Anderson et al., 1998). Our pull down assays clearly showed a higher affinity –of about 3 folds- for the constitutively non-phosphorylated Myo5-C_{ext}-S1205C, as compared with Myo5-C_{ext}-S1205D. The differential interaction was also confirmed *in vivo* using a yeast two hybrid assay (Figure 41). The decreased affinity of the Myo5-S1205D for Vrp1 was probably not the result of the missfolding of the mutant protein because the phospho-mimicking mutant interacted with even better affinity than Myo5-S1205C with other functionally relevant myosin interacting partners such as Sla1, Pan1 and Bzz1. Given that Vrp1 is a big protein (of 82.6 kDa), its association with Myo5 might sterically hinder binding of the myosin to other endocytic proteins. Therefore, down-regulation of the Myo5/Vrp1 interaction could secondarily promote the association of the myosin with other interacting partners. However, we cannot rule out that phosphorylation of the S1205 directly promotes binding of the myosin to Sla1, Pan1 or Bzz1 and it is actually binding to these proteins what secondarily prevents the interaction of the myosin with Vrp1. Experiments with purified components will now be required to discern between these possibilities.

Given the functional implications of the Vrp1/Myo5 interaction, we hypothesized that the phosphorylation of the Myo5 S1205 might impact the recruitment of the myosin to the endocytic sites and/or its NPA activity, which is required for the internalization of the endocytic coat. The live-cell imaging experiments suggested that phosphorylation of Myo5 S1205 does not influence the recruitment of the myosin to the endocytic sites, since its arrival relative to Sla1 was not significantly altered by the S1205D mutation or by overexpression of Cka2. Under these circumstances Myo5 might be efficiently recruited to the endocytic sites by the cooperative interaction with other available binding partners such as Bzz1, Las17, Sla1 or Pan1. In contrast thought, and consistent with an impaired Myo5/Vrp1 NPA, the S1205D mutation and the overexpression of Cka2 significantly slowed down the internalization process. Surprisingly, we also observed that phosphorylation of Myo5 S1205 delays dissociation of Myo5 from the plasma

membrane after fission of the endocytic vesicles. An increased interaction of the Myo5-S1205D mutant with Bzz1 might explain this phenotype (Figure 41).

When and where Cka2-dependent phosphorylation of Myo5 actually occurs in wild type yeast is a still completely open question. Given that the CK2 activity phosphorylating Myo5 *in vitro* does not seem to be cytosolic (see below), we tend to favor the hypothesis that Myo5 is phosphorylated at the plasma membrane to down-regulate the Myo5-NPA towards the end of the budding process (see below). On the other hand, Myo5 S1205 phosphorylation increases the affinity of Myo5 for the endocytic coat components Sla1 and Pan1. Therefore, phosphorylation of Myo5 might also favor its recruitment at the invagination tip previous to the fission event (see section 3.2.3.1.1.3. and Figure 23). Nevertheless, we cannot rule out at the moment that Myo5 is constitutively phosphorylated at the cytosol to promote binding to different components of the endocytic machinery and thereby promote efficient recruitment at endocytic sites. Local de-phosphorylation of Myo5 (by for example the Scd5-mediated targeting of protein phosphatase-1 Glc7 (Chang et al., 2002; Zeng et al., 2007)) would then trigger association to Vrp1 and activation of its NPA. We think though that this possibility is unlikely because, already in very short invaginations, Myo5 is tightly associated with the base of the endocytic invaginations, where it tightly co-localizes with Vrp1 (Idrissi et al., 2012). Only in longer, more mature profiles, co-localization of Myo5 with Bzz1, Pan1, and Sla1 can be demonstrated (Idrissi et al., 2012). Given that CK2-dependent phosphorylation of Myo5 down-regulates binding to Vrp1 but favors the binding to Bzz1, Pan1, and Sla1, our data suggest that the phosphorylation of Myo5 S1205 by Ck2 occurs towards the end of the budding process.

What may trigger activation of CK2 at this point is an open question. Interestingly though, Korolchuk et al. have observed that the catalytic activity CK2 is potently inhibited by direct interaction with PIP_2 (Korolchuk et al., 2005). PIP_2 turnover is required for efficient endocytic internalization in yeast. Mutations in the genes codifying for the PI(4)P-5-kinase *MSS4* or for the PIP_2-5-phosphatases *SJL1 SJL2* cause endocytic defects (Desrivieres et al., 2002; Singer-Kruger et al., 1998) and PIP_2 seems to accumulate at cortical patches upon assembly of the endocytic coat (Homma et al., 1998; Sun et al., 2007). It has been proposed that PIP_2 might concentrate at endocytic sites concomitantly and probably synergistically with endocytic coat components such as Sla2, yAP1801/yAP1802, and Ent1/Ent2, which contain PIP_2-binding domains (Sun et al., 2007). After assembly of the actin cap, the synaptojanin Slj2 is recruited and hydrolyze the PIP_2 in the highly curved membranes not protected by BAR domain proteins, promoting the uncoating of Sla2, yAP1801/yAP1802, and Ent1/Ent2 (Chang-Ileto et al., 2011; Liu et al., 2009; Stefan et al., 2005; Sun et al., 2007). We hypothesize that recruitment of Sjl1/2 might also locally activate the membrane-associated CK2, which will then phosphorylate the Myo5 S1205 to facilitate translocation of Bzz1 to the invagination base and the recruitment of Myo5 to the endocytic coat. This hypothesis would integrate the timing of recruitment of Sjl1/2, the activation of CK2 by hydrolysis of PIP_2 and the effects of CK2-dependent phosphorylation on the myosin-I interactome to explain the dynamics of endocytic proteins at the ultrastructural level (Figure 60) (Idrissi et al., 2012; Idrissi et al., 2008).

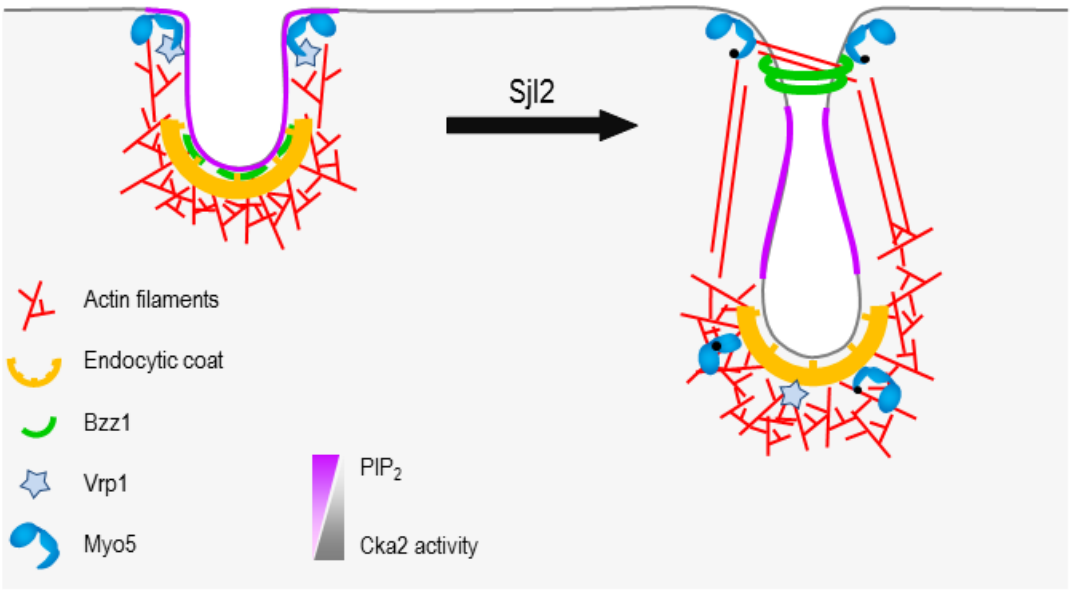

Figure 60. Model for the regulation of Cka2 by PIP2 at endocytic sites

The figure shows a proposed model for the regulation of a particulate-associated Cka2 activity at endocytic sites. Briefly, PIP_2 might inhibit the catalytic Cka2 activity at the initial phases of endocytic invagination. Upon Sjl2 recruitment, restricted PIP_2 hydrolysis might release Cka2 inactivation to promote the association of Myo5 to the endocytic coat and the rearrangement of Bzz1 to the base of the endocytic profile. The black dot represents Cka2-mediated Myo5 S1205 phosphorylation. See text for further details.

Besides the proposed mechanism for the regulation of the Myo5 NPA by Cka2-mediated Myo5 S1205 phosphorylation, the data presented in this study strongly suggest that Cka2-substrates other than the Myo5 S1205 are important to regulate this myosin function. Overexpression of Cka2 reduced the number of actin structures on the surface of Myo5-C_{ext} coated beads and the Myo5-C_{ext}-S1205C mutation was not able to suppress this phenotype. Further, although the Myo5-C_{ext}-S1205D mutation down-regulated the assembly of actin structures, more actin patches could be formed in this mutant upon depletion of Cka2 (compare Figure 38B to 39B). Moreover, depletion of Cka2 *in vivo* could partially rescue not only the endocytic defects of a *myo5Δ* mutant but also those installed by depletion of Sac6, a protein that is not required to ignite actin polymerization but it is essential to structure the endocytic actin cap (Figure 57). Conversely, overexpression of Cka2, but not a kinase dead mutant, caused synthetic dosage sickness with the *sac6Δ* strain (data not shown). The data suggested that the construction, the stability and/or the structure of endocytic actin structures might be negatively influenced by CK2-dependent phosphorylation of several endocytic targets.

An *in silico* search for endocytic proteins containing predicted CK2-mediated phosphorylation sites was performed and is shown in Table 8. Several actin regulatory factors, including NPFs, actin bundling proteins, and actin disassembly factors, contain predicted Cka2-mediated

phosphorylation sites. Some of these residues have actually been demonstrated to be phosphorylated *in vivo* using mass spectrometry, but the kinase effecting the phosphorylation and their functional significance have not been investigated. Future experiments are now being designed to investigate if some of these proteins are in fact phosphorylated by the protein kinase CK2 *in vivo* using Phos-tag™ Acrylamide system (Wako). If that is the case, further investigations will assess whether their phosphorylation state modulates the Myo5 NPA or the actin architecture of the structures generated on the surface of Myo5-C_{ext} covered glutathione-Sepharose beads. Two of our preferred candidates for the regulation of Myo5 NPA by Cka2-mediated phosphorylation of actin regulators others than Myo5 are Pan1 and Sla1. Pan1 contains 3 serines phosphorylated *in vivo* that perfectly fit the consensus site for CK2 and might regulate its NPA (see below). Besides, Pan1 contains 3 other residues located on CK2 consensus phosphorylation sites, but whether they are phosphorylated *in vitro* or *in vivo* has not been addressed so far. Interestingly, these residues (Pan1 S1435, Pan1 S1437, and Pan1 T1450) lie within the proline-rich region of Pan1, a domain that physically interacts with the Myo5 SH3 domain and enhances Myo5/Vrp1 actin polymerization activity (Barker et al., 2007). On the other hand, Sla1 contains a putative CK2-mediated phosphorylation site in its first SH3 domain, a region involved in the direct interaction of Sla1 and Myo5, and in the Sla1-mediated down-regulation of Myo5-dependent actin polymerization (Figure 45). Other factors present in the cell extract that might regulate the structural organization of the actin cap and its disassembly also contain putative CK2 consensus phosphorylation sites, including Abp1, the actin bundling proteins Sac6, Scp1, and Ysc84, Crn1, Lsb5, or the actin debranching protein Aim7 (Table 8). In the near future we aim to find out whether some of these proteins are indeed phosphorylated *in vivo* by CK2.

Yeast protein	Homolog	Residue	Sequence	Reference	Confidence
Early					
Ede1	Eps15	S964 S1096 S1161 S1130 S1131 S1132	LGSQS*DSEN ESVSS*IQES AQPTS*SLEI ESDSSSSDD SDSSSSDDD DSSSSDDDE		High Low Low High High High
Syp1	FCho1/2	.	.	.	.
Early coat					
Chc1/Clc1	Clathrin	.	.	.	.
yAP1801/2	AP180	.	.	.	.
Pal1	-	T304	GRDDT*DDSD		High
Apl3	α-adaptin (AP2)	S736 S738 S146	NSKIS*SSED KISSS*EDFS KSLSSSDDN		Medium Medium High
Apl1	β-adaptin (AP2)	.	.	.	.
Apm4	μ-adaptin (AP2)	S263	LGMQSEDE		High
Aps2	σ-adaptin (AP2)	.	.	.	.

Intermediate coat					
Sla2	Hip1R	.	.	.	.
Ent1	Epsin	S163 T180 S134	GTGRS*DEND ASRLT*AEED TALLSDDER		Medium Medium High
Ent2	Epsin	.	.	.	.
Late coat					
End3	-	.	.	.	.
Pan1	Intersectin	S1135 S1180 S1281 S1435 S1437 T1450	AKQES*DDED AQNES*DEEE DDGWS*DEDE GAYGSDSDD YGSDSDDDV ESVGTDEEE	(Li et al., 2007), (Albuquerque et al., 2008)	High High High High High High
Sla1	Intersectin/CIN85	S51	RVIGSDSEE		High
WASP/Myosin					
Las17	WASP	.	.	.	.
Vrp1	WIP	.	.	.	.
Bzz1	Syndapin	S472	AGEDS*DNN	(Albuquerque et al., 2008)	Medium
Myo3	Myosin-I	S1257	MRAESADDD		High
Myo5	Myosin-I	S1205	MRLES*DDEE	(Li et al., 2007)	High
Bbc1	-	S602 S854 S410 S545 T549	TAEVS*HDIE TSVLS*GAEK EEEDSEENR SDHDSDEDT SDEDTDDHE	(Albuquerque et al., 2008)	Low Low High High High
Actin					
Arp2/3	Arp2/3	.	.	.	.
Abp1	ABP1	S365	GLAAS*EKEE	(Li et al., 2007)	Medium
Sac6	Fimbrin	S318	SKDVSDGEN		High
Scp1	Transgelin	T10 S11	KADVT*SLDE ADVTS*LDED	(Li et al., 2007), (Albuquerque et al., 2008)	Low Medium
Cap1	Capping protein	.	.	.	.
Cap2	Capping protein	S267 S268	AAIAS*SAEE AIASS*AEEA	(Albuquerque et al., 2008)	Low Low
Ysc84	-	S301 S228 S255	GDFDS*EDED DDNAS*GDDF DSFDSTDES		High High High
Amphiphysin					
Rvs161/167	Amphiphysin	.	.	.	.
Vps1	Dynamin	.	.	.	.
Uncoating/Disassembly					
Ark1	AAK	S535 S568 S569 S460 S461	TIDNS*KDDL DKLNS*SEES KLNSS*EESF EDSSSSSDE DSSSSSDES		Medium Medium Low High High
Prk1	AAK	.	.	.	.
Sjl2	Synaptojanin-1	S1146 S1148	SPSNS*KSEE SNSKS*EEEL		Medium Medium
Cof1	Cofilin	.	.	.	.

Aip1	Aip1	.	.	.	.
Crn1	Coronin	S441 S443	EKPIS*ESEK PISES*EKEV	(Chi et al., 2007), (Albuquerque et al., 2008)	High Medium
Lsb5	-	S243 S301 S302 S330 S331	GKFSTDDEE AQDDSSDES QDDSSDESD IDSESSEEE DSESSEEES		High High High High High
Aim7	GMF	S137	LEDDS*DVEE	(Albuquerque et al., 2008)	High

Table 8. Putative CK2-mediated phosphorylation of different endocytic factors.
Table displaying identified and putative CK2 phosphorylation sites (highlighted in red; identified phosphorylation residues are followed by an asterisk). The acidic residues are boxed in green. A putative CK2-mediated phosphorylation site was annotated when it appeared in both kinase-specific phosphorylation databases consulted: NetphosK and PPSP (Prediction of protein kinase-specific phosphorylation). High-confidence is associated to a PPSP score ≥ 7,5. Low-confidence is associated to a PPSP score ≤ 5,5.

4.3. Mammalian and pathogenic NPFs are also modulated by CK2-dependent phosphorylation

Since the consensus domain of protein kinase CK2 is a serine or threonine surrounded by an acidic environment (Meggio et al., 1994; Pinna, 2002), regulation of nucleation by CK2-mediated phosphorylation at the acidic domain of NPFs might be a conserved mechanism. In fact, i*n vivo* and *in vitro* phosphorylation of mammalian and pathogenic NPFs by CK2 has previously been described (Table 9). However, how CK2 phosphorylation impacts their NPA and the molecular mechanism involved is far from being understood.

The first NPF shown to be phosphorylated by CK2 was WASP (Cory et al., 2003). The authors provided good evidence indicating that S483 and S484 located upstream of the acidic peptide required for binding and activation of the Arp2/3 complex, were phosphorylated by CK2 *in vivo* and *in vitro*. The authors also demonstrated that the phosphorylation of the full length WASP by CK2 increased the affinity of the NPF for the Arp2/3 complex and activated its NPA in pyrene-actin polymerization assays with pure components or in the presence of cellular extracts. Interestingly though, the effect of the CK2-dependent phosphorylation of these residues was minor when only the VCA domain of WASP was used in the pyrene actin polymerization assays. The data suggested that CK2 might work to release autoinhibition of the full length protein.

A few years later though, opposite effects of CK2-dependent phosphorylation on the NPA activity of the closely-related N-WASP was reported (Galovic et al., 2011). Galovic and coworkers also demonstrated *in vivo* and *in vitro* phosphorylation of the N-WASP S480 and S481 by CK2. However, in contrast to WASP, phosphorylation of these residues had a clear inhibitory effect on the NPA of N-WASP, when the full length protein was used in pyrene-actin polymerization assays with purified components. Surprisingly though, and similar to WASP, phosphorylation by CK2 increased the affinity of N-WASP for the Arp2/3 complex. Also similar to WASP, phosphorylation of N-WASP by CK2 had little effect when only the N-WASP VCA domain was used in the assay, indicating that CK2 also regulates the N-WASP autoinhibition, even

though conversely, as compared to WASP. Whether the discrepancies between WASP and N-WASP are due to the structural differences between these NPFs or to technical issues (including protein conformation, presence of co-purifying inhibitors and/or co-activators, among others) is still unknown.

Similar to N-WASP, phosphorylation of WAVE2 by CK2 also increases its affinity for the Arp2/3 complex but inhibits its NPA in pyrene-actin polymerization assays with purified components. However, the ultimate molecular mechanisms responsible for the inhibition of WAVE2 and N-WASP by CK2 might differ because WAVE2 is not regulated by autoinhibition (Bompard and Caron, 2004), and actually the effects of CK2 phosphorylation on WAVE2 on the pyrene-actin polymerization assay could be demonstrated using only the VCA domain (Pocha and Cory, 2009).

Finally, evidence for the regulation of the *Listeria monocytogenes* ActA by CK2 was also provided by Chong and co-workers. In the case of the pathogenic NPF, phosphorylation of ActA S155 and S157 by CK2 also increased its affinity for the Arp2/3 complex, but similar to WASP, it seemed to down-regulate its NPA. The authors showed that mutation of these serines to alanines or depletion of the cellular CK2 impairs recruitment of the Arp2/3 complex close to the bacteria and impairs the formation of *L. monocytogenes* induced actin tails (Chong et al., 2009). Interestingly though, mutation of the serines to negatively charged residues also altered the formation of actin tail. Actin still polymerized on the bacteria expressing the constitutively phospho-mimicking ActA mutants but it assembled as clumps rather tails. The data suggested that a phosphorylation/dephosphorylation cycle of the *Listeria* NPF by CK2 and a still unidentified phosphatase was required for the generation of actin-polymerization-based productive forces (Chong et al., 2009).

In *S. cerevisiae*, only Myo5 and Myo3 contain phosphorylatable residues immediately upstream of the acidic domain. Las17 does not contain any CK2 consensus site, while Pan1 contains a phosphorylatable serine in an acidic region downstream to the acidic domain, just after the conserved tryptophan (Pan1 S1281). Both Myo5 S1205 and Pan1 S1281 have been found phosphorylated *in vivo* by high throughput phospho-proteomics assays (Li et al., 2007). In addition to S1281, Pan1 also contains 2 more serines (Pan1 S1135 and Pan1 S1180) that are phosphorylated *in vivo* and perfectly fit the consensus site for casein kinase 2 (Li et al., 2007), see Table 8. Pan1 S1135 and Pan1 S1180 lie on the coiled coil domain of Pan1, a region that interacts with F-actin to promote Pan1-mediated actin polymerization (Toshima et al., 2005). Whether CK2-mediated Pan1 phosphorylation might regulate the nucleation promoting activity of the protein is an important question that we will like to address in a near future.

Similar to N-WASP, WAVE2 and ActA, phosphorylation of the Myo5 S1205 by CK2 down-regulates its NPA activity. Similar also to ActA, a cycle of phosphorylation and dephosphorylation of the Myo5 S1205 might be required for generation of productive actin-polymerization-based forces. However, our data suggest that the molecular mechanism explaining the regulation of the myosins-I NPA by CK2 differs from those described for the

mammalian and pathogenic NPFs. In contrast to WASP, N-WASP, WAVE2 and ActA, phosphorylation of the Myo5 S1205 does not seem to increase its affinity for the Arp2/3 complex, if at all, it rather decreases it. Regulation of the Myo5 NPA seems to rather rely on the impact of the Myo5 S1205 phosphorylation/dephosphorylation events on its binding to the co-activator Vrp1 and/or the inhibitor Sla1. It should be noticed though that we have analyzed the influence of the Myo5 S1205 phosphorylation using the C_{ext} only, and not the full length Myo5. Similar to WASP and N-WASP, Myo5 is modulated by an intramolecular autoinhibitory interaction between the C_{ext} and the neck and TH1 domains (see section 3.1.2.1.2.1). Therefore, we cannot rule out at the moment that, similar to N-WASP, phosphorylation of the Myo5 S1205 influences this autoinhibitory interaction and secondarily affects binding to the Arp2/3 complex in the context of the full length myosin. Further experiments are now being directed to test this hypothesis.

Organism	Protein	Sequence	Reference
Hs	WASP	481 HIS*S*DEGEDQAGDEDEDDEWDD 502	(Cory et al., 2003)
Hs	N-WASP	481 HIS*S*DEDEDEDDEEDFEDDDEWED 504	(Galovic et al., 2011)
Hs	WAVE1	541 VEYSDSEDDSEFDEVDWLE 559	
Hs	WAVE2	479 VEYS*DS*EDDS*S*EFDEDDWS*D 498	(Pocha and Cory, 2009)
Hs	WAVE3	484 VEYSDSDDDSEFDENDWSD 502	
Hs	WASH	445 IPPLPPPQQPQAEEDEDDWES 465	
Hs	WHAMM	791 VSADS*EEDS*DEQDPGQWDG 809	(Christensen et al., 2010)
Hs	JMY	970 ASPES*EDEEEALPCTDWEN 988	(Dephoure et al., 2008)
Ls	ActA	152 IASS*DS*ELESLTYPDKPTKANKRK 41 DEWEE 45	(Chong et al., 2009)
Rr	RickA	437 IEMSDSSSSESDSGNWSDVSVNRN 460	
AcMNPV	p78/83	373 MAKSSSEATSNDEGWDDDD 391	
Sc	Las17	621 VGAHDDMDNGDDW 633	
Sc	Myo3	1253 MRAESADDDDNDDGDDDDDW 1272	
Sc	Myo5	1201 MRLES*DDEEANEDEEEDDW 1219	(Li et al., 2007)
Sc	Pan1	1271 GLDEDEDDGWS*DEDESNNRV 1290	(Li et al., 2007)
Sc	Abp1	196 DNNDDDDWNEPELKE 210 425 EADNEEEPEENDDDWDDDEDEAAQPP 450	

Table 9. Putative CK2-mediated phosphorylation of different nucleation promoting factors
Table displaying identified and putative CK2 phosphorylation sites (highlighted in red; identified phosphorylation sites are followed by an asterisk) within the acidic domain of representative NPFs. The conserved acidic residues and the tryptophan of the acidic domain region are boxed in green and highlighted in lilac, respectively. Hs: *Homo sapiens*; Lm: *Listeria monocytogenes*; Rr: *Rickettsia rickettsii*; AcMNPV: Autographa californica nucleopolyhedrovirus ; Sc: *Saccharomyces cerevisiae*. Note that only human WASH and budding yeast Las17 do not contain putative CK2 phosphorylation sites.

4.4. Cka2 might regulate the assembly and disassembly of the endocytic coat

Our data indicates that CK2 phosphorylates Myo5 S1205 and probably other unidentified substrates to regulate the formation, reorganization, and/or disassembly of actin structures during endocytic invagination. In addition, the data suggests that Cka2 also plays a regulatory role in the assembly/disassembly of the endocytic coat.

In higher eukaryotes, CK2 has been proposed to function together with the Ark1/Prk1 homologous kinases GAK/AAK1 in the uncoating of clathrin coated vesicles (Korolchuk and Banting, 2003). Protein kinase CK2 participates in the endocytic uptake of transferrin (Cotlin et al., 1999), and seem to be enriched in clathrin coated vesicles after fractionation assays (Bar-Zvi and Branton, 1986). Mammalian CK2 is able to phosphorylate the human clathrin light chain, the clathrin adaptors AP-2 and AP-180, amphiphysin, and dynamin *in vitro* (Bar-Zvi and Branton, 1986; Doring et al., 2006; Hao et al., 1999; Korolchuk and Banting, 2002; Slepnev et al., 1998; Wilde and Brodsky, 1996). Phosphorylation of these factors seems to inhibit their interaction with endocytic binding partners, suggesting a role for CK2-mediated phosphorylation in the clathrin coat assembly/disassembly cycle (Georgieva-Hanson et al., 1988; Hao et al., 1999; Wilde and Brodsky, 1996). Whether budding yeast Cka2 might also have a regulatory function in the assembly/disassembly cycle of the endocytic coat is still not known. However, preliminary data indicates that it might be the case. As shown in Figure 58, we observed a slight increase in the number of endocytic sites in a *CKA2* depleted strain, which was probably not a consequence of the accumulation of non-productive endocytic events since the life span of the coat endocytic coat marker Sla1 was slightly reduced. A number of coat proteins and factors that function in the assembly and disassembly of the endocytic coat also contain consensus Cka2-mediated phosphorylation sites (Table 8) including Ede1, Pal1, Ent1, Pan1, Sla1, Ark1, Sjl2, or Lsb5. In the near future, we aim to find out whether any of these endocytic proteins are indeed phosphorylated *in vivo* by CK2.

It is interesting noticing that PIP_2 and CK2 have somehow opposite effects on the assembly/disassembly of endocytic coat complexes and on the polymerization of actin (Figure 61). PIP_2 might directly regulate proteins with lipid binding domains such the clathrin adaptors, the epsins, the BAR domain-containing proteins, or some NPFs such as WASP or the type I myosins. However, it will not be able to directly affect the activity of other proteins that do not contact the lipid bilayer. In this context, a secondary regulatory mechanism that tightly cross-talks with the local levels of PIP_2 and modulates the cytosolic components of the functional networks might shorten the time of response to sharp changes in the concentration of the phosphoinositide and will warranty the efficiency and reproducibility of the process. The PIP_2/CK2 pair might not only modulate that fast assembly/disassembly cycle of the clathrin coat and the actin structures during constitutive endocytic uptake, as discussed, but it might also favor rapid response to environmental changes that signal via a general increase in the cellular levels of PIP_2. Accordingly, the endocytic uptake rate is up-regulated upon several environmental stresses such as heat shock or low pH (Jenness and Spatrick, 1986; Motizuki et

al., 2008). Under these conditions, the total cellular PIP_2 levels increase twofold (Desrivieres et al., 1998; Motizuki et al., 2008) and cortical actin patches, presumably corresponding to endocytic structures, accumulate in the mother cells (Chowdhury et al., 1992; Delley and Hall, 1999; Desrivieres et al., 1998; Motizuki et al., 2008). Our preliminary data indicate that the life span of endocytic proteins does not seem to be altered upon heat stress, suggesting that more endocytic patches assemble under these experimental conditions (Dr. Maribel Geli, unpublished results). An increase in the levels of PIP_2 accompanied by a decrease in the CK2 activity might promote endocytic uptake under these experimental conditions. In order to investigate a possible functional cross-talk between the levels of PIP_2 and the activity of CK2, extracts from the *mss4-2* and *sjl1Δ sjl2Δ* strains will be assayed for their ability to phosphorylate Cka2 substrates. As discussed, Sjl2 and Sjl1 encode the synaptojanin that hydrolyze PIP_2 and promotes disassembly of endocytic structures shortly before or concomitant to vesicle fission. Mss4 encodes for a plasma membrane-associated PI(4)P-5-kinase that generates $PIns(4,5)P_2$ by the phosphorylation of PIns4P (Desrivieres et al., 2002; Singer-Kruger et al., 1998).

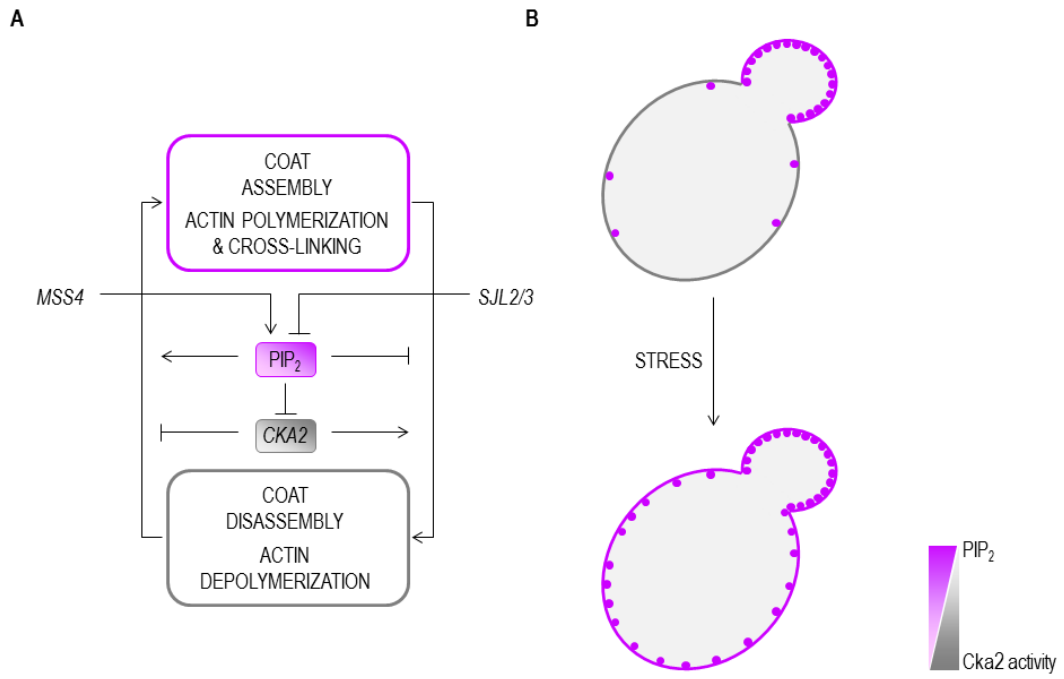

Figure 61. Model for the regulation of Cka2 by PIP2 upon environmental changes
The figure shows a proposed model for the regulation of Cka2 activity during endocytic internalization. (A) Mss4-mediated production of PIP_2 might inhibit the catalytic Cka2 activity and would promote coat assembly and formation of an actin cap at endocytic sites. Upon Sjl2 recruitment, PIP_2 hydrolysis might release Cka2 inactivation to promote uncoating and actin disassembly. (B) In particular stress conditions a general increase in the PIP_2 levels might likewise down-regulate Cka2 activity to promote endocytic coat assembly. Lilac dots represent endocytic sites. See text for further details.

4.5. A particulate-associated non-canonical CK2 phosphorylates Myo5

A striking observation derived from this study was that the CK2 activity responsible for Myo5 S1205 phosphorylation *in vitro* and the regulation of actin polymerization and endocytosis *in vivo* only involved the catalytic Cka2 subunit, but not the regulatory subunits Ckb1 and Ckb2 or the other catalytic subunit Cka1. We found that deletion of *CKA2* but not of *CKA1* impaired Myo5 S1205 phosphorylation and up-regulated Myo5-induced actin polymerization *in vitro* (Figures 35, 37, and 39). Second, overexpression of Cka2 but not of Cka1 or a catalytically inactive form of Cka2 was able to hyper-phosphorylate Myo5 S1205 and down-regulate Myo5-mediated actin polymerization (Figures 36 and 40). Third, a null mutation of *CKA2* but not of *CKA1* slightly accelerated the endocytic uptake and was able to partially suppress the endocytic defect of a *myo5Δ* mutant *in vivo* (Figures 55 and 57). And four, overexpression of Cka2 but not of Cka1 slightly delayed endocytic internalization as observed by live imaging (Figure 52 and Table 6). Surprisingly also, we observed that Cka2-mediated phosphorylation of Myo5 was associated to a particulate fraction, membranes and/or cytoskeletal elements (Figure 37B and 37C). Consistent with a specific role for Cka2 in Myo5 phosphorylation, Cka2 was also enriched in these particulate fraction, as compared to Cka1 (Figure 37A).

As explained in section 5.1.1, protein kinase CK2 (formerly known as casein kinase II) is an essential, ubiquitous, and highly conserved threonine/serine kinase that was traditionally envisioned as a holoenzyme composed by 2 catalytic and 2 regulatory subunits (α and β, respectively) (Litchfield, 2003). CK2 was reported to phosphorylate more than 300 substrates till 2003, and the number of reported targets subsequently increased (Meggio and Pinna, 2003). Therefore, protein kinase CK2 has not been assigned to a specific functional pathway but seems to play important roles in a number of physiological and pathological processes including cell cycle progression, proliferation, survival, transformation or tumorigenesis (Ahmed et al., 2002; Duncan and Litchfield, 2008; Guerra and Issinger, 2008; St-Denis and Litchfield, 2009).

Organisms ranging from yeast to mammals contain typically two catalytic isoforms encoded by two different genes (α and α'), but others including *D. melanogaster*, *C. elegans*, or *S. pombe* appear to have a single catalytic subunit (Litchfield, 2003; Shi et al., 2001). The regulatory β subunit is generally codified by a single gene, but distinct isoforms have also been reported in some organisms, such as *S. cerevisiae* (Bidwai et al., 1994). The holoenzyme can contain identical – the homotetramers $\alpha_2\beta_2$ and $\alpha'_2\beta_2$- or different –the heterotetramer $\alpha\alpha'\beta_2$- catalytic subunits (Gietz et al., 1995). The sequences of the CK2 subunits and the tetrameric structure of the holoenzyme are highly conserved from yeast to mammals. Budding yeast CK2 is composed of two catalytic subunits (α and α', *CKA1* and *CKA2*, respectively) and two regulatory subunits (β and β', CKB1 and CKB2, respectively) (Bidwai et al., 1995; Chen-Wu et al., 1988; Padmanabha et al., 1990; Reed et al., 1994). Like in higher eukaryotes, the tetrameric structure can contain identical or different catalytic isoforms, but it requires both regulatory subunits (Bidwai et al., 1995; Domanska et al., 2005; Kubinski et al., 2007). Disruption of either *CKA1* or *CKA2* does not cause any obvious phenotype but deletion of both genes is lethal,

indicating that CK2 is essential and that the catalytic subunits can compensate for each other in the context of viability (Chen-Wu et al., 1988; Padmanabha et al., 1990).

Interestingly, previous genetic evidence suggested some functional specialization for the individual catalytic subunit isoforms in budding yeast. First, functional analysis of thermo-sensitive *cka1* and *cka2* alleles as the sole source of catalytic CK2 activity early evidenced their physiological differences, suggesting that even though each of them can phosphorylate the essential CK2 substrates, Cka1 would preferentially phosphorylate cell cycle targets and Cka2 would preferentially phosphorylate proteins involved in cell polarity (Glover, 1998; Hanna et al., 1995; Rethinaswamy et al., 1998). Shortly later, another study pointed out a specific role for *CKA2* in the ceramide synthesis pathway and in the regulation of chronological life span (Fabrizio et al., 2010; Kobayashi and Nagiec, 2003). Further, large-scale survey analysis for drug target discovery exposes that *CKA1* or *CKA2*-depleted yeast cells are differentially sensitive/resistant to drugs displaying different mechanisms of action. Thus, while mutation of *CKA2* is associated to increased/decreased resistance to drugs that disturb the integrity of cellular membranes or the cell wall, mutation of *CKA1* is mostly associated to decreased resistance to drugs that prevents DNA replication or translational elongation (Kapitzky et al., 2010; Markovich et al., 2004; Xie et al., 2005; Yu et al., 2008). Analysis of gene expression profiles performed in strains lacking either catalytic subunit also show that the two isoforms have different effects on whole-genome expression (Ackermann et al., 2001). Finally, increasing evidence also indicates the differential dependence of some CK2 targets for a specific catalytic subunit: while phosphorylation of the transcriptional repressor Nrg1 requires the presence of Cka1 and the regulatory Ckb1 and Ckb2 subunits in the cytosolic extracts, phosphorylation of the mitochondrial TOM (Translocase of outer mitochondrial membrane) complex subunit Tom22 seems to be mediated by Cka2 -whether Ckb1/Ckb2 are required for Tom22 phosphorylation is unknown- (Berkey and Carlson, 2006; Schmidt et al., 2011).

An unexpected observation from our experiments was that the Cka2 activity responsible for the phosphorylation of Myo5 S1205 did not correspond to the canonical tetramer, since the regulatory subunits Ckb1 and Ckb2 seemed to be dispensable for the process (Figures 35 and 36). CK2 had typically been considered a holoenzyme because the catalytic subunits of CK2 appear to be accompanied by equivalent amounts of regulatory subunits when purified from different sources (Bidwai et al., 1994; Jauch et al., 2002; Litchfield et al., 1990). However, the only observed phenotype after deletion of both *CKB1* and *CKB2* in budding yeast was an ion specific salt-sensitivity, which means that the catalytic subunits maintain a significant level of enzymatic activity outside the tetrameric complex (Bidwai et al., 1995). Moreover, live-cell imaging, biochemical analysis, and structural examination of CK2 from different organisms suggest that, in addition to the multisubunit structure, free populations of α and β subunits can exist and are functional outside the holoenzyme complex (Abramczyk et al., 2003; Faust et al., 1999; Filhol et al., 2003; Guerra et al., 1999; Niefind et al., 2001). Consistently with this data, a monomeric kinase isolated from budding yeast cytosol was identified as a free catalytic α' subunit of CK2, indicating that at least the catalytic subunit Cka2 exists as a non-tetrameric

enzymatic activity in the cell (Abramczyk et al., 2003). Although the CK2 catalytic and regulatory subunits seem to localize predominantly at the nucleus, CK2 can be found at other subcellular compartments. In mammalian cells, both the catalytic and regulatory subunits localize at the smooth ER and the Golgi, but only the catalytic subunits could be detected in the rough ER and centromeres (Faust et al., 2002; Faust et al., 2001). CK2 can also associate to the plasma membrane through the regulatory subunits in the rat liver and insect cells (Sarrouilhe et al., 1998). In addition, the PH-domain containing protein CKIP-1/ PKHO1 also targets the protein kinase to the plasma membrane (Bosc et al., 2000; Olsten et al., 2004). Thus, targeting of the CK2 holoenzyme or of their individual subunits to different cellular compartments might contribute to the physiological regulation of the kinase (Filhol and Cochet, 2009). Future experiments are now being designed to analyze the composition of CK2 from particulate and cytosolic fractions -and purified plasma membrane- with the help of native electrophoresis.

5. CONCLUSIONS

Based on the results described in this study, we confirmed that Myo5 S1205 is phosphorylated by CK2 *in vitro* and we can conclude that:

- The CK2 activity responsible for the phosphorylation at Myo5 S1205 *in vitro* involves a particulate-associated catalytic Cka2 subunit, but not the other catalytic subunit Cka1.
- The CK2 activity responsible for the phosphorylation at Myo5 S1205 *in vitro* involves a non-tetrameric catalytic Cka2 subunit, since the regulatory subunits Ckb1 and Ckb2 are not required.
- The Cka2-mediated phosphorylation at Myo5 S1205 down-regulates the assembly of complex actin structures *in vitro*, which recapitulate those required for endocytic internalization *in vivo*.
- The Cka2-mediated phosphorylation at Myo5 S1205 does not influence the recruitment of the myosin to the endocytic sites but slows down the internalization process and the dissociation of the myosin from the plasma membrane.
- A cycle of Myo5 phosphorylation and dephosphorylation at S1205 is required to sustain efficient endocytic internalization in the absence of other NPFs.
- The Cka2-mediated phosphorylation at Myo5 S1205 does not seem to regulate the affinity of the NPF for the Arp2/3 complex but rather down-regulates the interaction of Myo5 with its co-activator Vrp1. This phosphorylation also increases directly or indirectly the binding of the myosin to Bzz1, Sla1, and Pan1, suggesting that the phosphorylation event occurs late during the maturation of the endocytic invagination.
- Cka2-substrates other than the Myo5 S1205 seem to be involved in the formation, reorganization, and/or disassembly of endocytic actin structures both *in vitro* and *in vivo*.
- Myo5 is phosphorylated on several residues not previously identified.
- In addition to its regulatory role in the generation and/or reorganization of endocytic actin structures, Cka2 might also have a regulatory function in the assembly/disassembly cycle of the endocytic coat.

6. MATERIALS & METHODS

6.1. Cell culture

6.1.1. Cell culture of *Escherichia coli*

E. coli cell culture was performed according to standard protocols (Sambrook and Russell, 2001). The DH5α strain was used for molecular cloning. DH5α cells were grown at 37ºC in LB media (0.5% yeast extract, 1% bacto tryptone, 0.5% NaCl) supplemented with 50 mg/L ampicillin, when selection was required. The BL21 strain was used for the expression of GST-fusion proteins (see section 6.4.3.2). BL21 cells were grown at 37ºC in LB supplemented with 50 mg/L ampicillin and transferred to minimal media (0.2% glucose, 0.4% casamino acids, 48 mM Na_2HPO_4 x $7H_2O$, 22 mM KH_2PO_4, 8.5 mM NaCl, 19 mM NH_4Cl, 1 mM $MgSO_4$ and 0.3 mM $CaCl_2$) supplemented with 50 mg/L ampicillin. Cells were grown at 37°C to an OD_{600} of 0.4, shifted to 24°C, and induced at an OD_{600} of 0.7-0.8 with 0.1 mM isopropyl-β-D-thiogalactopyranoside (IPTG) for 2 h.

E.coli was stored at -80ºC in 15% glycerol added to fresh culture.

6.1.2. Cell culture of *Saccharomyces cerevisiae*

S. cerevisiae cell culture was performed as described (Sambrook and Russell, 2001). Yeast cells were grown at 28ºC unless otherwise mentioned. Strains were grown in complete yeast peptone dextrose media (YPD) or, if selection was required, in appropriate synthetic dextrose minimal media (SDC) (Sherman, 1991). Complete YPD media contained 1% yeast extract (Difco), 2% peptone (Difco) and 2% glucose (Duchefa or Difco). Synthetic minimal media consisted of 2% glucose (Duchefa), 0.67% yeast nitrogen base (Difco) and 0.075% of CSM (Complete Synthetic Mix, Qbiogene), which contains all required amino acids, purine- and pyrimidine-bases except those required for auxotrophic marker selection. The concentration of amino acids, purine- and pyrimidine-bases used in CSM were: 10 mg/l adenine, 50 mg/l L-arginine, 80 mg/l L-aspartate, 20 mg/l L-histidine-HCl, 50 mg/l L-leucine, 50 mg/l L-lysine, 20 mg/l L-methionine, 50 mg/l L-phenylalanine, 100 mg/l L-threonine, 50 mg/l tryptophan, 50 mg/l L-tyrosine, 20 mg/l uracil and 140 mg/l valine. Solid media additionally contained 2% agar (Pronadisa or Difco). SDYE media used for the carboxypeptidase Y maturation assay (see section 6.9.2.) consisted of 2% glucose (Duchefa), 0.67% yeast nitrogen base (Difco), 0.2% yeast extract (Difco), and 40 mg/l of uracil, L-leucine, L-lysine, adenine, L-histidine, tryptophan and L-tyrosine. The SD media used in this assay was equally made, except that it did not contain the yeast extract. SD-Leu-SO_4^{2-} used for ^{35}S-radiolabelled α-factor purification (see section 6.4.3.3.) consisted of 2% glucose SO_4^{2-} free (Aristar), 0,67% yeast nitrogen base SO_4^{2-} free (Difco), and 40 mg /l of uracil, L-lysine, adenine, L-histidine, and tryptophan, pH 5.5. For YPD solid media containing Geneticin (Roche) the drug was added at a concentration of 0.03 mg/ml. In FOA-containing plates, 5'-fluoro-orotic acid (Fluorochem) was added to synthetic minimal solid medium at a concentration of 1 mg/ml. For the induction of proteins under a *GAL1*-promoter, yeast cells were grown until early logarithmic phase ($D.O_{600}$~0.3) in synthetic raffinose minimal media (SRC). Then, galactose (Fluka) was added to a final concentration of 2% and cells were grown

for 3 more hours. For qualitative detection of β-galactosidase, cells were grown in plates containing 80 mg/L X-Gal (5-bromo-4-cloro-3-indolil-β-D-galactopiranoside), 1% raffinose (Sigma), 2% galactose (Sigma), 0.67% yeast nitrogen base (Difco) and 0.054% of CSM-all amino acids (Complete Synthetic Mix, Qbiogene), 26 mM Na_2HPO_4, 25 mM NaH_2PO_4, 100 mg/l leucine, 2% agar, pH 7.0. For sporulation, diploid cells were grown for 1 day on complete solid media and subsequently transferred to sporulation media (1% potassium acetate, 0.1% yeast extract, 0.05% glucose). When cells were grown in the presence of α-factor (Sigma), the peptide was used at a concentration of 1 μg/ml cell culture.

S. cerevisiae was stored at -80ºC in 20% glycerol added to fresh culture.

6.2. Genetic techniques

6.2.1. Transformation of *Escherichia coli*

Transformation of *E.coli* strains was performed according to standard protocols (Sambrook and Russell, 2001). Chemical transformation was used to transform intact plasmids in BL21 cells and DH5α cells. Electroporation was used to transform DNA ligations in DH5α cells.

6.2.2. Transformation of *Saccharomyces cerevisiae*

Transformation of yeast was accomplished by the lithium acetate method (Ito et al., 1983). Briefly, yeast cells were grown on the appropriate media and recovered at exponential phase. Approximately 1-2 x 10^8 pelleted cells were washed on LiAc-TE buffer (100 mM lithium acetate, 10 mM Tris-HCl pH 7.5, 1 mM EDTA), mixed with the required DNA (0.5 μg of plasmid DNA or 2 to 5 μg of linear DNA for genomic integration), 25 μg of herring sperm DNA (Clonthech), which act as carrier, and 75 μg of PEG-4000. Cells were incubated at room temperature for 30 min, and heat shocked at 42ºC for 15 min. The PEG was eliminated by centrifugation; cells were diluted with TE (10 mM Tris pH 7.5, 1 mM EDTA) and plated on the adequate SDC media for selection.

6.2.3. Generation of yeast strains

6.2.3.1. Generation of yeast strains by mating, sporulation and tetrad dissection

Sporulation, tetrad dissection and scoring of genetic markers were performed as described (Sherman et al., 1974). Briefly, in order to obtain diploid yeast cells, haploids cells of opposite mating types, *MAT***a** and *MAT*α, were mixed on YPD plates and incubated for approximately 12 hours at room temperature. Subsequently, diploid cells were selected on appropriate minimal media (SDC lacking all amino acids, purine- or pyrimidine-bases that could be synthesized by the diploid but not by the haploid yeast cells). For sporulation, diploid cells were grown for 1 day on complete solid media and subsequently transferred to sporulation media (see section 6.1.2). The spores were separated under a tetrad dissection microscope (TDM50™, Micro Video Instruments, Inc) and allowed to germinate and grow on complete media at room temperature.

6.2.3.2. Generation of yeast strains by homologous recombination

For gene disruption by homologous recombination, PCR fragments that contained a yeast marker flanked by DNA sequences homologous to the gene of interest (approximately 40 nucleotides upstream and downstream of the region to be disrupted) were generated. Alternately, an integration cassette cloned in a plasmid, in which the ORF of the gene of interest was replaced by a yeast marker, was used. In this case the cassette was excised by restriction digests and the DNA fragment was purified from an agarose gel. The PCR fragment or the excised integration cassette was transformed into yeast cells as detailed in section 6.2.2. The DNA fragments containing the marker do not have origin of replication, so cells that grow in the selected marker might have incorporated the DNA in its genome. Replacement of the gene of interest was confirmed by PCR analysis.

For epitope tagging, a PCR-product encoding the epitope of interest with a yeast marker flanked by DNA sequences homologous to the upstream and downstream sequences adjacent the stop codon of the gene of interest was generated. . The PCR fragment was transformed into yeast cells as detailed in section 6.2.2. The DNA fragments containing the epitope plus the marker do not have origin of replication, so cells that grow in the selected marker might have incorporated the DNA in its genome. Epitope tagging was confirmed by PCR analysis, immunoblot, or scoring under the fluorescent microscope depending on the tag adjoined to the gene of interest.

6.2.3.3. Scoring of genetic markers

Scoring of genetic markers was accomplished as indicated below. When the methods listed were not sufficient to distinguish the desired genotype, scoring was performed by PCR of genomic DNA (see section 6.3.1 and 6.3.2.2) and/or by immunoblot (see section 6.4.1) and/or scoring under the fluorescent microscope.

6.2.3.3.1. Scoring for auxotrophies and temperature sensitivity

Analysis of the nutritional requirements and temperature sensitivity of yeast cells was done by replica plating. Briefly, a master plate containing the strains of interest was stamped onto a velvet. A copy of this impression was transferred to plates made with the relevant selective media. For analysis of temperature sensitive mutations, a replica of the imprint was transferred to YPD plates and incubated at 37ºC.

6.2.3.3.2. Scoring of the mating type

The mating type of haploid cells was tested by plating the corresponding yeast either with *MAT***a** and *MAT*α tester strains bearing a *his1* mutation (not present in any other laboratory strain) on minimal media lacking amino acids, purine- or pyrimidine-bases that cannot be synthesized by the haploid cells. Only yeasts of mating type opposite to the testers were able to produce diploids that grew on the minimal media.

6.2.3.3.3. Halo assay for detection of *bar1* mutants

Deletion of the *BAR1* gene, which codes for a secreted protease that cleaves the α-factor pheromone, was tested using a plate assay. The assay is based on the observation that *MAT***a** cells bearing double mutations in the *BAR1*/*SST1* and the *SST2* genes cannot recover from the cell cycle arrest induced by the α-factor pheromone.

A lawn of a yeast strain hyper-sensitive to α-factor (*MAT***a** *ssa1 ssa2,* strain RH123) was plated on YPD. A line of a *MAT*α strain arrested growth of the *MAT***a** *ssa1 ssa2* cells, therefore producing a halo in the middle of the plate. To identify *bar1* mutant yeast, the strains to be tested were streaked perpendicular to the line of the *MAT*α strain. Wild type *BAR1* cells secreted the protease and degraded the α-factor, thus allowing the lawn of the α-factor hyper-sensitive strain to grow closer to the *MAT*α strain middle line. When *BAR1* is knocked out, the secreted pheromone is not cleaved and the *MAT***a** *ssa1 ssa2* strain is not able to grow close to the *MAT*α strain.

A halo assay was also used to estimate the amount of α-factor purified (see section 6.4.3.3.) In this case, a lawn of *MAT***a** *ssa1 ssa2* cells was plated on YPD and 1 μl of purified α-factor from different fractions was spotted on the plate. Fractions that produced a clear halo were kept to be used for internalization assays.

6.2.3.3.4. Scoring of *S. cerevisiae* synthetic lethality after contra-selection of cells bearing plasmids expressing *URA3* in a *ura3* mutant background

For contra-selection of cells expressing *URA3* plasmids, 5'-fluoro-orotic acid (FOA) (Fluorochem) was added to synthetic minimal solid medium at a concentration of 1 mg/ml. Cells were transferred by replica plating to FOA-containing plates. Cells encoding the wild type *URA3* convert 5'-fluoro-orotic acid to 5'-fluoro-uracil, which is toxic for the yeast cell.

6.2.3.4. Construction of strains generated for this study

Yeast strains used in this study are listed in Table I. Not previously published strains were generated as follows.

Table I. Yeast strains

Strain	Genotype	Reference
BY4741	*MAT***a** *his3 leu2 met15 ura3*	Euroscarf
BY4742	*MAT*α *his3 leu2 lys2 ura3*	Euroscarf
Y01428	*MAT***a** *cka1Δ::kanMX4 ura3 leu2 his3 met15*	Euroscarf
Y01837	*MAT***a** *cka2Δ::kanMX4 ura3 leu2 his3 met15*	Euroscarf
Y03033	*MAT***a** *sla1Δ::kanMX4 ura3 leu2 his3 met15*	Euroscarf
Y04387	*MAT***a** *ckb1Δ::kanMX4 ura3 leu2 his3 met15*	Euroscarf
Y06549	*MAT***a** *myo5Δ::kanMX4 ura3 leu2 his3 met15*	Euroscarf

Y11815	*MATα ckb2Δ::kanMX4 ura3 leu2 his3 lys2*	Euroscarf
Y11837	*MATα cka2Δ::kanMX4 ura3 leu2 his3 lys2*	Euroscarf
Y16549	*MATα myo5Δ::kanMX4 ura3 leu2 his3 lys2*	Euroscarf
EGY48	*MAT**a** ura3 trp1 his3 leu2::lexAop6-LEU2*	(Gyuris et al., 1993)
RH123	*MAT**a** ssa1 ssa2*	H. Riezman
RH449	*MATα his4 leu2 lys2 ura3 bar1*	H. Riezman
RH2565	*MAT**a** sac6Δ::URA3 ura3 bar1 his3 leu2*	(Kubler and Riezman, 1993)
RH2881	*MAT**a** his3 leu2 trp1 ura3 bar1*	(Geli et al., 2000)
RH3377	*MAT**a** his3 leu2 trp1 ura3 bar1 ade2 myo3Δ::HIS3*	(Geli and Riezman, 1996)
RH3654	*MAT**a** his3 trp1 lys2 leu2 ade bar1Δ::LYS2 ura3 pan1-4*	H. Riezman
RH3977	*MATα his3 leu2 trp1 ura3 bar1 myo3Δ::HIS3*	(Geli et al., 1998)
RH4157	*MAT**a** ura3 his3 leu2 lys2 arp3HIS3 pDW20 (pCEN URA3 ARP3-5MYC6HIS)*	(Idrissi et al., 2002)
RH4165	*MAT**a** arp2-2 URA3 ade2 trp1 leu2 his ura3 bar1*	(Idrissi et al., 2002)
SL5156	*MATα leu2 ura3 trp1 his3 ABP1-mRPF::kanMX4*	S. Lemmon
YDH13	*MAT**a** lys2 his3 leu2 ura3 cka1Δ::HIS3 cka2Δ::TRP1 bar1::URA3 pcka2-13 (LEU2, CEN)*	(Hanna et al., 1995)
SCI284	*MATα his3 leu2 lys2 ura3 CKA1-13myc::HIS3MX6*	This study
SCI285	*MAT**a** myo5Δ::kanMX4 leu2 his3 ura3 met15 CKA2-3HA::HIS3MX6*	This study
SCMIG48	*MATα ade2 vrp1Δ::ura3 his3 leu2 lys2 trp1 ura3 bar1*	(Geli et al., 2000)
SCMIG100	*MAT**a** his3 leu2 met15 ura3 bar1Δ::URA3*	(Idrissi et al., 2002)
SCMIG275	*MAT**a** his3 leu2 lys2 trp1 ura3 bar1 myo5Δ::TRP1*	(Idrissi et al., 2002)
SCMIG276	*MATα his3 leu2 lys2 trp1 ura3 bar1 myo5Δ::TRP1*	(Geli et al., 2000)
SCMIG516	*MAT**a** his3 leu2 ura3 trp1 bar1 LAS17-3HA::TRP1*	(Idrissi et al., 2008)
SCMIG518	*MAT**a** his3 leu2 trp1 ura3 bar1 las17-waΔ-3HA::TRP1*	M.I. Geli
SCMIG716	*MAT**a** cka1Δ::kanMX4 ura3 leu2 his3 met15 bar1Δ::URA3*	This study
SCMIG717	*MAT**a** cka2Δ::kanMX4 ura3 leu2 his3 met15 bar1Δ::URA3*	This study
SCMIG723	*MAT**a** his3 ura3 leu2 met15 bar1Δ ::URA3 ABP1-3HA::HIS3MX*	(Idrissi et al., 2008)
SCMIG809	*MATα cka2Δ::kanMX4 ura3 leu2 his3 trp1 bar1*	This study
SCMIG811	*MAT**a** myo5Δ::TRP1 cka2Δ::HIS3 ura3 leu2 his3 trp1 lys2 bar1*	This study
SCMIG812	*MAT**a** myo5Δ::TRP1 cka1Δ::HIS3 ura3 leu2 his3 trp1 lys2 bar1*	This study
SCMIG814	*MAT**a** sac6Δ::URA3 cka2Δ::kanMX4 ura3 leu2 his3 bar1*	This study
SCMIG881	*MATα ura3 leu2 his4 trp1 lys2 myo5Δ::TRP1 ABP1-mRFP::kanMX4 bar1?*	This study
SCMIG903	*MAT**a** his3 ura3 leu2 met15 bar1Δ ::URA3 BBC1-3HA::HIS3MX*	(Idrissi et al., 2008)
SCMIG1077	*MAT**a** his3 leu2 trp1 ura3 met15 cmd1Δ::kanMX4 myo5Δ::kanMX4 SLA1-mCherry::HIS3MX6 pTRP1CMD1*	(Grotsch et al., 2010)
SCMIG1078	*MAT**a** his3 leu2 trp1 ura3 met15 cmd1Δ::kanMX4 myo5Δ::kanMX4 SLA1-mCherry::HIS3MX6 pTRP1cmd1-226*	(Grotsch et al., 2010)
SCMIG1097	*MAT**a** his3 leu2 trp1 ura3 bar1 myo3Δ::HIS3 myo5Δ::TRP1 p33myc-MYO5 (URA3, CEN)*	This study
SCMIG1098	*MATα his3 leu2 trp1 ura3 bar1 myo3Δ::HIS3 myo5Δ::TRP1 p33myc-MYO5 (URA3, CEN)*	This study
SCMIG1099	*MAT**a** his3 leu2 trp1 ura3 bar1 myo3Δ::HIS3 myo5Δ::TRP1 p33myc-myo5-S1205C (URA3, CEN)*	This study
SCMIG1100	*MATα his3 leu2 trp1 ura3 bar1 lys2 myo3Δ::HIS3 myo5Δ::TRP1 p33myc-myo5-S1205C (URA3, CEN)*	This study

SCMIG1101	*MAT**a** his3 leu2 trp1 ura3 bar1 myo3Δ::HIS3 myo5Δ::TRP1 p33myc-myo5-S1205D (URA3, CEN)*	This study
SCMIG1102	*MATα his3 leu2 trp1 ura3 bar1 myo3Δ::HIS3 myo5Δ::TRP1 p33myc-myo5-S1205D (URA3, CEN)*	This study
SCMIG1103	*MAT**a** ade2? ade3? his3 leu2 trp1 ura3 bar1 pan1-4 myo3Δ::HIS3 myo5Δ::TRP1 p33myc-MYO5 (URA3, CEN)*	This study
SCMIG1105	*MAT**a** ade2? ade3? his3 leu2 trp1 ura3 bar1::LYS pan1-4 myo3Δ::HIS3 myo5Δ::TRP1 p33myc-myo5-S1205C (URA3, CEN)*	This study
SCMIG1107	*MAT**a** ade2? ade3? his3 leu2 trp1 ura3 bar1::LYS pan1-4 myo3Δ::HIS3 myo5Δ::TRP1 p33myc-myo5-S1205D (URA3, CEN)*	This study
SCMIG1108	*MAT**a** his3 leu2 trp1 ura3 bar1 las17-waΔ-3HA::TRP1 myo3Δ::HIS3 myo5Δ::TRP1 p33myc-MYO5 (URA3, CEN)*	This study
SCMIG1110	*MAT**a** his3 leu2 trp1 ura3 bar1 lys? las17-waΔ-3HA::TRP1 myo3Δ::HIS3 myo5Δ::TRP1 p33myc-myo5-S1205C (URA3, CEN)*	This study
SCMIG1112	*MAT**a** his3 leu2 trp1 ura3 bar1 las17-waΔ-3HA::TRP1 myo3Δ::HIS3 myo5Δ::TRP1 p33myc-myo5-S1205D (URA3, CEN)*	This study
SCMIG1126	*MAT**a** his3? his4 leu2 ura3 trp1 myo3Δ::HIS3 myo5Δ::TRP1 ABP1-mRFP::kanMX4 p33GFP-MYO5 (URA3, CEN)*	This study
SCMIG1127	*MAT**a** his3? leu2 ura3 trp1 myo3Δ::HIS3 myo5Δ::TRP1 ABP1-mRFP::kanMX4 p33GFP-myo5-S1205C (URA3, CEN)*	This study
SCMIG1128	*MAT**a** his3? leu2 ura3 trp1 myo3Δ::HIS3 myo5Δ::TRP1 ABP1-mRFP::kanMX4 p33GFP-myo5-S1205D*	This study
SCMIG1135	*MAT**a** his3 leu2 ura3 cka2Δ::kanMX4 myo5Δ::kanMX4 p33GFP-MYO5 (URA3, CEN)*	This study
SCMIG1137	*MAT**a** his3 leu2 ura3 myo5Δ::kanMX4 p33GFP-MYO5*	This study
SCMIG1141	*MAT**a** his3 leu2 trp1 ura3 bar1 SLA1-mCherry::HIS3MX6*	This study
SCMIG1145	*MAT**a** his3 leu2 trp1 lys2 ura3 bar1 myo5Δ::TRP1 SLA1- mCherry::HIS3MX6*	This study
SCMIG1147	*MATα his3 leu2 trp1 ura3 lys2 myo3Δ::HIS3 myo5Δ::TRP1 p33GFP-MYO5 (URA3, CEN)*	This study
SCMIG1149	*MATα his3 leu2 trp1 ura3 lys2 myo3Δ::HIS3 myo5Δ::TRP1 p33GFP-myo5-S1205C (URA3, CEN)*	This study
SCMIG1151	*MATα his3 leu2 trp1 ura3 lys2 myo3Δ::HIS3 myo5Δ::TRP1 p33GFP-myo5-S1205D (URA3, CEN)*	This study
SCMIG1152	*MAT**a** his3 leu2 lys2 met15 ura3 CKA1-13myc::HIS3MX6 CKA2-3HA::HIS3MX6*	This study
SCMIG1155	*MAT**a** his3 leu2 ura3 CKA2-3HA::HIS3MX*	This study
SCMIG1160	*MAT**a** his3 leu2 lys2 ura3 trp1 bar1? myo3Δ::HIS3 myo5Δ::TRP1 SLA1- mCherry::HIS3MX6 p33GFP-MYO5 (URA3, CEN)*	This study
SCMIG1162	*MAT**a** his3 leu2 lys2 ura3 trp1 bar1? myo3Δ::HIS3 myo5Δ::TRP1 SLA1- mCherry::HIS3MX6 p33GFP-myo5-S1205C (URA3, CEN)*	This study
SCMIG1163	*MAT**a** his3 leu2 lys2 ura3 trp1 bar1? myo3Δ::HIS3 myo5Δ::TRP1 SLA1- mCherry::HIS3MX6 p33GFP-myo5-S1205D (URA3, CEN)*	This study
SCMIG1164	*MAT**a** his3 leu2 lys2 ura3 myo5Δ::kanMX4 sla1Δ::kanMX4 p111SLA1-HA (LEU2, CEN)*	This study
SCMIG1169	*MATα his3 leu2 lys2 ura3 met15 myo5Δ::kanMX4 cka2Δ::kanMX4*	This study
SCMIG1172	*MAT**a** his3 leu2 ura3 met15? SLA1- mCherry::HIS3MX6 cka2Δ::kanMX4*	This study
SCMIG1173	*MAT**a** his3 leu2 ura3 lys2 ckb1Δ::kanMX4 ckb2Δ::kanMX4*	This study
SCMIG1176	*MAT**a** his3 leu2 ura3 met15 cka1Δ::kanMX4 cka2Δ::kanMX4 pcka2-13 (LEU2, CEN)*	This study
SCMIG1178	*MAT**a** his3 leu2 ura3 met15 cka1Δ::kanMX4 cka2Δ::kanMX4 pCKA2 (LEU2, CEN)*	This study
SCMIG1180	*MAT**a** his3 leu2 ura3 met15 cka1Δ::kanMX4 cka2Δ::kanMX4 pcka1-13 (LEU2, CEN)*	This study
SCMIG1182	*MAT**a** his3 leu2 ura3 met15 cka1Δ::kanMX4 cka2Δ::kanMX4 pCKA1 (LEU2, CEN)*	This study
SCMIG1200	*MAT**a** his3 leu2 ura3 lys2 ckb1Δ::kanMX4 ckb2Δ::kanMX4 CKA2-3HA::HIS3MX6*	This study
SCMIG1202	*MAT**a** his3 leu2 met15 ura3 CKA1-3HA::HIS3MX6*	This study
SCMIG1216	*MAT**a** his3 leu2 met15 ura3 bar1Δ::URA3 BZZ1-3HA::HIS3MX6*	(Idrissi et al., 2012)

SCMIG716 and SCMIG717

SCMIG716 and SCMIG717 were generated by substituting the chromosomal copy of the gene encoding the protease Bar1, which cleaves the α-factor pheromone, by the auxotrophically selectable *URA3* gene. To do this, we used a *bar1Δ::URA3* knockout cassette (pLH309, kindly provided by Dr. Linda Hicke), which contains the *URA3* marker flanked with 600 base pairs of the region downstream and 700 base pairs of the region upstream of the *BAR1* open reading frame. The knockout cassette was excised with *Eco*RI, purified from an agarose gel and used to transform Y01428 and Y01837, respectively. Transformants were selected on SDC-Ura and scored for deletion of the *BAR1* gene using the halo assay (see above, section 6.2.3.3.3.)

SCMIG1097, SCMIG1098, SCMIG1099, SCMIG1100, SCMIG1101, SCMIG1102, SCMIG1103, SCMIG1105, SCMIG1107, SCMIG1108, SCMIG1110, SCMIG1112, SCMIG 518, SCMIG814 and SCMIG809

SCMIG1097 and SCMIG1098 were generated by mating SCMIG275 to RH3977 followed by selection of the diploid strains in SDC-His-Trp and transformation with p33*myc-MYO5*. Transformants were selected on SCD-Ura and forced to sporulate. Tetrads were dissected and spores were scored for the mating type and for the *HIS3, TRP1* and *URA3* markers to identify *myo3Δ myo5Δ* cells covered with p33*myc-MYO5*. The same procedure was followed to generate the SCMIG1099 and SCMIG1100 and the SCMIG1101 and SCMIG1102 strains, but in this case, the diploid strains were transformed with p33*myc-myo5-S1205C* or p33*myc-myo5-S1205D,* respectively.

SCMIG1103, SCMIG1105, and SCMIG1107 were generated by mating RH3654 to SCMIG1098, SCMIG1100 and SCMIG1102, respectively. Diploid cells were identified by visual inspection under the microscope and forced to sporulate. Tetrads were dissected and spores were scored for the mating type and for the *HIS3, TRP1* and *URA3* markers to identify *myo3Δ myo5Δ* segregants covered with p33*myc-MYO5,* p33*myc-myo5-S1205C* or p33*myc-myo5-S1205D* and for temperature sensitivity to identify the *pan1-4* allele.

SCMIG1108, SCMIG1110 and SCMIG1112 were obtained by mating SCMIG518 to SCMIG1098, SCMIG1100 and SCMIG1102, respectively. Diploid cells were identified by visual inspection under the microscope and forced to sporulate. Since deletion of *MYO5* and the *las17-waΔ-3HA* allele were both tagged with *TRP1*, the *las17-waΔ-3HA* genotype was scored by immunoblot using antibodies against the HA epitope. The *myo3Δ myo5Δ* genotype was confirmed by scoring for synthetic lethality after contra-selection of cells bearing p33*myc-MYO5,* p33*myc-myo5-S1205C* or p33*myc-myo5-S1205D* on FOA plates (see section 6.2.3.3.4). SCMIG518 was generated by substituting the chromosomal region of the *LAS17* gene that encodes the WH2 and acidic domains (amino acids 529 to 633) for a DNA fragment encoding 3HA with the auxotrophically selectable *TRP1* gene by homologous recombination. To do this, a PCR product encoding the *3HA::TRP1* cassette flanked by 50 nucleotides upstream the WH2 domain and 40 nucleotides downstream the STOP codon was generated using the plasmid pFA6a-3HA-Trp1 as

template and primers Las17.1530D.F2 and Las17.1899U.R1. The amplified fragment was transformed into the RH2881 and transformants were selected on SDC-Trp. Successful recombination was verified by immunoblot using an antibody against the HA epitope.

SCMIG814 was generated by mating SCMIG809 to RH2565. Diploids cells were identified by visual inspection under the microscope and forced to sporulate. Tetrads were dissected and spores were scored for the *URA3* and *kanMX4* markers to identify the *sac6Δ cka2Δ* double knockouts. SCMIG809 was constructed crossing SCMIG276 to SCMIG717. Diploids were selected on SDC-Ura-Trp and forced to sporulate. Spores were scored for the Trp auxotrophy and the *kanMX4* marker to identify the *cka2Δ trp1* strains.

SCMIG811 and SCMIG812

SCMIG811 and SCMIG812 were generated by substituting the chromosomal copies of the genes encoding the casein kinase catalytic subunits Cka1 and Cka2 by the auxotrophically selectable *HIS3* gene, respectively. To do this, a PCR-generated *cka1Δ::HIS3* knockout cassette containing the *HIS3* marker and flanking sequences of approximately 40 nucleotides corresponding to the upstream and downstream sequences of the *CKA1* ORF, was generated using the Cka1.20.YDp.D and Cka1.1080.YDp.U primers and YDp-H as template. The PCR fragment was transformed into SCMIG275 and transformants were selected on SDC-His. Knock out of the *CKA1* gene was confirmed by PCR (using primers Cka1.-498D.HindIII and Cka1.1317U.EcoRI, and genomic DNA of the putative *cka1Δ* cells as template), followed by restriction analysis. The same procedure was followed to knock out the *CKA2* gene, but in this case, primers Cka2.28.YDp.D and Cka2.1002.YDp.U and YDp-H were used to generate the knockout cassette, and primers Cka2.-480D.HindIII and Cka2.1220U.EcoRI were used to confirm the knockout by PCR and restriction analysis.

SCMIG1126, SCMIG1127, SCMIG1128, and SCMIG881

To obtain the SCMIG1126, SCMIG1127, and SCMIG1128 strains, SCMIG881 was mated to RH3377 and transformed with the p33*GFP-Myo5*, p33*GFP-Myo5-S1205C or* p33*GFP-Myo5-S1205D,* as indicated. Diploid cells were selected on SDC-His-Trp-Ura and forced to sporulate. Tetrads were dissected and spores were scored for the mating type, geneticin sensitivity, and the *HIS3, TRP1* and *URA3* markers to identify the *myo3Δ myo5Δ* or the *myo3Δ myo5Δ ABP1-mRFP* segregants bearing the plasmids expressing the corresponding GFP-Myo5 versions. SCMIG881 was generated by mating SCMIG811 to SL5156, kindly provided by Dr. Sandra Lemmon. Diploid cells were identified by visual inspection under the microscope and forced to sporulate. Tetrads were dissected and spores were scored for the mating type, geneticin sensitivity, and the *TRP1* marker to identify the *myo5Δ ABP1-mRFP* segregants.

SCMIG1160, SCMIG1162, SCMIG1163, SCMIG1147, SCMIG1149, SCMIG1151, SCMIG1164, SCMIG1172 and SCMIG1169

To obtain the SCMIG1160, SCMIG1162, and SCMIG1163 strains, SCMIG1145 was mated to SCMIG1147, SCMIG1149, and SCMIG1151, respectively. Diploid cells were identified by visual inspection under the microscope and forced to sporulate. Tetrads were dissected and spores were scored for the mating type and the *HIS3, TRP1* and *URA3* markers to identify the *myo3Δ myo5Δ Sla1-mCherry* segregants bearing the plasmids expressing the corresponding GFP-Myo5 versions. Since deletion of *MYO3* and Sla1-mCherry were both tagged with *HIS3*, the myo3*Δ* and *Sla1-mCherry* genotypes were scored for synthetic lethality after contra-selection of the GFP-Myo5 versions on FOA plates (section 6.2.3.3.4), to identify the *myo3Δ myo5Δ* genotype complemented by the corresponding Myo5 versions. Tagging of Sla1 was scored under the fluorescent microscope by verifying recruitment of the tagged proteins to the cortical actin patches. SCMIG1147, SCMIG1149, and SCMIG1151 were generated by mating RH3377 to SCMIG275 transformed with the p33*GFP-MYO5*, p33*GFP-myo5-S1205C or* p33*GFP-myo5-S1205D,* respectively. Diploid cells were selected on SDC-His-Trp-Ura and forced to sporulate. Tetrads were dissected and spores were scored for the mating type and the *HIS3, TRP1* and *URA3* markers to identify the *myo3Δ myo5Δ* segregants bearing the plasmids expressing the corresponding Myo5 versions.

SCMIG1164 was originated by mating Y16549 to Y03033. Diploid cells were identified by visual inspection under the microscope and forced to sporulate. Tetrads were dissected and scored for the mating type and the *kanMX4* marker to identify the *myo5Δ sla1Δ* segregants. Only tetrads with two of the four spores growing on YPD geneticin plates were selected to assure co-segregation of the *MYO5* and the *SLA1* knock outs.

SCMIG1172 was generated by mating SCMIG1141 to SCMIG1169. Diploid cells were identified by visual inspection under the microscope and forced to sporulate. Tetrads were dissected and spores were scored for the mating type and the *HIS3MX6* and *kanMX4* markers to identify the *cka2Δ SLA1-mCherry* segregants. Since deletion of *MYO5* and deletion of *CKA2* were both tagged with *kanMX4,* immunoblot using an antibody against Myo5 was used to verify that the *kanMX4* marker was not tagging the *MYO5* deletion. SCMIG1169 was constructed by mating Y06549 to Y11837. Diploid cells were identified by visual inspection under the microscope and forced to sporulate. Tetrads were dissected and scored for the *kanMX4* marker. Tetrads with two of the four spores growing on YPD-geneticin were selected for further analysis to assure co-segregation of the *MYO5* and the *CKA2* knock outs.

SCMIG1141 and SCMIG1145

SCMIG1141 and SCMIG1145 were generated by adjoining the gene encoding the monomeric fluorescent protein mCherry with the auxotrophically selectable *HIS3MX6* gene after the chromosomal copy of the gene encoding the endocytic marker Sla1 in a wild type cell or a *myo5Δ* strain, respectively. To do this, a PCR-product encoding the *mCherry::HIS3MX6* cassette

flanked by approximately 40 nucleotides corresponding to the upstream and downstream sequences adjacent the stop codon of the *SLA1* gene was obtained used the primers Sla1.3695D.F2 and Sla1.3775U.R1 and the plasmid pBS34 as a template (kindly provided by Dr. Sandra Lemmon). The PCR fragment was transformed into RH2881 and SCMIG275 to generate SCMIG1141 and SCMIG1145, respectively. Transformants were selected on SDC-His. Tagging of Sla1 was scored under the fluorescent microscope by verifying recruitment of the tagged proteins to the cortical actin patches.

SCMIG1135 and SCMIG1137

SCMIG1135 and SCMIG1137 strains were constructed by mating Y11837 to Y06549 transformed with p33*GFP-Myo5*. Diploid cells were identified by visual inspection under the microscope and forced to sporulate. Tetrads were dissected and spores were scored for the *kanMX4* and *URA3* markers to identify the *myo5Δ cka2Δ* and *myo5Δ CKA2* cells bearing p33*GFP-Myo5*, respectively. Since deletion of *MYO5* and deletion of *CKA2* were both tagged with *kanMX4,* co-segregation of the *MYO5* and the *CKA2* knock outs was assured by selecting tetrads with two of the four spores grew on YPD geneticin plates (only to generate SCMIG1135) and by immunoblot using an antibody against Myo5 (Myo5 and GFP-Myo5 show different SDS-PAGE mobility).

SCMIG1173, SCMIG1176, SCMIG1178, SCMIG1180, and SCMIG1182

SCMIG1173 was originated by mating Y04387 to Y11815. Diploid cells were identified by visual inspection under the microscope and forced to sporulate. Tetrads were dissected and scored for the *kanMX4* markers. Only tetrads with two of the four spores growing on YPD-geneticin plates were selected for further analysis to assure co-segregation of the *CKB1* and the *CKB2* knock outs. SCMIG1176, SCMIG1178, SCMIG1180, and SCMIG1182 were originated by mating Y11837 to Y01428 transformed with p*cka2-13*, p*CKA2*, p*cka1-13* and p*CKA1*, kindly provided by Dr. C. V. Glover, respectively. Cells were selected on SDC-Leu, and diploid cells were identified by visual inspection under the microscope and forced to sporulate. Tetrads were dissected and scored for the mating type and for the *kanMX4* and *LEU2* markers to identify cka1*Δ cka2Δ* segregants covered with p*cka2-13*, p*CKA2*, p*cka1-13* and p*CKA1*, respectively. Only tetrads with two of the four spores growing on YPD geneticin plates were selected for further analysis to assure co-segregation of the *CKA1* and the *CKA2* knock outs. Temperature sensitivity was scored to identify the cka1*Δ cka2Δ* segregants covered with p*cka2-13* or p*cka1-13.* PCR of genomic DNA using the Cka1.-498D.HindIII and Cka1.1317U.EcoRI primers or the Cka2.-498D.HindIII and Cka2.1220U primers was used to confirm the genotype of *cka1Δcka2Δ* segregants covered with p*CKA1*, and p*CKA2*, respectively.

SCI285, SCMIG1200, SCMIG1202, SCI284, SCMIG1152, and SCMIG1155

SCI285, SCMIG1200, SCMIG1202, SCI284 were generated by homologous recombination. SCI285 and SCMIG1200 were generated by adjoining a DNA fragment encoding 3HA plus the auxotrophically selectable *HIS3MX6* gene after the chromosomal copy of the gene encoding

Cka2 in a *myo5Δ* strain or in a *ckb1Δ ckb2Δ* strain, respectively. To do this, a PCR-product encoding the *3HA::HIS3MX6* cassette flanked by approximately 40 nucleotides corresponding to the upstream and downstream sequences adjacent the stop codon of the *CKA2* gene was obtained using the primers Cka2.980.F2 and Cka2.1060.R1 and the plasmid pFA6a-3HA-His3MX6. The PCR fragment was transformed into Y06549 and SCMIG1173 to generate SCI285 and SCMIG1200, respectively. The same strategy was used to generate the SCMIG1202 and SCI284 strains. A DNA fragment encoding either the *3HA::HIS3MX6* or the *13myc::HIS3MX6* cassettes flanked by approximately 40 nucleotides corresponding to the upstream and downstream sequences adjacent the stop codon of the *CKA1* gene were amplified using the primers Cka1.1079.F2 and Cka1.1159.R1 and either the plasmids pFA6a-3HA-His3MX6 or pFA6a-13myc-His3MX6, respectively. The PCR product encoding the *3HA::HIS3MX6* sequence was transformed into BY4741 to generate the SCMIG1202 strain, while the DNA fragment encoding the *13myc::HIS3MX6* cassette was transformed into BY4742 to generate the SCI284 strain. Transformants were selected on SDC-His. Tagging of Cka1 and Cka2 was scored by immunoblot using antibodies against the HA and/or myc epitopes.

SCMIG1152 and SCMIG1155 were generated by mating SCI284 to SCI285. Diploid cells were identified by visual inspection under the microscope and forced to sporulate. Tetrads were dissected and spores were scored for the mating type and the *HIS3* marker to identify the *CKA1-13myc* and *CKA2-3HA* segregants. Since *CKA1-13myc* and *CKA2-3HA* were both tagged with *HIS3MX6*, co-segregation of the *CKA1-13myc* and *CKA2-3HA* tagging was assured by selecting tetrads with two of the four spores growing on SDC-His plates (only to generate SCMIG1152), while immunoblot using antibodies against the HA and/or myc epitopes was used to identify the SCMIG55 strain (and verify the double tagging of the SCMIG1152 strain)

6.2.4. Serial dilution cell growth assays

Cells from mid-log phase cultures were diluted to 10^7 cells/ml in the adequate fresh media and 4 x 1 to 10 serial dilutions were prepared on sterile 1.5 ml Eppendorf tubes. 5 μl of each dilution were spotted on plates with the adequate solid media. After the liquid was evaporated, plates were incubated for two days at the indicated temperature.

6.3. DNA and RNA techniques and plasmid construction

6.3.1. Standard molecular biology techniques: amplification and purification of plasmids in *E. coli*, enzymatic restriction of DNA, PCR, agarose gels, purification of DNA fragments, and DNA sequencing

Standard DNA manipulations such as polymerase chain reaction (PCR), gel electrophoresis, enzymatic digestion, DNA ligation, and plasmid purification were performed as described (Sambrook and Russel, 2001). Standard PCRs were performed with a DNA polymerase with proof reading activity (Vent polymerase, New England Biolabs) and a TRIO-thermoblock (Biometra GmbH). Oligonucletides were synthesized by Genotek MWG or by Bonsai

Technologies. Restriction endonucleases were obtained from New England Biolabs or from Roche. DNA was purified using PCR- or gel extraction kits from Qiagen. Analytical agarose gel electrophoresis was performed using Sub-Cell cells from Bio-Rad Laboratories. Unless otherwise mentioned, cloning of DNA fragments was performed with the T4 DNA ligase (New England Biolabs). Occasionally, molecular cloning of DNA fragments in plasmids was accomplished by homologous recombination in yeast followed by plasmid purification (see below). Plasmids were amplified and purified from *E. coli* with the Nucleospin plasmid purification kit (Macherey-Nagel). DNA sequencing was performed in the DNA-Sequencing Facility of the Center for Research in Agricultural Genomics (CRAG) or by Macrogen Inc.

6.3.2. Purification of DNA from *S. cerevisiae*

6.3.2.1. Extraction and purification of plasmid DNA

A 5 ml yeast culture in stationary phase was harvested at 2,300 g for 5 min. Cells were suspended in 0.4 ml of lysis buffer (0.2 M Tris-HCl pH 7.5, 0.5 mM NaCl, 1% SDS, 10 mM EDTA) and transferred to a 1.5 ml Eppendorf tube. 150 μl of glass beads and 300 μl of phenol:chloroform:isoamyl alcohol (25:24:1) were added and cells were lysed by vortexing for 2 min. Upon centrifugation at 20,000 g for 5 min, the aqueous phase (upper phase) was transferred into a new 1.5 ml tube and the DNA was further purified by phenol:chloroform extraction. The plasmid DNA was then concentrated by ethanol precipitation and finally resuspended in 50 μl of double distilled water. To obtain pure plasmid DNA, electro-competent *E.coli* cells were transformed with the plasmid recovered from yeast cells. Plasmid DNA was purified from single colonies and analyzed by digestion with restriction enzymes and analytical agarose gel electrophoresis.

6.3.2.2. Extraction and purification of genomic DNA

Approximately 2 x 10^8 yeast cells were harvested (at a culture density of 10^7 cells/ml) and resuspended in 1 ml of 1 M sorbitol. Cells were collected in 1.5 ml Eppendorf tubes, centrifuged at 5,200 g for 2 min, and resuspended in 0.5 ml of Spheroplasting buffer (1 M sorbitol, 50 mM KPO_4 buffer, pH 7.5, 14 mM β-mercaptoethanol, and either 100 U/ml zymolyase 20T (Seikagaku) or 250 U/ml lyticase (Sigma-Aldrich)). After incubation for 30 min at 30ºC, spheroplasts were collected at 5,200 g and resuspended in 0.5 ml of 50 mM EDTA pH 8.0, 0.2% SDS. Samples were then incubated for 15 min at 65ºC. 50 μl of 5 M KAc pH 7.5 was added and the tube was incubated on ice for 1h. The precipitate was sedimented at 20.000 x g for 15 min and the supernatant was transferred into a new 1.5 ml Eppendorf tube carefully, in order not to fragment the chromosomes. 1 ml ethanol was added and the genomic DNA precipitate was collected at 20,000 g for 15 s. The supernatant was discarded and the pellet was air-dried and resuspended in 200 μl of TE buffer (10 mM Tris pH 7.5, 1 mM EDTA). DNA was then incubated at 37º C for 15 min in the presence of RNAse A (50 μg/ml). For further purification the sample was extracted 3 times with phenol:chloroform:isoamyl alcohol (25:24:1). Finally, the genomic DNA was precipitated with ethanol and resuspended in 50 μl of TE.

6.3.3. Construction of plasmids generated for this study

Plasmids used in this study are listed in Table II. Not previously published plasmids constructed for this study were generated as follows.

Table II. Plasmids

Plasmid	E.coli features	Yeast features	Insert	Reference
pGEX-5X-3	*ori* AMP^R	-	GST	Pharmacia
pGST-Myo5-C_{ext}	*ori* AMP^R	-	GST-*MYO5* (aa 984-1219)	(Geli et al., 2000)
pGST-Myo5-(SH3, $TH2_C$)	*ori* AMP^R	-	GST-*MYO 5* (aa 1085-1219)	(Geli et al., 2000)
pGST-Myo5-($TH2_C$)	*ori* AMP^R	-	GST-*MYO5* (aa 1142-1219)	(Geli et al., 2000)
pGST-Myo5-C_{ext}-S1205A	*ori* AMP^R	-	GST-*myo5-S1205A* (aa 984-1219)	B. Grosshans
pGST-Myo5-C_{ext}-S1205C	*ori* AMP^R	-	GST-*myo5-S1205C* (aa 984-1219)	This study
pGST-Myo5-C_{ext}-S1205D	*ori* AMP^R	-	GST-*myo5-S1205D* (aa 984-1219)	This study
YCplac111	*ori* AMP^R	*CEN4* *LEU2*	-	(Gietz and Sugino, 1988)
YEplac181	*ori* AMP^R	2μ *LEU2*	-	(Gietz and Sugino, 1988)
YDp-H	*ori* AMP^R	- *HIS3*	-	(Berben et al., 1991)
YDp-U	*ori* AMP^R	- *URA3*	-	(Berben et al., 1991)
pLH309	*ori* AMP^R	- *URA3*	*bar1Δ::URA3*	L. Hicke
pFA6a-3HA-Trp1	*ori* AMP^R	- *TRP1*	*3HA*	(Longtine et al., 1998)
pFA6a-3HA-HisMX6	*ori* AMP^R	- *HIS3MX6*	*3HA*	(Longtine et al., 1998)
pFA6a-13myc-HisMX6	*ori* AMP^R	- *HIS3MX6*	*13myc*	(Longtine et al., 1998)
pFA6a-GFP(S65T)-HisMX6	*ori* AMP^R	- *HIS3MX6*	*GFP(S65T)*	(Longtine et al., 1998)
pBS34	*ori* AMP^R	- *HIS3MX6*	*mCherry*	S. Lemmon
pDA6300	*ori* AMP^R	2μ *LEU2*	MFα1	H. Riezman
p*CKA1*	*ori* AMP^R	*CEN4* *LEU2*	*CKA1*	(Rethinaswamy et al., 1998)
p*CKA2*	*ori* AMP^R	*CEN4* *LEU2*	*CKA2*	(Hanna et al., 1995)
p*cka1-13*	*ori* AMP^R	*CEN4* *LEU2*	*cka1-13 (D253N)*	(Rethinaswamy et al., 1998)
p*cka2-13*	*ori* AMP^R	*CEN4* *LEU2*	*cka2-13 (D225N)*	(Hanna et al., 1995)
p*CKA2.leu2Δ::URA3*	*ori* AMP^R	*CEN4* *URA3*	*CKA2*	This study
p111*CKA1*	*ori* AMP^R	*CEN4* *LEU2*	*CKA1*	This study
p111*CKA2*	*ori* AMP^R	*CEN4* *LEU2*	*CKA2*	This study
p111*STE2-GFP*	*ori* AMP^R	*CEN4* *LEU2*	*STE2GFP*	This study
p111*STE2*	*ori* AMP^R	*CEN4* *LEU2*	*STE2*	This study
p181*STE2*	*ori* AMP^R	2μ *LEU2*	*STE2*	This study
p181*CKA1*	*ori* AMP^R	2μ *LEU2*	*CKA1*	This study
p181*CKA2*	*ori* AMP^R	2μ *LEU2*	*CKA2*	This study
p181*cka2-K79A*	*ori* AMP^R	2μ *LEU2*	*cka2-K79A*	This study
p181*CKA1-HA*	*ori* AMP^R	2μ *LEU2*	*CKA1-HA*	This study
p181*CKA2-HA*	*ori* AMP^R	2μ *LEU2*	*CKA2-HA*	This study
p181*cka2-K79A-HA*	*ori* AMP^R	2μ *LEU2*	*cka2-K79A-HA*	This study
p33*MYO5*	*ori* AMP^R	*CEN4* *URA3*	*MYO5*	(Grotsch et al., 2010)
p33*myc-MYO5*	*ori* AMP^R	*CEN4* *URA3*	*myc-MYO5*	(Grotsch et al., 2010)
p33*myc-myo5-S1205C*	*ori* AMP^R	*CEN4* *URA3*	*myc-myo5-S1205C*	This study
p33*myc-myo5-S1205D*	*ori* AMP^R	*CEN4* *URA3*	*myc-myo5-S1205D*	This study
p33*GFP-MYO5*	*ori* AMP^R	*CEN4* *URA3*	*GFP-MYO5*	(Grotsch et al., 2010)
p33*GFP-myo5-S1205D*	*ori* AMP^R	*CEN4* *LEU2*	*GFP-myo5-S1205D*	This study
p33*GFP-myo5-S1205C*	*ori* AMP^R	*CEN4* *LEU2*	*GFP-myo5-S1205D*	This study
p111*SLA1*	*ori* AMP^R	*CEN4* *LEU2*	*SLA1*	H. Grötsch

p111*SLA1-HA*	*ori*	AMP^R	*CEN4*	*LEU2*	*SLA1-HA*	(Idrissi et al., 2008)
p111*VRP1-HA*	*ori*	AMP^R	*CEN4*	*LEU2*	*VRP1-HA*	M. I. Geli
p195*PAN1-HA*	*ori*	AMP^R	*CEN4*	*URA3*	*PAN1-HA*	M. I. Geli
p111*sla1-SH3(1,2)Δ-HA*	*ori*	AMP^R	*CEN4*	*LEU2*	*sla1-HA* (aa 131-1244)	This study
p33*ProtA-MYO5*	*ori*	AMP^R	*CEN4*	*URA3*	ProtA-*MYO5*	(Grotsch et al., 2010)
p33*ProtA-myo5-CextΔ*	*ori*	AMP^R	*CEN4*	*URA3*	ProtA-*myo5* (aa 1- 996)	(Grotsch et al., 2010)
pSH18-34	*ori*	AMP^R	*2μ*	*URA3*	8 lexA Op. lacZ	(Gyuris et al., 1993)
pLexA-BCD1	*ori*	AMP^R	*2μ*	*HIS3*	LexA-*BCD1*	(Gyuris et al., 1993)
pLexA	*ori*	AMP^R	*2μ*	*HIS3*	LexA	(Gyuris et al., 1993)
pLexA -MYO5-C_{ext}	*ori*	AMP^R	*2μ*	*HIS3*	LexA-*myo5* (aa 984-1219)	(Geli et al., 2000)
pLexA -MYO5-C_{ext}-S1205C	*ori*	AMP^R	*2μ*	*HIS3*	LexA-*myo5* (aa 984-1219)	This study
pLexA -MYO5-C_{ext}-S1205D	*ori*	AMP^R	*2μ*	*HIS3*	LexA-*myo5* (aa 984-1219)	This study
pLexA -MYO5$_{SH3.TH2c.A}$	*ori*	AMP^R	*2μ*	*HIS3*	LexA-*myo5* (aa 1085-1219)	(Geli et al., 2000)
pLexA -MYO5$_{TH2c.A}$	*ori*	AMP^R	*2μ*	*HIS3*	LexA-*myo5* (aa 1142-1219)	(Geli et al., 2000)
pLexA -MYO5$_{TH2n}$	*ori*	AMP^R	*2μ*	*HIS3*	LexA-*myo5* (aa 984-1091)	(Geli et al., 2000)
pLexA -MYO5$_{SH3}$	*ori*	AMP^R	*2μ*	*HIS3*	LexA-*myo5* (aa 1085-1181)	(Geli et al., 2000)
pLexA -MYO5$_{TH2n.SH3}$	*ori*	AMP^R	*2μ*	*HIS3*	LexA-*myo5* (aa 984-1181)	(Geli et al., 2000)
pLexA -MYO5$_{TH2.A}$	*ori*	AMP^R	*2μ*	*HIS3*	LexA-*myo5* (aa 984-1091)+(aa1142-1219)	(Geli et al., 2000)
pLexA -MYO5$_{SH3\ (W1123S).TH2c}$	*ori*	AMP^R	*2μ*	*HIS3*	LexA-*myo5* (aa 1085-1219), W1123S	(Geli et al., 2000)
pB42	*ori*	AMP^R	*2μ*	*TRP1*	B42	(Gyuris et al., 1993)
pB42-SLA1	*ori*	AMP^R	*2μ*	*TRP1*	B42-*HA-SLA1*	M. I. Geli
pB42-SLA1$_{SH3(1,2).P.SH3(3)}$	*ori*	AMP^R	*2μ*	*TRP1*	B42- *HA -sla1* (aa 1-418)	F. Idrissi
pB42-SLA1$_{SH3(1,2).P}$	*ori*	AMP^R	*2μ*	*TRP1*	B42- *HA -sla1* (aa 1-357)	F. Idrissi
pB42-SLA1$_{SH3(1,2)}$	*ori*	AMP^R	*2μ*	*TRP1*	B42- *HA -sla1* (aa 1-136)	F. Idrissi
pB42-SLA1$_{SH3(1)}$	*ori*	AMP^R	*2μ*	*TRP1*	B42- *HA -sla1* (aa 1-75)	F. Idrissi
pB42-SLA1$_{SH3(2).P.SH3(3)}$	*ori*	AMP^R	*2μ*	*TRP1*	B42- *HA -sla1* (aa 69-418)	F. Idrissi
pB42-SLA1$_{P.SH3(3)}$	*ori*	AMP^R	*2μ*	*TRP1*	B42- *HA -sla1* (aa 131-418)	F. Idrissi
pB42-SLA1$_{SH3(3)}$	*ori*	AMP^R	*2μ*	*TRP1*	B42- *HA -sla1* (aa 350-418)	F. Idrissi
pB42-SLA1$_{SH3(2)}$	*ori*	AMP^R	*2μ*	*TRP1*	B42- *HA -sla1* (aa 69-136)	F. Idrissi
pB42-SLA1$_{P}$	*ori*	AMP^R	*2μ*	*TRP1*	B42- *HA -sla1* (aa 131-357)	F. Idrissi
pB42-ARC40	*ori*	AMP^R	*2μ*	*TRP1*	B42- *HA –ARC40*	M. I. Geli
pB42-VRP1	*ori*	AMP^R	*2μ*	*TRP1*	B42- *HA –VRP1*	M. I. Geli

p33*myc-myo5-S1205C* and p33*myc-myo5-S1205D*

p33*myc-myo5-S1205C* and p33*myc-myo5-S1205D* were obtained by site-directed mutagenesis using the overlap extension PCR technique. In a first step, two PCR fragments (A and B) containing the S1205C or S1205D mutation were obtained using p33*MYO5* as template and the primers listed below. The two DNA products were then used as template in a second round of PCR with the flanking primers Myo5.2746D and Myo5T.U to generate the mutated *myo5* fragment. The obtained DNA fragment was digested with *Bst*EII and *Sph*I and ligated into the *Bst*EII/*Sph*I digested p33*myc-MYO5*. The mutations were confirmed by sequencing.

First step	Primers (A)	Primers (B)
S1205C	Myo5.2746D, Myo5-S1205C-3626U	Myo5-S1205C-3594D, Myo5T.U
S1205D	Myo5.2746D, Myo5-S1205D-3626U	Myo5-S1205D-3594D, Myo5T.U

Second step	Primers
	Myo5.2746D, Myo5T.U

p181*cka2-K79A*

Site-directed mutagenesis by the overlap extension PCR technique was also used to construct p181*cka2-K79A*. In the first step, two PCR fragments (A and B) containing the K79A mutation were obtained using p111*CKA2* as template and the primers Cka2.-498D.HindIII and Cka2.K79A.U (to obtain the fragment A) and Cka2.1220U.EcoRI and Cka2.K79A.D (to obtain the fragment B). The two DNA products were then used as template in a second round of PCR with the flanking primers Cka2.-498D.HindIII and Cka2.1220U.EcoRI to generate the mutated *cka2* fragment. The obtained DNA fragment was digested with *Hind*III and *EcoR*I and ligated into the *Hind*III/*EcoR*I digested YEplac181. The mutation was confirmed by sequencing.

pGST-Myo5-C_{ext}-S1205C and pGST-Myo5-C_{ext}-S1205D

pGST-Myo5-C_{ext}-S1205C and pGST-Myo5-C_{ext}-S1205D were constructed following the strategy used for pGST-*MYO5-C_{ext}* (pGST-(TH2,SH3) from Geli et al, 2000). DNA fragments containing the TH2, SH3 and AS domains (aa 984 to 1219) of *myo5* mutants bearing either the S1205C or S1205D mutation were amplified by PCR using p33*myc-myo5-S1205C* and p33*myc-myo5-S1205D* as templates and primers Myo5.GST.2937.D and Myo5T.U. These fragments were digested with *BamH*I and *Xho*I and ligated into the *BamH*I/*Xho*I digested pGEX-5X-3.

pLexA-MYO5-C_{ext}-S1205C and pLexA-MYO5-C_{ext}-S1205D

pLexA-MYO5-C_{ext}-S1205C and pLexA-MYO5-C_{ext}-S1205D were constructed following the strategy used for pEG202-*MYO5-C_{ext}* (pEG202*(TH2,SH3)* from Geli et al, 2000). DNA fragments containing the TH2, SH3 and Acidic domains (aa 984 to 1219) of *myo5* mutants bearing either the S1205C or S1205D mutation were amplified by PCR using p33*myc-myo5-S1205C* and p33*myc-myo5-S1205D* as templates and primers Myo5.2948D and Myo5T.U. These fragments were digested with *BamH*I and *Xho*I and ligated into the *BamH*I/*Xho*I digested pEG202.

p33*GFP-myo5-S1205C* and p33*GFP-myo5-S1205D*

A fragment containing 203 nucleotides upstream of the START (ATG) codon followed by GFP and 2873 of the *MYO5* gene was generated by digesting the p33*GFP-MYO5* with *SnaB*I and *BstE*II. This DNA fragment was ligated into the *SnaBI/BstE*II digested p33*myc-myo5.S1205C* and p33*myc-myo5.S1205D* to generate p33*GFP-myo5.S1205C* and p33*GFP-myo5.S1205D*, respectively.

p111*CKA1*, p111*CKA2*, p181*CKA1*, p181*CKA2*, p111*STE2*, and p181*STE2*

p111*CKA1* and p181*CKA1* were constructed by amplifying the *CKA1* gene by PCR using the primers Cka1.-498D.HindIII and Cka1.1317U.EcoRI and genomic DNA from a wild type strain as template. The fragment was digested with *Hind*III and *EcoR*I and ligated into the *Hind*III/*EcoR*I digested YCplac111 or YEplac181, respectively. The same strategy was used to generate the p111*CKA2* and p181*CKA2*, but in this case, primers Cka2.-498D.HindIII and Cka2.1220U.EcoRI were used to amplify the *CKA2* gene.

p111*STE2* and p181*STE2* were obtained following the same approach as p111CKA1, p111CKA2, p181CKA1, and p181CKA2, but using primers Ste2.-480D.BamHI and Ste2.1810U.EcoRI. The amplified *STE2* gene was digested with *BamH*I and *EcoR*I, and ligated into the *BamH*I/*EcoR*I digested YCplac111 and YEplac181 plasmids.

p111*STE2-GFP*, p181*CKA1-HA*, p181*CKA2-HA,* and p181*cka2-K79A-HA*

A DNA fragment coding for GFP was inserted downstream of *STE2* by recombination in yeast. The GFP-fragment was amplified by PCR with primers Ste2.R1 and Ste2.F2, and pFA6a-GFP(S65T)-His3MX6 as template. The amplified fragment was then co-transformed in yeast with p111*STE2* and transformants selected on SDC-Leu-His. Plasmid was recovered and successful recombination was tested by restriction analysis.

A DNA fragment coding for 3-HA was inserted downstream of *CKA1*, *CKA2*, and *cka2-K79A* by homologous recombination in yeast. The HA-fragment was amplified by PCR with either primers Cka1.1079.F2 and Cka1.1159.R1 or Cka2.980.F2 and Cka2.1060.R1 and pFA6a-3HA-His3MX6 as template. The amplified fragment was then co-transformed in yeast with either p181*CKA1*, p181*CKA2,* or p181*cka2-K79A* and transformants were selected on SDC-Leu-His. Plasmids were recovered and successful recombination tested by restriction analysis.

p*CKA2.leu2Δ::URA,* p*sla1-SH3(1,2)Δ-HA*

p*CKA2.leu2Δ::URA3* was constructed by substituting the *LEU2* marker of the p*CKA2* plasmid (kindly provided by Dr. C.V. Glover) by *URA3* by homologous recombination in yeast. The *URA3* gene was amplified by PCR using the YDp-U plasmid as a template and primers Leu2.YDp.D and Leu2.YDp.U. The amplified fragment was then co-transformed in yeast with the p*CKA2* plasmid

and transformants selected on SDC-Ura. Plasmids were recovered and successful substitution of the marker tested by restriction analysis.

Homologous recombination in yeast was also used to construct the p*sla1-SH3(1,2)Δ-HA*. A PCR fragment containing 36 nucleotides upstream of the START (ATG) codon followed by a fragment of the *SLA1* gene missing the first 390 nucleotides (corresponding to amino acids 1 to 130) was amplified by PCR using the p111*SLA1* plasmid as template and primers Sla1.-36.ATG.391D and Sla1.2570U. The amplified fragment was co-transformed in yeast with the p111*SLA1-HA* fragment previously digested with *Msc*I and *Apa*I and transformants selected on SDC-Leu. Plasmids were recovered and successful recombination tested by restriction analysis.

pJG4-5*SLA1*

DNA fragments containing the ORF of *SLA1* was amplified by PCR using p111*SLA1* as template and primers Sla1.1D.SmaI and Sla1.3735.XhoI. These fragments were digested with *Sma*I and *Xho*I. pJG4-5 was digested with EcoRI and the 5' overhangs were filled in by using the Klenow DNA polymerase fragment, yielding a blunt ended DNA. Subsequently, the linearized plasmid was digested with XhoI and the SmaI/XhoI digested PCR fragments were ligated into it.

6.3.4. Primers

Primers used in this study are listed in Table III.

Table III. Primers
The sequences of the primers are written from the 5' to the 3' end. Primers amplifying the coding strand are named 5' primers, primers amplifying the complementary strand are 3' primers. Restriction sites are underlined. Mutated codon sites are shown in bold characters.

Name	Sequence	Restriction site	Direction
Cka1.20.YDp.D	GGAATATTTGATTCGAACTATGAAATGCAGGGTATGGTCGAATTCCCGG GGATCCGG		5'
Cka1.1080.YDp.U	CTTATTTTTCAATTTGTTCCCTTATTGGGGCAACCACGGGTGCAGGTCG ACGGATCCGG		3'
Cka1.-498D.HindIII	AAGGAAAAGCTTTAATTTGGGTTCCTTAATTGAGG	*Hind*III	5'
Cka1.1317U.EcoRI	AAGGAAGAATTCATTTTGCATGTATGAAATTTGCT	*Eco*RI	3'
Cka1.1079.F2	ACACCCGTGGTTTGCCCCAATAAGGGAACAAATTGAAAAA CGGATCCCCGGGTTAATTAA		5'
Cka1.1159.R1	CAGTGATTTTTTTTTTTTTATTTCATTCATTATTTATTTC GAATTCGAGCTCGTTTAAAC		3'
Cka2.28.YDp.D	GAAGAAACAGAATGCAATTACCTCCGTCAACATTGAACCGAATTCCCGG GGATCCGG		5'
Cka2.1002.YDp.U	GCTAAGAGTATTGTTGTCCAATTATTCAAACTTCGTTTTGTGCAGGTCGA CGGATCCGG		3'
Cka2.-498D.HindIII	AAGGAAAAGCTTTGTCCCCTCAACTCTGAAGTTGA	*Hind*III	5'
Cka2.1220U.EcoRI	AAGGAAGAATTCCGGAAGGCTCTTATATCTATATA	*Eco*RI	3'
Cka2.980.F2	GGAGGCTATGGATCATAAGTTTTTCAAAACGAAGTTTGAA CGGATCCCCGGGTTAATTAA		5'
Cka2.1060.R1	GTGGAAAAAGAATTGCCTTGCTAAGAGTATTGTTGTCCAA GAATTCGAGCTCGTTTAAAC		3'

Cka2.K79A.D	CAGAAGTGTGTTATT**GCA**GTTTTAAAACCAGTTAAAATG		5’
Cka2.K79A.U	CATTTTAACTGGTTTTAAAAC**TGC**AATAACACACTTCTG		3’
Las17.1530D.F2	CAACAACCTCAATCTGGAGGAGCTCCAGCTCCACCCCCACCTCCTCAA ATG CGGATCCCCGGGTTAATTAA		5’
Las17.1899U.R1	CCAATCATCACCATTGTCCATATCGTCATGAGCTCCCACT GAATTCGAGCTCGTTTAAAC		3’
Leu2.YDp.D	ATATATATATTTCAAGGATATACCATTCTAGAATTCCCGGGGATCCGG		5’
Leu2.YDp.U	GTACAAATATCATAAAAAAAGAGAATCTTTTTGGCTGCAGGTCGACGG		3’
Myo5.2746D	TAGGCTCGGCGATAGAGTACC		5’
Myo5.2948D	AAGGAAGGAAGGATCCCCTCGCAAGCAACGAGGAG		5’
Myo5-S1205C-3594D	CAATAAAATGAGATTAGAG**TGT**GATGACGAGGA		5’
Myo5-S1205C-3626U	TCCTCGTCATC**ACA**CTCTAATCTCATTTTATTG		3’
Myo5-S1205D-3594D	CAATAAAATGAGATTAGAG**GAT**GATGACGAGGA		5’
Myo5-S1205D-3626U	TCCTCGTCATC**ATC**CTCTAATCTCATTTTATTG		3’
Myo5.GST.2937D	ACACACACACGGATCCCCAGTTCCTCGCAAGCAAC	*BamH*I	5’
Myo5T.U	AAGGAAGGAACTCGAGACCATGATTACGCCAAGCTTGC	*Xho*I	3’
Sla1.-36.ATG.391D	GGCGACAGAGTGTGTTATATACAAAAGAGCTAGAGTATGAATGGGTCCA CTTCC		5’
Sla1.2570U	TTGAATGGATCCAATGGAGCG		3’
Sla1.3695D.F2	CAACATATTCAATGCTACTGCATCAAATCCGTTTGGATTCTAG CGGATCCCCGGGTTAATTAA		5’
Sla1.3775U.R1	GTTTTAGTTATTATCCTATAAAATCTTAAAATACATTAA GAATTCGAGCTCGTTTAAAC		3’
Sla1.1D.SmaI	AACCAACCCGGGAATGACTGTGTTTCTGGGCATC	*SmaI*	5’
Sla1.3735.XhoI	AACCAACTCGAGCTAGAATCCAAACGGATTTGATGC	*XhoI*	3’
Ste2.1810U.EcoRI	AACCAACCGAATTCGCCAAACAGCGTACCTTTAGACACGTGGGATGG	*EcoR*I	3’
Ste2.-480D.BamHI	AACCAACCGGATCCGCCTGCCAAAATGCATTGTCACACGCTGTAGTGC	*BamH*I	5’
Ste2.F2	AGAAAGTTCTGGACTGAAGATAATAATAATTTA CGGATCCCCGGGTTAATTAA		5’
Ste2.R1	ACGAAATTACTTTTTCAAAGCCGTAAATTTTGA GAATTCGAGCTCGTTTAAAC		3’

6.4. Biochemistry techniques

6.4.1. SDS-PAGE, immunoblots, and antibodies

SDS-PAGE was performed as described (Laemmli, 1970) using a Minigel system (Bio-Rad Laboratories). High and low range SDS-PAGE molecular weight standards (Bio-Rad Laboratories) were used for determination of apparent molecular weights. Coomassie Brilliant Blue or Colloidal Brilliant Blue G staining (Sigma) was used for detection of total protein on Acrylamide gels. Protein concentration was determined with a Bio-Rad Protein assay (Bio-Rad).

Immunoblots were performed as described (Geli et al., 1998). Nitrocellulose membranes (Schleicher and Schuell) were stained with Ponceau Red for detection of total protein. 3% Not

Fat Lyophilized Milk with 0.1% (v/v) Nonidet P-40 in PBS buffer (137 mM NaCl, 2.7 mM KCl, 10 mM Na_2HPO_4, 2 mM KH_2PO_4) was used as blocking solution. For detection of peroxidase-conjugated antibodies, an enhanced chemoluminiscence (ECL) detection kit (Amersham Biosciences) was used.

The primary and secondary antibodies used for detection of proteins are listed in Table IV.

Table IV. Antibodies

Antigen	Source	Dilution	Reference
MYC	Rabbit polyclonal antibody, peroxidase conjugated	1:2000	Sigma
HA	Mouse monoclonal antibody (clone HA-7), peroxidase conjugated	1:1000	Sigma
Peroxidase	Rabbit antibody, peroxidase conjugated, peroxidase complex (PAP)	1:1000	DAKO
Act1	Rat monoclonal antibody (clone MAC 237)	1:1000	Abcam
Myo5	Rabbit serum (EW)	1:1000	(Geli et al., 1998)
Myo5	Rabbit serum (IK)	1:1000	(Geli et al., 1998)
Gas1	Rabbit serum	1:50000	(Muniz et al., 2001)
Hxk1	Rabbit serum	1:2000	(van Tuinen and Riezman, 1987)
CPY	Rabbit serum	1:500	(Geli and Riezman, 1996)
Rabbit IgG	Goat antibody, peroxidase conjugated	1:8000	Sigma
Rat IgG	Goat antibody, peroxidase conjugated	1:5000	Sigma

6.4.2. Protein extraction from yeast

6.4.2.1. Quick yeast protein extract

Approximately 2-4 x 10^8 cells were harvested (at a culture density of 1-2 x 10^7 cells/ml), transferred to a 1.5 ml Eppendorf tube, and washed twice with 1 ml of IP buffer (50 mM Tris pH 7.5, 150 mM NaCl, 5 mM EDTA). Harvested cells were frozen at -20ºC. After thawing, the pellet was suspended in 100 μl of ice-cold IP buffer containing protease inhibitors (0.5 mM PMSF, 1 μg/ml aprotinin, 1 μg/ml antipain, 1 μg/ml leupeptin, 1 μg/ml pepstatin) and glass bead lysed for 15 min at 4ºC. The lysate was resuspended in 100 μl of IP2T buffer (IP buffer + 2% Triton) with protease inhibitors, and transferred to another tube. Unbroken cells and debris were eliminated by centrifugation at 13.000 g for 10 min at 4ºC. Total protein concentration was determined before boiling the cells extracts in Laemmli sample buffer (final concentration 1% SDS, 100 mM DTT, 10% glycerol, 60 mM Tris-HCl pH 6.8, Bromophenol blue) to be analyzed by SDS-PAGE.

6.4.2.2. Low speed pelleted (LSP) yeast protein extract

Low speed pelleted (LSP) yeast extracts were prepared as follows: approximately 4 x 10^9 cells were harvested (at a culture density of 1.5 x 10^7 cells/ml) and washed twice with XB (10 mM

Hepes pH 7.7, 100 mM KCl, 2 mM $MgCl_2$, 0.1 mM $CaCl_2$, 5 mM EGTA, 1 mM DTT, 1 mM ATP K^+ salt) 50 mM sucrose, and finally frozen at -20ºC. After thawing, one-tenth volume of ice-cold XB 50 mM sucrose containing protease inhibitors (0.5 mM PMSF, 1 μg/ml aprotinin, 1 μg/ml antipain, 1 μg/ml leupeptin, 1 μg/ml pepstatin) was added for each gram of pellet, and cells were glass bead-lysed (10 x 1 min) on ice. Samples were centrifuged at 2.500 g at 4°C and the supernatant was clarified at 13,000 g for 10 min. Protein and sucrose concentrations were adjusted to 20 μg/μl and 200 mM, respectively. Extracts were frozen in liquid N_2 and stored at –80°C until use in phosphorylation experiments or actin polymerization assays.

The LSP yeast extracts used for the pharmacological analysis of the *in vitro* actin polymerization assay (performed by Dr. Bianka Grosshans, section 2.1.2 and Figure 31) were equally prepared except that the following kinase or phosphatase inhibitors were added to the extracts at the following final concentrations: 10 mM sodium pyrophosphate, 10 mM NaN_3, 10 mM NaF, 0.4 mM EDTA, 0.4 mM $NaVO_3$, 0.4 mM Na_3VO_4, 2 μM cyclosporin A and 0.5 μM okadaic acid (phosphatase inhibitors), or 4 μM K252A and 1mM A3 (kinase inhibitors).

6.4.3. Protein purification

6.4.3.1. Purification of HA-tagged and ProtA-tagged proteins from yeast by affinity chromatography

For purification of HA-tagged proteins from yeast, agarose conjugated to a mouse anti-HA antibody (Sigma) was used. Approximately 4 x 10^9 yeast cells expressing HA-tagged protein of interest were harvested at a culture density of 1.5 x 10^7 cells/ml, washed twice with IP buffer (50 mM Tris pH 7.5, 150 mM NaCl, 5 mM EDTA), and frozen at -20ºC. After thawing, cells were resuspended in 100 μl of ice-cold IP buffer containing protease inhibitors (0.5 mM PMSF, 1 μg/ml aprotinin, 1 μg/ml antipain, 1 μg/ml leupeptin, 1 μg/ml pepstatin) and glass bead-lysed (10 x 1 min) on ice. Triton-X100 and NaCl were adjusted to 1% and 0.5 M, respectively, and the extract was then centrifuged twice at 13,000 g to eliminate unbroken cells and cell debris. The total protein extract was resuspended in 1 ml of IPTN (IP buffer containing protease inhibitors, 1% Triton-X100, and 0.5 M NaCl), transferred into a siliconized tube, and incubated with 40 μl of 50% anti-HA agarose equilibrated in IP buffer, for 2h in a turning wheel at 4ºC. The agarose beads were collected on Mobicol columns bearing 35 μm pore filters (MoBiTec), washed 3 times with IPTN, and twice with IP buffer. Proteins were then eluted from the anti-HA agarose by adding 20 μl EB buffer (0.5 M acetic acid pH 3.4 adjusted with ammonium acetate, 0.5 M NaCl, 0.1% Tween) and rapidly neutralized with 10 μl 1 M Tris pH 9.0. Purified tagged proteins were used for pull down assays (see section 6.4.4.1.)

For purification of ProtA-tagged Myo5 from yeast for mass spectrometry analysis, IgG-Sepharose 6 Fast Flow (GE Healthcare) was used. Approximately 4 x 10^9 yeast cells expressing ProA-tagged Myo5 were harvested at a culture density of 1.5 x 10^7 cells/ml, washed twice with IP buffer (50 mM Tris pH 7.5, 150 mM NaCl, 5 mM EDTA), and frozen at -20ºC. After thawing, cells were resuspended in 1150 μl of ice-cold IP buffer containing protease inhibitors (0.5 mM

PMSF, 1 μg/ml aprotinin, 1 μg/ml antipain, 1 μg/ml leupeptin, 1 μg/ml pepstatin) and phosphatase inhibitors (5 mM NaF, and 1 mM Na_3VO_4), and glass bead-lysed (10 x 1 min) on ice. Triton-X100 and NaCl were adjusted to 1% and 0.5 M, respectively, and the extract was then centrifuged twice at 13,000 g to eliminate unbroken cells and cell debris. The total protein extract was resuspended in 1 ml of IPTN (IP buffer containing protease inhibitors, phosphatase inhibitors, 1% Triton-X100, and 1 M NaCl), transferred into a siliconized tube, and incubated with 40 μl of 50% IgG-Sepharose 6 Fast Flow (equilibrated following the manufacturer instructions) for 1h in a turning wheel at 4ºC. The Sepharose beads were collected on Mobicol columns bearing 35 μm pore filters (MoBiTec), washed 3 times with IPTN, and 2 times with IP buffer. Proteins were then eluted from the Sepharose by adding 40 μl of Laemmli sample buffer (1% SDS, 100 mM DTT, 10% glycerol, 60 mM Tris-HCl pH 6.8, Bromophenol blue). Elutions were subjected to SDS-PAGE, proteins detected by Colloidal Brilliant Blue G staining (Sigma), and the gel region corresponding to purified ProtA-Myo5 sent to Dr. Judit Villén (Steve Gygi lab, Harvard Medical School, Boston) for mass spectrometric analysis.

6.4.3.2. Purification of recombinant GST-fusion proteins from *E. coli* by affinity chromatography

Recombinant glutathione-S-transferase-tagged proteins (GST-fusion proteins) were purified from BL21 *E. coli* cells according to (Geli et al., 2000). Briefly, 1/100 of an overnight *E. coli* culture was inoculated into minimal media (see section 6.1.1) containing 50 mg/l ampicillin. The culture was grown at 37 °C to an OD_{600} of 0.4. Cells were shifted to 24°C and induced at an OD_{600} of 0.7-0.8 with 0.1 mM isopropyl-β-D-thiogalactopyranoside (IPTG) for 2 hrs. Cells were harvested and frozen at –20°C.

For protein purification, cells were thawed in PBST buffer (137 mM NaCl, 2.7 mM KCl, 10 mM Na_2HPO_4, 2 mM KH_2PO_4, 0.5% Tween; 25 ml buffer for each L culture of bacteria) and lysed by sonication (10 pulses of x 30 seconds at 30 second intervals and amplitude of 30%) in the presence of protease inhibitors (1 tablet cOmplete Protease Inhibitor Cocktail Tablets (Roche)/50 ml of buffer). Cell debris was pelleted by centrifugation. Depending on whether GST-fusion proteins were subjected to pull down, used for the *in vitro* visual actin polymerization assay, or *in vitro* phosphorylation assays, GST-fusion protein purification was performed as follows:

- For pull down assays, 25 μl of glutathione-Sepharose beads (Amersham Biosciences) equilibrated in PBST were added to the protein extracts obtained from a culture of 100 ml of *E.coli* transformed with pGST, or a culture of 1 L of cells transformed with pGST-Myo5-C_{ext}, pGST-Myo5-C_{ext}-S1205C or pGST-Myo5-C_{ext}-S1205D cultures, and incubated for 2 h shaking at 4°C. Beads were recovered by using Econo Columns (Bio-Rad Laboratories), washed 3 times with 10 ml of PBST, 2 times with 10 ml of PBS, and equilibrated and adjusted to 50% in the buffer used for the binding experiment: XB200 buffer (10 mM Hepes pH 7.7, 100 mM KCl, 2 mM $MgCl_2$, 0.1 mM $CaCl_2$, 5 mM EGTA, 1 mM DTT, 1 mM ATP K^+ salt, 200 mM sucrose) when total

yeast extracts were used, or TBST (10 mM Tris pH 8.0, 150 mM NaCl) for the pull down of purified components.

- For the visual actin polymerization assay, 15 μl of glutathione-Sepharose beads (Amersham Biosciences) equilibrated in PBST were added to the protein extracts obtained from a culture of 1 L of cells transformed with pGST-Myo5-C_{ext}, pGST-Myo5-C_{ext}-S1205C or pGST-Myo5-C_{ext}-S1205D cultures, and incubated for 2 h shaking at 4°C. Beads were recovered by using Econo Columns (Bio-Rad Laboratories), washed 3 times with 10 ml of PBST, 2 times with 10 ml of PBS, and equilibrated and adjusted to 50% in XB200 buffer (10 mM Hepes pH 7.7, 100 mM KCl, 2 mM $MgCl_2$, 0.1 mM $CaCl_2$, 5 mM EGTA, 1 mM DTT, 1 mM ATP K^+ salt, 200 mM sucrose).

- For the *in vitro* phosphorylations assays, 50 μl of glutathione-Sepharose beads (Amersham Biosciences) equilibrated in PBST were added to the protein extracts obtained from 1 L of BL21 cells transformed with pGST-Myo5-C_{ext} or pGST-Myo5-C_{ext}-S1205C, and incubated for 2 hrs shaking at 4°C. Beads were recovered by using Econo Columns (Bio-Rad Laboratories), washed 3 times with 10 ml of PBST, 2 times with 10 ml of PBS, and equilibrated and adjusted to 50% in XB200 buffer (10 mM Hepes pH 7.7, 100 mM KCl, 2 mM $MgCl_2$, 0.1 mM $CaCl_2$, 5 mM EGTA, 1 mM DTT, 1 mM ATP K^+ salt, 200 mM sucrose).

6.4.3.3. Purification of ^{35}S-radiolabelled α-factor by ion exchange chromatography

The purification of ^{35}S-radiolabelled α-factor was performed according to (Dulic et al., 1991). The α-factor was overproduced in a *MAT*α strain (RH449) bearing a 2μ plasmid that carries the gene encoding the prepro-α-factor (*MFα1*, pDA6300) and the protease required for its processing (*STE13*). Cells were grown in freshly made SDC-Leu to a culture density of 0.5 x 10^7 cells/ml. 4 x 10^7 cells were harvested, washed twice with double distilled sterile water, resuspended in 25 ml of freshly prepared SD-Leu-SO_4^{2-} (see section 6.1.2.), and incubated for 30 min at 30ºC in a 500 ml siliconized Erlenmeyer. Cells were then metabolically labelled with 25 mCi $^{35}SO_4^{2-}$ and incubated for 4 more hours at 30ºC. Cells were separated from the supernatant by centrifugation at 2500 g and the supernatant was collected. 25 μl of 0.2 M EDTA, 10 mg of TAME (N-tosyl-L-Arginine-methylesterhydrocloride) and 1.75 μl of 2-β-mercaptoethanol was added to the supernatant, which was carefully transferred to a mild cationic exchange column. Preparation of the resin was accomplished as follows: 2.5 ml of Amberlite CG-50 (Sigma) was swollen with 20 ml of a buffer composed of 3 N HCl, 1 mM 2–β–mercaptoethanol, washed twice with 20 ml of double-distilled sterile water, washed with 20 ml of elution buffer (0.01 N HCl, 80% ethanol, 1 mM 2-β-mercaptoethanol) and finally, 20 ml of equilibration buffer (0.1 M HAc, 1 mM 2-β-mercaptoethanol) was added to transfer the resin into a siliconized Econo column (Bio-Rad Laboratories) to a final bed volume of 3.5 ml. After pouring the supernatant into de exchange column, washing buffer was added (50% ethanol, 1 mM 2–β–mercaptoethanol) to approximately 25 times the bed volume (80-100 ml). Elution buffer was then added to the column, fractions were collected on siliconized 1.5 ml Eppendorf tubes, and 1 μl of each fraction was measured in a β-counter (Beckman LS 6000 TA).

α-factor purification was examined by assaying the radioactive positive fractions for its ability to inhibit growth of a α-factor hypersensitive strain (*sst1 sst2*) (Halo assays, see section 6.2.3.3.3).

6.4.4. Analysis of protein-protein interactions

6.4.4.1. Pull down assays

In order to perform pull down assays from total yeast extracts, 70 µl of LSP yeast extracts (see section 6.4.2.2.) were placed in Mobicol tubes bearing 35 µm filters (MoBiTec) together with 12.5 µl of GST-Myo5-C_{ext}, GST-Myo5-C_{ext}-S1205C or GST-Myo5-C_{ext}-S1205D coated glutathione-Sepharose beads diluted to 50% in XB200 buffer (see section 6.4.3.2.). The tubes were incubated on ice for 7 min and the binding reactions were stopped by eluting the yeast extract and washing the beads with XB buffer without sucrose (10 mM Hepes pH 7.7, 100 mM KCl, 2 mM $MgCl_2$, 0.1 mM $CaCl_2$, 5 mM EGTA, 1 mM DTT, 1 mM ATP). 25 µl of Laemmli sample buffer (1% SDS, 100 mM DTT, 10% glycerol, 60 mM Tris-HCl pH 6.8, Bromophenol blue) was added; samples were boiled for 3 min and stored at -20ºC until analysis by SDS-PAGE and immunoblot.

For the pull down assay with purified components, 15 µl of GST-Myo5-C_{ext} or the equivalent amount of GST-coated glutathione-Sepharose beads diluted to 50% in TBST (10 mM Tris pH 8.0, 150 mM NaCl)(see section 6.4.3.2.) was incubated with 90 µl of eluted HA-tagged protein (see section 6.4.3.1) in a total volume of 1 ml of TBST-TB (10 mM Tris pH 8.0, 150 mM NaCl, 0.1% Tween-20, 1.5% BSA) in siliconized 1.5 ml Eppendorf tubes for 2h at 4ºC. Beads were collected, washed with TBS-TB and TBS-T (10 mM Tris pH 8.0, 150 mM NaCl, 0.1% Tween-20) and finally eluted in 25 µl of Laemmli sample buffer (1% SDS, 100 mM DTT, 10% glycerol, 60 mM Tris-HCl pH 6.8, Bromophenol blue).

6.4.4.2. Immunoprecipitation of proteins from yeast extracts

For the immunoprecipitations of myc- and HA-tagged proteins from different subcellular fractions, yeast protein extracts were obtained as described in section 6.7. After measuring protein concentration for each fraction, 400 µg of protein were mixed with 10 µl of anti-myc- or anti-HA-agarose in a final volume of 1 ml adjusted with IP buffer (50 mM Tris pH 7.5, 150 mM NaCl, 5 mM EDTA) with a final concentration of 1% Triton-X100 plus protein inhibitors (0.5 mM PMSF, 1 µg/ml aprotinin, 1 µg/ml antipain, 1 µg/ml leupeptin, 1 µg/ml pepstatin), and incubated for 2h at 4ºC in a turning wheel. The agarose beads were collected on Mobicol columns bearing 35 µm pore filters (MoBiTec), washed 3 times with IPTN (IP buffer, 1% Triton-X100, 0.5 M NaCl), and twice with IP buffer. Proteins were then eluted from the agarose by adding 50 µl of Laemmli sample buffer (1% SDS, 100 mM DTT, 10% glycerol, 60 mM Tris-HCl pH 6.8, Bromophenol blue). Elutions were stored at -20ºC until analysis by SDS-PAGE and immunoblot.

For immunoprecipitation of ProtA-tagged Myo5, the same procedure as the one explained in section 6.4.3.1 was followed, with three modifications: 1) the IPT buffer contained 0.5 M NaCl

instead of 1 M NaCl; 2) no phosphatase inhibitors were added to the yeast extract; and 3) ProtA-Myo5 was eluted from the Sepharose by adding 50 μl of Laemmli sample buffer, and elutions were stored at -20ºC until analysis by SDS-PAGE and immunoblot.

6.4.4.3. Yeast two hybrid assay

The Interaction Trap two-hybrid system was used (Gyuris et al., 1993). Plasmids pEG202, pJG4-5, pSH18-34 and the strain EGY48 were kindly provided by Dr. R. Brent (MGM, Boston). To measure β-galactosidase activity, EGY48 cells bearing the lexAop-lacZ reporter plasmid pSH18-34 were co-transformed with the appropriate pEG202 and pJG4-5 derived plasmids (see below) and selected in SDC-Ura-His-Trp. Co-transformants were grown in SDC-Ura-His-Trp plates containing 80 mg/L X-Gal (5-bromo-4-cloro-3-indolil-β-D-galactopiranoside, see section 1.2) for 2 days at 28ºC. For the induction of proteins under a *GAL1*-promoter, yeast cells were grown until early logarithmic phase ($D.O_{600}$~0.3) in synthetic raffinose minimal media (SRC). Then, galactose (Fluka) was added to a final concentration of 2% and cells were grown for 3 more hours.

Name	Promoter	Functional domains
pEG202	*ADH1* (full length, constitutive)	LexA (DNA-binding domain)
pJG4-5	*GAL1* (full length, inducible)	B42 (transcription activation domain) + SV40 nuclear localization signal+ HA-tag

When the quantitative two-hybrid method was used (Figure 41), induction of proteins under the *GAL1*-promoter was performed as explained in section 1.2, with the exception of the B42-Sla1 chimeric protein, which was not induced in order not to saturate the assay (see discussion). 1.5 x 10^6 co-transformants grown at a culture density of 1.5 x 10^7 cells/ml were mixed with 100 μl Y-PER protein extraction reagent (Thermo Scientific) and incubated 20 min at 30ºC with gentle shaking. 100 μl of MUGAL buffer (60 mM Na_2HPO_4, 40 mM NaH_2PO_4, 10 mM KCl, 1 mM $MgSO_4$, 0.3% β-mercaptoethanol and 0.62 mM 4-methylumbelliferyl-β-D-galactopyranoside) was added to the permeabilized cells, and plates were then read either in a Victor3 Wallac (Perkin Elmer Inc.) or FL800 (Bio-Tek) spectrofluorometer, at 340/60 nm excitation and 440/60 emission wavelengths. Fluorescence was recorded for 20 min (one measurement per min), and β-galactosidase activity values were calculated as the rate of increase in arbitrary fluorescence units along time using standard regression methods.

6.5. *In vitro* phosphorylation assays

Recombinant glutathione-S-transferase-tagged proteins (GST-fusion proteins) were purified as described above (section 6.4.3.2.). For *in vitro* phosphorylation with protein extracts, 10 μl of

GST-Myo5-C_{ext} or GST-Myo5-C_{ext}-S1205C coated glutathione-Sepharose beads were mixed with 10 μl empty glutathione-Sepharose beads. 28 μl LSP protein extract and 20 μCi γ-^{33}P-ATP (Amersham) were added and the reaction was allowed to proceed for 30 min at 24°C. The beads were washed 3 times with PBS containing protease inhibitors (0.5 mM PMSF, 1 μg/ml aprotinin, 1 μg/ml pepstatin, 1 μg/ml leupeptin, 1 μg/ml antipain) and finally boiled in 30 μl Laemmli sample buffer (1% SDS, 100 mM DTT, 10% glycerol, 60 mM Tris-HCl pH 6.8, Bromophenol blue). 15 μl were loaded on NuPAGE Bis-Tris 4-12% gradient gels. The *in vitro* phosphorylation assays performed by Dr. B. Grosshans (section 2.1.3, Figures 32 and 33) were equally made except that γ-^{32}P-ATP (Amersham) instead of γ-^{33}P-ATP was used.

6.6. *In vitro* actin polymerization assay

The *in vitro* actin polymerization assay was designed according to Ma *et al.*, 1998a and Ma *et al.*, 1998b. Briefly, 14 μl of LSP yeast extracts (see section 6.4.2.2) were mixed with 2 μl of ARS (10 mg/ml creatine kinase, 10 mM ATP, 10 mM $MgCl_2$, 400 mM creatine phosphate) and 2 μl of 10 μM rhodamine-actin (APHR-C, Cytoskeleton, Inc.) or unlabeled actin (APHL99-A, Cytoskeleton, Inc) from human platelet (non-muscle). The polymerization reaction was initiated by adding 2.5 μl of 50% coated glutathione-Sepharose beads (see section 6.4.3.2). Samples were incubated at room temperature (26°C) for 7 min and stopped by adding 5 μl of 16% methanol-free formaldehyde (Polyscience).

Samples were visualized after 10 min using an *AxioPhot* fluorescence microscope (Zeiss) or an E600 fluorescent microscope (Nikon) equipped with rhodamine and GFP filters and an Olympus DP72 camera. For quantification of the actin *foci* density, an area of 25 x 25 μm was defined and the patches were counted in at least 8 different randomly chosen beads. At least two independent experiments were performed per each sample. The average actin *foci* density was normalized with respect to the average density of actin *foci* generated on beads incubated with the wild type yeast extract.

When the actin polymerization assay was used to collect the components of actin *foci* for mass spectrometry analysis (performed by Dr. Maribel Geli, section 2.1.1.3 and Figure 30), the reaction was performed on Mobicol columns bearing 35 μm pore filters (MoBiTec) and scaled to a final volume of 100 μl. Samples were incubated at room temperature (26°C) for 15 min, yeast extract was discarded, and the glutathione-Sepharose covered beads were washed with XB buffer (10 mM Hepes pH 7.7, 100 mM KCl, 2 mM $MgCl_2$, 0.1 mM $CaCl_2$, 5 mM EGTA, 1 mM DTT, 1 mM ATP K^+ salt). Proteins were then eluted from the glutathione-Sepharose beads by adding XB containing increasing amounts of salt (200 to 400 mM KCl). The eluted fractions were precipitated with TCA 12.5%, boiled in 20 μl Laemmli sample buffer (1% SDS, 100 mM DTT, 10% glycerol, 60 mM Tris-HCl pH 6.8, Bromophenol blue), and stored at -20ºC until analysis by SDS-PAGE and mass spectrometry.

6.7. Subcellular fractionation

Subcellular fractionation was performed by differential centrifugation of yeast extracts. Briefly, 1.5 x 10^{10} yeast cells grown in the appropriate media (YPD or SDC when plasmid maintenance was required) were harvested at a culture density of 1.5 x 10^7 cells/ml, washed with IP buffer (50 mM Tris pH 7.5, 150 mM NaCl, 5 mM EDTA), and frozen at -20ºC. After thawing, 100 µl of ice-cold IP buffer in the presence of protease inhibitors (0.5 mM PMSF, 1 µg/ml aprotinin, 1 µg/ml antipain, 1 µg/ml leupeptin, 1 µg/ml pepstatin, and 0.8 mM Pefabloc) were added for each gram of pellet, and cells were subjected to glass bead lysis. About 300 µl of yeast extract were recovered, centrifuged at 300 g for 20 min at 4ºC to discard unbroken cells. The supernatant was then centrifuged 45 min at 700 g at 4ºC. A 100 µl aliquot of the 700 g supernatant was stored ($S_{0.7}$) and the rest was subsequently centrifuged at 13,000 g for 45 min at 4ºC. After centrifugation, of the 13,000 g pellet was resuspended with IP buffer bearing protease inhibitors to the same volumen of the supernatant, and a 100 µl aliquot of the supernatant (S_{13}) and the resuspended pellet (P_{13}) was stored. The rest of the S_{13} supernatant was transferred to a polyallomer tube (Beckman Coulter), and subjected to a new round of centrifugation for 1 hour at 100.000 g at 4ºC in a Optima™ TLX ultracentrifuge (Beckman Coulter). The 100,000 g pellet (P_{100}) volume was adjusted to that of the 100,000 g supernatant (S_{100}) with IP buffer containing protease inhibitors. Protein concentrations were determined, and extracts were mixed with Laemmli sample buffer (final concentration 1% SDS, 100 mM DTT, 10% glycerol, 60 mM Tris-HCl pH 6.8, Bromophenol blue) to be analyzed by SDS-PAGE.

When subcellular fractions were used for phosphorylation assays (see section 6.5), XB50 was used (10 mM Hepes pH 7.7, 100 mM KCl, 2 mM $MgCl_2$, 0.1 mM $CaCl_2$, 5 mM EGTA, 1 mM DTT, 1 mM ATP K^+ salt, 50 mM sucrose) instead of IP buffer. After the differential centrifugation steps were made, protein and sucrose concentration from S_{13} were adjusted to 20 µg/µl and 200 mM, respectively. The protein concentration of the other fractions was adjusted with equivalent volumes of the buffers used. Extracts were frozen in liquid N_2 and stored at –80ºC until use.

6.8. Live cell fluorescence imaging of yeast cells

Cells encoding GFP- or mCherry-tagged proteins were grown to a cell density of 0.75 x 10^7 cells/ml in the appropriate SDC media. The SDC media used for imaging was filtered or autoclaved at 116ºC to avoid quenching. Cells were harvested, diluted in 25 – 50 µl SCD-M media (SDC media, 20 mM $KiPO_4$, pH 6.5), and directed visualized on poly-lysine coated slides using an AF7000 fluorescence microscope (Leica) equipped with a TRICT-filter (excitation 515-560, LP590). Images were taken with a Hammamatsu Orca CCD digital camera.

For the time-lapse fluorescence microscopy cells were grown as described above but subsequently immobilized in 0.8% low-melt agarose (Bio-Rad) prepared in SDC-M medium. Cells were observed in a Perkin Elmer UltraView ERS Spinning-Disk microscope equipped with Argon (488, 514 nm), Argon/Krypton (568 nm) and HeNe (405, 440, 640 nm) lasers, a 405/488/568/640 Dichroic filter, and a 63x 1.4NA Oil DIC Plan-Apochromat objective. Collection

of images was performed with a Hamamatsu C9100-50 EMCCD camera. Time-lapse microscopy images were taken every 2 seconds using Volocity from Improvision (Perkin Elmer). All images were collected with identical sensitivity and exposure times of 650 ms, 450 ms and 1 s for GFP-Myo5, Abp1-RFP and Sla1-mCherry, respectively. Volocity files were converted to multi-tiff for imaging processing.

To examine the lifespan of GFP- and mCherry-tagged proteins at endocytic sites, minimum fluorescence intensity (background) and maximum fluorescence intensity fluorescence intensity were computed using Volocity from a cropped area of 0'68 μm^2 that comprise a cortical patch. Volocity files were then converted to cvs files (comma separated values) to perform calculations with Microsoft Excel. Briefly, the value resulting from subtracting the minimum fluorescence intensity from the maximum fluorescence intensity for each time point was used to obtain the Fluorescence Intensity (FI). The maximal fluorescence intensity within a given peak was the used to normalize and obtain the Relative Fluorescence Intensity (RFI). RFI was plotted against time and the lifespan of the endocytic protein was calculated as the time lapse during which the RFI was above 0.5. Only bright well defined endocytic patches were used for the analysis. No significant differences between the maximal fluorescence intensity of the endocytic patches analyzed was detected in the different mutants for a given protein. A minimum of 75 cortical patches were analyzed from a minimum of 20 different cells. Average lifespan, standard deviation, and p-values for the two-tailed Student's t-test were also calculated with Microsoft Excel. For analysis of arrival and departure times of GFP-Myo5 relative to Sla1-mCherry or Abp1-RFP, Relative Fluorescence Intensity (RFI) curves plotted against time (seconds) were calculated for each pair and the time point when Sla1-mCherry or Abp1-RFP reached RFI = 0.5 was subtracted from the time point when GFP-Myo5 reached RFI = 0.5 either before (arrival) or after (departure) the time point when Sla1-mCherry or Abp1-RFP reached RFI = 1.

6.9. *In vivo* protein transport assays

6.9.1. Ste2 internalization assays using ^{35}S-α-factor

6.9.1.1. Ligand-induced Ste2 internalization

The α-factor pheromone is a small peptide secreted by yeast cells of the mating type α (*MAT***α**). The peptide binds to a G-coupled receptor (Ste2) that is exclusively expressed in cells of the opposite mating type (*MAT***a** cells). After binding of the α-factor to its receptor the complex is rapidly internalized by endocytosis and is then transported to the vacuole for degradation. Based on the observation that the α–factor bound to its receptor on the cell surface -but not internalized α-factor- can be dissociated from the cells by a short incubation in an acidic buffer, a quantitative assay to monitor the internalization kinetics of [^{35}S] radiolabelled α-factor was developed by Dulic *et al*. (Dulic et al., 1991). Briefly, cells were grown to 0.5 - 1 x 10^7 cells/ml, harvested, resuspended at 5 x 10^8 cells/ml in pre-warmed YPD and incubated at the desired temperature for 10 min. Uptake was initiated by adding 10.000 dpm/ml of purified ^{35}S-α-factor. Samples were taken at the indicated time points into ice-cold pH 1 (50 mM sodium citrate) and

pH 6 (50 mM potassium phosphate) buffers. Cells were recovered by filtration onto GF/C filters (Whatman) and associated counts were measured in a β-counter (Beckman LS 6000 TA). Internalized counts were calculated by dividing pH 1 wash resistant (internal) by pH 6 wash resistant (total cell-bound) counts, per time point. In experiments in which *cka2Δ* strains were used, the low amounts of Ste2 observed in the surface of these mutants prompt us to transform the strains analyzed with the p181*STE2* plasmid to obtain surface expression of Ste2 similar to wild type cells. Uptake assays were performed at least three times and the mean and standard deviations calculated per time point.

6.9.1.2. Constitutive Ste2 internalization

To measure constitutive internalization of Ste2, cells were grown to 0.5 – 1 x 10^7 cells/ml, harvested and resuspended in fresh media at 0.5 x 10^7 cells/ml. Cycloheximide was added to 10 μg/ml and cells were incubated for 10 min to stop protein synthesis and to allow all Ste2 in transit to the plasma membrane to reach the cell surface (time point 0). 20 ml samples were taken at the indicated time points into pre-chilled tubes containing 1 ml of 20 x inhibitor media (YPD 200 mM NaN_3 and 200 mM NaF). Cells were harvested at 4ºC and resuspended in 0.5 ml of pre-chilled inhibitor media (YPD 10 mM NaN_3 and 10 mM NaF). To measure surface-exposed Ste2, 0.1 ml of each sample were incubated in the presence of 10,000 d.p.m. of ^{35}S-radiolabelled α-factor for one hour at RT. Cells were recovered by filtration onto GF/C filters (Whatman) and associated counts were measured in a β-counter (Beckman LS 6000 TA). Unspecific binding was monitored by performing replicas for each sample using isogenic α strains. Background was subtracted from each sample and the percentage of cell surface-exposed Ste2 was calculate with respect to time point 0 (10 min after addition of cycloheximide).

6.9.2. Maturation of Carboxypeptidase Y (CPY) assay

Carboxypeptidase Y is a vacuolar protease. It is synthesized on ER-bound ribosomes as an inactive glycosylated precursor (proCPY). From the ER, proCPY is transported to the Golgi, where its carbohydrate is further elaborated before delivery to the vacuole. At late endosomal compartments or upon arrival to the vacuole, proCPY is protealytically cleaved to produce its mature active form. The maturation of Carboxypeptidase Y assay was performed according to (Stevens et al., 1982). Briefly, yeast cells were grown at 24°C in SDYE media (see section 6.1.2.) to early log phase. 2.5 x 10^7 cells per time point were harvested and washed in SD media and finally resuspended at 2.5 x 10^7 cells/ml. Cells were then pulsed for 5 min with 100 μCi of ^{35}S-labeling mix (PRO-MIX™, Amersham Biosciences) per time point and chased by addition of 0.3% methionine, 0.3% cysteine, 300 mM $(NH_4)_2SO_4$. 2.5 x 10^7 cells per time point were harvested and glass bead-lysed in 200 μl of TEPI (50 mM Tris, pH 7.5, 5 mM EDTA, 5 μg/ml chymostatin, 5 μg/ml leupeptine, 5 μg/ml antipain and 5 μg/ml pepstatin). SDS was added to 0.5% and samples were incubated at 95ºC for 5 min. 800 μl of TNET (30 mM Tris, pH 7.5, 120 mM NaCl, 5 mM EDTA, 1% Triton X-100) were added, samples were mixed and cell debris were pelleted. CPY was immunoprecipitated for 2 hours at room temperature using a

polyclonal antibody against this protein (Geli and Riezman, 1996) and Protein A-coupled Sepharose (Sigma). Immunocomplexes were washed with TNET 0.1% SDS and TNET 2 M Urea and finally resuspended in Laemmli sample buffer (final concentration 1% SDS, 100 mM DTT, 10% glycerol, 60 mM Tris-HCl pH 6.8, Bromophenol blue), and subjected to SDS-PAGE electrophoresis.

7. BIBLIOGRAPHY

- Abramczyk, O., Zien, P., Zielinski, R., Pilecki, M., Hellman, U., and Szyszka, R. (2003). The protein kinase 60S is a free catalytic CK2alpha' subunit and forms an inactive complex with superoxide dismutase SOD1. Biochem Biophys Res Commun *307*, 31-40.
- Adams, A.E., Botstein, D., and Drubin, D.G. (1989). A yeast actin-binding protein is encoded by SAC6, a gene found by suppression of an actin mutation. Science *243*, 231-233.
- Adams, A.E., Botstein, D., and Drubin, D.G. (1991). Requirement of yeast fimbrin for actin organization and morphogenesis in vivo. Nature *354*, 404-408.
- Adams, R.J., and Pollard, T.D. (1989). Binding of myosin I to membrane lipids. Nature *340*, 565-568.
- Aguilar, R.C., Watson, H.A., and Wendland, B. (2003). The yeast Epsin Ent1 is recruited to membranes through multiple independent interactions. J Biol Chem *278*, 10737-10743.
- Ahmed, K., Gerber, D.A., and Cochet, C. (2002). Joining the cell survival squad: an emerging role for protein kinase CK2. Trends Cell Biol *12*, 226-230.
- Ahuja, R., Pinyol, R., Reichenbach, N., Custer, L., Klingensmith, J., Kessels, M.M., and Qualmann, B. (2007). Cordon-bleu is an actin nucleation factor and controls neuronal morphology. Cell *131*, 337-350.
- Akin, O., and Mullins, R.D. (2008). Capping protein increases the rate of actin-based motility by promoting filament nucleation by the Arp2/3 complex. Cell *133*, 841-851.
- Albanesi, J.P., Hammer, J.A., 3rd, and Korn, E.D. (1983). The interaction of F-actin with phosphorylated and unphosphorylated myosins IA and IB from Acanthamoeba castellanii. J Biol Chem *258*, 10176-10181.
- Albuquerque, C.P., Smolka, M.B., Payne, S.H., Bafna, V., Eng, J., and Zhou, H. (2008). A multidimensional chromatography technology for in-depth phosphoproteome analysis. Mol Cell Proteomics *7*, 1389-1396.
- Amann, K.J., and Pollard, T.D. (2001). Direct real-time observation of actin filament branching mediated by Arp2/3 complex using total internal reflection fluorescence microscopy. Proc Natl Acad Sci U S A *98*, 15009-15013.
- Amatruda, J.F., and Cooper, J.A. (1992). Purification, characterization, and immunofluorescence localization of Saccharomyces cerevisiae capping protein. J Cell Biol *117*, 1067-1076.
- Amatruda, J.F., Gattermeir, D.J., Karpova, T.S., and Cooper, J.A. (1992). Effects of null mutations and overexpression of capping protein on morphogenesis, actin distribution and polarized secretion in yeast. J Cell Biol *119*, 1151-1162.
- Amberg, D.C., Basart, E., and Botstein, D. (1995). Defining protein interactions with yeast actin in vivo. Nat Struct Biol *2*, 28-35.
- Amberg, D.C., Zahner, J.E., Mulholland, J.W., Pringle, J.R., and Botstein, D. (1997). Aip3p/Bud6p, a yeast actin-interacting protein that is involved in morphogenesis and the selection of bipolar budding sites. Mol Biol Cell *8*, 729-753.
- Anderson, B.L., Boldogh, I., Evangelista, M., Boone, C., Greene, L.A., and Pon, L.A. (1998). The Src homology domain 3 (SH3) of a yeast type I myosin, Myo5p, binds to verprolin and is required for targeting to sites of actin polarization. J Cell Biol *141*, 1357-1370.
- Andrianantoandro, E., and Pollard, T.D. (2006). Mechanism of actin filament turnover by severing and nucleation at different concentrations of ADF/cofilin. Mol Cell *24*, 13-23.
- Asakura, T., Sasaki, T., Nagano, F., Satoh, A., Obaishi, H., Nishioka, H., Imamura, H., Hotta, K., Tanaka, K., Nakanishi, H.*, et al.* (1998). Isolation and characterization of a novel actin filament-binding protein from Saccharomyces cerevisiae. Oncogene *16*, 121-130.
- Aschenbrenner, L., Lee, T., and Hasson, T. (2003). Myo6 facilitates the translocation of endocytic vesicles from cell peripheries. Mol Biol Cell *14*, 2728-2743.
- Ayscough, K.R. (2000). Endocytosis and the development of cell polarity in yeast require a dynamic F-actin cytoskeleton. Curr Biol *10*, 1587-1590.
- Ayscough, K.R., and Drubin, D.G. (1996). ACTIN: general principles from studies in yeast. Annu Rev Cell Dev Biol *12*, 129-160.

- Ayscough, K.R., Stryker, J., Pokala, N., Sanders, M., Crews, P., and Drubin, D.G. (1997). High rates of actin filament turnover in budding yeast and roles for actin in establishment and maintenance of cell polarity revealed using the actin inhibitor latrunculin-A. J Cell Biol *137*, 399-416.
- Baines, I.C., Corigliano-Murphy, A., and Korn, E.D. (1995). Quantification and localization of phosphorylated myosin I isoforms in Acanthamoeba castellanii. J Cell Biol *130*, 591-603.
- Balasubramanian, M.K., Bi, E., and Glotzer, M. (2004). Comparative analysis of cytokinesis in budding yeast, fission yeast and animal cells. Curr Biol *14*, R806-818.
- Balcer, H.I., Daugherty-Clarke, K., and Goode, B.L. (2010). The p40/ARPC1 subunit of Arp2/3 complex performs multiple essential roles in WASp-regulated actin nucleation. J Biol Chem *285*, 8481-8491.
- Balcer, H.I., Goodman, A.L., Rodal, A.A., Smith, E., Kugler, J., Heuser, J.E., and Goode, B.L. (2003). Coordinated regulation of actin filament turnover by a high-molecular-weight Srv2/CAP complex, cofilin, profilin, and Aip1. Curr Biol *13*, 2159-2169.
- Bamburg, J.R. (1999). Proteins of the ADF/cofilin family: essential regulators of actin dynamics. Annu Rev Cell Dev Biol *15*, 185-230.
- Bar-Zvi, D., and Branton, D. (1986). Clathrin-coated vesicles contain two protein kinase activities. Phosphorylation of clathrin beta-light chain by casein kinase II. J Biol Chem *261*, 9614-9621.
- Barker, S.L., Lee, L., Pierce, B.D., Maldonado-Baez, L., Drubin, D.G., and Wendland, B. (2007). Interaction of the endocytic scaffold protein Pan1 with the type I myosins contributes to the late stages of endocytosis. Mol Biol Cell *18*, 2893-2903.
- Bashkirov, P.V., Akimov, S.A., Evseev, A.I., Schmid, S.L., Zimmerberg, J., and Frolov, V.A. (2008). GTPase cycle of dynamin is coupled to membrane squeeze and release, leading to spontaneous fission. Cell *135*, 1276-1286.
- Bement, W.M., and Mooseker, M.S. (1995). TEDS rule: a molecular rationale for differential regulation of myosins by phosphorylation of the heavy chain head. Cell Motil Cytoskeleton *31*, 87-92.
- Berben, G., Dumont, J., Gilliquet, V., Bolle, P.A., and Hilger, F. (1991). The YDp plasmids: a uniform set of vectors bearing versatile gene disruption cassettes for Saccharomyces cerevisiae. Yeast *7*, 475-477.
- Berg, J.S., Powell, B.C., and Cheney, R.E. (2001). A millennial myosin census. Mol Biol Cell *12*, 780-794.
- Berkey, C.D., and Carlson, M. (2006). A specific catalytic subunit isoform of protein kinase CK2 is required for phosphorylation of the repressor Nrg1 in Saccharomyces cerevisiae. Curr Genet *50*, 1-10.
- Bernstein, B.W., and Bamburg, J.R. (1982). Tropomyosin binding to F-actin protects the F-actin from disassembly by brain actin-depolymerizing factor (ADF). Cell Motil *2*, 1-8.
- Bertling, E., Quintero-Monzon, O., Mattila, P.K., Goode, B.L., and Lappalainen, P. (2007). Mechanism and biological role of profilin-Srv2/CAP interaction. J Cell Sci *120*, 1225-1234.
- Bi, E. (2001). Cytokinesis in budding yeast: the relationship between actomyosin ring function and septum formation. Cell Struct Funct *26*, 529-537.
- Bi, E., Maddox, P., Lew, D.J., Salmon, E.D., McMillan, J.N., Yeh, E., and Pringle, J.R. (1998). Involvement of an actomyosin contractile ring in Saccharomyces cerevisiae cytokinesis. J Cell Biol *142*, 1301-1312.
- Bidwai, A.P., Reed, J.C., and Glover, C.V. (1994). Casein kinase II of Saccharomyces cerevisiae contains two distinct regulatory subunits, beta and beta'. Arch Biochem Biophys *309*, 348-355.
- Bidwai, A.P., Reed, J.C., and Glover, C.V. (1995). Cloning and disruption of CKB1, the gene encoding the 38-kDa beta subunit of Saccharomyces cerevisiae casein kinase II (CKII). Deletion of CKII regulatory subunits elicits a salt-sensitive phenotype. J Biol Chem *270*, 10395-10404.
- Blanchoin, L., Pollard, T.D., and Hitchcock-DeGregori, S.E. (2001). Inhibition of the Arp2/3 complex-nucleated actin polymerization and branch formation by tropomyosin. Curr Biol *11*, 1300-1304.

- Blanchoin, L., Pollard, T.D., and Mullins, R.D. (2000). Interactions of ADF/cofilin, Arp2/3 complex, capping protein and profilin in remodeling of branched actin filament networks. Curr Biol *10*, 1273-1282.
- Block, S.M. (1996). Fifty ways to love your lever: myosin motors. Cell *87*, 151-157.
- Bobkov, A.A., Muhlrad, A., Shvetsov, A., Benchaar, S., Scoville, D., Almo, S.C., and Reisler, E. (2004). Cofilin (ADF) affects lateral contacts in F-actin. J Mol Biol *337*, 93-104.
- Boettner, D.R., D'Agostino, J.L., Torres, O.T., Daugherty-Clarke, K., Uygur, A., Reider, A., Wendland, B., Lemmon, S.K., and Goode, B.L. (2009). The F-BAR protein Syp1 negatively regulates WASp-Arp2/3 complex activity during endocytic patch formation. Curr Biol *19*, 1979-1987.
- Boettner, D.R., Friesen, H., Andrews, B., and Lemmon, S.K. (2011). Clathrin light chain directs endocytosis by influencing the binding of the yeast Hip1R homologue, Sla2, to F-actin. Mol Biol Cell *22*, 3699-3714.
- Bompard, G., and Caron, E. (2004). Regulation of WASP/WAVE proteins: making a long story short. J Cell Biol *166*, 957-962.
- Bosc, D.G., Graham, K.C., Saulnier, R.B., Zhang, C., Prober, D., Gietz, R.D., and Litchfield, D.W. (2000). Identification and characterization of CKIP-1, a novel pleckstrin homology domain-containing protein that interacts with protein kinase CK2. J Biol Chem *275*, 14295-14306.
- Boulant, S., Kural, C., Zeeh, J.C., Ubelmann, F., and Kirchhausen, T. (2011). Actin dynamics counteract membrane tension during clathrin-mediated endocytosis. Nat Cell Biol *13*, 1124-1131.
- Brandt, D.T., Marion, S., Griffiths, G., Watanabe, T., Kaibuchi, K., and Grosse, R. (2007). Dia1 and IQGAP1 interact in cell migration and phagocytic cup formation. J Cell Biol *178*, 193-200.
- Brieher, W.M., Kueh, H.Y., Ballif, B.A., and Mitchison, T.J. (2006). Rapid actin monomer-insensitive depolymerization of Listeria actin comet tails by cofilin, coronin, and Aip1. J Cell Biol *175*, 315-324.
- Brockerhoff, S.E., Stevens, R.C., and Davis, T.N. (1994). The unconventional myosin, Myo2p, is a calmodulin target at sites of cell growth in Saccharomyces cerevisiae. J Cell Biol *124*, 315-323.
- Brower, S.M., Honts, J.E., and Adams, A.E. (1995). Genetic analysis of the fimbrin-actin binding interaction in Saccharomyces cerevisiae. Genetics *140*, 91-101.
- Bryce, N.S., Schevzov, G., Ferguson, V., Percival, J.M., Lin, J.J., Matsumura, F., Bamburg, J.R., Jeffrey, P.L., Hardeman, E.C., Gunning, P.*, et al.* (2003). Specification of actin filament function and molecular composition by tropomyosin isoforms. Mol Biol Cell *14*, 1002-1016.
- Brzeska, H., Hwang, K.J., and Korn, E.D. (2008). Acanthamoeba myosin IC colocalizes with phosphatidylinositol 4,5-bisphosphate at the plasma membrane due to the high concentration of negative charge. J Biol Chem *283*, 32014-32023.
- Brzeska, H., Knaus, U.G., Wang, Z.Y., Bokoch, G.M., and Korn, E.D. (1997). p21-activated kinase has substrate specificity similar to Acanthamoeba myosin I heavy chain kinase and activates Acanthamoeba myosin I. Proc Natl Acad Sci U S A *94*, 1092-1095.
- Brzeska, H., Lynch, T.J., and Korn, E.D. (1988). Localization of the actin-binding sites of Acanthamoeba myosin IB and effect of limited proteolysis on its actin-activated Mg2+-ATPase activity. J Biol Chem *263*, 427-435.
- Burston, H.E., Maldonado-Baez, L., Davey, M., Montpetit, B., Schluter, C., Wendland, B., and Conibear, E. (2009). Regulators of yeast endocytosis identified by systematic quantitative analysis. J Cell Biol *185*, 1097-1110.
- Buzan, J.M., and Frieden, C. (1996). Yeast actin: polymerization kinetic studies of wild type and a poorly polymerizing mutant. Proc Natl Acad Sci U S A *93*, 91-95.
- Cai, L., Holoweckyj, N., Schaller, M.D., and Bear, J.E. (2005). Phosphorylation of coronin 1B by protein kinase C regulates interaction with Arp2/3 and cell motility. J Biol Chem *280*, 31913-31923.
- Campellone, K.G., Webb, N.J., Znameroski, E.A., and Welch, M.D. (2008). WHAMM is an Arp2/3 complex activator that binds microtubules and functions in ER to Golgi transport. Cell *134*, 148-161.
- Campellone, K.G., and Welch, M.D. (2010). A nucleator arms race: cellular control of actin assembly. Nat Rev Mol Cell Biol *11*, 237-251.

- Carlier, M.F., and Pantaloni, D. (1988). Binding of phosphate to F-ADP-actin and role of F-ADP-Pi-actin in ATP-actin polymerization. J Biol Chem *263*, 817-825.
- Carlier, M.F., and Pantaloni, D. (1997). Control of actin dynamics in cell motility. J Mol Biol *269*, 459-467.
- Carroll, S.Y., Stimpson, H.E., Weinberg, J., Toret, C.P., Sun, Y., and Drubin, D.G. (2012). Analysis of yeast endocytic site formation and maturation through a regulatory transition point. Mol Biol Cell *23*, 657-668.
- Chang, J.S., Henry, K., Wolf, B.L., Geli, M., and Lemmon, S.K. (2002). Protein phosphatase-1 binding to scd5p is important for regulation of actin organization and endocytosis in yeast. J Biol Chem 277, 48002-48008.
- Coluccio, L.M. (2008). Myosins: A Superfamily of Molecular Motors (Springer).
- Collins, A., Warrington, A., Taylor, K.A., and Svitkina, T. (2011). Structural organization of the actin cytoskeleton at sites of clathrin-mediated endocytosis. Curr Biol *21*, 1167-1175.
- Cooper, J.A., and Sept, D. (2008). New insights into mechanism and regulation of actin capping protein. Int Rev Cell Mol Biol *267*, 183-206.
- Cope, M.J., Yang, S., Shang, C., and Drubin, D.G. (1999). Novel protein kinases Ark1p and Prk1p associate with and regulate the cortical actin cytoskeleton in budding yeast. J Cell Biol *144*, 1203-1218.
- Cory, G.O., Cramer, R., Blanchoin, L., and Ridley, A.J. (2003). Phosphorylation of the WASP-VCA domain increases its affinity for the Arp2/3 complex and enhances actin polymerization by WASP. Mol Cell *11*, 1229-1239.
- Cote, G.P., Albanesi, J.P., Ueno, T., Hammer, J.A., 3rd, and Korn, E.D. (1985). Purification from Dictyostelium discoideum of a low-molecular-weight myosin that resembles myosin I from Acanthamoeba castellanii. J Biol Chem *260*, 4543-4546.
- Cotlin, L.F., Siddiqui, M.A., Simpson, F., and Collawn, J.F. (1999). Casein kinase II activity is required for transferrin receptor endocytosis. J Biol Chem *274*, 30550-30556.
- Cyr, J.L., Dumont, R.A., and Gillespie, P.G. (2002). Myosin-1c interacts with hair-cell receptors through its calmodulin-binding IQ domains. J Neurosci *22*, 2487-2495.
- Chang-Ileto, B., Frere, S.G., Chan, R.B., Voronov, S.V., Roux, A., and Di Paolo, G. (2011). Synaptojanin 1-mediated PI(4,5)P2 hydrolysis is modulated by membrane curvature and facilitates membrane fission. Dev Cell *20*, 206-218.
- Chen-Wu, J.L., Padmanabha, R., and Glover, C.V. (1988). Isolation, sequencing, and disruption of the CKA1 gene encoding the alpha subunit of yeast casein kinase II. Mol Cell Biol *8*, 4981-4990.
- Chereau, D., Boczkowska, M., Skwarek-Maruszewska, A., Fujiwara, I., Hayes, D.B., Rebowski, G., Lappalainen, P., Pollard, T.D., and Dominguez, R. (2008). Leiomodin is an actin filament nucleator in muscle cells. Science *320*, 239-243.
- Chesarone, M., Gould, C.J., Moseley, J.B., and Goode, B.L. (2009). Displacement of formins from growing barbed ends by bud14 is critical for actin cable architecture and function. Dev Cell *16*, 292-302.
- Chesarone, M.A., DuPage, A.G., and Goode, B.L. (2010). Unleashing formins to remodel the actin and microtubule cytoskeletons. Nat Rev Mol Cell Biol *11*, 62-74.
- Chi, A., Huttenhower, C., Geer, L.Y., Coon, J.J., Syka, J.E., Bai, D.L., Shabanowitz, J., Burke, D.J., Troyanskaya, O.G., and Hunt, D.F. (2007). Analysis of phosphorylation sites on proteins from Saccharomyces cerevisiae by electron transfer dissociation (ETD) mass spectrometry. Proc Natl Acad Sci U S A *104*, 2193-2198.
- Chong, R., Swiss, R., Briones, G., Stone, K.L., Gulcicek, E.E., and Agaisse, H. (2009). Regulatory mimicry in Listeria monocytogenes actin-based motility. Cell Host Microbe *6*, 268-278.
- Chowdhury, S., Smith, K.W., and Gustin, M.C. (1992). Osmotic stress and the yeast cytoskeleton: phenotype-specific suppression of an actin mutation. J Cell Biol *118*, 561-571.

- Christensen, G.L., Kelstrup, C.D., Lyngso, C., Sarwar, U., Bogebo, R., Sheikh, S.P., Gammeltoft, S., Olsen, J.V., and Hansen, J.L. (2010). Quantitative phosphoproteomics dissection of seven-transmembrane receptor signaling using full and biased agonists. Mol Cell Proteomics *9*, 1540-1553.
- Chung, S., and Takizawa, P.A. (2010). Multiple Myo4 motors enhance ASH1 mRNA transport in Saccharomyces cerevisiae. J Cell Biol *189*, 755-767.
- D'Agostino, J.L., and Goode, B.L. (2005). Dissection of Arp2/3 complex actin nucleation mechanism and distinct roles for its nucleation-promoting factors in Saccharomyces cerevisiae. Genetics *171*, 35-47.
- D'Silva, S., Haider, S.J., and Phizicky, E.M. (2011). A domain of the actin binding protein Abp140 is the yeast methyltransferase responsible for 3-methylcytidine modification in the tRNA anti-codon loop. RNA *17*, 1100-1110.
- Damke, H., Baba, T., Warnock, D.E., and Schmid, S.L. (1994). Induction of mutant dynamin specifically blocks endocytic coated vesicle formation. J Cell Biol *127*, 915-934.
- Daugherty, K.M., and Goode, B.L. (2008). Functional surfaces on the p35/ARPC2 subunit of Arp2/3 complex required for cell growth, actin nucleation, and endocytosis. J Biol Chem *283*, 16950-16959.
- Dayel, M.J., Holleran, E.A., and Mullins, R.D. (2001). Arp2/3 complex requires hydrolyzable ATP for nucleation of new actin filaments. Proc Natl Acad Sci U S A *98*, 14871-14876.
- Dayel, M.J., and Mullins, R.D. (2004). Activation of Arp2/3 complex: addition of the first subunit of the new filament by a WASP protein triggers rapid ATP hydrolysis on Arp2. PLoS Biol *2*, E91.
- De La Cruz, E.M., and Ostap, E.M. (2004). Relating biochemistry and function in the myosin superfamily. Curr Opin Cell Biol *16*, 61-67.
- Delley, P.A., and Hall, M.N. (1999). Cell wall stress depolarizes cell growth via hyperactivation of RHO1. J Cell Biol *147*, 163-174.
- Dephoure, N., Zhou, C., Villen, J., Beausoleil, S.A., Bakalarski, C.E., Elledge, S.J., and Gygi, S.P. (2008). A quantitative atlas of mitotic phosphorylation. Proc Natl Acad Sci U S A *105*, 10762-10767.
- Derivery, E., Sousa, C., Gautier, J.J., Lombard, B., Loew, D., and Gautreau, A. (2009). The Arp2/3 activator WASH controls the fission of endosomes through a large multiprotein complex. Dev Cell *17*, 712-723.
- Desrivieres, S., Cooke, F.T., Morales-Johansson, H., Parker, P.J., and Hall, M.N. (2002). Calmodulin controls organization of the actin cytoskeleton via regulation of phosphatidylinositol (4,5)-bisphosphate synthesis in Saccharomyces cerevisiae. Biochem J *366*, 945-951.
- Desrivieres, S., Cooke, F.T., Parker, P.J., and Hall, M.N. (1998). MSS4, a phosphatidylinositol-4-phosphate 5-kinase required for organization of the actin cytoskeleton in Saccharomyces cerevisiae. J Biol Chem *273*, 15787-15793.
- Di Fiore, P.P., and Scita, G. (2002). Eps8 in the midst of GTPases. Int J Biochem Cell Biol *34*, 1178-1183.
- Di Paolo, G., and De Camilli, P. (2006). Phosphoinositides in cell regulation and membrane dynamics. Nature *443*, 651-657.
- Doberstein, S.K., and Pollard, T.D. (1992). Localization and specificity of the phospholipid and actin binding sites on the tail of Acanthamoeba myosin IC. J Cell Biol *117*, 1241-1249.
- Doherty, G.J., and McMahon, H.T. (2008). Mediation, modulation, and consequences of membrane-cytoskeleton interactions. Annu Rev Biophys *37*, 65-95.
- Doherty, G.J., and McMahon, H.T. (2009). Mechanisms of endocytosis. Annu Rev Biochem *78*, 857-902.
- Domanska, K., Zielinski, R., Kubinski, K., Sajnaga, E., Maslyk, M., Bretner, M., and Szyszka, R. (2005). Different properties of four molecular forms of protein kinase CK2 from Saccharomyces cerevisiae. Acta Biochim Pol *52*, 947-951.
- Dong, Y., Pruyne, D., and Bretscher, A. (2003). Formin-dependent actin assembly is regulated by distinct modes of Rho signaling in yeast. J Cell Biol *161*, 1081-1092.

- Donnelly, S.F., Pocklington, M.J., Pallotta, D., and Orr, E. (1993). A proline-rich protein, verprolin, involved in cytoskeletal organization and cellular growth in the yeast Saccharomyces cerevisiae. Mol Microbiol *10*, 585-596.
- Dores, M.R., Schnell, J.D., Maldonado-Baez, L., Wendland, B., and Hicke, L. (2010). The function of yeast epsin and Ede1 ubiquitin-binding domains during receptor internalization. Traffic *11*, 151-160.
- Doring, M., Loos, A., Schrader, N., Pfander, B., and Bauerfeind, R. (2006). Nerve growth factor-induced phosphorylation of amphiphysin-1 by casein kinase 2 regulates clathrin-amphiphysin interactions. J Neurochem *98*, 2013-2022.
- Drees, B., Brown, C., Barrell, B.G., and Bretscher, A. (1995). Tropomyosin is essential in yeast, yet the TPM1 and TPM2 products perform distinct functions. J Cell Biol *128*, 383-392.
- Drubin, D.G., Miller, K.G., and Botstein, D. (1988). Yeast actin-binding proteins: evidence for a role in morphogenesis. J Cell Biol *107*, 2551-2561.
- Dulic, V., Egerton, M., Elguindi, I., Raths, S., Singer, B., and Riezman, H. (1991). Yeast endocytosis assays. Methods Enzymol *194*, 697-710.
- Duncan, J.S., and Litchfield, D.W. (2008). Too much of a good thing: the role of protein kinase CK2 in tumorigenesis and prospects for therapeutic inhibition of CK2. Biochim Biophys Acta *1784*, 33-47.
- Duncan, M.C., Cope, M.J., Goode, B.L., Wendland, B., and Drubin, D.G. (2001). Yeast Eps15-like endocytic protein, Pan1p, activates the Arp2/3 complex. Nat Cell Biol *3*, 687-690.
- Dunn, B.D., Sakamoto, T., Hong, M.S., Sellers, J.R., and Takizawa, P.A. (2007). Myo4p is a monomeric myosin with motility uniquely adapted to transport mRNA. J Cell Biol *178*, 1193-1206.
- Durrbach, A., Louvard, D., and Coudrier, E. (1996). Actin filaments facilitate two steps of endocytosis. J Cell Sci *109 (Pt 2)*, 457-465.
- Eads, J.C., Mahoney, N.M., Vorobiev, S., Bresnick, A.R., Wen, K.K., Rubenstein, P.A., Haarer, B.K., and Almo, S.C. (1998). Structure determination and characterization of Saccharomyces cerevisiae profilin. Biochemistry *37*, 11171-11181.
- Egile, C., Rouiller, I., Xu, X.P., Volkmann, N., Li, R., and Hanein, D. (2005). Mechanism of filament nucleation and branch stability revealed by the structure of the Arp2/3 complex at actin branch junctions. PLoS Biol *3*, e383.
- Eitzen, G., Wang, L., Thorngren, N., and Wickner, W. (2002). Remodeling of organelle-bound actin is required for yeast vacuole fusion. J Cell Biol *158*, 669-679.
- Engqvist-Goldstein, A.E., and Drubin, D.G. (2003). Actin assembly and endocytosis: from yeast to mammals. Annu Rev Cell Dev Biol *19*, 287-332.
- Epp, J.A., and Chant, J. (1997). An IQGAP-related protein controls actin-ring formation and cytokinesis in yeast. Curr Biol *7*, 921-929.
- Evangelista, M., Blundell, K., Longtine, M.S., Chow, C.J., Adames, N., Pringle, J.R., Peter, M., and Boone, C. (1997). Bni1p, a yeast formin linking cdc42p and the actin cytoskeleton during polarized morphogenesis. Science *276*, 118-122.
- Evangelista, M., Klebl, B.M., Tong, A.H., Webb, B.A., Leeuw, T., Leberer, E., Whiteway, M., Thomas, D.Y., and Boone, C. (2000). A role for myosin-I in actin assembly through interactions with Vrp1p, Bee1p, and the Arp2/3 complex. J Cell Biol *148*, 353-362.
- Evangelista, M., Pruyne, D., Amberg, D.C., Boone, C., and Bretscher, A. (2002). Formins direct Arp2/3-independent actin filament assembly to polarize cell growth in yeast. Nat Cell Biol *4*, 260-269.
- Fabrizio, P., Hoon, S., Shamalnasab, M., Galbani, A., Wei, M., Giaever, G., Nislow, C., and Longo, V.D. (2010). Genome-wide screen in Saccharomyces cerevisiae identifies vacuolar protein sorting, autophagy, biosynthetic, and tRNA methylation genes involved in life span regulation. PLoS Genet *6*, e1001024.
- Falck, S., Paavilainen, V.O., Wear, M.A., Grossmann, J.G., Cooper, J.A., and Lappalainen, P. (2004). Biological role and structural mechanism of twinfilin-capping protein interaction. Embo J *23*, 3010-3019.

- Fan, X., Martin-Brown, S., Florens, L., and Li, R. (2008). Intrinsic capability of budding yeast cofilin to promote turnover of tropomyosin-bound actin filaments. PLoS One *3*, e3641.
- Fang, X., Luo, J., Nishihama, R., Wloka, C., Dravis, C., Travaglia, M., Iwase, M., Vallen, E.A., and Bi, E. (2010). Biphasic targeting and cleavage furrow ingression directed by the tail of a myosin II. J Cell Biol *191*, 1333-1350.
- Faust, M., Gunther, J., Morgenstern, E., Montenarh, M., and Gotz, C. (2002). Specific localization of the catalytic subunits of protein kinase CK2 at the centrosomes. Cell Mol Life Sci *59*, 2155-2164.
- Faust, M., Jung, M., Gunther, J., Zimmermann, R., and Montenarh, M. (2001). Localization of individual subunits of protein kinase CK2 to the endoplasmic reticulum and to the Golgi apparatus. Mol Cell Biochem *227*, 73-80.
- Faust, M., Schuster, N., and Montenarh, M. (1999). Specific binding of protein kinase CK2 catalytic subunits to tubulin. FEBS Lett *462*, 51-56.
- Fedor-Chaiken, M., Deschenes, R.J., and Broach, J.R. (1990). SRV2, a gene required for RAS activation of adenylate cyclase in yeast. Cell *61*, 329-340.
- Feeser, E.A., Ignacio, C.M., Krendel, M., and Ostap, E.M. (2010). Myo1e binds anionic phospholipids with high affinity. Biochemistry *49*, 9353-9360.
- Ferguson, S.M., and De Camilli, P. (2012). Dynamin, a membrane-remodelling GTPase. Nat Rev Mol Cell Biol *13*, 75-88.
- Ferguson, S.M., Raimondi, A., Paradise, S., Shen, H., Mesaki, K., Ferguson, A., Destaing, O., Ko, G., Takasaki, J., Cremona, O.*, et al.* (2009). Coordinated actions of actin and BAR proteins upstream of dynamin at endocytic clathrin-coated pits. Dev Cell *17*, 811-822.
- Ficarro, S.B., McCleland, M.L., Stukenberg, P.T., Burke, D.J., Ross, M.M., Shabanowitz, J., Hunt, D.F., and White, F.M. (2002). Phosphoproteome analysis by mass spectrometry and its application to Saccharomyces cerevisiae. Nat Biotechnol *20*, 301-305.
- Field, J., Vojtek, A., Ballester, R., Bolger, G., Colicelli, J., Ferguson, K., Gerst, J., Kataoka, T., Michaeli, T., Powers, S.*, et al.* (1990). Cloning and characterization of CAP, the S. cerevisiae gene encoding the 70 kd adenylyl cyclase-associated protein. Cell *61*, 319-327.
- Filhol, O., and Cochet, C. (2009). Protein kinase CK2 in health and disease: Cellular functions of protein kinase CK2: a dynamic affair. Cell Mol Life Sci *66*, 1830-1839.
- Filhol, O., Nueda, A., Martel, V., Gerber-Scokaert, D., Benitez, M.J., Souchier, C., Saoudi, Y., and Cochet, C. (2003). Live-cell fluorescence imaging reveals the dynamics of protein kinase CK2 individual subunits. Mol Cell Biol *23*, 975-987.
- Foth, B.J., Goedecke, M.C., and Soldati, D. (2006). New insights into myosin evolution and classification. Proc Natl Acad Sci U S A *103*, 3681-3686.
- Frantz, C., Barreiro, G., Dominguez, L., Chen, X., Eddy, R., Condeelis, J., Kelly, M.J., Jacobson, M.P., and Barber, D.L. (2008). Cofilin is a pH sensor for actin free barbed end formation: role of phosphoinositide binding. J Cell Biol *183*, 865-879.
- Fujiwara, I., Takahashi, S., Tadakuma, H., Funatsu, T., and Ishiwata, S. (2002). Microscopic analysis of polymerization dynamics with individual actin filaments. Nat Cell Biol *4*, 666-673.
- Galovic, M., Xu, D., Areces, L.B., van der Kammen, R., and Innocenti, M. (2011). Interplay between N-WASP and CK2 optimizes clathrin-mediated endocytosis of EGFR. J Cell Sci *124*, 2001-2012.
- Galletta, B.J., Chuang, D.Y., and Cooper, J.A. (2008). Distinct roles for Arp2/3 regulators in actin assembly and endocytosis. PLoS Biol *6*, e1.
- Gandhi, M., Achard, V., Blanchoin, L., and Goode, B.L. (2009). Coronin switches roles in actin disassembly depending on the nucleotide state of actin. Mol Cell *34*, 364-374.
- Gandhi, M., Smith, B.A., Bovellan, M., Paavilainen, V., Daugherty-Clarke, K., Gelles, J., Lappalainen, P., and Goode, B.L. (2010). GMF is a cofilin homolog that binds Arp2/3 complex to stimulate filament debranching and inhibit actin nucleation. Curr Biol *20*, 861-867.
- Gasman, S., Kalaidzidis, Y., and Zerial, M. (2003). RhoD regulates endosome dynamics through Diaphanous-related Formin and Src tyrosine kinase. Nat Cell Biol *5*, 195-204.

- Geli, M.I., Lombardi, R., Schmelzl, B., and Riezman, H. (2000). An intact SH3 domain is required for myosin I-induced actin polymerization. Embo J *19*, 4281-4291.
- Geli, M.I., and Riezman, H. (1996). Role of type I myosins in receptor-mediated endocytosis in yeast. Science *272*, 533-535.
- Geli, M.I., Wesp, A., and Riezman, H. (1998). Distinct functions of calmodulin are required for the uptake step of receptor-mediated endocytosis in yeast: the type I myosin Myo5p is one of the calmodulin targets. Embo J *17*, 635-647.
- Georgieva-Hanson, V., Schook, W.J., and Puszkin, S. (1988). Brain coated vesicle destabilization and phosphorylation of coat proteins. J Neurochem *50*, 307-315.
- Gerst, J.E., Ferguson, K., Vojtek, A., Wigler, M., and Field, J. (1991). CAP is a bifunctional component of the Saccharomyces cerevisiae adenylyl cyclase complex. Mol Cell Biol *11*, 1248-1257.
- Gheorghe, D.M., Aghamohammadzadeh, S., Smaczynska-de, R., II, Allwood, E.G., Winder, S.J., and Ayscough, K.R. (2008). Interactions between the yeast SM22 homologue Scp1 and actin demonstrate the importance of actin bundling in endocytosis. J Biol Chem *283*, 15037-15046.
- Gietz, R.D., Graham, K.C., and Litchfield, D.W. (1995). Interactions between the subunits of casein kinase II. J Biol Chem *270*, 13017-13021.
- Gietz, R.D., and Sugino, A. (1988). New yeast-Escherichia coli shuttle vectors constructed with in vitro mutagenized yeast genes lacking six-base pair restriction sites. Gene *74*, 527-534.
- Girao, H., Geli, M.I., and Idrissi, F.Z. (2008). Actin in the endocytic pathway: From yeast to mammals. FEBS Lett *582*, 2112-2119.
- Glover, C.V., 3rd (1998). On the physiological role of casein kinase II in Saccharomyces cerevisiae. Prog Nucleic Acid Res Mol Biol *59*, 95-133.
- Gnad, F., de Godoy, L.M., Cox, J., Neuhauser, N., Ren, S., Olsen, J.V., and Mann, M. (2009). High-accuracy identification and bioinformatic analysis of in vivo protein phosphorylation sites in yeast. Proteomics *9*, 4642-4652.
- Goldschmidt-Clermont, P.J., Furman, M.I., Wachsstock, D., Safer, D., Nachmias, V.T., and Pollard, T.D. (1992). The control of actin nucleotide exchange by thymosin beta 4 and profilin. A potential regulatory mechanism for actin polymerization in cells. Mol Biol Cell *3*, 1015-1024.
- Goley, E.D., Ohkawa, T., Mancuso, J., Woodruff, J.B., D'Alessio, J.A., Cande, W.Z., Volkman, L.E., and Welch, M.D. (2006). Dynamic nuclear actin assembly by Arp2/3 complex and a baculovirus WASP-like protein. Science *314*, 464-467.
- Goley, E.D., Rodenbusch, S.E., Martin, A.C., and Welch, M.D. (2004). Critical conformational changes in the Arp2/3 complex are induced by nucleotide and nucleation promoting factor. Mol Cell *16*, 269-279.
- Gomez, T.S., and Billadeau, D.D. (2009). A FAM21-containing WASH complex regulates retromer-dependent sorting. Dev Cell *17*, 699-711.
- Goode, B.L., Drubin, D.G., and Lappalainen, P. (1998). Regulation of the cortical actin cytoskeleton in budding yeast by twinfilin, a ubiquitous actin monomer-sequestering protein. J Cell Biol *142*, 723-733.
- Goode, B.L., Rodal, A.A., Barnes, G., and Drubin, D.G. (2001). Activation of the Arp2/3 complex by the actin filament binding protein Abp1p. J Cell Biol *153*, 627-634.
- Goode, B.L., Wong, J.J., Butty, A.C., Peter, M., McCormack, A.L., Yates, J.R., Drubin, D.G., and Barnes, G. (1999). Coronin promotes the rapid assembly and cross-linking of actin filaments and may link the actin and microtubule cytoskeletons in yeast. J Cell Biol *144*, 83-98.
- Goodman, A., Goode, B.L., Matsudaira, P., and Fink, G.R. (2003). The Saccharomyces cerevisiae calponin/transgelin homolog Scp1 functions with fimbrin to regulate stability and organization of the actin cytoskeleton. Mol Biol Cell *14*, 2617-2629.
- Goodson, H.V., Anderson, B.L., Warrick, H.M., Pon, L.A., and Spudich, J.A. (1996). Synthetic lethality screen identifies a novel yeast myosin I gene (MYO5): myosin I proteins are required for polarization of the actin cytoskeleton. J Cell Biol *133*, 1277-1291.

- Goodson, H.V., and Spudich, J.A. (1995). Identification and molecular characterization of a yeast myosin I. Cell Motil Cytoskeleton *30*, 73-84.
- Goroncy, A.K., Koshiba, S., Tochio, N., Tomizawa, T., Sato, M., Inoue, M., Watanabe, S., Hayashizaki, Y., Tanaka, A., Kigawa, T.*, et al.* (2009). NMR solution structures of actin depolymerizing factor homology domains. Protein Sci *18*, 2384-2392.
- Gottwald, U., Brokamp, R., Karakesisoglou, I., Schleicher, M., and Noegel, A.A. (1996). Identification of a cyclase-associated protein (CAP) homologue in Dictyostelium discoideum and characterization of its interaction with actin. Mol Biol Cell *7*, 261-272.
- Gouin, E., Egile, C., Dehoux, P., Villiers, V., Adams, J., Gertler, F., Li, R., and Cossart, P. (2004). The RickA protein of Rickettsia conorii activates the Arp2/3 complex. Nature *427*, 457-461.
- Graziano, B.R., DuPage, A.G., Michelot, A., Breitsprecher, D., Moseley, J.B., Sagot, I., Blanchoin, L., and Goode, B.L. (2011). Mechanism and cellular function of Bud6 as an actin nucleation-promoting factor. Mol Biol Cell *22*, 4016-4028.
- Greer, C., and Schekman, R. (1982). Actin from Saccharomyces cerevisiae. Mol Cell Biol *2*, 1270-1278.
- Grosshans, B.L., Grotsch, H., Mukhopadhyay, D., Fernandez, I.M., Pfannstiel, J., Idrissi, F.Z., Lechner, J., Riezman, H., and Geli, M.I. (2006). TEDS site phosphorylation of the yeast myosins I is required for ligand-induced but not for constitutive endocytosis of the G protein-coupled receptor Ste2p. J Biol Chem *281*, 11104-11114.
- Grotsch, H., Giblin, J.P., Idrissi, F.Z., Fernandez-Golbano, I.M., Collette, J.R., Newpher, T.M., Robles, V., Lemmon, S.K., and Geli, M.I. (2010). Calmodulin dissociation regulates Myo5 recruitment and function at endocytic sites. Embo J *29*, 2899-2914.
- Gruhler, A., Olsen, J.V., Mohammed, S., Mortensen, P., Faergeman, N.J., Mann, M., and Jensen, O.N. (2005). Quantitative phosphoproteomics applied to the yeast pheromone signaling pathway. Mol Cell Proteomics *4*, 310-327.
- Guerra, B., and Issinger, O.G. (2008). Protein kinase CK2 in human diseases. Curr Med Chem *15*, 1870-1886.
- Guerra, B., Siemer, S., Boldyreff, B., and Issinger, O.G. (1999). Protein kinase CK2: evidence for a protein kinase CK2beta subunit fraction, devoid of the catalytic CK2alpha subunit, in mouse brain and testicles. FEBS Lett *462*, 353-357.
- Gyuris, J., Golemis, E., Chertkov, H., and Brent, R. (1993). Cdi1, a human G1 and S phase protein phosphatase that associates with Cdk2. Cell *75*, 791-803.
- Haarer, B.K., Lillie, S.H., Adams, A.E., Magdolen, V., Bandlow, W., and Brown, S.S. (1990). Purification of profilin from Saccharomyces cerevisiae and analysis of profilin-deficient cells. J Cell Biol *110*, 105-114.
- Haarer, B.K., Petzold, A., Lillie, S.H., and Brown, S.S. (1994). Identification of MYO4, a second class V myosin gene in yeast. J Cell Sci *107 (Pt 4)*, 1055-1064.
- Hanks, S.K., and Hunter, T. (1995). Protein kinases 6. The eukaryotic protein kinase superfamily: kinase (catalytic) domain structure and classification. Faseb J *9*, 576-596.
- Hanna, D.E., Rethinaswamy, A., and Glover, C.V. (1995). Casein kinase II is required for cell cycle progression during G1 and G2/M in Saccharomyces cerevisiae. J Biol Chem *270*, 25905-25914.
- Hao, W., Luo, Z., Zheng, L., Prasad, K., and Lafer, E.M. (1999). AP180 and AP-2 interact directly in a complex that cooperatively assembles clathrin. J Biol Chem *274*, 22785-22794.
- Hayden, S.M., Wolenski, J.S., and Mooseker, M.S. (1990). Binding of brush border myosin I to phospholipid vesicles. J Cell Biol *111*, 443-451.
- Helfer, E., Nevalainen, E.M., Naumanen, P., Romero, S., Didry, D., Pantaloni, D., Lappalainen, P., and Carlier, M.F. (2006). Mammalian twinfilin sequesters ADP-G-actin and caps filament barbed ends: implications in motility. Embo J *25*, 1184-1195.
- Henry, K.R., D'Hondt, K., Chang, J., Newpher, T., Huang, K., Hudson, R.T., Riezman, H., and Lemmon, S.K. (2002). Scd5p and clathrin function are important for cortical actin organization, endocytosis, and localization of sla2p in yeast. Mol Biol Cell *13*, 2607-2625.

- Herskovits, J.S., Burgess, C.C., Obar, R.A., and Vallee, R.B. (1993). Effects of mutant rat dynamin on endocytosis. J Cell Biol *122*, 565-578.
- Hess, D.C., Myers, C.L., Huttenhower, C., Hibbs, M.A., Hayes, A.P., Paw, J., Clore, J.J., Mendoza, R.M., Luis, B.S., Nislow, C*., et al.* (2009). Computationally driven, quantitative experiments discover genes required for mitochondrial biogenesis. PLoS Genet *5*, e1000407.
- Higgs, H.N., Blanchoin, L., and Pollard, T.D. (1999). Influence of the C terminus of Wiskott-Aldrich syndrome protein (WASp) and the Arp2/3 complex on actin polymerization. Biochemistry *38*, 15212-15222.
- Higgs, H.N., and Pollard, T.D. (2000). Activation by Cdc42 and PIP(2) of Wiskott-Aldrich syndrome protein (WASp) stimulates actin nucleation by Arp2/3 complex. J Cell Biol *150*, 1311-1320.
- Higgs, H.N., and Pollard, T.D. (2001). Regulation of actin filament network formation through ARP2/3 complex: activation by a diverse array of proteins. Annu Rev Biochem *70*, 649-676.
- Hirono, M., Denis, C.S., Richardson, G.P., and Gillespie, P.G. (2004). Hair cells require phosphatidylinositol 4,5-bisphosphate for mechanical transduction and adaptation. Neuron *44*, 309-320.
- Hitchcock-DeGregori, S.E., and Heald, R.W. (1987). Altered actin and troponin binding of amino-terminal variants of chicken striated muscle alpha-tropomyosin expressed in Escherichia coli. J Biol Chem *262*, 9730-9735.
- Hokanson, D.E., Laakso, J.M., Lin, T., Sept, D., and Ostap, E.M. (2006). Myo1c binds phosphoinositides through a putative pleckstrin homology domain. Mol Biol Cell *17*, 4856-4865.
- Holt, L.J., Tuch, B.B., Villen, J., Johnson, A.D., Gygi, S.P., and Morgan, D.O. (2009). Global analysis of Cdk1 substrate phosphorylation sites provides insights into evolution. Science *325*, 1682-1686.
- Holtzman, D.A., Yang, S., and Drubin, D.G. (1993). Synthetic-lethal interactions identify two novel genes, SLA1 and SLA2, that control membrane cytoskeleton assembly in Saccharomyces cerevisiae. J Cell Biol *122*, 635-644.
- Homma, K., Terui, S., Minemura, M., Qadota, H., Anraku, Y., Kanaho, Y., and Ohya, Y. (1998). Phosphatidylinositol-4-phosphate 5-kinase localized on the plasma membrane is essential for yeast cell morphogenesis. J Biol Chem *273*, 15779-15786.
- Huang, M.E., Souciet, J.L., Chuat, J.C., and Galibert, F. (1996). Identification of ACT4, a novel essential actin-related gene in the yeast Saccharomyces cerevisiae. Yeast *12*, 839-848.
- Hubberstey, A.V., and Mottillo, E.P. (2002). Cyclase-associated proteins: CAPacity for linking signal transduction and actin polymerization. Faseb J *16*, 487-499.
- Huckaba, T.M., Gay, A.C., Pantalena, L.F., Yang, H.C., and Pon, L.A. (2004). Live cell imaging of the assembly, disassembly, and actin cable-dependent movement of endosomes and actin patches in the budding yeast, Saccharomyces cerevisiae. J Cell Biol *167*, 519-530.
- Huckaba, T.M., Lipkin, T., and Pon, L.A. (2006). Roles of type II myosin and a tropomyosin isoform in retrograde actin flow in budding yeast. J Cell Biol *175*, 957-969.
- Hug, C., Jay, P.Y., Reddy, I., McNally, J.G., Bridgman, P.C., Elson, E.L., and Cooper, J.A. (1995). Capping protein levels influence actin assembly and cell motility in dictyostelium. Cell *81*, 591-600.
- Humphries, C.L., Balcer, H.I., D'Agostino, J.L., Winsor, B., Drubin, D.G., Barnes, G., Andrews, B.J., and Goode, B.L. (2002). Direct regulation of Arp2/3 complex activity and function by the actin binding protein coronin. J Cell Biol *159*, 993-1004.
- Huxley, A.F., and Niedergerke, R. (1954). Structural changes in muscle during contraction; interference microscopy of living muscle fibres. Nature *173*, 971-973.
- Huxley, H., and Hanson, J. (1954). Changes in the cross-striations of muscle during contraction and stretch and their structural interpretation. Nature *173*, 973-976.
- Huxley, H.E. (1963). Electron Microscope Studies on the Structure of Natural and Synthetic Protein Filaments from Striated Muscle. J Mol Biol *7*, 281-308.
- Ichetovkin, I., Grant, W., and Condeelis, J. (2002). Cofilin produces newly polymerized actin filaments that are preferred for dendritic nucleation by the Arp2/3 complex. Curr Biol *12*, 79-84.

- Idrissi, F.Z., Blasco, A., Espinal, A., and Geli, M.I. (2012). Ultrastructural dynamics of proteins involved in endocytic budding. Proc Natl Acad Sci U S A.
- Idrissi, F.Z., Grotsch, H., Fernandez-Golbano, I.M., Presciatto-Baschong, C., Riezman, H., and Geli, M.I. (2008). Distinct acto/myosin-I structures associate with endocytic profiles at the plasma membrane. J Cell Biol *180*, 1219-1232.
- Idrissi, F.Z., Wolf, B.L., and Geli, M.I. (2002). Cofilin, but not profilin, is required for myosin-I-induced actin polymerization and the endocytic uptake in yeast. Mol Biol Cell *13*, 4074-4087.
- Iida, K., Moriyama, K., Matsumoto, S., Kawasaki, H., Nishida, E., and Yahara, I. (1993). Isolation of a yeast essential gene, COF1, that encodes a homologue of mammalian cofilin, a low-M(r) actin-binding and depolymerizing protein. Gene *124*, 115-120.
- Imamura, H., Tanaka, K., Hihara, T., Umikawa, M., Kamei, T., Takahashi, K., Sasaki, T., and Takai, Y. (1997). Bni1p and Bnr1p: downstream targets of the Rho family small G-proteins which interact with profilin and regulate actin cytoskeleton in Saccharomyces cerevisiae. Embo J *16*, 2745-2755.
- Jauch, E., Melzig, J., Brkulj, M., and Raabe, T. (2002). In vivo functional analysis of Drosophila protein kinase casein kinase 2 (CK2) beta-subunit. Gene *298*, 29-39.
- Jeng, R.L., Goley, E.D., D'Alessio, J.A., Chaga, O.Y., Svitkina, T.M., Borisy, G.G., Heinzen, R.A., and Welch, M.D. (2004). A Rickettsia WASP-like protein activates the Arp2/3 complex and mediates actin-based motility. Cell Microbiol *6*, 761-769.
- Jenness, D.D., and Spatrick, P. (1986). Down regulation of the alpha-factor pheromone receptor in S. cerevisiae. Cell *46*, 345-353.
- Johnston, G.C., Prendergast, J.A., and Singer, R.A. (1991). The Saccharomyces cerevisiae MYO2 gene encodes an essential myosin for vectorial transport of vesicles. J Cell Biol *113*, 539-551.
- Jonsdottir, G.A., and Li, R. (2004). Dynamics of yeast Myosin I: evidence for a possible role in scission of endocytic vesicles. Curr Biol *14*, 1604-1609.
- Jung, G., and Hammer, J.A., 3rd (1994). The actin binding site in the tail domain of Dictyostelium myosin IC (myoC) resides within the glycine- and proline-rich sequence (tail homology region 2). FEBS Lett *342*, 197-202.
- Jung, G., Remmert, K., Wu, X., Volosky, J.M., and Hammer, J.A., 3rd (2001). The Dictyostelium CARMIL protein links capping protein and the Arp2/3 complex to type I myosins through their SH3 domains. J Cell Biol *153*, 1479-1497.
- Kabsch, W., Mannherz, H.G., Suck, D., Pai, E.F., and Holmes, K.C. (1990). Atomic structure of the actin:DNase I complex. Nature *347*, 37-44.
- Kaksonen, M., Peng, H.B., and Rauvala, H. (2000). Association of cortactin with dynamic actin in lamellipodia and on endosomal vesicles. J Cell Sci *113 Pt 24*, 4421-4426.
- Kaksonen, M., Sun, Y., and Drubin, D.G. (2003). A pathway for association of receptors, adaptors, and actin during endocytic internalization. Cell *115*, 475-487.
- Kaksonen, M., Toret, C.P., and Drubin, D.G. (2005). A modular design for the clathrin- and actin-mediated endocytosis machinery. Cell *123*, 305-320.
- Kapitzky, L., Beltrao, P., Berens, T.J., Gassner, N., Zhou, C., Wuster, A., Wu, J., Babu, M.M., Elledge, S.J., Toczyski, D*., et al.* (2010). Cross-species chemogenomic profiling reveals evolutionarily conserved drug mode of action. Mol Syst Biol *6*, 451.
- Karcher, R.L., Roland, J.T., Zappacosta, F., Huddleston, M.J., Annan, R.S., Carr, S.A., and Gelfand, V.I. (2001). Cell cycle regulation of myosin-V by calcium/calmodulin-dependent protein kinase II. Science *293*, 1317-1320.
- Karlsson, R., Aspenstrom, P., and Bystrom, A.S. (1991). A chicken beta-actin gene can complement a disruption of the Saccharomyces cerevisiae ACT1 gene. Mol Cell Biol *11*, 213-217.
- Karpova, T.S., McNally, J.G., Moltz, S.L., and Cooper, J.A. (1998). Assembly and function of the actin cytoskeleton of yeast: relationships between cables and patches. J Cell Biol *142*, 1501-1517.
- Karpova, T.S., Tatchell, K., and Cooper, J.A. (1995). Actin filaments in yeast are unstable in the absence of capping protein or fimbrin. J Cell Biol *131*, 1483-1493.

- Kato, M., and Takenawa, T. (2005). WICH, a member of WASP-interacting protein family, cross-links actin filaments. Biochem Biophys Res Commun *328*, 1058-1066.
- Kilchert, C., and Spang, A. (2011). Cotranslational transport of ABP140 mRNA to the distal pole of S. cerevisiae. Embo J *30*, 3567-3580.
- Kim, E., Miller, C.J., and Reisler, E. (1996). Polymerization and in vitro motility properties of yeast actin: a comparison with rabbit skeletal alpha-actin. Biochemistry *35*, 16566-16572.
- Kim, K., Galletta, B.J., Schmidt, K.O., Chang, F.S., Blumer, K.J., and Cooper, J.A. (2006). Actin-based motility during endocytosis in budding yeast. Mol Biol Cell *17*, 1354-1363.
- Kim, K., Yamashita, A., Wear, M.A., Maeda, Y., and Cooper, J.A. (2004). Capping protein binding to actin in yeast: biochemical mechanism and physiological relevance. J Cell Biol *164*, 567-580.
- Kim, S.V., and Flavell, R.A. (2008). Myosin I: from yeast to human. Cell Mol Life Sci *65*, 2128-2137.
- Kinley, A.W., Weed, S.A., Weaver, A.M., Karginov, A.V., Bissonette, E., Cooper, J.A., and Parsons, J.T. (2003). Cortactin interacts with WIP in regulating Arp2/3 activation and membrane protrusion. Curr Biol *13*, 384-393.
- Kishimoto, T., Sun, Y., Buser, C., Liu, J., Michelot, A., and Drubin, D.G. (2011). Determinants of endocytic membrane geometry, stability, and scission. Proc Natl Acad Sci U S A *108*, E979-988.
- Kjeken, R., Egeberg, M., Habermann, A., Kuehnel, M., Peyron, P., Floetenmeyer, M., Walther, P., Jahraus, A., Defacque, H., Kuznetsov, S.A*., et al.* (2004). Fusion between phagosomes, early and late endosomes: a role for actin in fusion between late, but not early endocytic organelles. Mol Biol Cell *15*, 345-358.
- Kobayashi, S.D., and Nagiec, M.M. (2003). Ceramide/long-chain base phosphate rheostat in Saccharomyces cerevisiae: regulation of ceramide synthesis by Elo3p and Cka2p. Eukaryot Cell *2*, 284-294.
- Korolchuk, V., and Banting, G. (2003). Kinases in clathrin-mediated endocytosis. Biochem Soc Trans *31*, 857-860.
- Korolchuk, V.I., and Banting, G. (2002). CK2 and GAK/auxilin2 are major protein kinases in clathrin-coated vesicles. Traffic *3*, 428-439.
- Korolchuk, V.I., Cozier, G., and Banting, G. (2005). Regulation of CK2 activity by phosphatidylinositol phosphates. J Biol Chem *280*, 40796-40801.
- Kovar, D.R., Harris, E.S., Mahaffy, R., Higgs, H.N., and Pollard, T.D. (2006). Control of the assembly of ATP- and ADP-actin by formins and profilin. Cell *124*, 423-435.
- Kovar, D.R., and Pollard, T.D. (2004). Insertional assembly of actin filament barbed ends in association with formins produces piconewton forces. Proc Natl Acad Sci U S A *101*, 14725-14730.
- Kreis, T., and Vale, R. (1999). Guidebook to the cytoskeletal and motor proteins, 2nd edn (Oxford ; New York, Oxford University Press).
- Kron, S.J., Drubin, D.G., Botstein, D., and Spudich, J.A. (1992). Yeast actin filaments display ATP-dependent sliding movement over surfaces coated with rabbit muscle myosin. Proc Natl Acad Sci U S A *89*, 4466-4470.
- Kubinski, K., Domanska, K., Sajnaga, E., Mazur, E., Zielinski, R., and Szyszka, R. (2007). Yeast holoenzyme of protein kinase CK2 requires both beta and beta' regulatory subunits for its activity. Mol Cell Biochem *295*, 229-236.
- Kubler, E., and Riezman, H. (1993). Actin and fimbrin are required for the internalization step of endocytosis in yeast. Embo J *12*, 2855-2862.
- Kukulski, W., Schorb, M., Welsch, S., Picco, A., Kaksonen, M., and Briggs, J.A. (2011). Correlated fluorescence and 3D electron microscopy with high sensitivity and spatial precision. J Cell Biol *192*, 111-119.
- Kuriyan, J., and Cowburn, D. (1997). Modular peptide recognition domains in eukaryotic signaling. Annu Rev Biophys Biomol Struct *26*, 259-288.
- Laemmli, U.K. (1970). Cleavage of structural proteins during the assembly of the head of bacteriophage T4. Nature *227*, 680-685.

- Lappalainen, P. (2007). Actin-monomer-binding proteins (Austin, Tex.
- New York, N.Y., Landes Bioscience ;
- Springer).
- Lappalainen, P., and Drubin, D.G. (1997). Cofilin promotes rapid actin filament turnover in vivo. Nature *388*, 78-82.
- Lappalainen, P., Fedorov, E.V., Fedorov, A.A., Almo, S.C., and Drubin, D.G. (1997). Essential functions and actin-binding surfaces of yeast cofilin revealed by systematic mutagenesis. Embo J *16*, 5520-5530.
- Lassing, I., and Lindberg, U. (1985). Specific interaction between phosphatidylinositol 4,5-bisphosphate and profilactin. Nature *314*, 472-474.
- Le Clainche, C., Didry, D., Carlier, M.F., and Pantaloni, D. (2001). Activation of Arp2/3 complex by Wiskott-Aldrich Syndrome protein is linked to enhanced binding of ATP to Arp2. J Biol Chem *276*, 46689-46692.
- Le Clainche, C., Pantaloni, D., and Carlier, M.F. (2003). ATP hydrolysis on actin-related protein 2/3 complex causes debranching of dendritic actin arrays. Proc Natl Acad Sci U S A *100*, 6337-6342.
- LeClaire, L.L., 3rd, Baumgartner, M., Iwasa, J.H., Mullins, R.D., and Barber, D.L. (2008). Phosphorylation of the Arp2/3 complex is necessary to nucleate actin filaments. J Cell Biol *182*, 647-654.
- Lechler, T., Jonsdottir, G.A., Klee, S.K., Pellman, D., and Li, R. (2001). A two-tiered mechanism by which Cdc42 controls the localization and activation of an Arp2/3-activating motor complex in yeast. J Cell Biol *155*, 261-270.
- Lechler, T., Shevchenko, A., and Li, R. (2000). Direct involvement of yeast type I myosins in Cdc42-dependent actin polymerization. J Cell Biol *148*, 363-373.
- Lee, S.F., Egelhoff, T.T., Mahasneh, A., and Cote, G.P. (1996). Cloning and characterization of a Dictyostelium myosin I heavy chain kinase activated by Cdc42 and Rac. J Biol Chem *271*, 27044-27048.
- Lee, W.L., Bezanilla, M., and Pollard, T.D. (2000). Fission yeast myosin-I, Myo1p, stimulates actin assembly by Arp2/3 complex and shares functions with WASp. J Cell Biol *151*, 789-800.
- Lees-Miller, J.P., Henry, G., and Helfman, D.M. (1992). Identification of act2, an essential gene in the fission yeast Schizosaccharomyces pombe that encodes a protein related to actin. Proc Natl Acad Sci U S A *89*, 80-83.
- Legesse-Miller, A., Zhang, S., Santiago-Tirado, F.H., Van Pelt, C.K., and Bretscher, A. (2006). Regulated phosphorylation of budding yeast's essential myosin V heavy chain, Myo2p. Mol Biol Cell *17*, 1812-1821.
- Li, C.R., Wang, Y.M., and Wang, Y. (2008). The IQGAP Iqg1 is a regulatory target of CDK for cytokinesis in Candida albicans. Embo J *27*, 2998-3010.
- Li, X., Gerber, S.A., Rudner, A.D., Beausoleil, S.A., Haas, W., Villen, J., Elias, J.E., and Gygi, S.P. (2007). Large-scale phosphorylation analysis of alpha-factor-arrested Saccharomyces cerevisiae. J Proteome Res *6*, 1190-1197.
- Lila, T., and Drubin, D.G. (1997). Evidence for physical and functional interactions among two Saccharomyces cerevisiae SH3 domain proteins, an adenylyl cyclase-associated protein and the actin cytoskeleton. Mol Biol Cell *8*, 367-385.
- Lin, M.C., Galletta, B.J., Sept, D., and Cooper, J.A. (2010). Overlapping and distinct functions for cofilin, coronin and Aip1 in actin dynamics in vivo. J Cell Sci *123*, 1329-1342.
- Lippincott, J., and Li, R. (1998). Sequential assembly of myosin II, an IQGAP-like protein, and filamentous actin to a ring structure involved in budding yeast cytokinesis. J Cell Biol *140*, 355-366.
- Litchfield, D.W. (2003). Protein kinase CK2: structure, regulation and role in cellular decisions of life and death. Biochem J *369*, 1-15.

- Litchfield, D.W., Lozeman, F.J., Piening, C., Sommercorn, J., Takio, K., Walsh, K.A., and Krebs, E.G. (1990). Subunit structure of casein kinase II from bovine testis. Demonstration that the alpha and alpha' subunits are distinct polypeptides. J Biol Chem *265*, 7638-7644.
- Liu, H.P., and Bretscher, A. (1989a). Disruption of the single tropomyosin gene in yeast results in the disappearance of actin cables from the cytoskeleton. Cell *57*, 233-242.
- Liu, H.P., and Bretscher, A. (1989b). Purification of tropomyosin from Saccharomyces cerevisiae and identification of related proteins in Schizosaccharomyces and Physarum. Proc Natl Acad Sci U S A *86*, 90-93.
- Liu, J., Kaksonen, M., Drubin, D.G., and Oster, G. (2006). Endocytic vesicle scission by lipid phase boundary forces. Proc Natl Acad Sci U S A *103*, 10277-10282.
- Liu, J., Sun, Y., Drubin, D.G., and Oster, G.F. (2009). The mechanochemistry of endocytosis. PLoS Biol *7*, e1000204.
- Loisel, T.P., Boujemaa, R., Pantaloni, D., and Carlier, M.F. (1999). Reconstitution of actin-based motility of Listeria and Shigella using pure proteins. Nature *401*, 613-616.
- Longtine, M.S., McKenzie, A., 3rd, Demarini, D.J., Shah, N.G., Wach, A., Brachat, A., Philippsen, P., and Pringle, J.R. (1998). Additional modules for versatile and economical PCR-based gene deletion and modification in Saccharomyces cerevisiae. Yeast *14*, 953-961.
- Lord, M., Laves, E., and Pollard, T.D. (2005). Cytokinesis depends on the motor domains of myosin-II in fission yeast but not in budding yeast. Mol Biol Cell *16*, 5346-5355.
- Luo, J., Vallen, E.A., Dravis, C., Tcheperegine, S.E., Drees, B., and Bi, E. (2004). Identification and functional analysis of the essential and regulatory light chains of the only type II myosin Myo1p in Saccharomyces cerevisiae. J Cell Biol *165*, 843-855.
- Lynch, T.J., Brzeska, H., Miyata, H., and Korn, E.D. (1989). Purification and characterization of a third isoform of myosin I from Acanthamoeba castellanii. J Biol Chem *264*, 19333-19339.
- Llado, A., Timpson, P., Vila de Muga, S., Moreto, J., Pol, A., Grewal, T., Daly, R.J., Enrich, C., and Tebar, F. (2008). Protein Kinase C{delta} and Calmodulin Regulate Epidermal Growth Factor Receptor Recycling from Early Endosomes through Arp2/3 Complex and Cortactin. Mol Biol Cell *19*, 17-29.
- Machesky, L.M., Atkinson, S.J., Ampe, C., Vandekerckhove, J., and Pollard, T.D. (1994). Purification of a cortical complex containing two unconventional actins from Acanthamoeba by affinity chromatography on profilin-agarose. J Cell Biol *127*, 107-115.
- Machesky, L.M., Mullins, R.D., Higgs, H.N., Kaiser, D.A., Blanchoin, L., May, R.C., Hall, M.E., and Pollard, T.D. (1999). Scar, a WASp-related protein, activates nucleation of actin filaments by the Arp2/3 complex. Proc Natl Acad Sci U S A *96*, 3739-3744.
- Magdolen, V., Oechsner, U., Muller, G., and Bandlow, W. (1988). The intron-containing gene for yeast profilin (PFY) encodes a vital function. Mol Cell Biol *8*, 5108-5115.
- Maldonado-Baez, L., Dores, M.R., Perkins, E.M., Drivas, T.G., Hicke, L., and Wendland, B. (2008). Interaction between Epsin/Yap180 adaptors and the scaffolds Ede1/Pan1 is required for endocytosis. Mol Biol Cell *19*, 2936-2948.
- Maldonado-Baez, L., and Wendland, B. (2006). Endocytic adaptors: recruiters, coordinators and regulators. Trends Cell Biol *16*, 505-513.
- Malik, R., Lenobel, R., Santamaria, A., Ries, A., Nigg, E.A., and Korner, R. (2009). Quantitative analysis of the human spindle phosphoproteome at distinct mitotic stages. J Proteome Res *8*, 4553-4563.
- Marchand, J.B., Kaiser, D.A., Pollard, T.D., and Higgs, H.N. (2001). Interaction of WASP/Scar proteins with actin and vertebrate Arp2/3 complex. Nat Cell Biol *3*, 76-82.
- Markovich, S., Yekutiel, A., Shalit, I., Shadkchan, Y., and Osherov, N. (2004). Genomic approach to identification of mutations affecting caspofungin susceptibility in Saccharomyces cerevisiae. Antimicrob Agents Chemother *48*, 3871-3876.
- Martin, A.C., Welch, M.D., and Drubin, D.G. (2006). Arp2/3 ATP hydrolysis-catalysed branch dissociation is critical for endocytic force generation. Nat Cell Biol *8*, 826-833.

- Martin, A.C., Xu, X.P., Rouiller, I., Kaksonen, M., Sun, Y., Belmont, L., Volkmann, N., Hanein, D., Welch, M., and Drubin, D.G. (2005). Effects of Arp2 and Arp3 nucleotide-binding pocket mutations on Arp2/3 complex function. J Cell Biol *168*, 315-328.
- Martinez-Quiles, N., Rohatgi, R., Anton, I.M., Medina, M., Saville, S.P., Miki, H., Yamaguchi, H., Takenawa, T., Hartwig, J.H., Geha, R.S.*, et al.* (2001). WIP regulates N-WASP-mediated actin polymerization and filopodium formation. Nat Cell Biol *3*, 484-491.
- Maruta, H., and Korn, E.D. (1977). Acanthamoeba cofactor protein is a heavy chain kinase required for actin activation of the Mg2+-ATPase activity of Acanthamoeba myosin I. J Biol Chem *252*, 8329-8332.
- Matheos, D., Metodiev, M., Muller, E., Stone, D., and Rose, M.D. (2004). Pheromone-induced polarization is dependent on the Fus3p MAPK acting through the formin Bni1p. J Cell Biol *165*, 99-109.
- Mattila, P.K., Quintero-Monzon, O., Kugler, J., Moseley, J.B., Almo, S.C., Lappalainen, P., and Goode, B.L. (2004). A high-affinity interaction with ADP-actin monomers underlies the mechanism and in vivo function of Srv2/cyclase-associated protein. Mol Biol Cell *15*, 5158-5171.
- Mayor, S., and Pagano, R.E. (2007). Pathways of clathrin-independent endocytosis. Nat Rev Mol Cell Biol *8*, 603-612.
- Maytum, R., Geeves, M.A., and Konrad, M. (2000). Actomyosin regulatory properties of yeast tropomyosin are dependent upon N-terminal modification. Biochemistry *39*, 11913-11920.
- McCann, R.O., and Craig, S.W. (1997). The I/LWEQ module: a conserved sequence that signifies F-actin binding in functionally diverse proteins from yeast to mammals. Proc Natl Acad Sci U S A *94*, 5679-5684.
- McGough, A., Pope, B., Chiu, W., and Weeds, A. (1997). Cofilin changes the twist of F-actin: implications for actin filament dynamics and cellular function. J Cell Biol *138*, 771-781.
- Meggio, F., Marin, O., and Pinna, L.A. (1994). Substrate specificity of protein kinase CK2. Cell Mol Biol Res *40*, 401-409.
- Meggio, F., and Pinna, L.A. (2003). One-thousand-and-one substrates of protein kinase CK2? Faseb J *17*, 349-368.
- Melki, R., Fievez, S., and Carlier, M.F. (1996). Continuous monitoring of Pi release following nucleotide hydrolysis in actin or tubulin assembly using 2-amino-6-mercapto-7-methylpurine ribonucleoside and purine-nucleoside phosphorylase as an enzyme-linked assay. Biochemistry *35*, 12038-12045.
- Merrifield, C.J., Moss, S.E., Ballestrem, C., Imhof, B.A., Giese, G., Wunderlich, I., and Almers, W. (1999). Endocytic vesicles move at the tips of actin tails in cultured mast cells. Nat Cell Biol *1*, 72-74.
- Miyata, H., Bowers, B., and Korn, E.D. (1989). Plasma membrane association of Acanthamoeba myosin I. J Cell Biol *109*, 1519-1528.
- Moon, A.L., Janmey, P.A., Louie, K.A., and Drubin, D.G. (1993). Cofilin is an essential component of the yeast cortical cytoskeleton. J Cell Biol *120*, 421-435.
- Moore, P.B., Huxley, H.E., and DeRosier, D.J. (1970). Three-dimensional reconstruction of F-actin, thin filaments and decorated thin filaments. J Mol Biol *50*, 279-295.
- Moreau, V., Frischknecht, F., Reckmann, I., Vincentelli, R., Rabut, G., Stewart, D., and Way, M. (2000). A complex of N-WASP and WIP integrates signalling cascades that lead to actin polymerization. Nat Cell Biol *2*, 441-448.
- Moreau, V., Galan, J.M., Devilliers, G., Haguenauer-Tsapis, R., and Winsor, B. (1997). The yeast actin-related protein Arp2p is required for the internalization step of endocytosis. Mol Biol Cell *8*, 1361-1375.
- Moreau, V., Madania, A., Martin, R.P., and Winson, B. (1996). The Saccharomyces cerevisiae actin-related protein Arp2 is involved in the actin cytoskeleton. J Cell Biol *134*, 117-132.
- Moriyama, K., and Yahara, I. (2002). Human CAP1 is a key factor in the recycling of cofilin and actin for rapid actin turnover. J Cell Sci *115*, 1591-1601.

- Moseley, J.B., and Goode, B.L. (2006). The yeast actin cytoskeleton: from cellular function to biochemical mechanism. Microbiol Mol Biol Rev *70*, 605-645.
- Moseley, J.B., Okada, K., Balcer, H.I., Kovar, D.R., Pollard, T.D., and Goode, B.L. (2006). Twinfilin is an actin-filament-severing protein and promotes rapid turnover of actin structures in vivo. J Cell Sci *119*, 1547-1557.
- Moseley, J.B., Sagot, I., Manning, A.L., Xu, Y., Eck, M.J., Pellman, D., and Goode, B.L. (2004). A conserved mechanism for Bni1- and mDia1-induced actin assembly and dual regulation of Bni1 by Bud6 and profilin. Mol Biol Cell *15*, 896-907.
- Motizuki, M., Yokota, S., and Tsurugi, K. (2008). Effect of low pH on organization of the actin cytoskeleton in Saccharomyces cerevisiae. Biochim Biophys Acta *1780*, 179-184.
- Mullins, R.D., Heuser, J.A., and Pollard, T.D. (1998). The interaction of Arp2/3 complex with actin: nucleation, high affinity pointed end capping, and formation of branching networks of filaments. Proc Natl Acad Sci U S A *95*, 6181-6186.
- Muniz, M., Morsomme, P., and Riezman, H. (2001). Protein sorting upon exit from the endoplasmic reticulum. Cell *104*, 313-320.
- Munn, A.L., and Riezman, H. (1994). Endocytosis is required for the growth of vacuolar H(+)-ATPase-defective yeast: identification of six new END genes. J Cell Biol *127*, 373-386.
- Munn, A.L., Stevenson, B.J., Geli, M.I., and Riezman, H. (1995). end5, end6, and end7: mutations that cause actin delocalization and block the internalization step of endocytosis in Saccharomyces cerevisiae. Mol Biol Cell *6*, 1721-1742.
- Nakano, K., Satoh, K., Morimatsu, A., Ohnuma, M., and Mabuchi, I. (2001). Interactions among a fimbrin, a capping protein, and an actin-depolymerizing factor in organization of the fission yeast actin cytoskeleton. Mol Biol Cell *12*, 3515-3526.
- Nannapaneni, S., Wang, D., Jain, S., Schroeder, B., Highfill, C., Reustle, L., Pittsley, D., Maysent, A., Moulder, S., McDowell, R.*, et al.* (2010). The yeast dynamin-like protein Vps1:vps1 mutations perturb the internalization and the motility of endocytic vesicles and endosomes via disorganization of the actin cytoskeleton. Eur J Cell Biol *89*, 499-508.
- Naqvi, S.N., Feng, Q., Boulton, V.J., Zahn, R., and Munn, A.L. (2001). Vrp1p functions in both actomyosin ring-dependent and Hof1p-dependent pathways of cytokinesis. Traffic *2*, 189-201.
- Naqvi, S.N., Zahn, R., Mitchell, D.A., Stevenson, B.J., and Munn, A.L. (1998). The WASp homologue Las17p functions with the WIP homologue End5p/verprolin and is essential for endocytosis in yeast. Curr Biol *8*, 959-962.
- Newpher, T.M., and Lemmon, S.K. (2006). Clathrin is important for normal actin dynamics and progression of Sla2p-containing patches during endocytosis in yeast. Traffic *7*, 574-588.
- Newpher, T.M., Smith, R.P., Lemmon, V., and Lemmon, S.K. (2005). In vivo dynamics of clathrin and its adaptor-dependent recruitment to the actin-based endocytic machinery in yeast. Dev Cell *9*, 87-98.
- Niefind, K., Guerra, B., Ermakowa, I., and Issinger, O.G. (2001). Crystal structure of human protein kinase CK2: insights into basic properties of the CK2 holoenzyme. Embo J *20*, 5320-5331.
- Nikolov, M., Schmidt, C., and Urlaub, H. (2012). Quantitative mass spectrometry-based proteomics: an overview. Methods Mol Biol *893*, 85-100.
- Nishida, E. (1985). Opposite effects of cofilin and profilin from porcine brain on rate of exchange of actin-bound adenosine 5'-triphosphate. Biochemistry *24*, 1160-1164.
- Noma, A., Yi, S., Katoh, T., Takai, Y., and Suzuki, T. (2011). Actin-binding protein ABP140 is a methyltransferase for 3-methylcytidine at position 32 of tRNAs in Saccharomyces cerevisiae. RNA *17*, 1111-1119.
- Novak, K.D., and Titus, M.A. (1998). The myosin I SH3 domain and TEDS rule phosphorylation site are required for in vivo function. Mol Biol Cell *9*, 75-88.
- Ojala, P.J., Paavilainen, V., and Lappalainen, P. (2001). Identification of yeast cofilin residues specific for actin monomer and PIP2 binding. Biochemistry *40*, 15562-15569.

- Okada, K., Ravi, H., Smith, E.M., and Goode, B.L. (2006). Aip1 and cofilin promote rapid turnover of yeast actin patches and cables: a coordinated mechanism for severing and capping filaments. Mol Biol Cell *17*, 2855-2868.
- Okreglak, V., and Drubin, D.G. (2007). Cofilin recruitment and function during actin-mediated endocytosis dictated by actin nucleotide state. J Cell Biol *178*, 1251-1264.
- Okreglak, V., and Drubin, D.G. (2010). Loss of Aip1 reveals a role in maintaining the actin monomer pool and an in vivo oligomer assembly pathway. J Cell Biol *188*, 769-777.
- Olsen, J.V., Vermeulen, M., Santamaria, A., Kumar, C., Miller, M.L., Jensen, L.J., Gnad, F., Cox, J., Jensen, T.S., Nigg, E.A*., et al.* (2010). Quantitative phosphoproteomics reveals widespread full phosphorylation site occupancy during mitosis. Sci Signal *3*, ra3.
- Olsten, M.E., Canton, D.A., Zhang, C., Walton, P.A., and Litchfield, D.W. (2004). The Pleckstrin homology domain of CK2 interacting protein-1 is required for interactions and recruitment of protein kinase CK2 to the plasma membrane. J Biol Chem *279*, 42114-42127.
- Oosawa, F., and S. Asakura. (1975). Thermodynamics of the Polymerization of Protein. (New York.).
- Orlova, A., and Egelman, E.H. (1992). Structural basis for the destabilization of F-actin by phosphate release following ATP hydrolysis. J Mol Biol *227*, 1043-1053.
- Padmanabha, R., Chen-Wu, J.L., Hanna, D.E., and Glover, C.V. (1990). Isolation, sequencing, and disruption of the yeast CKA2 gene: casein kinase II is essential for viability in Saccharomyces cerevisiae. Mol Cell Biol *10*, 4089-4099.
- Palmgren, S., Ojala, P.J., Wear, M.A., Cooper, J.A., and Lappalainen, P. (2001). Interactions with PIP2, ADP-actin monomers, and capping protein regulate the activity and localization of yeast twinfilin. J Cell Biol *155*, 251-260.
- Pan, F., Egile, C., Lipkin, T., and Li, R. (2004). ARPC1/Arc40 mediates the interaction of the actin-related protein 2 and 3 complex with Wiskott-Aldrich syndrome protein family activators. J Biol Chem *279*, 54629-54636.
- Pantaloni, D., and Carlier, M.F. (1993). How profilin promotes actin filament assembly in the presence of thymosin beta 4. Cell *75*, 1007-1014.
- Payne, G.S., Baker, D., van Tuinen, E., and Schekman, R. (1988). Protein transport to the vacuole and receptor-mediated endocytosis by clathrin heavy chain-deficient yeast. J Cell Biol *106*, 1453-1461.
- Pinna, L.A. (2002). Protein kinase CK2: a challenge to canons. J Cell Sci *115*, 3873-3878.
- Pocha, S.M., and Cory, G.O. (2009). WAVE2 is regulated by multiple phosphorylation events within its VCA domain. Cell Motil Cytoskeleton *66*, 36-47.
- Pollard, T.D. (1986). Rate constants for the reactions of ATP- and ADP-actin with the ends of actin filaments. J Cell Biol *103*, 2747-2754.
- Pollard, T.D. (2007). Regulation of actin filament assembly by Arp2/3 complex and formins. Annu Rev Biophys Biomol Struct *36*, 451-477.
- Pollard, T.D., Blanchoin, L., and Mullins, R.D. (2000). Molecular mechanisms controlling actin filament dynamics in nonmuscle cells. Annu Rev Biophys Biomol Struct *29*, 545-576.
- Pollard, T.D., and Borisy, G.G. (2003). Cellular motility driven by assembly and disassembly of actin filaments. Cell *112*, 453-465.
- Pollard, T.D., and Cooper, J.A. (1984). Quantitative analysis of the effect of Acanthamoeba profilin on actin filament nucleation and elongation. Biochemistry *23*, 6631-6641.
- Pollard, T.D., and Cooper, J.A. (1986). Actin and actin-binding proteins. A critical evaluation of mechanisms and functions. Annu Rev Biochem *55*, 987-1035.
- Pollard, T.D., Doberstein, S.K., and Zot, H.G. (1991). Myosin-I. Annu Rev Physiol *53*, 653-681.
- Pollard, T.D., and Korn, E.D. (1973). Acanthamoeba myosin. I. Isolation from Acanthamoeba castellanii of an enzyme similar to muscle myosin. J Biol Chem *248*, 4682-4690.

- Pring, M., Evangelista, M., Boone, C., Yang, C., and Zigmond, S.H. (2003). Mechanism of formin-induced nucleation of actin filaments. Biochemistry *42*, 486-496.
- Pring, M., Weber, A., and Bubb, M.R. (1992). Profilin-actin complexes directly elongate actin filaments at the barbed end. Biochemistry *31*, 1827-1836.
- Prosser, D.C., Drivas, T.G., Maldonado-Baez, L., and Wendland, B. (2011). Existence of a novel clathrin-independent endocytic pathway in yeast that depends on Rho1 and formin. J Cell Biol *195*, 657-671.
- Pruyne, D., Evangelista, M., Yang, C., Bi, E., Zigmond, S., Bretscher, A., and Boone, C. (2002). Role of formins in actin assembly: nucleation and barbed-end association. Science *297*, 612-615.
- Pruyne, D., Gao, L., Bi, E., and Bretscher, A. (2004a). Stable and dynamic axes of polarity use distinct formin isoforms in budding yeast. Mol Biol Cell *15*, 4971-4989.
- Pruyne, D., Legesse-Miller, A., Gao, L., Dong, Y., and Bretscher, A. (2004b). Mechanisms of polarized growth and organelle segregation in yeast. Annu Rev Cell Dev Biol *20*, 559-591.
- Pucadyil, T.J., and Schmid, S.L. (2008). Real-time visualization of dynamin-catalyzed membrane fission and vesicle release. Cell *135*, 1263-1275.
- Quinlan, M.E., Heuser, J.E., Kerkhoff, E., and Mullins, R.D. (2005). Drosophila Spire is an actin nucleation factor. Nature *433*, 382-388.
- Quintero-Monzon, O., Jonasson, E.M., Bertling, E., Talarico, L., Chaudhry, F., Sihvo, M., Lappalainen, P., and Goode, B.L. (2009). Reconstitution and dissection of the 600-kDa Srv2/CAP complex: roles for oligomerization and cofilin-actin binding in driving actin turnover. J Biol Chem *284*, 10923-10934.
- Raijmakers, R., Kraiczek, K., de Jong, A.P., Mohammed, S., and Heck, A.J. (2010). Exploring the human leukocyte phosphoproteome using a microfluidic reversed-phase-TiO2-reversed-phase high-performance liquid chromatography phosphochip coupled to a quadrupole time-of-flight mass spectrometer. Anal Chem *82*, 824-832.
- Rao, Y., and Haucke, V. (2011). Membrane shaping by the Bin/amphiphysin/Rvs (BAR) domain protein superfamily. Cell Mol Life Sci *68*, 3983-3993.
- Raths, S., Rohrer, J., Crausaz, F., and Riezman, H. (1993). end3 and end4: two mutants defective in receptor-mediated and fluid-phase endocytosis in Saccharomyces cerevisiae. J Cell Biol *120*, 55-65.
- Reck-Peterson, S.L., Tyska, M.J., Novick, P.J., and Mooseker, M.S. (2001). The yeast class V myosins, Myo2p and Myo4p, are nonprocessive actin-based motors. J Cell Biol *153*, 1121-1126.
- Redowicz, M.J. (2001). Regulation of nonmuscle myosins by heavy chain phosphorylation. J Muscle Res Cell Motil *22*, 163-173.
- Reed, J.C., Bidwai, A.P., and Glover, C.V. (1994). Cloning and disruption of CKB2, the gene encoding the 32-kDa regulatory beta'-subunit of Saccharomyces cerevisiae casein kinase II. J Biol Chem *269*, 18192-18200.
- Reider, A., Barker, S.L., Mishra, S.K., Im, Y.J., Maldonado-Baez, L., Hurley, J.H., Traub, L.M., and Wendland, B. (2009). Syp1 is a conserved endocytic adaptor that contains domains involved in cargo selection and membrane tubulation. Embo J *28*, 3103-3116.
- Rethinaswamy, A., Birnbaum, M.J., and Glover, C.V. (1998). Temperature-sensitive mutations of the CKA1 gene reveal a role for casein kinase II in maintenance of cell polarity in Saccharomyces cerevisiae. J Biol Chem *273*, 5869-5877.
- Ridley, A.J. (2006). Rho GTPases and actin dynamics in membrane protrusions and vesicle trafficking. Trends Cell Biol *16*, 522-529.
- Robinson, R.C., Turbedsky, K., Kaiser, D.A., Marchand, J.B., Higgs, H.N., Choe, S., and Pollard, T.D. (2001). Crystal structure of Arp2/3 complex. Science *294*, 1679-1684.
- Rodal, A.A., Manning, A.L., Goode, B.L., and Drubin, D.G. (2003). Negative regulation of yeast WASp by two SH3 domain-containing proteins. Curr Biol *13*, 1000-1008.
- Rodal, A.A., Sokolova, O., Robins, D.B., Daugherty, K.M., Hippenmeyer, S., Riezman, H., Grigorieff, N., and Goode, B.L. (2005). Conformational changes in the Arp2/3 complex leading to actin nucleation. Nat Struct Mol Biol *12*, 26-31.

- Rohatgi, R., Ma, L., Miki, H., Lopez, M., Kirchhausen, T., Takenawa, T., and Kirschner, M.W. (1999). The interaction between N-WASP and the Arp2/3 complex links Cdc42-dependent signals to actin assembly. Cell *97*, 221-231.
- Rosenfeld, S.S., and Rener, B. (1994). The GPQ-rich segment of Dictyostelium myosin IB contains an actin binding site. Biochemistry *33*, 2322-2328.
- Rouiller, I., Xu, X.P., Amann, K.J., Egile, C., Nickell, S., Nicastro, D., Li, R., Pollard, T.D., Volkmann, N., and Hanein, D. (2008). The structural basis of actin filament branching by the Arp2/3 complex. J Cell Biol *180*, 887-895.
- Roux, A., Uyhazi, K., Frost, A., and De Camilli, P. (2006). GTP-dependent twisting of dynamin implicates constriction and tension in membrane fission. Nature *441*, 528-531.
- Safer, D., Elzinga, M., and Nachmias, V.T. (1991). Thymosin beta 4 and Fx, an actin-sequestering peptide, are indistinguishable. J Biol Chem *266*, 4029-4032.
- Safer, D., Golla, R., and Nachmias, V.T. (1990). Isolation of a 5-kilodalton actin-sequestering peptide from human blood platelets. Proc Natl Acad Sci U S A *87*, 2536-2540.
- Sagot, I., Klee, S.K., and Pellman, D. (2002a). Yeast formins regulate cell polarity by controlling the assembly of actin cables. Nat Cell Biol *4*, 42-50.
- Sagot, I., Rodal, A.A., Moseley, J., Goode, B.L., and Pellman, D. (2002b). An actin nucleation mechanism mediated by Bni1 and profilin. Nat Cell Biol *4*, 626-631.
- Sambrook, J., and Russell, D.W. (2001). Molecular cloning : a laboratory manual, 3rd edn (Cold Spring Harbor, N.Y., Cold Spring Harbor Laboratory Press).
- Sarrouilhe, D., Filhol, O., Leroy, D., Bonello, G., Baudry, M., Chambaz, E.M., and Cochet, C. (1998). The tight association of protein kinase CK2 with plasma membranes is mediated by a specific domain of its regulatory beta-subunit. Biochim Biophys Acta *1403*, 199-210.
- Schmidt, O., Harbauer, A.B., Rao, S., Eyrich, B., Zahedi, R.P., Stojanovski, D., Schonfisch, B., Guiard, B., Sickmann, A., Pfanner, N.*, et al.* (2011). Regulation of mitochondrial protein import by cytosolic kinases. Cell *144*, 227-239.
- Schutt, C.E., Myslik, J.C., Rozycki, M.D., Goonesekere, N.C., and Lindberg, U. (1993). The structure of crystalline profilin-beta-actin. Nature *365*, 810-816.
- Schwob, E., and Martin, R.P. (1992). New yeast actin-like gene required late in the cell cycle. Nature *355*, 179-182.
- Seeley, E.S., Kato, M., Margolis, N., Wickner, W., and Eitzen, G. (2002). Genomic analysis of homotypic vacuole fusion. Mol Biol Cell *13*, 782-794.
- Sekiya-Kawasaki, M., Groen, A.C., Cope, M.J., Kaksonen, M., Watson, H.A., Zhang, C., Shokat, K.M., Wendland, B., McDonald, K.L., McCaffery, J.M.*, et al.* (2003). Dynamic phosphoregulation of the cortical actin cytoskeleton and endocytic machinery revealed by real-time chemical genetic analysis. J Cell Biol *162*, 765-772.
- Sellers, J.R. (2000). Myosins: a diverse superfamily. Biochim Biophys Acta *1496*, 3-22.
- Sellers, J.R., and Veigel, C. (2006). Walking with myosin V. Curr Opin Cell Biol *18*, 68-73.
- Sept, D., and McCammon, J.A. (2001). Thermodynamics and kinetics of actin filament nucleation. Biophys J *81*, 667-674.
- Shannon, K.B., and Li, R. (2000). A myosin light chain mediates the localization of the budding yeast IQGAP-like protein during contractile ring formation. Curr Biol *10*, 727-730.
- Shao, J., Welch, W.J., Diprospero, N.A., and Diamond, M.I. (2008). Phosphorylation of profilin by ROCK1 regulates polyglutamine aggregation. Mol Cell Biol *28*, 5196-5208.
- Sherman, F. (1991). Getting started with yeast. Methods Enzymol *194*, 3-21.
- Shi, X., Potvin, B., Huang, T., Hilgard, P., Spray, D.C., Suadicani, S.O., Wolkoff, A.W., Stanley, P., and Stockert, R.J. (2001). A novel casein kinase 2 alpha-subunit regulates membrane protein traffic in the human hepatoma cell line HuH-7. J Biol Chem *276*, 2075-2082.

- Singer-Kruger, B., Nemoto, Y., Daniell, L., Ferro-Novick, S., and De Camilli, P. (1998). Synaptojanin family members are implicated in endocytic membrane traffic in yeast. J Cell Sci *111 (Pt 22)*, 3347-3356.
- Slepnev, V.I., Ochoa, G.C., Butler, M.H., Grabs, D., and De Camilli, P. (1998). Role of phosphorylation in regulation of the assembly of endocytic coat complexes. Science *281*, 821-824.
- Smaczynska-de, R., II, Allwood, E.G., Aghamohammadzadeh, S., Hettema, E.H., Goldberg, M.W., and Ayscough, K.R. (2010). A role for the dynamin-like protein Vps1 during endocytosis in yeast. J Cell Sci *123*, 3496-3506.
- Smolka, M.B., Albuquerque, C.P., Chen, S.H., and Zhou, H. (2007). Proteome-wide identification of in vivo targets of DNA damage checkpoint kinases. Proc Natl Acad Sci U S A *104*, 10364-10369.
- Soldati, T., and Schliwa, M. (2006). Powering membrane traffic in endocytosis and recycling. Nat Rev Mol Cell Biol *7*, 897-908.
- Soulard, A., Lechler, T., Spiridonov, V., Shevchenko, A., Shevchenko, A., Li, R., and Winsor, B. (2002). Saccharomyces cerevisiae Bzz1p is implicated with type I myosins in actin patch polarization and is able to recruit actin-polymerizing machinery in vitro. Mol Cell Biol *22*, 7889-7906.
- Southwick, F.S., Li, W., Zhang, F., Zeile, W.L., and Purich, D.L. (2003). Actin-based endosome and phagosome rocketing in macrophages: activation by the secretagogue antagonists lanthanum and zinc. Cell Motil Cytoskeleton *54*, 41-55.
- St-Denis, N.A., and Litchfield, D.W. (2009). Protein kinase CK2 in health and disease: From birth to death: the role of protein kinase CK2 in the regulation of cell proliferation and survival. Cell Mol Life Sci *66*, 1817-1829.
- Stefan, C.J., Padilla, S.M., Audhya, A., and Emr, S.D. (2005). The phosphoinositide phosphatase Sjl2 is recruited to cortical actin patches in the control of vesicle formation and fission during endocytosis. Mol Cell Biol *25*, 2910-2923.
- Stevens, R.C., and Davis, T.N. (1998). Mlc1p is a light chain for the unconventional myosin Myo2p in Saccharomyces cerevisiae. J Cell Biol *142*, 711-722.
- Stevens, T., Esmon, B., and Schekman, R. (1982). Early stages in the yeast secretory pathway are required for transport of carboxypeptidase Y to the vacuole. Cell *30*, 439-448.
- Stimpson, H.E., Toret, C.P., Cheng, A.T., Pauly, B.S., and Drubin, D.G. (2009). Early-arriving Syp1p and Ede1p function in endocytic site placement and formation in budding yeast. Mol Biol Cell *20*, 4640-4651.
- Sun, Y., Carroll, S., Kaksonen, M., Toshima, J.Y., and Drubin, D.G. (2007). PtdIns(4,5)P2 turnover is required for multiple stages during clathrin- and actin-dependent endocytic internalization. J Cell Biol *177*, 355-367.
- Sun, Y., Kaksonen, M., Madden, D.T., Schekman, R., and Drubin, D.G. (2005). Interaction of Sla2p's ANTH domain with PtdIns(4,5)P2 is important for actin-dependent endocytic internalization. Mol Biol Cell *16*, 717-730.
- Sun, Y., Martin, A.C., and Drubin, D.G. (2006). Endocytic internalization in budding yeast requires coordinated actin nucleation and myosin motor activity. Dev Cell *11*, 33-46.
- Suzuki, R., Toshima, J.Y., and Toshima, J. (2012). Regulation of clathrin coat assembly by Eps15 homology domain-mediated interactions during endocytosis. Mol Biol Cell *23*, 687-700.
- Takenawa, T., and Suetsugu, S. (2007). The WASP-WAVE protein network: connecting the membrane to the cytoskeleton. Nat Rev Mol Cell Biol *8*, 37-48.
- Tang, H.Y., and Cai, M. (1996). The EH-domain-containing protein Pan1 is required for normal organization of the actin cytoskeleton in Saccharomyces cerevisiae. Mol Cell Biol *16*, 4897-4914.
- Taunton, J., Rowning, B.A., Coughlin, M.L., Wu, M., Moon, R.T., Mitchison, T.J., and Larabell, C.A. (2000). Actin-dependent propulsion of endosomes and lysosomes by recruitment of N-WASP. J Cell Biol *148*, 519-530.
- Taylor, M.J., Lampe, M., and Merrifield, C.J. (2012). A feedback loop between dynamin and actin recruitment during clathrin-mediated endocytosis. PLoS Biol *10*, e1001302.

- Theriot, J.A., and Mitchison, T.J. (1991). Actin microfilament dynamics in locomoting cells. Nature *352*, 126-131.
- Tolliday, N., VerPlank, L., and Li, R. (2002). Rho1 directs formin-mediated actin ring assembly during budding yeast cytokinesis. Curr Biol *12*, 1864-1870.
- Tonikian, R., Xin, X., Toret, C.P., Gfeller, D., Landgraf, C., Panni, S., Paoluzi, S., Castagnoli, L., Currell, B., Seshagiri, S.*, et al.* (2009). Bayesian modeling of the yeast SH3 domain interactome predicts spatiotemporal dynamics of endocytosis proteins. PLoS Biol *7*, e1000218.
- Toret, C.P., Lee, L., Sekiya-Kawasaki, M., and Drubin, D.G. (2008). Multiple pathways regulate endocytic coat disassembly in Saccharomyces cerevisiae for optimal downstream trafficking. Traffic *9*, 848-859.
- Toshima, J., Toshima, J.Y., Duncan, M.C., Cope, M.J., Sun, Y., Martin, A.C., Anderson, S., Yates, J.R., 3rd, Mizuno, K., and Drubin, D.G. (2007). Negative regulation of yeast Eps15-like Arp2/3 complex activator, Pan1p, by the Hip1R-related protein, Sla2p, during endocytosis. Mol Biol Cell *18*, 658-668.
- Toshima, J., Toshima, J.Y., Martin, A.C., and Drubin, D.G. (2005). Phosphoregulation of Arp2/3-dependent actin assembly during receptor-mediated endocytosis. Nat Cell Biol *7*, 246-254.
- Toshima, J.Y., Toshima, J., Kaksonen, M., Martin, A.C., King, D.S., and Drubin, D.G. (2006). Spatial dynamics of receptor-mediated endocytic trafficking in budding yeast revealed by using fluorescent alpha-factor derivatives. Proc Natl Acad Sci U S A *103*, 5793-5798.
- Trybus, K.M. (2008). Myosin V from head to tail. Cell Mol Life Sci *65*, 1378-1389.
- Uruno, T., Liu, J., Zhang, P., Fan, Y., Egile, C., Li, R., Mueller, S.C., and Zhan, X. (2001). Activation of Arp2/3 complex-mediated actin polymerization by cortactin. Nat Cell Biol *3*, 259-266.
- Vaduva, G., Martin, N.C., and Hopper, A.K. (1997). Actin-binding verprolin is a polarity development protein required for the morphogenesis and function of the yeast actin cytoskeleton. J Cell Biol *139*, 1821-1833.
- Vaduva, G., Martinez-Quiles, N., Anton, I.M., Martin, N.C., Geha, R.S., Hopper, A.K., and Ramesh, N. (1999). The human WASP-interacting protein, WIP, activates the cell polarity pathway in yeast. J Biol Chem *274*, 17103-17108.
- van der Bliek, A.M., Redelmeier, T.E., Damke, H., Tisdale, E.J., Meyerowitz, E.M., and Schmid, S.L. (1993). Mutations in human dynamin block an intermediate stage in coated vesicle formation. J Cell Biol *122*, 553-563.
- van Deurs, B., Holm, P.K., Kayser, L., and Sandvig, K. (1995). Delivery to lysosomes in the human carcinoma cell line HEp-2 involves an actin filament-facilitated fusion between mature endosomes and preexisting lysosomes. Eur J Cell Biol *66*, 309-323.
- Van Troys, M., Huyck, L., Leyman, S., Dhaese, S., Vandekerkhove, J., and Ampe, C. (2008). Ins and outs of ADF/cofilin activity and regulation. Eur J Cell Biol *87*, 649-667.
- van Tuinen, E., and Riezman, H. (1987). Immunolocalization of glyceraldehyde-3-phosphate dehydrogenase, hexokinase, and carboxypeptidase Y in yeast cells at the ultrastructural level. J Histochem Cytochem *35*, 327-333.
- Vavylonis, D., Kovar, D.R., O'Shaughnessy, B., and Pollard, T.D. (2006). Model of formin-associated actin filament elongation. Mol Cell *21*, 455-466.
- Vilk, G., Saulnier, R.B., St Pierre, R., and Litchfield, D.W. (1999). Inducible expression of protein kinase CK2 in mammalian cells. Evidence for functional specialization of CK2 isoforms. J Biol Chem *274*, 14406-14414.
- Vojtek, A., Haarer, B., Field, J., Gerst, J., Pollard, T.D., Brown, S., and Wigler, M. (1991). Evidence for a functional link between profilin and CAP in the yeast S. cerevisiae. Cell *66*, 497-505.
- Vorobiev, S., Strokopytov, B., Drubin, D.G., Frieden, C., Ono, S., Condeelis, J., Rubenstein, P.A., and Almo, S.C. (2003). The structure of nonvertebrate actin: implications for the ATP hydrolytic mechanism. Proc Natl Acad Sci U S A *100*, 5760-5765.
- Waddle, J.A., Cooper, J.A., and Waterston, R.H. (1993). The alpha and beta subunits of nematode actin capping protein function in yeast. Mol Biol Cell *4*, 907-917.

- Wang, J., Neo, S.P., and Cai, M. (2009). Regulation of the yeast formin Bni1p by the actin-regulating kinase Prk1p. Traffic *10*, 528-535.
- Wang, L., Seeley, E.S., Wickner, W., and Merz, A.J. (2002). Vacuole fusion at a ring of vertex docking sites leaves membrane fragments within the organelle. Cell *108*, 357-369.
- Watts, F.Z., Miller, D.M., and Orr, E. (1985). Identification of myosin heavy chain in Saccharomyces cerevisiae. Nature *316*, 83-85.
- Wawro, B., Greenfield, N.J., Wear, M.A., Cooper, J.A., Higgs, H.N., and Hitchcock-DeGregori, S.E. (2007). Tropomyosin regulates elongation by formin at the fast-growing end of the actin filament. Biochemistry *46*, 8146-8155.
- Weaver, A.M., Karginov, A.V., Kinley, A.W., Weed, S.A., Li, Y., Parsons, J.T., and Cooper, J.A. (2001). Cortactin promotes and stabilizes Arp2/3-induced actin filament network formation. Curr Biol *11*, 370-374.
- Weber, A., Pennise, C.R., Babcock, G.G., and Fowler, V.M. (1994). Tropomodulin caps the pointed ends of actin filaments. J Cell Biol *127*, 1627-1635.
- Wegner, A. (1976). Head to tail polymerization of actin. J Mol Biol *108*, 139-150.
- Weinberg, J., and Drubin, D.G. (2012). Clathrin-mediated endocytosis in budding yeast. Trends Cell Biol *22*, 1-13.
- Welch, M.D., Iwamatsu, A., and Mitchison, T.J. (1997). Actin polymerization is induced by Arp2/3 protein complex at the surface of Listeria monocytogenes. Nature *385*, 265-269.
- Welch, M.D., Rosenblatt, J., Skoble, J., Portnoy, D.A., and Mitchison, T.J. (1998). Interaction of human Arp2/3 complex and the Listeria monocytogenes ActA protein in actin filament nucleation. Science *281*, 105-108.
- Wen, K.K., and Rubenstein, P.A. (2005). Acceleration of yeast actin polymerization by yeast Arp2/3 complex does not require an Arp2/3-activating protein. J Biol Chem *280*, 24168-24174.
- Wendland, B., Steece, K.E., and Emr, S.D. (1999). Yeast epsins contain an essential N-terminal ENTH domain, bind clathrin and are required for endocytosis. Embo J *18*, 4383-4393.
- Whittaker, M., and Milligan, R.A. (1997). Conformational changes due to calcium-induced calmodulin dissociation in brush border myosin I-decorated F-actin revealed by cryoelectron microscopy and image analysis. J Mol Biol *269*, 548-557.
- Wickner, W. (2002). Yeast vacuoles and membrane fusion pathways. Embo J *21*, 1241-1247.
- Wickstead, B., and Gull, K. (2011). The evolution of the cytoskeleton. J Cell Biol *194*, 513-525.
- Wilde, A., and Brodsky, F.M. (1996). In vivo phosphorylation of adaptors regulates their interaction with clathrin. J Cell Biol *135*, 635-645.
- Williams, R., and Coluccio, L.M. (1994). Novel 130-kDa rat liver myosin-1 will translocate actin filaments. Cell Motil Cytoskeleton *27*, 41-48.
- Winder, S.J., Jess, T., and Ayscough, K.R. (2003). SCP1 encodes an actin-bundling protein in yeast. Biochem J *375*, 287-295.
- Winter, D., Lechler, T., and Li, R. (1999a). Activation of the yeast Arp2/3 complex by Bee1p, a WASP-family protein. Curr Biol *9*, 501-504.
- Winter, D., Podtelejnikov, A.V., Mann, M., and Li, R. (1997). The complex containing actin-related proteins Arp2 and Arp3 is required for the motility and integrity of yeast actin patches. Curr Biol *7*, 519-529.
- Winter, D.C., Choe, E.Y., and Li, R. (1999b). Genetic dissection of the budding yeast Arp2/3 complex: a comparison of the in vivo and structural roles of individual subunits. Proc Natl Acad Sci U S A *96*, 7288-7293.
- Wolven, A.K., Belmont, L.D., Mahoney, N.M., Almo, S.C., and Drubin, D.G. (2000). In vivo importance of actin nucleotide exchange catalyzed by profilin. J Cell Biol *150*, 895-904.

- Woodrum, D.T., Rich, S.A., and Pollard, T.D. (1975). Evidence for biased bidirectional polymerization of actin filaments using heavy meromyosin prepared by an improved method. J Cell Biol *67*, 231-237.
- Wu, C., Lytvyn, V., Thomas, D.Y., and Leberer, E. (1997). The phosphorylation site for Ste20p-like protein kinases is essential for the function of myosin-I in yeast. J Biol Chem *272*, 30623-30626.
- Wu, R., Dephoure, N., Haas, W., Huttlin, E.L., Zhai, B., Sowa, M.E., and Gygi, S.P. (2011). Correct interpretation of comprehensive phosphorylation dynamics requires normalization by protein expression changes. Mol Cell Proteomics *10*, M111 009654.
- Xie, M.W., Jin, F., Hwang, H., Hwang, S., Anand, V., Duncan, M.C., and Huang, J. (2005). Insights into TOR function and rapamycin response: chemical genomic profiling by using a high-density cell array method. Proc Natl Acad Sci U S A *102*, 7215-7220.
- Yamada, H., Padilla-Parra, S., Park, S.J., Itoh, T., Chaineau, M., Monaldi, I., Cremona, O., Benfenati, F., De Camilli, P., Coppey-Moisan, M.*, et al.* (2009). Dynamic interaction of amphiphysin with N-WASP regulates actin assembly. J Biol Chem *284*, 34244-34256.
- Yang, H.C., and Pon, L.A. (2002). Actin cable dynamics in budding yeast. Proc Natl Acad Sci U S A *99*, 751-756.
- Yang, S., Cope, M.J., and Drubin, D.G. (1999). Sla2p is associated with the yeast cortical actin cytoskeleton via redundant localization signals. Mol Biol Cell *10*, 2265-2283.
- Yao, X., and Rubenstein, P.A. (2001). F-actin-like ATPase activity in a polymerization-defective mutant yeast actin (V266G/L267G). J Biol Chem *276*, 25598-25604.
- Yarar, D., To, W., Abo, A., and Welch, M.D. (1999). The Wiskott-Aldrich syndrome protein directs actin-based motility by stimulating actin nucleation with the Arp2/3 complex. Curr Biol *9*, 555-558.
- Yarar, D., Waterman-Storer, C.M., and Schmid, S.L. (2005). A dynamic actin cytoskeleton functions at multiple stages of clathrin-mediated endocytosis. Mol Biol Cell *16*, 964-975.
- Young, M.E., Cooper, J.A., and Bridgman, P.C. (2004). Yeast actin patches are networks of branched actin filaments. J Cell Biol *166*, 629-635.
- Yu, L., Lopez, A., Anaflous, A., El Bali, B., Hamal, A., Ericson, E., Heisler, L.E., McQuibban, A., Giaever, G., Nislow, C.*, et al.* (2008). Chemical-genetic profiling of imidazo[1,2-a]pyridines and -pyrimidines reveals target pathways conserved between yeast and human cells. PLoS Genet *4*, e1000284.
- Zahner, J.E., Harkins, H.A., and Pringle, J.R. (1996). Genetic analysis of the bipolar pattern of bud site selection in the yeast Saccharomyces cerevisiae. Mol Cell Biol *16*, 1857-1870.
- Zeng, G., and Cai, M. (1999). Regulation of the actin cytoskeleton organization in yeast by a novel serine/threonine kinase Prk1p. J Cell Biol *144*, 71-82.
- Zeng, G., Huang, B., Neo, S.P., Wang, J., and Cai, M. (2007). Scd5p mediates phosphoregulation of actin and endocytosis by the type 1 phosphatase Glc7p in yeast. Mol Biol Cell 18, 4885-4898.
- Zeng, G., Yu, X., and Cai, M. (2001). Regulation of yeast actin cytoskeleton-regulatory complex Pan1p/Sla1p/End3p by serine/threonine kinase Prk1p. Mol Biol Cell *12*, 3759-3772.
- Zuchero, J.B., Coutts, A.S., Quinlan, M.E., Thangue, N.B., and Mullins, R.D. (2009). p53-cofactor JMY is a multifunctional actin nucleation factor. Nat Cell Biol *11*, 451-459.

8. RESUMEN DEL PROYECTO

8.1. Introducción

La levadura *S. cerevisiae* es un organismo modelo muy utilizado para estudiar los mecanismos moleculares que regulan el citoesqueleto actina y su función biológica, debido a que se pueden aplicar con relativa facilidad métodos de biología molecular, genética, bioquímica, o microscopía de fluorescencia *in vivo*. Asimismo, los mecanismos moleculares que controlan la organización del citoesqueleto de actina están conservados, por lo que muchos de los descubrimientos realizados en *S. cerevisiae* son aplicables también en eucariotas superiores.

8.1.1. Mecanismos moleculares de la remodelación del citoesqueleto de actina

La primera fase de formación de un filamento de actina, que consiste en la asociación de dos o tres subunidades de actina unidas a ATP, se denomina nucleación. Una vez formado el núcleo la G-actina (forma monomérica) se une al filamento en función de su concentración. En el estado estacionario la adición de ATP-actina es favorable en el denominado extremo (+). Una vez la actina se une al filamento el ATP se hidroliza, produciendo ADP + P_i unido al monómero. La consiguiente liberación del P_i provoca la disociación de ADP-actina en el extremo (-). Posteriormente se intercambia el nucleótido ADP por ATP para empezar un nuevo ciclo de polimerización (Figura 1). Aunque la secuencia de aminoácidos de la actina de *S. cerevisiae* (Act1) sólo difiere en un 9% a la actina de mamíferos y su estructura es prácticamente idéntica, su actividad bioquímica es ligeramente diferente. Por ejemplo, en la actina de levadura liberación del P_i es simultánea a la hidrólisis de ATP, por lo que la polimerización de actina de levadura es más rápida que la de su homólogo en mamíferos. En la Tabla 1 se muestra un listado con los reguladores de actina de *S. cerevisiae,* y en la figura 2 se ilustran sus funciones moleculares más relevantes.

La estabilización del núcleo de actina es realizada por los nucleadores de actina. *S. cerevisiae* contiene 2 tipos de nucleadores: las forminas y el complejo Arp2/3, dos tipos de nucleadores altamente conservados en organismos eucariotas. Las forminas catalizan la formación de estructuras de actina lineales, como las fibras de estrés, filopodia, o los cables de actina polarizados. *S. cerevisiae* contiene 2 forminas funcionalmente redundantes, Bni1 y Bnr1. El mecanismo de nucleación y elongación del filamento de actina mediante las forminas se resume en la Figura 4A. Por su parte el complejo Arp2/3, formado por 7 proteínas -Arp2, Arp3 (estas dos proteínas son muy similares a la actina y mimetizan la formación de un dímero de actina), Arpc1 (Arc40 en levadura), Arpc2 (Arc35), Arpc3 (Arc18), Arpc4 (Arc19), y Arpc5 (Arc15)-, se acopla en un filamento preexistente con un ángulo de aproximadamente 70º dando lugar a una estructura de actina ramificada con el complejo Arp2/3 en la junta entre el filamento inicial y el extremo (-) del nuevo filamento (ver mecanismo en la Figura 4B). El complejo Arp2/3 de levadura tiene mayor actividad basal que el de organismos superiores, pero en todos los casos la acción de proteínas activadoras conocidas como NPFs aumenta la formación de nuevos extremo (+) varios órdenes de magnitud. *S. cerevisiae* contiene 5 NPFs: Las17, que es el homólogo de WASP, las miosinas de tipo I Myo3 y Myo5, Pan1, y Abp1. Todos los NPFs contienen una secuencia rica en aminoácidos ácidos (CA) de unión al complejo Arp2/3, pero

para activarlo Las17 y Myo3/Myo5 (NPFs de tipo I) interaccionan con G-actina a través de su dominio WH2 (que en el caso de las miosinas se ubica en otra molécula, la Vrp1) mientras que Pan1 y Abp1 (NPFs de tipo II) interaccionan con F-actina, que también actúa como activador del complejo Arp2/3. Esta diferencia es significativa puesto que los NPFs de tipo I son mucho más potentes que los de tipo II. En la Figura 6 se muestran los NPFs más representativos, mientras que su función biológica se resume brevemente en la sección 8.1.2. Además de los NPFs, la coronina (Crn1) también regula la actividad del complejo Arp2/3, restringiendo su actividad en los lugares donde abundan los filamentos de reciente creación.

Solo 6 proteínas que unen G-actina están conservadas en todos los organismos eucariotas: ADF/cofilina (Cof1 en *S. cerevisiae*, ver más abajo), profilina (Pfy1), Srv2/CAP, twinfilina (Twf1), verprolina (Vrp1), y WASP/WAVE (Las17). Pfy1 unido a ATP-actina constituye la mayor fuente de monómeros para la polimerización en el extremo (+), e impide la nucleación espontánea y la elongación en el extremo (-). Srv2 facilita el intercambio de nucleótido desde ADP-actina unido a cofilina (ver debajo) a ATP-actina, que se unirá a la Pfy1 para empezar una nueva ronda de polimerización. Twf1 inhibe el intercambio de nucleótido de ADP-actina a ATP-actina y a la vez estimula el desensamblaje del filamento de actina. Vrp1 recluta Las17 a los sitios donde se requiere la formación de un citoesqueleto de actina dinámico, y además activa la función NPA de Myo5 y Myo3 aportando los dominios de unión a G-actina (dominios WH2).

El recubrimiento de los filamentos de actina impide la adicción y disociación de monómeros. Dos tipos de proteínas con función 'capping' de extremo (+) se conservan en eucariotas: CP, formado por las subunidades Cap1/Cap2, y Aip1. CP restringe la longitud del filamento y aumenta la motilidad dependiente de actina modificando la arquitectura del entramado de redes de actina. Aip1 se une al extremo (+) de la F-actina fragmentada por la acción de Cof1, impidiendo su elongación y favoreciendo la conversión de oligómeros de actina en G-actina.

La rotura y posterior despolimerización de los filamentos de actina es importante para dinamizar la actina filamentosa, ya que proporciona nuevos extremos (+) e incrementa la disponibilidad de G-actina. En *S. cerevisiae* esta función la realiza la proteína Cof1, miembro de la familia ADF/cofilina. Cof1 también inhibe el intercambio de nucleótido de ADP-actina a ATP-actina, por lo que la presencia de Aip1, Srv2 y Pfy1 es necesaria para el reciclaje de los monómeros tras su disociación. Recientemente se ha identificado otro miembro de la familia ADF/cofilina en levadura, Aim7, pero su función se limita a eliminar las ramificaciones de actina producidas por el complejo Arp2/3 y a inhibir la formación de nuevos filamentos.

En *S. cerevisiae*, la actina se encuentra preferentemente en forma de F-actina, organizado en estructuras especializadas. Estas estructuras pueden contener proteínas que se asocian a lo largo de los filamentos de actina, proteínas que conectan diferentes filamentos de actina entre sí, o proteínas que enlazan los filamentos de actina con otras estructuras celulares. Las tropomiosinas son proteínas conservadas que se asocian a lo largo de los filamentos de actina, principalmente los nucleados por las forminas ya que no contienen ramificaciones que obstaculicen su unión. Dos tropomiosinas existen en *S. cerevisiae*, Tpm1 y Tpm2. La asociación

de filamentos de actina para formar estructuras complejas se realiza mediante proteínas que contienen varios dominios de unión a actina o bien dominios de oligomerización. *S. cerevisiae* contiene 4 proteínas que realizan esta función, 3 de ellas conservadas durante la evolución: la fimbrina Sac6, Scp1, y la IQGAP Igq1. Abp140, por el contrario, parece existir únicamente en *S. cerevisiae*. La asociación entre los filamentos de actina y estructuras celulares membranosas se realiza mediante proteínas que interaccionan con lípidos específicos o que están unidas covalentemente a lípidos, proteínas integrales de membrana, o proteínas que interaccionan con membranas a través de proteínas adaptadoras. En *S. cerevisiae* hay en concreto 2 tipos de proteínas de unión a actina que interaccionan directamente con membranas: las miosinas no convencionales y el homólogo de Hip1R Sla2. Sla2 interacciona con PIP_2 mediante su región N-terminal y a actina filamentosa mediante la región C-terminal.

Las miosinas son motores moleculares que se mueven a lo largo de los filamentos de actina y consisten en una o dos cadenas pesadas unidas a un número variable de cadenas ligeras. Existen alrededor de 25 tipos de miosinas; algunos de ellos se expresan en todos los organismos mientras que otros están presentes sólo en determinadas especies. La cadena pesada de las miosinas está constituida por la cabeza, que contiene la región motora, seguida de una cola responsable de la dimerización de la miosina o de la unión a su carga. Entre la cabeza y la cola se encuentra una región 'cuello' de unión a las cadenas ligeras de la miosina a través de sus motivos IQ. La región motora usa la energía química del ATP ara producir fuerza mecánica en un proceso denominado ciclo ATPasa de actomiosina, que se resume en la Figura 14. El cuello sirve como palanca, convirtiendo los pequeños cambios conformacionales de la región motora en importantes movimientos en la cola de la miosina. La cola de las miosinas difiere considerablemente entre los diferentes tipos de miosinas, y define la localización y función de dichas proteínas. *S. cerevisiae* contiene 5 miosinas: la miosina de tipo II Myo1, las miosinas de tipo V Myo2 y Myo4, y las miosinas de tipo I Myo3 y Myo5. Además, expresa 3 cadenas ligeras: la calmodulina Cmd1, y las proteínas Mlc1 y Mlc2. La organización funcional de las cadenas pesadas y ligeras de las miosinas de *S. cerevisiae* se representa en la Figura 15.

- La miosina de tipo II de mamíferos fue las primera miosina identificada, ya que es la proteína más abundante en el músculo esquelético. Además de formar parte de células musculares, las miosinas de tipo II no musculares funcionan en una gran variedad de procesos como la citoquinesis, la adhesión o la migración muscular, entre otros. Están constituidas por 2 cadenas pesadas que a su vez unen 2 cadenas ligeras, Mlc1 y Mlc2 en el caso de *S. cerevisiae*. El dominio C-terminal interviene en la dimerización entre cadenas pesadas. Myo1 participa en la separación entre célula madre y célula hija durante la citoquinesis.
- Las miosinas de tipo V transportan cargas dentro de la célula 'caminando' sobre los filamentos de actina. También están constituidas por 2 cadenas pesadas, pero cada una tiene 6 sitios de unión a cadenas ligeras. Tras la región de dimerización poseen un dominio globular (GTD) implicado en la unión y transporte de la carga. Las miosinas-V de S. cerevisiae Myo2 y Myo4 transportan diferentes cargas: Myo2 transporta vesículas,

orgánulos, y microtúbulos, mientras que Myo4 transporta retículo endoplasmático cortical y complejos de proteína-mRNA. No está claro si Myo4 también forma dímeros.

- Las miosinas de tipo I son monoméricas, y sus funciones varían entre diferentes tipos celulares. Poseen un número variable de motivos IQ, que en el caso de Myo3 y Myo5 son 2 regiones de unión a Cmd1. Pueden contener una versión de la cola C-terminal corta o larga. Ambas contienen una región rica en aminoácidos básicos que facilita la unión de la miosina a membranas (TH1). Además de la región TH1, la versión larga incluye una extensión C-terminal (C_{ext}) que contiene una región de unión a F-actina (TH2) y un dominio SH3 que media la interacción con motivos ricos en prolinas. Algunas miosinas de cola larga interaccionan con el complejo Arp2/3 mediante dos mecanismos alternativos: las miosinas de levadura contienen la región rica en aminoácidos ácidos involucrada en la activación del Arp2/3 (CA), mientras que algunas miosinas de protozoos reclutan al complejo indirectamente a través de la proteína CARMIL. Las miosinas de tipo I de *S. cerevisiae* Myo3 y Myo5 tienen la estructura típica de la miosinas de cola larga. Tienen una función esencial en la captación endocítica, y tanto su actividad motora como de activación del complejo Arp2/3 son imprescindibles para esta función (ver más abajo). La actividad motora está regulada por una fosforilación/defosforilación de una serina conservada situada en la región de unión de unión al filamento de actina (sitio TEDS). La actividad NPA se regula mediante una interacción autoinhibitoria entre el TH1 y el C_{ext} estabilizada por la Cmd1.

8.1.2. Funciones fisiológicas de la actina en *S. cerevisiae.*

En la levadura *S. cerevisiae*, los filamentos de actina se organizan en 3 estructuras principales: los cables de actina, el anillo contráctil de actomiosina, y los parches de actina. Los dos primeros están formados por haces paralelos de filamentos de actina nucleados por forminas, pero mientras los cables se polarizan a lo largo del eje célula madre y la gema o célula hija, el anillo contráctil se sitúa perpendicularmente a ese eje durante la transición G2-M. Los parches de actina están formados por una red de filamentos ramificados localizados en el córtex celular y nucleados por el complejo Arp2/3 que se localizan principalmente en las zonas de crecimiento celular. Sin embargo, la distribución y polarización de las 3 estructuras varían a lo largo del ciclo celular, ver Figura 16.

Aunque la formación de un anillo contráctil de actomiosina es fundamental para la división celular en casi todas las células eucariotas, en *S. cerevisiae* la formación del anillo facilita la citoquinesis pero no es esencial debido a la presencia de un mecanismo complementario, la deposición del septo. Estos dos mecanismos son interdependientes y cooperan para facilitar la separación celular. Además de actina y miosina, la formación del anillo de actomiosina en *S. cerevisiae* precisa la presencia de las forminas Bni1 y Bnr1, Pfy1, Iqg1, y Tpm1/2.

El transporte de vesículas secretoras y orgánulos hacia la célula hija está dirigido por los cables de actina, que se orientan con sus extremos (+) hacia la punta o el cuello de la gema debido a la localización restringida de las forminas Bni1 y Bnr1, respectivamente, en esas regiones.

Aunque la formación de los cables depende de las forminas, otras proteínas como Bud6 y Pfy1 participan en su formación y otras proteínas como Sac6, Tpm1/Tpm2, o Abp140 se ubican en los cables de actina. Los cables de actina sirven de guía a las miosinas Myo2 y Myo4 para el trasporte de vesículas secretoras, orgánulos, y mRNAs específicos de la célula hija hacia ésta. También están implicados en el movimiento retrógrado de endosomas y otras moléculas específicas de la célula madre, además de participar en la elongación del huso mitótico.

8.1.2.1. La función de la actina en endocitosis

La endocitosis en un proceso celular por el cual la membrana plasmática se curva formando una vesícula endocítica que se separa de la superficie celular y viaja a través del citosol para fusionarse con los endosomas, desde donde la carga internalizada se recicla a la membrana plasmática o se dirige al sistema endolisosomal para su degradación. Diferentes mecanismos de endocitosis se han descrito en mamíferos, incluyendo la fagocitosis, macropinocitosis, endocitosis mediada por caveolas, o la vía CLIC-GEEC. Sin embargo, en *S. cerevisiae* la vía endocítica clásica, dependiente de clatrina, ha sido el único mecanismo descrito hasta el pasado año, cuando se publicó la existencia de un mecanismo alternativo independiente de clatrina. Sin embargo, aún no se conoce ni la contribución de la vía alternativa en las células en las que la vía clásica permanece intacta, ni la carga que podría internalizarse a través de esta vía.

8.1.2.1.1. Formación de vesículas endocíticas en la membrana plasmática

La actina y diferentes proteínas asociadas a los parches de actina son necesarias para la formación de vesículas endocíticas, y multitud de proteínas endocíticas, como adaptadores y 'scaffolds' (andamios celulares), se localizan en estructuras corticales punteadas que colocalizan total o parcialmente con los parches de actina (Tabla 2). Los nuevos avances en la obtención de imágenes microscópicas en células vivas aplicadas a *S. cerevisiae* han sido cruciales para establecer un vínculo funcional entre los parches de actina corticales y la endocitosis, así como para establecer el orden de la secuencia de eventos moleculares implicados en la maduración de los parches de actina y la formación de las vesículas endocíticas. Las proteínas involucradas en la internalización endocítica se reclutan transitoriamente de forma invariable, secuencial, y parcialmente solapada en los parches corticales donde se está formando la vesícula, y según su dinámica se agrupan en módulos funcionales tal y como se indica en la Figura 17 o en la Tabla 2. Más recientemente, el aumento de la resolución espacial obtenida mediante la utilización de técnicas de microscopía electrónica e inmunomarcaje cuantitativo ha expuesto la naturaleza de los perfiles endocíticos primarios en la membrana plasmática y cómo los complejos moleculares que deforman la membrana plasmática se van reorganizando durante la maduración del perfil endocítico. En la Figura 18 se muestran 3 perfiles endocíticos, invaginaciones tubulares de 50 nm de diámetro y hasta 180 nm de longitud, revestidos por una cubierta de clatrina hemisférica de unos 40 nm, que se desplazan hacia el citosol durante su elongación y maduración. En la figura 19 se resume el modelo actual de la formación de vesículas endocíticas.

Las primeras proteínas reclutadas en el parche cortical son Ede1 y Syp1, componentes del llamado módulo temprano ('Early'), y los componentes del módulo de recubrimiento temprano ('Early coat') que incluye la clatrina, adaptadores como el AP-2 y el Yap1801/2, y Pal1. Los componentes del 'Early' y el 'Early coat' se clasifican en módulos distintos porque aunque llegan prácticamente a la vez, Ede1/Syp1 abandonan el parche endocítico antes que los componentes del 'Early coat'. La clatrina funciona clásicamente como 'scaffold' y fuerza motriz para la internación endocítica, aunque en *S. cerevisiae* podría más bien tener una función reguladora ya que la mutación de los genes *CHC1* y *CLC1* sólo disminuye la actividad endocítica en un 50% y no afecta a la morfología de los perfiles endocíticos, sino que reducen el número de lugares de endocitosis y disminuyen la vida de algunas proteínas endocíticas tardías; un fenotipo que también se observa tras la mutación de *EDE1*. Syp1 parece tener múltiples funciones: recluta carga endocítica, constriñe el cuello de la invaginación, inhibe la NPA de Las17, y localiza la endocitosis en el cuello de la gema. Tras el reclutamiento del 'Early' y del 'Early coat', aparecen los componentes del módulo de recubrimiento intermedio ('Intermediate coat'), que incluye las proteínas Sla2 y las epsinas Ent1/2. Tanto Sla2 como Ent1/2 enlazan proteínas endocíticas con la membrana plasmática a través de sus dominios de unión al PIP_2, pero Sla2, aparte de interaccionar con otras proteínas endocíticas, se une directamente a los filamentos de actina funcionando de vínculo entre el 'coat' endocítico y el citesqueleto de actina. Seguidamente los componentes del módulo de recubrimiento tardío ('Late coat') formado por End3, Pan1, y Sla1, se unen al parche endocítico. Estas 3 proteínas pueden formar un complejo y funcionar como adaptadores y/o 'scaffold' endocíticos y regular el citoesqueleto de actina, de forma similar a la intersectina de mamíferos. End3 y Pan1 contienen dominios de interacción con adaptadores endocíticos, Pan1 además de funcionar de 'scaffold' funciona como NPF, y Sla1 también tiene una doble función como adaptador/'scaffold' y regulador de la dinámica de actina en el parche endocítico. Junto a estas proteínas se recluta Las17, homólogo de WASP, pero se considera que forma parte de otro módulo ya que su dinámica difiere de la del 'coat'.

Pese a que Las17 posee una elevada NPA, la polimerización masiva de actina se detecta unos 10 segundos más tarde de la llegada de Las17 al parche endocítico. Esto se debe a que su función como activador del Arp2/3 está probablemente inhibida por las proteínas Syp1 y Sla1, que en esta fase inicial colocalizan con Las17 a nivel ultraestructural. De forma similar, la débil NPA de Pan1 podría estar inhibida por Sla2. Vrp1 y Bzz1 se reclutan en el parche endocítico unos 10 segundos después del reclutamiento de Las17, coincidiendo con un movimiento acotado del parche cortical y con la deformación inicial de la membrana plasmática. Bzz1 libera la función inhibidora de Sla1 sobre Las17, por lo que se ha propuesto que la curvatura inicial de la membrana reclutaría a Bzz1 a través de su dominio F-BAR, iniciando la polimerización de actina mediada por Las17 en los parches endocíticos. Aún no se sabe cómo se genera esta curvatura inicial en la membrana, pero los resultados obtenidos en nuestro laboratorio mediante el uso farmacológico del secuestrador de G-actina Latrunculin A indican que este tratamiento no evita el acoplamiento del 'coat' ni la deformación de la membrana plasmática. En esta fase inicial de la invaginación de membrana Las17 y Pan1 se localizan en el 'coat' que cubre el extremo de la invaginación endocítica. La polimerización de actina mediada por Arp2/3 e inducida por Pan1 y

Las17, y el reclutamiento de Abp1, Sac6, Scp1, y Cap1/2, que forman el módulo de actina ('Actin'), desencadena la formación de un 'cap' de actina que se organiza alrededor del 'coat' (ver Figura 19). La mutación de diferentes componentes del Arp2/3, o de Sac6/Scp1 o Cap1/Cap2 no impide la formación del 'cap' de actina pero sí la internalización productiva del 'coat', lo que indica que la formación de una red de actina con una arquitectura bien definida es esencial para generar fuerzas productivas capaces de deformar la membrana plasmática y producir la escisión de la vesícula.

Unos 10 segundos después de la llegada de Vrp1 y Bzz1 se observa la aparición de Myo5 y de un inhibidor de la NPA de Las17 y Myo5, la proteína Bbc1. La llegada del potente NPF Myo5 coincide con la polimerización masiva de actina y la elongación del perfil endocítico tubular de 70 a 200 nm previo a la fisión. Tanto la actividad motora como la NPA de Myo5 son necesarias para la elongación del perfil endocítico. Estudios ultraestructurales muestran que en invaginaciones de una longitud media (70 nm), Las17 colocaliza con sus inhibidores Bbc1 y Syp1 en el cuello de los perfiles mientras que Myo5 y su co-activador Vrp1 se acumulan en la base. Así, en este momento Myo5/Vrp1 remplazaría a Las17 como NPA produciendo la acumulación de filamentos de actina con sus extremos (+) hacia la membrana plasmática, que son empujados hacia el citosol por la actividad motora de la miosina (ver Figura 23). Si estos filamentos están bien conectados con el 'cap' de actina y con el 'coat' endocítico, la actividad de motora de la miosina estaría bien posicionada para producir el movimiento dirigido del 'coat' hacia el citosol.

La llegada de las anfifisinas Rvs161 y Rvs167 marca el momento de la escisión de la vesícula. Ambas proteína tienen dominios N-BAR y se localizan en el cuello de la invaginación, contribuyendo a su constricción. Además de Rvs161/167 otros factores son necesarios para la fisión. En eucariotas superiores la GTPasa dinamina es esencial para la escisión de las vesículas recubiertas de clatrina pero en *S. cerevisiae* el papel de la GTPasa Vps1 es discutible, ya que aparece en algunos parches corticales pero su contribución directa es controvertida. Algunos resultados recientes indican que una combinación de actividades bioquímicas tales como la deformación de membranas producidas por los dominios BAR, la reorganización de lípidos, y la polimerización de actina cooperarían para desencadenar la escisión de la vesícula, tanto en *S. cerevisiae* como en eucariotas superiores. En la levadura la mutación de Rvs167 muestra defectos sinergísticos en la constricción y escisión del túbulo cuando se combina con la mutación de Bzz1 o con la reducción de la NPA de Myo5 y Las17. En las invaginaciones muy largas (> 110 nm) Myo5 se reorganiza en la base y el extremo distal de la invaginación. Mientras la actina/miosina situada en la base de la invaginación podría promover a la constricción, la del extremo podría proporcionar la tensión necesaria para la escisión. Además de la acumulación de proteínas con dominios BAR y de la polimerización de actina, la reorganización de lípidos podría jugar un papel determinante en la fisión. PIP_2 se concentra en los parches corticales y desaparece simultáneamente a la escisión, poco después de la llegada de la fosfatasa de PIP_2 Sjl2. Se ha propuesto que PIP_2 podría hidrolizarse en la punta de la invaginación pero no en el

cuello, lo que crearía una segregación de lípidos que llevaría a la compresión del perfil endocítico.

Durante o tras la escisión, la vesícula se desprende del 'coat' y empieza el desensamblaje de la estructura de actina. Abp1 recluta varios factores como la fosfatasa de PIP_2 Slj2, o las quinasas de S/T Ark1 y Prk1. PIP_2 se acumula en los sitios de endocitosis donde facilita el reclutamiento de Ent1/2, Sla2, y Yap1801/1802. La llegada de Sjl2 facilitaría la desunión de dichas proteínas. La fosforilación de Sla1 y Pan1 mediada por Ark1/Prk1 impide su interacción, lo que conllevaría también a su disociación. Otros factores implicados en el desensamblaje de la actina, como Cof1, Aip1, o Crn1 (ver más arriba) también se reclutan en este periodo.

8.1.2.1.2. Funciones de la actina en el tráfico endocítico tras la internalización

Tras la fisión, la vesícula endocítica viaja en el citosol siguiendo una trayectoria aparentemente aleatoria. No se sabe si este movimiento requiere la presencia del Arp2/3 ya que tras la fisión, Myo5 y Las17 quedan retenidas en la membrana plasmática, la actividad NPA de Pan1 está inhibida por fosforilación vía Ark1/Prk1, y la mutación de Abp1 no impide su desplazamiento. Tras la trayectoria aleatoria, una subpoblación de vesículas endocíticas experimenta un movimiento lineal retrógrado asociado a cables de actina que se produce sin la ayuda de proteínas motoras. Los endosomas tempranos experimentan un movimiento anterógrado sobre los cables de actina, pero no se ha identificado el motor molecular responsable de este desplazamiento. En mamíferos el transporte de endosomas se realiza mediante microtúbulos, pero los movimientos de trayectoria corta en zonas ricas en actina también dependerían de la polimerización de actina inducida por Arp2/3 y/o forminas. En *S. cerevisiae*, Las17 podría participar en el movimiento de los endosomas tardíos. Por otra parte, varias de proteínas involucradas en la regulación de actina, como Vrp1, el complejo Arp2/3, Las17, Myo5, o Sac6 parecen participar también en la fusión homotípica de la vacuola. Todas estas funciones de la actina en se resumen en la Figura 26.

8.2. Resultados

8.2.1. Antecedentes

Con el objetivo de estudiar cómo se regula la NPA de Myo5, nuestro laboratorio ha establecido un ensayo de polimerización de actina *in vitro* que permite monitorizar visualmente la polimerización de actina mediada por la extensión C_{ext} de la Myo5. Brevemente, Myo5-C_{ext} (aminoácidos 984-1219) purificada de *E. coli* es inmovilizada en la superficie de bolas de Sepharosa e incubada a 26ºC en la presencia de extracto de levadura, un sistema regenerador de ATP, y actina marcada fluorescentemente. La polimerización de actina mediada por Myo5-C_{ext} recapitula un proceso fisiológico ya que las estructuras de actina formadas se asemejan morfológica y bioquímicamente a los parches de actina endocíticos: se requiere la presencia del complejo Arp2/3 y del co-activador de Myo5 Vrp1 para su formación, y contienen varios componentes de los parches corticales de actina como Arp2/3, Abp1, Sac6, o Crn1 (Geli et al.,

2000; Idrissi et al., 2002)(datos no publicados de F. Idrissi y M. Geli, Figura 30). Otras proteínas endocíticas como Sla1 y Bbc1 están presentes en las bolas de Sepharosa pero no se acumulan en las estructuras de actina.

La formación de los *foci* de actina está regulada por componentes citosólicos, ya que son estructuras discretas pero ni Myo5-C_{ext} ni la actina ni el Arp2/3 son limitantes en el ensayo. El análisis farmacológico del ensayo indica que una o más fosfatasas serían necesarias para iniciar la formación de las estructuras de actina mediadas por Myo5 mientras que una o más quinasas lo regularían negativamente (datos no publicados de B. Grosshans, Figura 31). La incorporación de ATP marcado radiactivamente demuestra que la fracción de la Myo5-C_{ext} correspondiente a los aminoácidos 1142-1219 se fosforila en condiciones en las que se realiza el ensayo de polimerización de actina (datos no publicados de B. Grosshans, Figura 32). El análisis de la secuencia del péptido indica la presencia de una serina susceptible de fosforilación, la S1205, cuya mutación a alanina evita la fosforilación de Myo5-C_{ext}. Dicho residuo se encuentra en un motivo consenso para la quinasa CK2, un entorno de residuos ácidos que puede extenderse desde la posición -2 a la +5. Mediante ensayos de fosforilación realizados en presencia de extracto de levadura de cepas salvajes o mutantes para la CK2 (*ck2-ts*) se demostró que la quinasa CK2 es capaz de fosforilar a Myo5 en la S1205, al menos *in vitro* (datos no publicados de B. Grosshans, Figura 33).

8.2.2. Análisis de la fosforilación de la S1205 de Myo5 por CK2

CK2 es una S/T quinasa pleiotrópica y altamente conservada que existe principalmente como un tetrámero compuesto de 2 subunidades catalíticas α y 2 reguladoras β, codificadas en *S. cerevisiae* por *CKA1* y *CKA2*, y *CKB1* y *CKB2*, respectivamente. Las subunidades reguladoras no son necesarias para la viabilidad en condiciones estándares, pero sí lo es la presencia de al menos una subunidad catalítica. Por otra parte, diferentes estudios indican que aunque la depleción de *CKA1* o *CKA2* no causa ningún fenotipo obvio, las dos subunidades catalíticas podrían tener funciones independientes. El análisis de la contribución de cada subunidad catalítica y de las subunidades reguladoras a la fosforilación de la S1205 de Myo5 indica que la subunidad Cka2 contribuye en mayor medida que la subunidad Cka1 a esta fosforilación y que las subunidades reguladoras parecen ser prescindibles (Figura 35). Para confirmar esta observación se sobreexpresó Cka1, Cka2, o una versión de Cka2 que tiene una mutación puntual en un residuo conservado de su centro catalítico (*cka2-K79A*) a partir de plásmidos multicopia. Según se muestra en la Figura 36, únicamente la sobreexpresión de Cka2 aumenta significativamente la fosforilación de la S1205 de Myo5. Además, la tetramerización no parece ser necesaria ya que la sobreexpresión de Cka2 en una cepa *ckb1Δ ckb2Δ* incrementa la fosforilación de la S1205 de Myo5 al mismo nivel que la sobreexpresión en la cepa salvaje.

También se investigó la localización subcelular de la actividad CK2 responsable de la fosforilación de Myo5-C_{ext}. Los extractos usados en los ensayos (S13, sobrenadante tras centrifugación a 13.000 g) se subfraccionaron por centrifugación a 100.000 g. El sobrenadante S100 corresponde al citosol y P100 contiene membranas celulares y posiblemente elementos del

citoesqueleto (Figura 37). Curiosamente, la fosforilación se ve reducida en la fracción S100 respecto la P100. Tanto en la fracción S100 como P100 la depleción de Cka2 reduce la fosforilación de la S1205 de Myo5. Análisis de las fracciones subcelulares que contienen membranas 'pesadas', como la membrana plasmática o la cubierta nuclear (P13) indican que la actividad que fosforila Myo5-C_{ext} también se asocia a dicha fracción. Consistentemente, Cka2 aparece enriquecido en el P13 y en menor medida en el P100 pero no en el S100, si se compara con Cka1.

8.2.3. Análisis del papel regulatorio de la fosforilación de la S1205 de Myo5 por CK2 en la polimerización de actina inducida por miosina

Puesto que la S1205 de Myo5 se sitúa junto a la secuencia rica en aminoácidos ácidos (CA) de unión al Arp2/3, se investigó si la fosforilación de este residuo regula la formación de las estructuras de actina *in vitro*. Para ello S1205 se sustituyó por ácido aspártico (D) o cisteína (C) para mimetizar el estado fosforilado o no fosforilado, respectivamente, de la miosina. Aunque las 2 construcciones unen Arp2/3 de forma similar, la formación de estructuras de actina aumenta significativamente en la forma no fosforilada de Myo5 (Myo5-S1205C) mientras que se reduce en la forma fosforilada (Myo5-S1205D), lo que sugiere que la fosforilación de Myo5 en el residuo S1205 regula negativamente la formación de parches de actina *in vitro* (Figura 38).

Los resultados de los ensayos de fosforilación indicaban que la subunidad Cka2 juega un papel predominante en la fosforilación de la S1205 de Myo5. Consistentemente, la formación de estructuras de actina aumenta significativamente en un mutante *cka2Δ* y disminuye en una cepa que sobreexpresa *CKA2*, mientras que ni la depleción ni la sobrexpresión de *CKA1* tienen un efecto significativo (Figuras 39 y 40). El efecto de la Cka2 es debido a su actividad quinasa, tal y como se demuestra mediante la sobreexpresión del mutante *cka2-K79A*, y al menos parcialmente causado por la fosforilación en la S1205 de Myo5, tal y como se observa por la supresión del efecto de la cepa *cka2Δ* en el mutante Myo5-S1205D. Pero además de Myo5-C_{ext}, Cka2 estaría regulando otras proteínas implicadas en la generación de los parches de actina, ya que la depleción de Cka2 es capaz de incrementar la polimerización de actina también sobre la construcción mutante Myo5-S1205D, y el mutante Myo5-S1205C por sí solo no puede impedir ni la inhibición ni el aumento de la polimerización de actina causada por la sobreexpresión de CKA2 o *cka2-K79A*, respectivamente.

8.2.4. Análisis de la influencia de la fosforilación de la S1205 de Myo5 en el interactoma de Myo5

Para averiguar qué mecanismos moleculares participan en la regulación de la polimerización de actina inducida por Myo5 a partir de la fosforilación de su residuo S1205, investigamos las afinidades relativas de los mutantes Myo5-S1205C y Myo5-S1205D por proteínas que interaccionan con Myo5: el complejo Arp2/3, Vrp1, Las17, Pan1, Bbc1, Abp1, and Sla1. Sorprendentemente, no se observaron diferencias en la afinidad de los mutantes con el complejo Arp2/3 mediante ensayos de 'pull-down'. Sin embargo, el co-activador de Myo5 Vrp1

mostraba una mayor afinidad por Myo5-S1205C mientras que los componentes del parche endocítico Sla1 y en menor medida Pan1 mostraban mayor afinidad por Myo5-S1205D. La interacción diferencial con Vrp1 y Sla1 se confirmó usando un ensayo de doble híbrido (Figura 41).

El hecho de que Vrp1 interaccione mejor con Myo5-S1205C, que muestra una mayor actividad NPA, es consistente con su función co-activadora de Myo5. Sla1, por su parte, es un inhibidor de la función NPA de Las17, y experimentos preliminares indicaban que también podría serlo de Myo5 (datos no publicados de F. Idrissi). Para confirmar este dato, se caracterizaron los dominios de interacción entre Sla1 y Myo5 y posteriormente se investigó si las mutaciones que evitan dicha interacción afectan también la función NPA de Myo5. Nuestros resultados indican que la interacción Myo5/Sla1 ocurre in vivo a través del dominio C_{ext} de Myo5, es directa, y se da específicamente entre el dominio TH2 de Myo5 y los 2 dominios SH3 N-terminales de Sla1 (Figuras 42, 43, y 44). Además, tanto la depleción completa de *SLA1* como la de los dominios SH3 N-terminales provocan un aumento significativo de la formación de estructuras de actina inducidas por Myo5, indicando que dichos dominios de Sla1 inhiben directamente la actividad NPA de Myo5-C_{ext} (Figura 45).

8.2.5. Análisis del papel regulatorio de la fosforilación de la S1205 de Myo5 por CK2 en la internalización endocítica

Nuestros datos indican que la subunidad Cka2 fosforila la S1205 de Myo5 y que esta fosforilación regula negativamente la formación de *foci* de actina *in vitro*. Como dichos *foci* recapitulan las estructuras de actina corticales necesarias para la formación de vesículas endocíticas en la membrana plasmática, decidimos analizar si la fosforilación de la S1205 de Myo5 por la quinasa Cka2 tiene influencia sobre la internalización endocítica.

Para ello usamos inicialmente un ensayo que evalúa el ritmo de internalización endocítica mediante el uso de un ligando marcado radiactivamente, la feromona α-factor, que se une y activa la internalización del GPCR Ste2. Sin embargo, aunque la fosforilación de la S1205 de Myo5 regula la formación de estructuras de actina *in vitro*, los mutantes que mimetizan las formas constitutivamente fosforilada y no fosforilada como única fuente de myosina-I (*myo3Δ myo5-S1205D* y *myo3Δ myo5-S1205C*, respectivamente) son capaces de alterar la cinética de internalización del Ste2 *in vivo*, posiblemente debido a la redundancia funcional con otros NPFs que enmascararían los efectos individuales de la miosina (Figura 46). Por esta razón dichas mutaciones fueron combinadas con mutaciones en el dominio necesario para la función NPA de Las17 o de Pan1. En estas condiciones sí pudimos observar una limitada pero significativa disminución del ritmo de internalización endocítica, independiente de la carga impuesta en la S1205 de Myo5, lo que indicaría la necesidad de un ciclo de fosforilación/defosforilación para la eficiente internalización del ligando (Figura 47).

El ensayo de internalización de Ste2 podría no ser lo suficientemente sensible para revelar el fenotipo de los mutantes *myo5-S1205C* y *myo5-S1205D* en presencia de mecanismos

redundantes. Por ejemplo, la disrupción de la secuencia de unión a Arp2/3 (CA) de Myo5 en una cepa *myo3Δ* no causa un defecto perceptible en la internalización del Ste2. Sin embargo, una fracción significativa de los parches corticales permanece en la membrana un largo periodo de tiempo y no son internalizados, tal y como se puede observar a partir de experimentos de microscopía de fluorescencia *in vivo*. Por esta razón, se investigaron los efectos de *myo5-S1205C* y *myo5-S1205D* en la dinámica cortical de la miosina y Abp1 en cepas *myo3Δ*. Sorprendentemente, el mutante *myo3Δ myo5-S1205C* no causa ningún efecto sobre la dinámica de GFP-Myo5 ni de Abp1-mRFP. Sin embargo, ambas proteínas permanecen más tiempo en los parches corticales en el mutante *myo3Δ myo5-S1205D* (Figura 48 y Tabla 3), aunque esta mutación no impide la internalización de Abp1 (Figura 49). El análisis de la llegada de la miosina respecto la proteína de la cubierta Sla1-mCherry indica que la prolongación del tiempo de residencia de Myo5 y Abp1 en el córtex en dicho mutante no es debido a un reclutamiento prematuro de la miosina acompañado de polimerización de actina, como es el caso del mutante de calmodulina *cmd1-226* (Grotsch et al., 2010). Por el contrario, la fosforilación de la S1205 de Myo5 dificulta la internalización del 'coat', ya que Sla1-mCherry permanece más tiempo en los parches corticales en el mutante. Además, la fosforilación de la S1205 de Myo5 también parece entorpecer la disociación de Myo5 de la membrana plasmática una vez la vesícula ha sido internalizada (Figura 50 y Tabla 4). Consecuentemente, la sobreexpresión de *CKA2* pero no de *CKA1* ni de la versión mutante de Cka2 *cka2-K79A* reproduce el fenotipo observado en la cepa mutante Myo5-S1205D (Figura 52 y 53 y Tabla 6). Además, se pudo demostrar que el efecto instalado por la sobreexpresión de Cka2 es al menos parcialmente dependiente de la fosforilación de la S1205 de Myo5, ya que dicha sobreexpresión no logra extender el tiempo de residencia del mutante constitutivamente desfosforilado Myo5-S1205C. Estos resultados indican que la fosforilación de la S1205 de Myo5 por Cka2 disminuye la polimerización de actina mediada por Myo5 en los parches endocíticos.

Nuestros datos sugieren que Cka2 posee otras funciones en endocitosis aparte de regular la NPA de Myo5. Los ensayos de polimerización *in vitro* ya indicaban que Cka2 probablemente fosforilaría otras proteínas involucradas en el proceso. El ensayo de internalización de Ste2 también revela la especificidad de la subunidad Cka2 en la internalización endocítica, cuyo ritmo se ve incrementado sutil pero significativamente en el mutante *cka2Δ* respecto el mutante *cka1Δ* o la cepa salvaje (Figura 55). Esta aceleración no es consecuencia de una aceleración general del tráfico de membranas, ya que el tráfico biosintético de la carboxipeptidasa CPY desde el retículo endoplasmático a la vacuola no se ve alterado en el mutante (Figura 56). Además, la depleción de *CKA2* es capaz de suprimir parcialmente los defectos endocíticos de *myo5Δ* pero también de *sac6Δ*, lo que confirma que, aparte de la regulación de la NPA de Myo5, la quinasa regula negativamente otras funciones necesarias para la internalización endocítica (Figura 57).

La aceleración de la internalización de Ste2 en el mutante *cka2Δ* es de aproximadamente 1,7 veces, y podría ser debido a un aumento del número de parches corticales endocíticos, a una maduración más rápida de estos parches, o a una mayor eficacia en el empaquetado de Ste2 en

las vesículas endocíticas. Nuestros datos indican que probablemente se deba a una combinación de factores, ya que tanto el número de parches corticales como el tiempo de retención del 'coat' en la membrana plasmática se ven levemente alterados en el mutante *cka2Δ* (Figura 58). Este efecto es al menos parcialmente independiente de la fosforilación en la S1205 de Myo5 ya que la dinámica de Myo5 no se ve alterada en el mutante *cka2Δ* y la dinámica de la cubierta endocítica tampoco se veía alterada en el mutante *myo3Δ GFP-Myo5-S1205C.*

8.3. Discusión

Resultados preliminares de nuestro grupo indicaban 1) que Myo5-C_{ext} induce la formación de estructuras de actina *in vitro* que recapitulan el ensamblaje de la estructura de actina que se forma alrededor del 'coat' endocítico in vivo, y 2) que la formación de dichas estructuras está negativamente regulada por la fosforilación del residuo S1205 de Myo5 mediada por la quinasa CK2. En el presente estudio hemos caracterizado la actividad CK2 que fosforila a Myo5-C_{ext} e investigado el significado funcional de este evento *in vitro* e *in vivo*. Hemos observado que una actividad CK2 no canónica y asociada a partículas que incluye a la subunidad catalítica Cka2, pero no a la subunidad catalítica Cka1 ni a las subunidades reguladoras, es responsable de la fosforilación de la S1205 de Myo5. Nuestros resultados también indican que esta fosforilación inhibe la actividad NPA de Myo5 necesaria para la internalización endocítica, que Cka2 seguramente tiene otras dianas además de Myo5, y que su actividad podría regular otras fases iniciales durante la formación de la vesícula endocítica.

8.3.1. La fosforilación de la S1205 de Myo5 por Cka2 regula la actividad NPA de la miosina

Nuestros experimentos de polimerización de actina *in vitro* usando mutantes que mimetizan la forma constitutivamente fosforilada o no fosforilada de la S1205 de Myo5 indican que dicha fosforilación inhibe la formación de *foci* de actina inducidos por Myo5-C_{ext}. Además, los experimentos de fosforilación revelan que la capacidad para fosforilar la S1205 de Myo5 de citosoles mutantes es inversamente proporcional con su habilidad para inducir la polimerización de actina. Así, la depleción de Cka2 -pero no de Cka1- inhibe la fosforilación de la S1205 de Myo5 y activa la actividad NPA de Myo5 al mismo nivel que el mutante Myo5-S1205C. El mutante Myo5-S1205D suprime parcialmente este fenotipo, indicando que dicha quinasa regula la actividad NPA de Myo5 a través de la fosforilación de la S1205 de Myo5, al menos parcialmente. De forma equivalente, la sobrexpresión de Cka2 –pero no de Cka1 ni de un mutante de Cka2 sin actividad quinasa- aumenta la fosforilación de la S1205 de Myo5 y disminuye el número de *foci* de actina.

La deformación de la membrana plasmática inducida por actina es un paso clave durante la internalización endocítica. La arquitectura de actina en los sitios de endocitosis debe ajustarse perfectamente en el tiempo y el espacio para generar las fuerzas productivas necesarias para impulsar este proceso. En especial, las fuerzas generadas por la polimerización de actina son esenciales para la elongación de las invaginaciones endocíticas tubulares recubiertas por el

'coat' de clatrina y para la escisión de la vesícula. Mediante técnicas de microscopía de fluorescencia *in vivo* pudimos observar que en un mutante que mimetiza la fosforilación de la S1205 de Myo5 (*myo3Δ myo5-S1205D*), así como en una cepa que sobreexpresa Cka2, la internalización del 'coat' endocítico se ve retardada. Aunque el fenotipo es sutil, nuestros datos indican que es consecuencia directa de la fosforilación de la S1205 de Myo5 por Cka2 ya que dicho fenotipo se ve suprimido tanto en la versión de Myo5 constitutivamente no fosforilada (*myo3Δ myo5-S1205C*) como por la sobreexpresión del mutante de Cka2 sin actividad quinasa (*cka2-K72A*). Aunque las deficiencias endocíticas observadas en estos mutantes son significativas, su efecto absoluto sobre la endocitosis es limitada. Varios estudios demuestran que cuando la actividad NPA de la Myo5 se ve reducida, otros NPFs pueden sustituirlo. Consistentemente, observamos un defecto en la internalización endocítica de Ste2 cuando los mutantes de la S1205 de Myo5 fueron combinados con un mutante Las17 que no conserva su dominio CA de unión al Arp2/3. Un resultado similar se observó tras combinar los mutantes de Myo5 con un mutante de Pan1 al que le falta la región C-terminal incluyendo el CA, pero como la depleción de los dominios ácidos de las miosinas-I y Pan1 no causan defectos aditivos, es posible que más que redundancia funcional el efecto observado sea causado por la falta de regulación de este mutante de Pan1 sobre la NPA de Myo5. Es estos momentos estamos generando cepas que combinen los mutantes *myo3Δ myo5-S1205C* o *myo3Δ myo5-S1205C* con los mutantes de Las17 y Pan1 para analizar la dinámica de los factores endocíticos por microscopía *in vivo* y la ultraestructura de los perfiles endocíticos por microscopía electrónica e inmunomarcaje.

Como nuestros datos indican que la fosforilación de la S1205 de Myo5 mediada por Cka2 regula la NPA de la miosina *in vitro* e *in vivo*, se ha dedicado mucho tiempo y esfuerzo intentando confirmar que la fosforilación *in vivo* depende de Cka2. Desafortunadamente ni mediante el uso de marcaje radiactivo *in vivo* ni con electroforesis de 2 dimensiones pudimos identificar la fosforilación de Myo5 en la S1205 usando proteína purificada. También colaboramos con uno de los grupos que identificaron esta modificación *in vivo* mediante espectometría de masas, y aun así, no fuimos capaces de detectar el residuo fosforilado en la miosina purificada. Curiosamente, todos los estudios de proteómica que han identificado *in vivo* esta modificación han usado extractos totales de levadura. Es posible que la fosforilación se pierda durante el proceso de purificación, o que la forma fosforilada esté poco representada tras la inmunoprecipitación. De hecho, hemos observado recientemente que la miosina asociada la membrana plasmática se purifica muy mal si se compara con la forma citosolica. Por tanto, estamos diseñando nuevos experimentos para detectar la fosforilación *in vivo* bien usando extractos totales o usando miosina asociada a membrana mediante el sistema Phos-tag™ Acrylamide (Wako), y para comparar el estado de fosforilación de Myo5 en una cepa salvaje y un mutante *cka2Δ* a partir de extractos totales usando técnicas de proteómica cuantitativa. Aunque no pudimos detectar la fosforilación de la S1205 de Myo5, el análisis proteómico de la miosina nos permitió identificar un residuo ubicuitinado y 11 residuos fosforilados, 6 de los cuales no habían sido descritos antes (Figura 59). Curiosamente, se identificaron 6 sitios de fosforilación en el extremo C_{ext} de Myo5, aunque en las condiciones del ensayo de fosforilación *in vitro* la S1205 de Myo5 es el residuo

predominantemente fosforilado. Es posible que estas modificaciones deriven de cascadas de transducción de señales no activadas en nuestro ensayo, o bien que las quinasa(s) responsables no estén presentes de forma significativa en los extractos. En cualquier caso, la fosforilación en alguno de estos residuos podría cooperar con la modificación de S1205 para regular la NPA de Myo5.

8.3.2. Los mecanismos moleculares que explican la inhibición de la NPA de Myo5 por CK2

El análisis de la influencia de la fosforilación de la S1205 de Myo5 en el interactoma de la miosina indica que aunque el residuo se localiza en el dominio que une Arp2/3, la fosforilación de S1205 no afecta gravemente esta interacción. Sin embargo, el estado de fosforilación de la S1205 de Myo5 regula la interacción de Myo5 con su co-activador Vrp1. Ensayos de interacción *in vitro* indican que Vrp1 interacciona preferentemente con el mutante de Myo5 no fosforilado, resultado que fue confirmado *in vivo*. El mutante constitutivamente fosforilado muestra mayor afinidad por otras proteínas que interaccionan con Myo5, como Sla1, Pan1, y Bzz1. No sabemos si la interacción con Vrp1 dificulta estéricamente la unión de la miosina a estas proteínas, o si la fosforilación favorece directamente la interacción con Sla1, Pan1, y Bzz1 previniendo de forma secundaria la interacción entre Myo5 y Vrp1. Experimentos con componentes purificados son necesarios para discriminar entre las 2 posibilidades. De cualquier forma, debido a que Vrp1 es necesaria tanto para el reclutamiento de la Myo5 como para activar su NPA, la fosforilación de Myo5 en la S1205 podría perturbar alguna de estas funciones. Nuestros experimentos de microscopía *in vivo* indican que el reclutamiento de Myo5 no se ve alterado, posiblemente debido a la interacción con otras proteínas presentes en el parche endocítico. Sin embargo, y de forma consistente con la menor NPA de Myo5/Vrp1 observada en estos mutantes, tanto la cepa *myo3Δ myo5-S1205D* como la que sobreexpresa Cka2 disminuyen la velocidad de internalización endocítica. Además, la fosforilación de la S1205 de Myo5 ralentiza la disociación de Myo5 de la membrana plasmática tras la internalización de la vesícula, quizá debido a su mayor interacción con Bzz1.

Aún no sabemos dónde y cuándo podría producirse la fosforilación de la S1205 de Myo5. Creemos que Myo5 se fosforila en la membrana plasmática inhibiendo la NPA de Myo5 hacia el final del proceso de deformación de la membrana, ya que al inicio Myo5 se asocia a la base de las invaginaciones endocíticas de longitud intermedia donde co-localiza con Vrp1, y sólo en los perfiles endocíticos más maduros la miosina co-localiza con Bzz1, Pan1, y Sla1. Si nuestra hipótesis es correcta, predice la existencia de algún mecanismo de activación de Cka2 hacia el final de la formación de la vesícula. Korolchuk et al. han observado que la actividad quinasa de CK2 se inhibe por interacción directa con PIP_2. PIP_2 es necesario para la internalización endocítica en *S. cerevisiae*, y se acumula en los sitios de endocitosis de forma simultánea al reclutamiento de proteínas del 'coat'. Tras la formación del 'cap' de actina, la sinaptojanina Sjl2 hidroliza el PIP_2, lo que provoca la disociación de algunos componentes del 'coat'. Creemos que el reclutamiento de Sjl1/2 también podría activar localmente la actividad Cka2 asociada a la

membrana, que fosforilaría la S1205 de Myo5 facilitando la translocación de Bzz1 a la base de la invaginación y el reclutamiento de Myo5 hacia el 'coat' endocítico. Esta hipótesis integraría el tiempo de reclutamiento de Sjl2, la activación de CK2 por la hidrólisis de PIP_2, y los efectos de la fosforilación de la S1205 de Myo5 por Cka2 en el interactoma de la miosina con la dinámica de las proteínas endocíticas a nivel ultraestructural.

Los datos presentados en este estudio indican que además de la S1205 de Myo5, otros sustratos de Cka2 son importantes para regular la actividad de la miosina. Por ejemplo, la mutación Myo5-S1205C no es capaz de suprimir el defecto en la actividad NPA de Myo5 provocado por la sobreexpresión de Cka2. Por su parte, la depleción de *CKA2* no sólo es capaz de rescatar los defectos endocíticos de un mutante *myo5Δ* sino que también suprime parcialmente el defecto endocítico instalado tras la mutación del gen de la fimbrina *SAC6*. Estos datos sugieren que la construcción, estabilidad, y organización de las estructuras de actina endocíticas podrían estar reguladas por la fosforilación de varias dianas endocíticas mediada por Cka2. En la Tabla 8 se muestra un listado de proteínas endocíticas con secuencias diana para la CK2, incluyendo NPFs, proteínas que organizan las superestructuras de actina, o factores que facilitan el desensamblaje de la actina. Algunos de los residuos indicados han sido identificados como residuos fosforilados por espectrometría de masas, pero no se ha investigado ni la quinasa responsable de la fosforilación ni su significado funcional. Actualmente estamos diseñando experimentos para averiguar si Cka2 fosforila alguna de estas proteínas, y si es así se estudiará si su estado de fosforilación modula la polimerización o la estructura de los *foci* de actina inducidos por Myo5. Dos de los candidatos más interesantes son Pan1 y Sla1. Pan1 contiene 3 residuos situados en secuencias consenso para CK2 en la región poli-prolina que interacciona con Myo5 activando su NPA, y Sla1 contiene 1 en la región SH3 que interacciona con Myo5 e inhibe su NPA.

8.3.3. Otros NPFs también se modulan por fosforilación dependiente de CK2

El hecho de que la secuencia consenso de CK2 sea una serina o treonina rodeada de una zona rica en aminoácidos ácidos, la fosforilación en el dominio CA de los NPFs podría ser un mecanismo conservado para su regulación. De hecho, se ha descrito la fosforilación en este dominio para varios NPFs (Tabla 9). Sin embargo, aún no está claro cómo esta fosforilación regula la NPA ni los mecanismos moleculares implicados en dicha regulación. La fosforilación de los residuos S483/S484 de WASP mediada por CK2 incrementa su interacción con el Arp2/3 y activa su NPA en ensayos de polimerización de actina con componentes purificados. Sin embargo, el efecto en la NPA es mucho menor cuando se usa solo la región VCA, lo que sugiere que la fosforilación podría estar liberando la autoinhibición de la proteína. Por el contrario N-WASP se fosforila en los residuos S480/S481 por CK2 pero dicha fosforilación inhibe la NPA de N-WASP. Curiosamente, la fosforilación también aumenta la afinidad de N-WASP por el Arp2/3 y tiene poco efecto en la NPA de la región VCA, lo que indicaría que CK2 también regularía la autoinhibición de N-WASP aunque de forma inversa que para WASP. No se sabe si estas discrepancias son debidas a diferencias entre las 2 proteínas o a aspectos técnicos. De forma

similar a N-WASP, la fosforilación de WAVE2 por CK2 incrementa su afinidad por Arp2/3 pero inhibe su NPA, aunque los mecanismos moleculares responsables de la inhibición de WAVE2 y N-WASP deben ser diferentes ya que WAVE2 no se regula por autoinhibición y el efecto sobre la NPA de WAVE2 también se observa cuando se usa únicamente la región VCA. También el NPF ActA de *Listeria* se fosforila en las S155/S157 por CK2, lo que aumenta su afinidad por Arp2/3. La mutación de las serinas a alanina o a ácido glutámico impide la formación de las colas de actina generadas por el patógeno o que éstas sean productivas, respectivamente.

En *S. cerevisiae* sólo Myo5 y Myo3 contienen residuos susceptibles de fosforilación antes del dominio CA. Las17 no contiene ninguna región consenso para CK2, mientras que Pan1 contiene una serina en una región ácida justo después del CA (S1281). Tanto la S1205 de Myo5 como la S1281 de Pan1 se fosforilan *in vivo*. Pan1 contiene otras 2 serinas fosforiladas *in vivo* en secuencias consenso para CK2 (S1135 y S1180) que se sitúan en una región de unión a F-actina necesaria para su NPA. En un futuro próximo nos gustaría estudiar si estas fosforilaciones están mediadas por CK2 y si regulan la NPA de la proteína. En el caso de la Myo5, hemos observado que la fosforilación de la S1205 de Myo5 regula negativamente su NPA. Similar a ActA, parece que un ciclo de fosforilación/defosforilación de Myo5 es necesario para generar fuerzas productivas basadas en la polimerización de actina. En todo caso, los mecanismos moleculares que explican la regulación de la NPA de la miosina difieren de los descritos en mamíferos ya que la fosforilación no aumenta su interacción con el complejo Arp2/3, sino que más bien influencia su interacción con su co-activador Vrp1 y el inhibidor Sla1. Cabe destacar que en nuestros ensayos hemos usado el fragmento de Myo5 C_{ext} y no la proteína entera. De forma similar a WASP y N-WASP, la actividad de Myo5 también se modula por una interacción autoinhibitoria entre el C_{ext} y el dominio nTH1, por lo que no podemos descartar que la fosforilación en la S1205 de Myo5 regule la interacción autoinhibitoria de la miosina. Se están llevando a cabo nuevos experimentos para sondear esta hipótesis.

8.3.4. Cka2 podría regular la asociación/disociación del 'coat' endocítico

En eucariotas superiores la fosforilación de diferentes proteínas endocíticas mediada por CK2 y por las quinasas GAK/AAK1 (homólogas de Ark1/Prk1) en las vesículas cubiertas de clatrina parece inhibir su interacción con componentes endocíticos provocando su desensamblaje. Nuestros datos preliminares indican que este fenómeno también podría darse en *S. cerevisiae*, ya que en la cepa *cka2Δ* se observa un aumento del número de parches endocíticos que no son consecuencia de la acumulación de eventos improductivos. Varias proteínas que forman parte del 'coat', así como factores que participan en la asociación y disociación del 'coat' endocítico, contienen secuencias diana para la CK2, incluyendo Ede1, Pal1, Ent1, Pan1, Sla1, Ark1, Sjl2, o Lsb5 (Tabla 8). En un futuro próximo nos gustaría averiguar si CK2 fosforila *in vitro* e *in vivo* alguna de estas proteínas.

PIP_2 y CK2 parecen tener efectos contrarios en la asociación/disociación del 'coat' endocítico y en la polimerización de actina (Figura 61). PIP_2 puede regular directamente a proteínas con dominios de unión a lípidos, pero no a proteínas que no contactan con la membrana. En este

contexto, un mecanismo regulatorio secundario que se comunique con los niveles de PIP_2 y regule los componentes citosólicos de las redes funcionales endocíticas podría acortar el tiempo de respuesta tras cambios bruscos en la concentración de fosfoinosítidos y garantizar la eficiencia y reproducibilidad del proceso. La pareja PIP_2/CK2 no solo modularía la asociación/disociación del 'coat' y las estructuras de actina durante la endocitosis sino que también podría dar rápida respuesta a los cambios ambientales que producen un incremento en los niveles celulares de PIP_2. De hecho, la capacidad endocítica de la célula aumenta cuando se somete a las células a choque térmico o bajo pH, lo que también produce un aumento de PIP_2 y la reorganización de los parches de actina corticales. En un futuro próximo queremos investigar si existe una comunicación entre los niveles de PIP_2 y la actividad de CK2. Para ello, analizaremos la actividad CK2 de extractos de cepas mutantes de la PI(4)P-5-quinasa *MSS4* y de las PI(4,5)P_2-fosfatasas *SJL1/2*.

8.3.5. Una actividad CK2 no canónica y asociada a partículas fosforila Myo5

Una de las observaciones más sorprendentes de este estudio es que la actividad CK2 responsable de la fosforilación de la S1205 de Myo5 *in vitro*, la regulación de la NPA de Myo5 *in vitro*, y la endocitosis *in vivo* sólo involucra a la actividad catalítica Cka2 pero no a la otra subunidad catalítica Cka1 ni a las subunidades reguladoras Ckb1 y Ckb2. Además, observamos que tanto la fosforilación de la S1205 de Myo5 como la subunidad Cka2 -cuando se compara con Cka1- se asocian a una fracción particulada de membranas y/o elementos del citoesqueleto. CK2 está constituida principalmente por 2 subunidades catalíticas α y 2 reguladoras β, compuestas en *S. cerevisiae* por *CKA1* y *CKA2*, y *CKB1* y *CKB2*, respectivamente. La estructura tetramérica puede contener idénticas o diferentes isoformas catalíticas, pero requiere las dos subunidades reguladoras. La depleción de *CKA1* o de *CKA2* no causa fenotipo obvio pero la disrupción de ambos genes es letal, lo que indica que CK2 es esencial y que una subunidad catalítica puede suplir la ausencia de la otra para la viabilidad celular. Aun así, existe especialización funcional entre las isoformas. Estudios genéticos, bioquímicos, y farmacológicos indican que aunque las dos pueden fosforilar todas las dianas esenciales, Cka1 tendría preferencia por dianas de ciclo celular y Cka2 por proteínas involucradas en la polaridad celular y la integridad de membranas. Además, se ha observado recientemente la fosforilación del represor transcripcional Nrg1 depende de Cka1 pero no de Cka2 mientras que la fosforilación de la proteína mitocondrial Tom22 depende de Cka2 pero no de Cka1.

Sorprendentemente, observamos también que la actividad Cka2 responsable de la fosforilación de la S1205 de Myo5 no se corresponde con la estructura tetramérica, ya que las subunidades reguladoras son dispensables para el proceso. Se considera habitualmente que CK2 es un tetrámero porque cuando se purifican las subunidades catalíticas suelen estar acompañadas por cantidades equivalentes de subunidades reguladoras. Sin embargo, la cepa *ckb1Δ ckb2Δ* es completamente viable, lo que indica que las subunidades catalíticas mantienen un nivel importante de actividad fuera del complejo. Además, diferentes estudios indican que existen poblaciones de subunidades α y β fuera de la estructura tetramérica clásica. Por ejemplo, una

quinasa monomérica aislada del citosol de *S. cerevisiae* fue identificada posteriormente como una subunidad Cka2 libre. Aunque CK2 se localiza predominantemente en el núcleo celular, se ha observado la presencia de las subunidades catalíticas y reguladoras en Golgi y retículo endoplasmático liso, y de subunidades catalíticas (pero no reguladoras) en el retículo endoplasmático rugoso y en centrómeros. CK2 también está presente en la membrana plasmática. La localización del holoenzima o de sus subunidades individuales a diferentes compartimentos celulares puede contribuir a la regulación de la quinasa. Actualmente estamos diseñando ensayos para analizar la composición de la CK2 en fracciones citosólicas y particuladas, así como en la membrana plasmática, mediante el uso de electroforesis con geles nativos.

8.4. Conclusiones

En este trabajo hemos confirmado que CK2 fosforila *in vitro* la S1205 de Myo5 y concluimos que:

- La actividad CK2 responsable de la fosforilación en la S1205 de la Myo5 *in vitro* está asociada a partículas y requiere la subunidad catalítica Cka2 pero no Cka1.
- La actividad CK2 responsable de la fosforilación en la S1205 de la Myo5 *in vitro* contiene una subunidad catalítica Cka2 no tetramérica, ya que no se requieren las subunidades reguladoras Ckb1 y Ckb2.
- La fosforilación de la S1205 de Myo5 mediada por Cka2 disminuye la formación de estructuras de actina complejas *in vitro* que recapitulan las estructuras de actina necesarias para la internalización endocítica *in vivo*.
- La fosforilación de la S1205 de Myo5 mediada por Cka2 no influencia el reclutamiento de la miosina a los sitios de endocitosis sino que disminuye la velocidad de la internalización y la disociación de la miosina de la membrana plasmática.
- La formación de un ciclo de fosforilación/defosforilación es importante para preservar de forma eficiente la internalización endocítica en ausencia de otros NPFs.
- La fosforilación de la S1205 de Myo5 mediada por Cka2 regula negativamente la interacción entre Myo5 y su co-activador Vrp1. Esta fosforilación también incrementa directa o indirectamente la interacción de la miosina con Bzz1, Sla1, y Pan1, lo que sugiere que la fosforilación ocurre tarde durante la maduración de la invaginación endocítica.
- Además de la S1205 de Myo5, otros sustratos de Cka2 participan en la formación y reorganización de las estructuras de actina *in vitro* e *in vivo*.
- Myo5 contiene otros residuos fosforilados que no han sido previamente identificados.
- Además de su papel en la regulación de la generación y/o reorganización de las estructuras de actina, la actividad de Cka2 podría tener una función en el ciclo de asociación/disociación de la cubierta endocítica.

9. APPENDIX: Publications

Contributions to other studies during the thesis period:

- Grosshans, B.L., Grotsch, H., Mukhopadhyay, D., Fernandez-Golbano, I.M., Pfannstiel, J., Idrissi, F.Z., Lechner, J., Riezman, H., and Geli, M.I. (2006). TEDS site phosphorylation of the yeast myosins I is required for ligand-induced but not for constitutive endocytosis of the G protein-coupled receptor Ste2p. J Biol Chem *281*, 11104-11114.
- Idrissi, F.Z., Grotsch, H., Fernandez-Golbano, I.M., Presciatto-Baschong, C., Riezman, H., and Geli, M.I. (2008). Distinct acto/myosin-I structures associate with endocytic profiles at the plasma membrane. J Cell Biol *180*, 1219-1232.
- Collette JR, Chi RJ, Boettner DR, Fernandez-Golbano IM, Plemel R, Merz AJ, Geli MI, Traub LM, Lemmon SK. (2009). Clathrin functions in the absence of the terminal domain binding site for adaptor-associated clathrin-box motifs. Mol Biol Cell. *20*, 3401-3413.
- Grotsch, H., Giblin, J.P., Idrissi, F.Z., Fernandez-Golbano, I.M., Collette, J.R., Newpher, T.M., Robles, V., Lemmon, S.K., and Geli, M.I. (2010). Calmodulin dissociation regulates Myo5 recruitment and function at endocytic sites. Embo J *29*, 2899-2914.
- Giblin J, Fernandez-Golbano IM, Idrissi FZ, Geli MI. (2011). Function and regulation of Saccharomyces cerevisiae myosins-I in endocytic budding. Biochem Soc Trans. 39, 1185-1190. Review.

In preparation:

- Fernandez-Golbano, I.M., Grosshans, B.L., Idrissi, F.Z., and Geli, M.I. A non-canonical CK2 activity modulates myosin-I-induced actin polymerization at endocytic sites.